



Petrology and geochemistry of granitoids and their mafic microgranular enclaves (MME) in marginal part of the Małopolska Block (S Poland)

Anna WOLSKA

Institute of Geological Sciences, Jagiellonian University, 30-063 Kraków, ul. Oleandry 2a,

e-mail: a.wolska@uj.edu.pl

Received: May 5, 2012

Received in revised form: November 27, 2012

Accepted: January 2, 2013

Available online: March 22, 2013

Abstract. Granitic plutons (the Dolina Będkowska valley and Pilica area) were found in a few boreholes in the Małopolska Block (MB). These granitic rocks may represent apical parts (apophyses) of a great magmatic bodies (batholiths) located in deeper level of the Ediacaran/Paleozoic basement. They are described as ‘stitching intrusions’, generated during/after collision in Carboniferous/Permian period (~300 Ma) between the Upper Silesian Block (USB) and the Małopolska Block (MB).

These rocks are fresh, unaltered granodiorites that are pale grey in colour. They have holocrystalline, medium- to coarse-grained structure and massive texture. For the first time, several mafic microgranular enclaves (MME), varying in size and colour, were found in the granodioritic host (HG). The occurrence of MME in the host granodioritic rocks is evidence of a mingling process between mafic and felsic magmas.

The MME are pale/dark grey in colour, fine-grained rocks with ‘porphyritic’ textures. They consist of large megacrysts/xenocrysts of plagioclase, quartz, alkali feldspars and the fine-grained groundmass of pseudo-doleritic textures (lath-shaped plagioclases, blade-shaped amphiboles/biotites). According to their modal/mineral composition, they represent Q-diorites and tonalites.

The MME, similar to the host granodiorites (HG), are I-type rocks, exhibit high Na₂O content >3.2 wt%; normative diopside or normative corundum occurs (mainly <1%). They are metaluminous to slightly peraluminous (ASI <1.1) and have calc-alkaline, medium-K to high-K character. They generally belong to magnesian series (#Mg=0.20-0.40) and have low algaite index (<0.87). They are low evolved magmatic rocks. The rocks studied are enriched in LREEs (La, Ce, Sm) compared to HREEs. The Eu* negative anomaly and high Sr contents point to varying degrees of plagioclase fractionation connected to the mixing process rather than simple fractional crystallization. Both rocks studied (HG and MME) are characterized by a high content of LILEs (K, Ba, Rb) in normalized patterns and a low HFS/LIL elements ratio (Ta, Nb)/(K, Rb, La). The projection points of the rocks

studied plot in different fields of various petrochemical diagrams: mainly in the arc granites that are rare in the pre-collisional granites as well as the syn-subductional to post-collisional granites fields.

For the first time, inner textures in rock-forming minerals related to mixing processes are described both in the granodioritic host (HG) and in the MME. Mantled boxy cellular plagioclase megacrysts with ‘old cores’ of labradorite composition, and amphibole aggregates with titanite and opaque minerals, represent peritectic rather than primary residual minerals. The plagioclase, quartz and alkali feldspar megacrysts/xenocrysts were mechanically transferred from the granodioritic host (HG) to MME. The presence of lath-shaped plagioclases, blade-shaped amphiboles/biotites and acicular-shaped apatites in the groundmass of the MME is evidence of undercooling of hot mafic blobs in a relatively cold granodioritic magma chamber. The MME were hybridized by leucocratic melt squeezed from the granodioritic magma in a later stage of the mixing process (quartz and alkali crystals in the interstices in the MME groundmass). In the granodiorites (HG), the spike and spongy cellular zones as well as biotite/amphibole zones in plagioclase megacrysts are connected to the mixing process.

Both of the rocks studied are characterized by different amounts of major elements (SiO_2 , Na_2O and K_2O), trace elements (Ni, Cr, V, Ti and P), #Mg and modified alkali–lime index (MALI) that is related to their origins from different sources. On the other hand, they have similar chondrite-normalized patterns (for trace elements and REE), LILEs contents (Sr, Ba, Rb), aluminum saturation index (ASI) and isotopic signatures (high $^{86}\text{Sr}/^{87}\text{Sr}$ (0.079–0.713) and low $^{143}\text{Nd}/^{144}\text{Nd}$ (0.512) values but lower than in continental crust), which are evidence of the strong hybridisation of mafic enclaves by the granodioritic host magma. The parental rocks of both rocks studied have a similar mafic signature but were generated in different sources: the host granodiorites (HG) magma in lower continental crust rocks, and the MME magma in enriched upper mantle. The MME crystallized from strongly hybridized magma of intermediate compositions (Q-diorite, tonalite) rather than from primary mafic magma. The host granodiorites (HG) originated from completely homogenized crustal granodioritic magma which inherited its geochemical signature from ancient arc-rocks in a subduction-related setting.

Key-words: the Małopolska Block (MB), host granodiorites (HG), mafic microgranular enclaves (MME), Q-diorites, tonalites, mixing, mingling, hybridisation process

Content

1. Introduction	5
2. Geological setting	6
3. Magmatic rock investigations	9
4. Methods	13
5. Results	15
5.1. Petrography of pale grey host granites (HG)	15
5.2. Petrography of mafic microgranular enclaves (MME)	29
5.3. Geochemistry of pale grey host granites (HG)	44
5.4. Geochemistry of mafic microgranular enclaves (MME)	69
6. Discussion	78
6.1. Variscan volcano-plutonic magmatic activity	78
6.2. Petrography of contrasted rocks – MME and host granites	79
6.3. Geochemistry of contrasted rocks – MME and host granites	90
7. Conclusions	110
8. References	112

1. Introduction

The Kraków-Lubliniec Fault Zone (KLFZ) separates the Małopolska Block (MB) from the Upper Silesian Block (USB). The KLFZ is part of the Hamburg-Kraków-Dobrogea transcontinental tectonic strike-slip zone which represents a larger Trans-European composite tectonic suture zone (TESZ). TESZ separates the East-European Craton (Laurussia-Baltica) from mosaic terranes in Western and Central Europe (Gondwana blocks).

The Upper Silesian Block (USB) is part of the Brunovistulicum composite terrane (BVT), whereas the Małopolska Block (MB) is a thinned marginal part of the Baltica/Laurussian craton (Fig. 1). The amalgamation of terranes during the Carboniferous-Permian was accompanied by intensive magmatic activity.

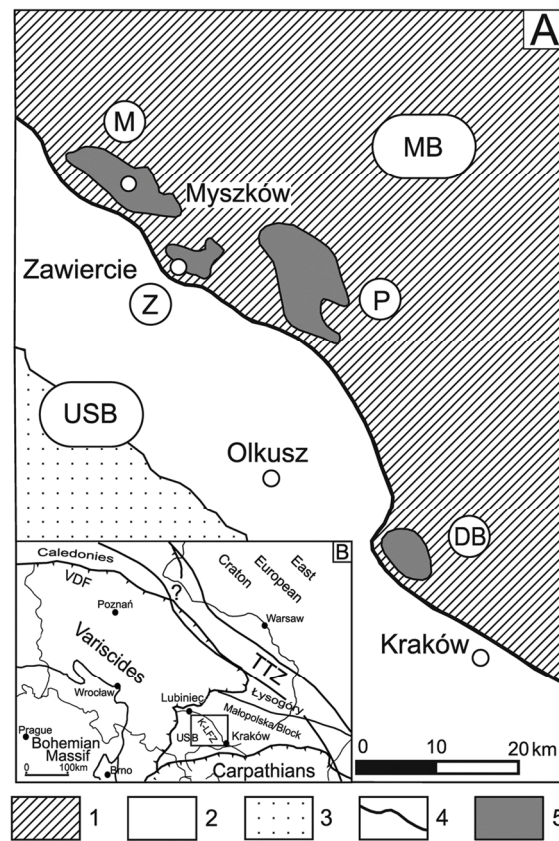


Fig. 1.A. Localization of granitoid intrusions at the boundary zone of the Upper Silesia (USB) and Małopolska (MB) blocks (after Żaba 1995). 1 – Małopolska Block (MB), 2 – Upper Silesia Block (USB), 3 – Upper Silesian Coal Basin, 4 – Kraków-Lubliniec Fault Zone (after Buła 1994), 5 – areas of granitoid intrusions and their contact interaction on host Paleozoic rocks. Symbols: M – Myszków-Mrzygłód, Z – Zawiercie, P – Pilica, BD – Dolina Będkowska valley; B. location of the Kraków-Lubliniec Fault Zone (KLFZ) in Poland (after Mazur, Jaroński 2006, modified by Żelaźniewicz et al. 2008; Pożaryski and Karnkowski 1997).

In the 60s of the 19th century, in the Krzeszowice area which represents a small part of boundary between the Upper Silesian Block (USB) and Małopolska Block (MB), several outcrops of volcanic rocks were described (Kreutz 1871; and other authors – see Chapter 3: Magmatic rock investigations). In the 70s of the 20th century, magmatic rocks (commonly granites with extrusive rocks) were found in several deep drill holes in Ediacaran/Paleozoic basement (see Chapter 3: Magmatic rock investigations).

The aims of this monograph are: (1) the detailed presentation of petrographical and geochemical features of dark/pale grey subtypes of mafic microgranular enclaves (MME) that occur in the host pale grey granites (HG); (2) the description, for the first time, of the occurrence of inner (mixing) textures in rock-forming minerals in the MME as well as in the host granites; (3) the presentation of similarities and differences in the petrographical and geochemical features of both magmatic rock types; (4) the detailed discussion about hybridisation, mixing, mingling, fractional crystallization and assimilation processes in the magmatic rocks studied; (5) for the first time, determination of the Sr and Nd isotope data in both host granites and MME; and (6) the geochemical characteristics (including isotopes) related to their origin and evolution in collision setting/environment during the Variscan orogeny. There are attempts to explain the problem of the specific geochemical signature of these magmatic rocks (VAG-type) in the context of the complex development and geological setting of this part of Southern Poland. The author hopes that this monograph should be helpful in extending the knowledge and answer some of the significant scientific problems relating to the evolution of plutonic activity in the Małopolska Block (MB).

The present monograph is also based on previous studies of magmatic rocks in the Małopolska Block (MB) and the Krzeszowice area (the KLFZ), their geochemical characteristics and geological setting context (see Chapter 2: Geological setting).

2. Geological setting

In the southern part of Poland, there are two, large regional tectonic units – the Upper Silesian Block (USB) and the Małopolska Block (MB). The Upper Silesian Block (USB) is one of numerous terranes, including the Bruno-Vistulian (the Moravian) one (Bukowy 1964; Herbich 1981; Kotas 1982), which presumably originated from the south-eastern part of East Avalonia. The Małopolska Block (MB) was probably formed from the southern part of the East European craton (EEC) – (Lewandowski 1994; Dadlez et al. 1994; Dadlez 1995; Moczydłowska 1995). According to the studies of Harańczyk (1994) and Unrug et al. (1999), a small Lubliniec-Zawiercie-Wieluń terrane also occurs in this area. These blocks are localized in the south-western foreland of the East European Craton (EEC), within the Central European part of the Paleozoic platform (Żaba 1999). These blocks represent the fragments of micro-continents (terranes), characterized by different lithologies of rock sequences, tectonic style, degree of consolidation, alteration processes and history (Żaba 1999).

The boundary between the Bruno-Vistulian Terrane (BVT) and the Małopolska Block (MB), in this part, is represented by the Kraków-Lubliniec fault zone (KLFZ) which is well defined and documented (Brochwicz-Lewiński et al. 1986; Harańczyk 1994; Dadlez 1995; Buła et al. 1997b; Żaba 1999; Nawrocki et al. 2004). This zone was also named the Kraków-Myszków Lineament, fracture of the Kraków-Myszków Zone, Zawiercie-

Rzeszotary Fault Zone, Kraków Lineament, Hamburg-Kraków Fracture and Kraków-Lubliniec Fault Zone (Bogacz 1980; Kotas 1982; Brochwicz-Lewiński et al. 1983; Harańczyk 1988, 1994; Oberc 1993, 1994; Buła 1994). The KLFZ was described as a segment of a larger transcontinental suture zone, Hamburg-Kraków (Brochwicz-Lewiński et al. 1983; Oberc 1993, 1994; Harańczyk 1994; Żaba 1994; Dadlez 1995; Buła, Żaba 2005). The KLFZ is continuation towards the south-east of the Elbe Lineament (Winchester, Team 2002) and is part of the major Hamburg-Kraków-Dobrogea transcontinental strike-slip tectonic zone (Słaby et al. 2010).

The KLFZ has a width of 0.5 to 2 km (Żaba 1994, 1995, 1996; Buła et al. 1997b) and stretches in a SE-NW direction. Its location and width are variously described by numerous authors (Bogacz 1980; Kotas 1982; Brochwicz-Lewiński et al. 1983; Harańczyk 1988, 1994; Oberc 1993, 1994; Dadlez 1995; Buła et al. 1997b; Nawrocki et al. 2004; Malinowski et al. 2005). Buła (1994) has established its exact location and direction (Fig. 1). The new seismic data – seismic refraction profile CEL-02 of the CELEBRATION 2000 experiment (Malinowski et al. 2005) confirm these interpretations. The KLFZ is a deep, intensive brittle fold and fault system that underwent repeated reactivation and multi-stage deformation (Żaba 1996, 1999, 2000). The boundary between the Upper Silesian Block (USB) and Małopolska Block (MB) forms a narrow fault zone (KLFZ), cutting and moving all rocks of Precambrian and Paleozoic age (Buła et al. 1997a; Żaba 1999; Buła 2000).

This deep tectonic zone (or suture zone, according to Harańczyk 1994) probably has a late Proterozoic foundation (Żaba 1999) and originated in Neoproterozoic-Cambrian periods, being repeatedly rejuvenated during the Paleozoic (Dadlez 1995; Żelaźniewicz 1998; Żaba 1999; Nawrocki et al. 2004). Many authors have shown that tectonic activity in this zone was active from the Early Paleozoic to the Cenozoic (vide Żaba 1999).

The Kraków-Lubliniec Fault Zone (KLFZ) was formed during the collision between the Upper Silesian (USB) and Małopolska (MB) blocks as a strongly deformed, marginal tectonic zone (brittle shear zone – Żaba 1999). The most important tectonic deformation in the border part of both blocks was related to increased strike-slip activity at the end of the Silurian period (sinistral transpression – Żaba 1994, 1995, 1996) and during the Late Carboniferous (dextral transpression and dextral, local sinistral transtension – Żaba 1996).

The tectonic structures and lithology of the Precambrian and Lower Paleozoic sequences (series) are different in both the Upper Silesian Block (USB) and the Małopolska Block (MB). The Upper Silesian Block (USB) may have Gondwana affinity (Buła et al. 1997a), whereas the Early Paleozoic rocks of the Małopolska Block (MB) exhibit faunal and lithological affinities to Baltica (Dzik 1983; Orłowski 1992; Moczydłowska 1995; Żylińska 2002).

Upper Silesian Block (USB)

The Precambrian basement of the Upper Silesian Block (USB) (the eastern part of the Bruno-Vistulian terrane (BVT)) consists of two complexes. The Archean crystalline rocks (amphibolites), 2.8-2.6 Ga old, formed the Rzeszotary Horst (Bylina et al. 2000; Żelaźniewicz et al. 2009; Buła, Żaba 2005, 2008). The Neoproterozoic crystalline rocks (540-600 Ma) are connected with the Cadomian tectonic and metamorphic processes

(Dudek 1980; Żelaźniewicz et al. 1997, 2002, 2009; Finger et al. 1999, 2000; Buła, Żaba 2005, 2008). The second complex, represented by the Ediacaran flish, is strongly tectonically deformed and composed from anchimetamorphic rocks (phyllites) (Cebulak, Kotas 1982; Żelaźniewicz et al., 2009; Buła, Żaba 2005, 2008) and polymictic conglomerates (Buła, Żaba 2005; Buła, Habryn 2008).

The Lower and Upper Paleozoic cover consist of Cambrian, Devonian and Carboniferous rocks. The Early and Middle Cambrian deposits are represented by clastic rocks – shallow-water sandstone succession (Buła, Jachowicz 1996; Buła et al. 1997a; Buła 2000; Buła, Żaba 2005; Jachowicz 2005).

The tectonic transport of the Bruno-Vistulian terrane (BVT) towards the Małopolska Block (MB) is postulated by Belka et al. (2002) and Nawrocki et al. (2007b) as being after the Ludlovian, but before the Early Devonian when ‘old red’ sandstones were deposited on the Upper Silesian Block (USB).

The Early Devonian ‘old red’ type deposits are common for both the blocks (Żaba 1999; Buła 2000) and strongly indicate the final amalgamation of the Bruno-Vistulian terrane (BVT) (Nawrocki, Poprawa 2006).

The Early Devonian rocks of ‘old red’ facies are covered by the Middle and Late Devonian carbonates (Narkiewicz 2005, 2007). The Early Carboniferous sequences begin carbonate deposits and later form clastic rocks of flish and flish-like (kulm) type. During the Namurian and Westphalian, coal-bearing deposits (molasse) were formed on the Upper Silesia Coal Basin (USCB) (Kotas 1982, 1985a, b) related to the Paralic and Limnic sandstones series. These deposits formed during compression and collision of the Bohemian Massif (BM) and the Bruno-Vistulian terrane (BVT). The Paleozoic formations built by the unit represent thrust fault structure (Buła et al. 2008). In the Late Carboniferous, the tectonic activity (strike-slip motions) is connected with dextral transpression and transtension (Bogacz, Krokowski 1981; Żaba 1999).

The paleomagmatic studies (Nawrocki et al. 2007a; Nawrocki et al. 2008) of Early Permian volcanic rocks from the Krzeszowice area explain the question of tectonic movements, which were induced by sinistral transtension after emplacement of these rocks.

Małopolska Block (MB)

The Małopolska Block (MB) consists of two main structural levels: Ediacaran/Paleozoic basement, and Mesozoic cover composed of Triassic, Jurassic and Cretaceous sedimentary rocks.

The Precambrian basement of the Małopolska Block (MB) consists of anchimetamorphosed and strongly tectonically deformed silicoclastic and pelitic rocks (flish deposits – Żelaźniewicz et al. 2009; Buła, Habryn 2008, 2010). In contrast to the geological setting of a crystalline basement of the Bruno-Vistulian terrane (BVT), the Małopolska Block (MB) shows the occurrence of the crystalline metamorphic rocks up to a 10 km depth (Malinowski et al. 2005). Lower Paleozoic rocks are overlain with Neoproterozoic deposits, and are represented by the Early Cambrian clastic rocks and clastic (psammitic to pelitic) rocks, as well as carbonate sediments of Ordovician and Silurian age (Buła, Habryn 2008). A clastic material of the Ludlovian sandstones, on the Małopolska Block (MB), did not originate from the Bruno-Vistulian Terrane (BVT) but

from the island arc (Kozłowski et al. 2004) which was located on the west of the Małopolska Block (MB), in the place where the Bruno-Vistulian terrane (BVT) now occurs (Nawrocki et al. 2007b).

The Precambrian and Lower Paleozoic rocks are covered by clastic rocks of 'old red' formation, as well as the Middle and Late Devonian carbonates, but also by carbonates/clastic sediments (kulm facies) of the Carboniferous age. The Paleozoic formations build numerous 'mosaic' block structures composed from the Ediacaran deposits and the Devonian-Carboniferous sequences with the Lower Paleozoic rocks (Buła et al. 2008).

3. Magmatic rock investigations

Volcanic rocks in the Krzeszowice area (a small part of the KLFZ) were mentioned in the 19th century (Kreutz 1871; Zuber 1886; Zaręczny 1894). These rocks occur as lavas, dykes and sills, but also as laccoliths and lava domes in several natural outcrops as well as quarries. In the 20s of the 20th century, the volcanic rocks in boreholes: Dziewki/k. Siewierza, Wielkie Drogi were founded (vide – Siedlecki 1954). Later, in the 60s of the 20th century, in Bębło and Czajowice boreholes were drilled in the hydrothermally altered rhyodacite with sulphide mineralization (Bukowy, Ślósarz 1968; Górecka 1972).

Several generations of scientists, of the last 100 years, described the mineralogical, petrographical and geochemical characteristics of volcanic rocks in the Krzeszowice area (Kreutz 1871; Zuber 1886; Zaręczny 1894; Rozen 1909; Broder 1931; Bolewski 1939; Siedlecki, Wieser 1947; Bukowy, Ślósarz 1968; Sutowicz 1984; Wolska 1984; Słaby 1987, 1990, 2000; Harańczyk, Wala 1982; Heflik, Muszyński 1993; Muszyński, Pieczka 1994; Muszyński 1995; Muszyński, Pieczka 1996; Czerny, Muszyński 1997; Muszyński, Czerny 1999; Czerny, Muszyński 2000; Lewandowska, Bochenek 2001; Podemski 2001; Lewandowska, Rospondek 2003; Falenty 2004 vide Słaby et al. 2010; Gniazdowska 2004 vide Słaby et al. 2010; Słaby et al. 2009, 2010; Lewandowska et al. 2010).

Volcanic rocks represent a bimodal suite of mafic-intermediate rocks (trachybasalts-trachyandesites with minor lamprophyres) and felsic rocks (dacites-trachydacites-rhyolites).

The pioneering papers of Kreutz (1871), Zuber (1886) and Zaręczny (1894) describe, for the first time, the mineralogical and petrographical characteristics of volcanic rocks from the Krzeszowice area. Rozen (1909) characterized the volcanic rocks, both mafic and felsic, as connected to a calc-alkaline differentiation trend. Bolewski (1939) distinguished the second trend represented by high-potassium alkaline rocks. The high-potassium nature of the original magmas was questioned by Słaby (1987, 1990, 2000). Harańczyk (1989) postulated the occurrence of four different magma types (basic, rhyodacitic, trachytic and lamprophyric) in the Silesian-Cracow region. Czerny and Muszyński (1997) argued that there are three types of magmas (basic, lamprophyric and rhyodacitic) and explain that the different geochemical features/characteristics of volcanic rocks is related to mixing between basic and lamprophyric magmas. Earlier, Bukowy and Cebulak (1964) postulated that magmatic rocks from the Silesian-Cracow region formed during mixing between mafic and felsic magmas. Rospondek et al. (2004) hypothesised that the formation of intermediate and felsic rocks may be related to fractional crystallization. Geochemical modelling showed that both magma suites evolved by fractional crystallization but they are not comagmatic

(Gniazdowska 2004; Falenty, 2004 – vide Słaby et al. 2010). Słaby et al. (2009) suggested that the magma for the Krzeszowice area volcanic rocks was generated in two different sources: the basalts-trachybasalts-trachyandesites in enriched (metasomatized) lithospheric mantle, and the dacites-trachydacites-rhyolites in the continental crust (which is composed from amphibolites).

Słaby et al. (2010) concluded, based on a geochemical study, that the magmatic rocks have collisional, arc-related features and calc-alkaline character which were inherited from an enriched, subduction-setting source correlated to Ediacaran/Cambrian reorganization – collision process of the Brunovistulia (the break-up of Rodinia) with Baltica. In Carboniferous/Permian period, magmatic processes active in situ in the KLFZ, were connected to lithospheric thickening, delamination and decompressional melting and lead to mantle metasomatism. Magmas interacted with material from the lithospheric boundary layer and induced crust-mantle melting.

Lewandowska et al. (2010) suggested, based on a geochemical study, that the basaltic trachyandesite magma from the Krzeszowice area indicates subduction-related characteristics and originated from a source containing hydrous phases (amphibole or phlogopite). Its generation was related to the formation of pull-apart basins in the late stages of the Variscan orogeny evolution.

In the felsic volcanic rocks (rhyodacites) from the Krzeszowice area, the enclaves of microgranodiorites and micromonzodiorites were described (Rozen 1909; Gawel 1955; Heflik, Muszyński 1993; Muszyński, Czerny 1999; Lewandowska, Bochenek 2001; Czerny et al. 2000; Czerny, Muszyński 2002). On the other hand, dark enclaves (mafic microgranular enclaves – MME) in the Małopolska granodiorites have not been investigated.

3.1. Granitoids

In the Małopolska Block (MB), granitoid bodies are known in four areas: Myszków-Mrzygłód, Zawiercie, Pilica and Dolina Będkowska valley (Fig. 1). They occur within host sedimentary rocks of the Ediacaran/Paleozoic basement in the border zone of the Małopolska Block (MB). Their emplacement is linear in character and shows the NW-SE strike. The occurrence of granitoid bodies was determined on the basis of magnetic and gravimetric anomalies (Skorupa 1953; Kurbiel 1978; Brochwicz-Lewiński et al. 1983; Królikowski, Petecki 1995). Harańczyk et al. (1995) has defined the character of their emplacement as 'stitching intrusions'. Granitoid bodies were intruded in Ediacaran age sedimentary rocks of (Jachowicz-Zdanowska 2010) but also in Early Paleozoic rocks (Harańczyk 1982; 1994). Numerous boreholes (vide Żaba 1999) drilled these granitoid bodies in various levels of the Ediacaran/Paleozoic basement.

Earlier authors considered them to represent small bodies, 2-3 km wide and 5-7 km long. They were considered to be hypoabissal intrusions, because of the occurrence of oscillatory zoning in plagioclase crystals (Kośnik, Muszyński 1990) and melt inclusions in quartz, apatite and zircon (Karwowski 1988). Based on these investigations, the estimated depth of solidification of granitic melt was 5-6 km (Żaba 1999). Granitic bodies were considered to represent apical parts of a great batholith about 100 km long that was

probably located in a deeper level of the basement in the border zone of Małopolska Block (Żaba 1999).

These magmatic rocks were described by numerous authors. They are represented mainly by granodiorites (Banaś et al. 1972; Mikrut 1977; Harańczyk 1982, 1985; Harańczyk, Wala 1982; Piekarski 1982b, 1985; Ślósarz 1982, 1985; Kośnik, Muszyński 1990; Harańczyk et al. 1995; Płonczyńska 2000; Wolska 2000, 2001; Truszel et al. 2006; Żelaźniewicz et al. 2008) as well as transition rocks to monzonites and granites and some diorites (Heflik et al. 1977; Markiewicz 1984, 1994; Kośnik, Muszyński 1990; Wolska 2009).

Kośnik and Muszyński (1990) described petrographical characteristics and mineral compositions of granites from the Dolina Będkowska valley, Pilica and Zawiercie areas. A detailed study of the Jerzmanowice granite, localized in the DB5 and WB102A boreholes in the Dolina Będkowska valley, was conducted by Harańczyk et al. (1995) in which the author paid attention to unequigranular structure, sometimes 'porphyritic', of the granites, but also described marked differences in its mineral composition, especially various amounts of femic minerals. Płonczyńska (2000) investigated mineral composition of granodiorites (especially the plagioclase characteristics) as well as their geochemical features (e.g. strongly peraluminous, S-type, highly fractionated granodiorites and granomonzonites which formed in COLG and VAG tectonic settings).

The petrographic investigations of the granodiorite from the Dolina Będkowska valley (the borehole WB102A) were presented by Markiewicz (2006 – vide Żelaźniewicz et al. 2008). The author determined the modal composition of granodiorites and implied that the rock-forming minerals markedly show various proportions. Plagioclases are the dominant minerals and exhibit andesine core and oligoclase-albite rim. Mafic minerals are represented by biotite and Mg-hornblende.

Żelaźniewicz et al. (2008) took note that the granitoids in the boundary of the Małopolska Block (MB) occur outside the orogenic belt, and suggested the hypothesis that the parent melt for the silicic rocks formed from the thickened lower crust of the Variscan orogenic belt during extensional decompression melting near the crust/mantle boundary, and was transported away to foreland setting along the crustal-scale fault zone (the KLFZ).

Żelaźniewicz et al. (2008) concluded, based on geochemical studies, that the granodiorites indicate strongly supra-subduction affinity, and originated during partial melting of metapsammitic or granodioritic to tonalitic precursors.

3.2. Geochronologic data

The majority of authors (Bukowy, Cebulak 1964; Bukowy 1984, 1994; Karwowski 1988; Kośnik, Muszyński 1990; Żaba 1994, 1995, 1996) connect the emplacement of granitic bodies in the basement of the Małopolska Block with the Variscan magmatic cycle – Late Carboniferous (Westphalian-Stephanian) (Żaba 1999) and close to the Carboniferous/Permian boundary (Nawrocki et al. 2008; Żelaźniewicz et al. 2008; Słaby et al. 2010). A close relationship between the occurrence of granitoid bodies in the basement, in the border zone of the Małopolska Block (MB), and the tectonic activity during the Late Carboniferous polyphase dextral shear zones was suggested by Żaba (1996). The emplacement of granitoid intrusions was due to the Late Carboniferous dextral

transpression (Żaba 1996). In the pre-intrusive Namurian A stage (no. 7 according to Żaba 1996) during the D3 deformation phase, the generation of granitoid magma in deep levels of basement in the border zone of the Małopolska Block (MB) took place. During the Westphalian B stage (no. 8 according to Żaba 1996), granitoid bodies began to rise from the basement to the upper crustal levels.

Granitoids of the Myszków-Mrzygłód area were examined using several geochronologic methods. According to the K/Ar method, their isotope age amounts to 312 Ma (Jarmołowicz-Szulc 1984, 1985), whereas $^{40}\text{Ar}/^{39}\text{Ar}$ investigation resulted in 298-300 Ma (Snee – vide Ślósarz 1985) and the volumetric K/Ar method resulted in 300 Ma (Depciuch 1971). Minerals from the Myszków granodiorite yielded a $^{40}\text{Ar}/^{39}\text{Ar}$ isotope age of 300-296 Ma for biotites, 297.5 ± 0.5 Ma for a white mica and 290-292 Ma for K-feldspars (Podemski et al. 2001). The granodiorite intrusion from the Dolina Będkowska valley has an isotope age of 293 ± 10 Ma (Olivier vide Harańczyk 1989), 292-284 Ma (Nawrocki et al. 2010) and 300 ± 3 Ma was estimated on the base of U-Pb zircon age data (SHRIMP II) (Żelaźniewicz et al. 2008).

3.3. Temperature and pressure conditions

Karwowski's (1988) investigations have shown that the temperature of intruding granitic magma in the Myszków-Mrzygłód area was below 800°C (zircon and apatite were formed in melt in the range 1260-820°C – Truszel et al. 2006) and the temperature of metasomatic fluids below 550°C. Fluid inclusion investigations of the quartz veins of the granites from the Pilica area allowed the temperature of K-feldspathic alteration processes to be determined in the interval from 400°C to 210°C (Harańczyk et al. 1988). Słaby et al. (2010) noted that the compositions of felsic volcanic rocks from the Krzeszowice area is close to the quartz-feldspar cotectics in the hydrous granitic system related to pressures between 5 and 10 kbars (Winkler 1974). The pressure was estimated, according to the Al-in-amphibole geobarometer (Schmidt 1992) in amphibole from felsic rocks (Miękinia and Żalas-Orlej), to be approximately $5.7\text{-}7.4 \pm 0.6$ kbar (Słaby et al. 2010).

3.4. Thermal metamorphism

Granitoid magma has produced broad contact aureoles (thermal and metasomatic) that have been mentioned and described by several authors (Łydka 1973; Ryka 1974; Heflik et al. 1975; Harańczyk et al. 1980, 1995, 1996; Piekarski 1982a, b, 1985; Markiewicz 1984, 1994, 1998, 2002; Karwowski 1988; Narkiewicz, Nehring-Lefeld 1993; Żaba 1994; Heflik, Piekarski 1992; Truszel 1994; Koszowska, Wolska 1994a, b, 2000a, b; Truszel et al. 2006).

Thermal activity of the granite magma intrusion on the carbonate rock complex in the Zawiercie area (Ordovician-Silurian age) was evaluated as 440-610°C (upper part) and 490-720°C (lower part) (Narkiewicz, Nehring-Lefeld 1993). According to Żaba (1994), the width of a thermal alteration zone of granitoids studied in the host sedimentary rocks amounts to several metres, and of metasomatic alterations up to 2 km.

In the Dolina Będkowska valley, the width of the contact aureole produced by granodiorite in the host sedimentary rocks reaches up to one hundred metres (Koszowska, Wolska 2000a). The occurrence of K-feldspar-cordierite-biotite mineral paragenesis

(Koszowska, Wolska 2000a) suggests variable temperature condition from 500°C to 630°C (Koszowska, Wolska 2000b), which corresponds to medium- and high-temperature facies of contact metamorphism – the hornblende-hornfels and orthoclase-cordierite-hornfels facies – according to Winkler (1986).

Markiewicz (2002) and Truszel et al. (2006) determined the contact and metasomatic action of magmatic intrusion on the host Lower Paleozoic rocks (Mrzygłód, Myszków, Zawiercie), and described several rocks in the thermal aureole (hornfels, hornfelsic schists, spotted slates and skarns) which formed under conditions of the albite-epidote-hornfels and hornblende-hornfels facies of thermal metamorphism.

3.5. Hydrothermal alteration

Granitoids from the Małopolska Block (MB) are often strongly metasomatically altered and are connected with the mineralization of Cu-Mo porphyry type deposits (Harańczyk 1978; Harańczyk et al. 1980, 1995; Piekarski 1982a, b, 1985, 1994; Ślósarz 1982, 1985, 1994; Wolska 2000, 2001; Podemski 2001; Truszel et al. 2006).

Harańczyk (1978) mentioned the hydrothermally altered magmatic rocks in the Pilica area and described various types of metasomatic alteration: K-silicate, sericitic, propylitic and argillic. In later papers Harańczyk et al. (1980, 1995) describe typical ore-bearing mineralization connected to porphyry copper deposits that occur in the granitoid bodies in both the Dolina Będkowska valley and Zawiercie area.

Piekarski (1982a, b, 1985, 1994) defined zones of Myszków ore deposit that relate to the Mo-W-Cu stockwork mineralization of porphyry copper type developed within granite intrusion as well as in host metamorphic rocks. Ślósarz (1982, 1985, 1994) described a magmatic body in Myszków-Mrzygłód area with a classical zonation connected to hydrothermal alteration of the porphyry copper type deposits (e.g. K-silicate zone in central part of intrusion while the sericitic and propylitic zones in the outer parts). Podemski et al. (2001) compile the knowledge about the Myszków deposit as the specific Mo-W porphyry copper deposit characterized by stockwork multiphase ore-bearing mineralization related to metasomatic hydrothermal alteration of magmatic and host metamorphic rocks.

Wolska (2000, 2001) investigated granitoids both from the Pilica area and from the Dolina Będkowska valley which show strongly hydrothermal alteration and divided a few zones of alteration: K-silicate, sericitic, chloritic (propylitic) and argillic. She remarked that a mineralization of the Mo-Cu-porphyry type deposits was commonly developed in granites as surrounding veins type and show pervasive, advanced character.

Truszel et al. (2006) described in magmatic rocks as well as in host rocks (Ediacaran/Paleozoic age) in the Zawiercie and Mysłów area ore mineralization (Cu, W and Mo) developed as vein and stockwork.

4. Methods

4.1. Sampling

More than 100 samples of granites (the drill core samples) were collected from six boreholes situated in the Silesian-Cracow region. Two boreholes (DB5 and WB102A) are

localized in the Dolina Będkowska valley and four boreholes (KH1, KH2, KH3 and WB 115) in Kocikowa near Pilica (Fig. 1A). These boreholes penetrated a complex of Ediacaran/Early Paleozoic folded and faulted rocks which were found under the Jurassic sequence. As previous investigators defined (see Chapter 3: Magmatic rock investigations), granitoids from various areas of the Małopolska Block (MB) are characterized by similar petrographical and geochemical features and may represent higher levels of a great batholith located in a basement of the border zone of this block (Żaba 1999).

The profile of the boreholes are elaborated and described in detail by Harańczyk (1984) and Harańczyk et al. (1995). The granitic bodies are cut by numerous ore-bearing quartz and feldspar veinlets as well as rhyolitic dykes and exhibit zones of pervasive alteration connected with hydrothermal mineralization of Cu-Mo porphyry type deposits. Therefore, detailed petrographic (microscopic) investigations were carried out on 60 selected rock samples from some drill core intervals which represent fresh, grey (in various shades) unaltered granites and their slightly hydrothermally altered pale pinkish varieties.

4.2. Microscopic study and modal mineralogy

Microscopic study was performed in the Department of Mineralogy, Petrology and Geochemistry, Institute of Geological Sciences, Jagiellonian University using a NIKON YM-EPI Eclipse E600POL (Japan) optical microscope. Modal mineralogy was determined by point counting with a Zeiss automatic counter, and on each thin section more than 1500 points were counted along 10-15 lines. The point numbers for different minerals were recalculated to 100 modal percentage. Microphotographic documentation was made using a Canon EOS 40D camera.

4.3. Microprobe analyses

Microprobe analyses were performed in the Laboratory of Scanning Electron Microscopy at the Institute of Zoology of the Jagiellonian University and in the Laboratory of Field Emission Scanning Electron Microscopy and Microanalysis at the Institute of Geological Sciences of the Jagiellonian University. The chemical composition of the main rock-forming minerals was determined using the SEM-EDS method. Carbon-coated polished thin section samples were analysed using a JEOL 5410 microscope with a Voyager 3100 (NORAN) EDS spectrometer and a HITASCHI S 4700 microscope with a Vantage (NORAN) spectrometer respectively. The time of analysis was 100 s for point at the acceleration voltage 20 kV. The ZAF correction algorithm was used.

4.4. Chemical analyses

After macroscopic and microscopic studies, only 30 samples were selected for major, trace and RE elements analyses. The representative fresh samples were powdered using an agate ball mill. The whole rock analysis was carried out in the ACME Analytical Laboratories Ltd., Vancouver, Canada. Total abundances of the major oxides and several minor elements are reported on a 0.1 g sample analysed by ICP-emission spectrometry following a lithium metaborate/tetraborate fusion and dilute nitric acid digestion. Loss on

ignition (LOI) is determined by weight difference after ignition at 1000°C for > 2 h. Rare earth and refractory elements are determined by ICP mass spectrometry following a lithium metaborate/tetraborate fusion and nitric acid digestion of a 0.1 g sample. Moreover, separate 0.5 g samples were digested in Aqua Regia and analysed by ICP mass spectrometry to report the precious and base metals. Detection limits range from 0.01 to 0.1 wt% for major oxides, from 0.1 to 10 ppm for trace elements, and from 0.01 to 0.5 ppm for the rare earth elements.

4.5. Isotopic investigations

Rb-Sr and Sm-Nd isotope analyses were performed in the Environmental Laboratory of Isotope Geochemistry, Polish Academy of Science (Kraków, Poland). The digestion of samples and separation of REE was carried out using the procedure according to Cohen et al. (1988) and Pin and Santos Zalduegui (1997). All the samples were analysed using the MC ICPMS 'Iso Prote' manufactured by Micromass (UK) Ltd. in static/stable method (Vance, Thirwall, 2002). Analytical blank and standard followed the Jd1Nd standard and gave $^{143}\text{Nd}/^{144}\text{Nd} = 0.512101 \pm 12 \text{ } 2\sigma$. Mass bias correction was made according to exponential law using $^{146}\text{Nd}/^{144}\text{Nd} = 0.7219$. The measured Sr isotopic ratio was normalized against $^{86}\text{Sr}/^{88}\text{Sr} = 0.1194$ and the $^{87}\text{Sr}/^{86}\text{Sr}$ ratio for the SRM 987 Sr standard was $0.710263 \pm 12 \text{ } 2\sigma$. Total procedural blanks for Nd were below 20 pg, and for Sr below 50 pg. The precision of the Rb/Sr abundance ratio determined with ICPMS was ca. 1%, the Sm/Nd abundance ratio ca. 0.5%. The $^{143}\text{Nd}/^{144}\text{Nd}$ ratios are quoted in the ϵ_{Nd} notation as derivations from a chondritic reference (CHUR) with present-day $^{143}\text{Nd}/^{144}\text{Nd}$ ratio.

5. Results

5.1. Petrography of pale grey host granites (HG)

Granitoids from the Ediacaran/Paleozoic basement of the Małopolska Block (MB) and hydrothermal alteration zones in granitoids of the Małopolska Block connected with ore-bearing mineralization of porphyry Cu-Mo deposits were described by many authors (see Chapter 3: Magmatic rock investigations). Therefore, for the present studies only several samples of unaltered pale grey granitoids or weakly altered granitoids with pale pinkish shades were selected from almost a hundred specimens. The location of samples studied in the boreholes is shown in Figure 2.

The fresh, unaltered host granites studied are pale grey in colour (Fig. 3). Płoczyńska (2000) provides information that the colours of granitoids from the Małopolska Block (Dolina Będkowska valley, Myszków-Mrzygłód, Pilica and Zawiercie) are grey or pinkish. Meanwhile, Żelaźniewicz et al. (2008) noticed that the colour of the granodiorite from the Dolina Będkowska valley is greyish red or occasionally a greyish green. The host granites studied have holocrystalline, medium- to coarse-grained structure (the grain size of rock-forming minerals is below 10 mm and variable) and massive texture (Fig. 3). A few rare samples of granitoids display inequigranular or 'porphyritic' character. The occurrence of porphyritic texture in granitoids from Dolina Będkowska valley was described by

Harańczyk et al. (1995), Płoczyńska (2000) and Wolska (2000, 2001), Markiewicz, (2006 vide Żelaźniewicz et al. 2008) and Żelaźniewicz et al. (2008).

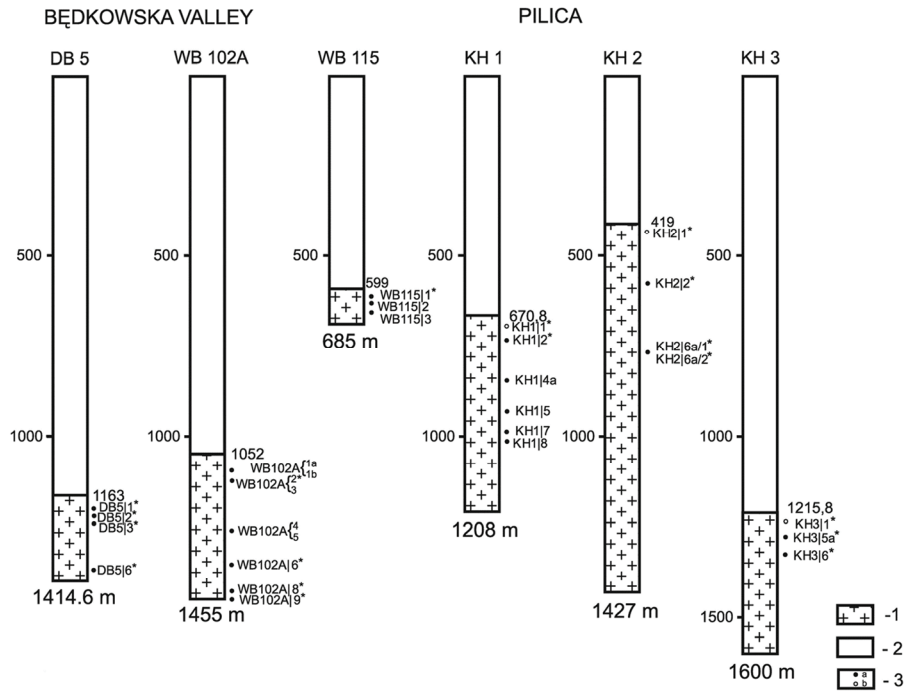


Fig. 2. Localization of the host granite samples in the sections of the boreholes: Dolina Będkowska valley (DB5, WB102A), Pilica (KH1, KH2, KH3 and WB115) after Harańczyk (1984), Harańczyk et al. (1995). 1 – granites, 2 – other rocks, 3 – a site of sampling (a number of samples); a – pale grey host granite samples; b – contact host granite samples.

The host granites from the contact zone with host sedimentary rocks (the cHG granite samples) are predominantly medium-grained and show variable colour from pale grey to greyish white and pale pinkish (Fig. 4).

Following from the present investigations, even the macroscopic observations of unaltered, fresh pale grey granite samples studied indicate that the colour of feldspars is diversified: crystals of plagioclase are white or pale green, while K-feldspar crystals are pale pinkish or exhibit various shades of pink colour.

The pale grey granites (pgHG) studied generally consist of plagioclase and quartz with variable amounts of K-feldspar, biotite and/or hornblende, accompanied by accessories: titanite, epidote, opaque minerals, allanite, zircon, apatite (Table 1). On the other hand, in the contact granites (cHG) only quartz and feldspars are observed. The dark minerals – biotite and amphiboles are strongly altered to chlorite.



Fig. 3. Pale grey host granites (sample no. KH3/6).

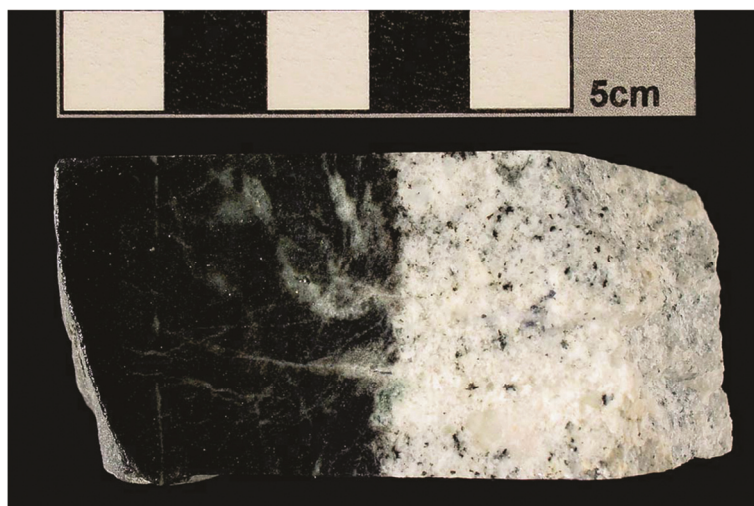


Fig. 4. Contact host granites (right) with metasedimentary wall-rocks (left) – (sample no. KH3/1).

5.1.1. Modal composition of pale grey host granites (HG)

The modal composition of the host granites studied is shown in Table 1. The amount of rock-forming minerals, especially feldspars and quartz in studied rocks, as shown by modal analysis varies in a broad range. Samples of the host granite are characterized by diverse mineral compositions. Similarly, the modal composition of the rock-forming minerals and their various proportions in the Dolina Będkowska valley granodiorite was described by Markiewicz (2006 vide Żelaźniewicz et al. 2008). Nevertheless, on the IUGS classification diagram the samples of pale grey (pgHG) granite studied plot in the granodiorite field (Fig. 5). According to Le Maitre (1989), granodiorites are characterized by a Q modal content ranging from 20 to 60%, the P' index ($100 \times P / (A + P)$ in %) from 65 to 95% and the colour index ($M' > 5\%$). Only the 'leuco' variety of granodiorite has the M' index $< 5\%$. All the samples of host

granite studied exhibit the content of Q (26-54vol%) and P (41-64vol%). The P' index ranges from 71 to 91% and the M' index from 18 to 6vol%. Only the samples from the contact zones with sedimentary rocks (contact host granites – KH1/1, KH2/1 and KH3/1 samples) have the M' index < 3 and represent the leuco-granodiorite variety.

5.1.2. Mineral characteristics of pale grey host granites (HG)

Plagioclases

Plagioclases are the most abundant minerals (38-59vol%) in the host granites studied (Table 1). The large euhedral, tabular crystals (up to 8 mm in size) are fresh and show composite inner textures. In plagioclase crystals, a multiple zoning as a combination of discontinuous oscillatory and convolute zoning can be seen (Fig. 6). Their cores are inhomogenous, and show textures resulting from resorption-regrowth processes. They are often filled with irregular inclusions of K-feldspars, biotite and quartz and display a speckled appearance of fine inclusions of white mica (sericite). Żelaźniewicz et al. (2008) mentioned that plagioclase crystals from the Dolina Będkowska valley granodiorite are slightly altered and exhibit various alteration processes (sericitization, carbonatization, albitization and rarely epidotization).

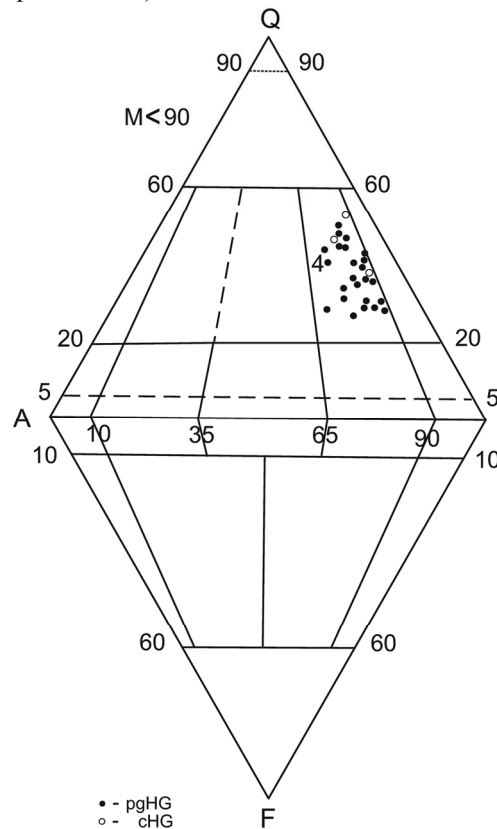


Fig. 5. Modal composition of pale grey host granites on the IUGS classification diagram. Symbols: pgHG – pale grey host granites, cHG – contact host granites; (4) – granodiorite.

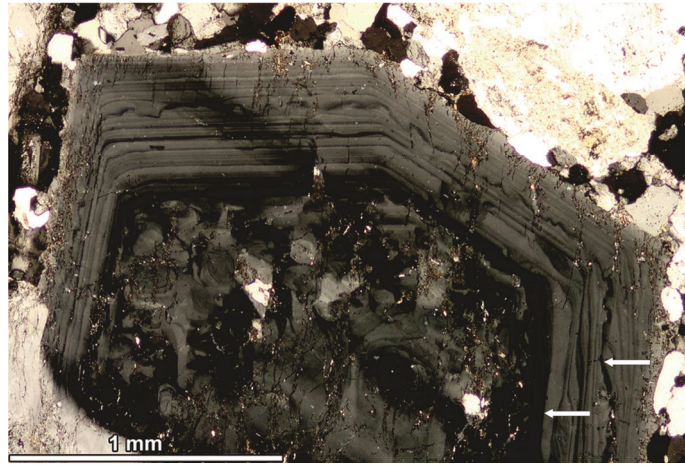


Fig. 6. Fragment of large plagioclase crystals with nonhomogeneous 'old core' and multiple zoning rim (arrows - resorption surface) – pale grey host granites (sample no. KH3/6). Crossed polars.

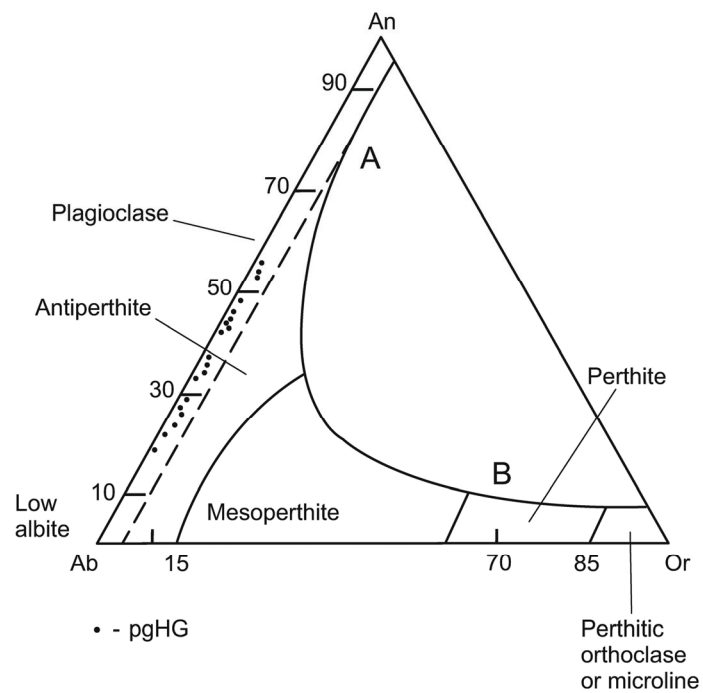


Fig. 7. Composition of plagioclases of pale grey host granites on the Ab-An-Or classification diagram. Symbol: pgHG – pale grey host granites.

Only locally in the samples studied of contact host granite (cHG), the cores of plagioclase crystals contain a dense mass of very fine white mica and clay minerals, related to alteration or which are crosscut by veinlets of K-feldspar.

Modal composition of pale grey host granites (HG).

Sample	KH1/2	KH1/4a	KH1/5	KH1/7	KH1/8	KH2/2	KH3/6	KH3/5a	WB115/1	WB115/2	WB115/3	WB102A/1a	WB102A/1b	WB102A/2
pale grey host granites (pgHG)														
plagioclase megacrysts	15.0	8.2	0.0	4.3	5.1	1.3	6.5	8.9	1.0	3.3	2.7	1.4	5.2	8.3
quartz megacrysts	10.1	2.3	0.0	3.8	0.9	2.6	3.2	0.0	0.0	0.0	2.2	0.0	0.0	3.0
plagioclases	34.3	41.6	42.4	35.3	39.8	35.1	42.5	44.2	36.8	49.5	37.6	45.0	46.9	34.8
quartz	29.4	27.7	27.3	34.7	24.6	35.9	27.6	26.9	34.1	31.1	40.1	36.7	25.8	33.5
hornblende	1.2	0.0	0.0	2.5	1.0	2.0	2.2	1.6	0.8	1.7	0.3	1.1	3.1	0.0
biotite	2.9	0.0	0.0	6.1	7.3	1.8	5.1	8.0	8.0	6.6	7.3	4.4	9.5	9.0
titanite	0.3	0.0	0.0	0.3	0.0	1.7	0.5	0.2	0.9	0.8	0.0	0.2	0.3	0.2
chlorite	0.3	11.8	0.0	0.4	0.4	5.3	0.0	0.2	2.0	0.5	1.1	0.0	0.3	1.2
K-feldspar	5.4	6.9	10.6	11.3	20.0	13.1	10.6	9.6	15.6	6.4	8.6	10.5	7.5	8.7
sercite	0.7	0.6	16.7	1.2	0.2	0.3	0.5	0.0	0.3	0.0	0.2	0.0	0.3	0.5
opaque minerals	0.5	0.8	3.0	0.3	0.7	0.6	1.2	0.5	0.5	0.0	0.0	0.5	1.0	0.5
epidote/zoisite	0.0	0.0	0.0	0.0	0.0	0.3	0.0	0.0	0.0	0.0	0.0	0.2	0.0	0.0
allanite	0.0	0.0	0.0	0.0	0.0	0.0	0.0	0.0	0.0	0.0	0.0	0.0	0.0	0.2
Total	100.1	99.9	100.0	100.2	100.2	100.0	99.9	100.1	100.1	100.1	100.1	100.0	99.9	99.9
P'index	90.1	87.8	80.0	77.4	69.2	73.5	82.2	84.5	70.8	89.2	82.4	81.5	87.4	83.2
M'index	5.9	13.2	19.7	10.8	9.6	12.0	9.4	10.5	12.5	9.6	9.0	6.4	14.5	11.6

P' index – 100xP/A+P (in%); M' index – the colour index

TABLE 1

WB102A/3	WB102A/4	WB102A/5	WB102A/6	WB102A/8	WB102A/9	DB5/1	DB5/2	DB5/3	DB5/6	KH1/1	KH2/1	KH3/1
contact host granites (cHG)												
0.8	3.5	7.3	9.1	5.1	1.3	6.1	6.1	2.3	6.6	1.2	2.3	3.5
4.3	1.0	0.0	1.6	2.3	5.2	1.5	4.6	0.0	2.2	1.4	4.5	7.7
39.0	41.7	42.9	44.6	53.4	40.5	42.2	41.0	43.4	43.4	48.6	38.3	37.7
37.2	24.7	22.7	24.9	24.3	25.8	29.5	29.5	28.9	20.8	32.9	48.2	38.4
0.0	2.7	1.4	2.3	1.4	2.3	3.0	1.3	1.1	2.0	0.0	0.0	0.2
7.1	9.3	9.6	4.9	4.6	7.7	7.1	8.0	7.4	11.1	0.0	0.7	0.7
0.5	1.5	1.0	0.6	1.5	1.0	0.5	0.2	9.4	0.8	0.0	0.0	0.0
0.8	0.3	0.4	0.0	0.0	0.4	0.0	0.2	0.7	0.7	2.5	0.4	1.4
8.1	14.5	13.3	11.4	6.0	14.3	8.4	7.8	13.9	8.7	6.4	4.6	10.3
0.0	0.3	0.2	0.0	0.8	0.4	0.0	0.2	0.7	0.8	6.7	1.1	0.0
2.0	0.5	1.2	0.7	0.6	1.2	1.7	1.0	1.3	2.8	0.4	0.0	0.0
0.3	0.0	0.0	0.0	0.0	0.0	0.0	0.0	0.0	0.0	0.0	0.0	0.2
100.1	100.0	100.0	100.1	100.0	100.1	100.0	99.9	100.1	99.9	100.1	100.1	100.1
83.1	75.1	79.1	82.5	90.7	74.5	85.2	85.8	76.7	85.2	88.6	89.8	80.0
10.7	14.6	13.8	8.5	8.9	13.0	12.3	10.9	11.6	18.1	9.6	2.2	2.5

As described by Płonczyńska (2000), plagioclases are characterized by multiple twinning according to albite, pericline and Carlsbad laws. They exhibit variable crystal sizes and an uneven degree of alteration (sericitization). The composition of the plagioclases is andesine ($\text{Ab}_{68-51} \text{An}_{48-30} \text{Or}_{2-1}$) in the core and oligoclase ($\text{Ab}_{81-71} \text{An}_{28-18} \text{Or}_{2-1}$) in some outer rims. Płonczyńska (2000) as well as Żelaźniewicz et al. (2008) display similar compositional variation (from core to rim) of plagioclase crystals. Four zones (zones: Ab_{54} , Ab_{57} , Ab_{62} , Ab_{67}), differing in the amount of Ab, are distinctly observed in the plagioclase cores of the samples studied. On the other hand, the broad outer plagioclase rims show merely three zones (Ab_{71} , Ab_{72-74} and Ab_{78} zones). The outer rims of albite composition were also mentioned by Płonczyńska (2000) and Żelaźniewicz et al. (2008).

In the host granites studied, the local occurrence of plagioclase boxy cellular crystals (megacrysts), with ‘old core’ was described (Fig. 6) for the first time. These cores have irregular boundaries (spike zones) and spongy cellular dissolution/melting textures, and are composed of labradorite ($\text{Ab}_{48-47} \text{An}_{52-51} \text{Or}_1$), containing an admixture of SrO (0.4wt%). In plagioclase boxy cellular crystals (megacrysts), the occurrence of two resorption zones between ‘old core’ and inner rim as well as between inner and outer rim (Fig. 6) is markedly visible. The composition of plagioclase crystals is presented on Figure 7.

In the contact host granites (cHG) a strong alteration of plagioclase crystals filled with secondary sericite and K-feldspar can be seen (Fig. 8).

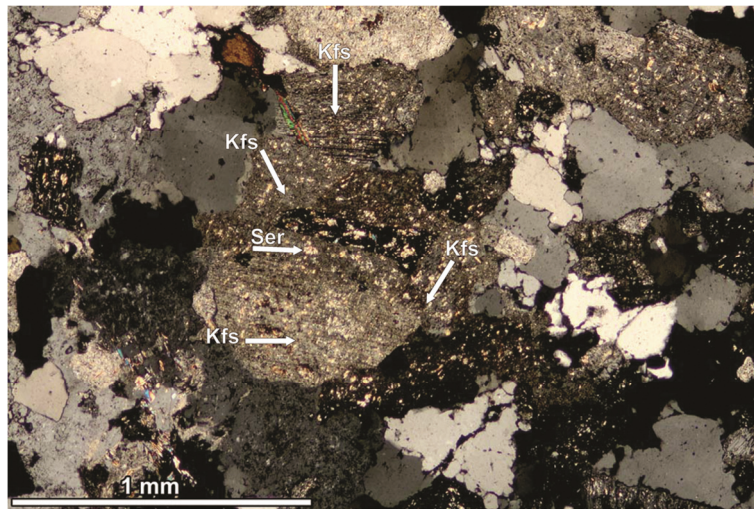


Fig. 8. Strongly altered plagioclase crystals filled with secondary sericite (Ser) and K-feldspar (Kfs) – contact host granites (sample no. KH3/1). Crossed polars.

Quartz

Quartz (23- 46vol% – Table 1) occurs as large subhedral and anhedral crystals (up to 0.7 mm in size). Sometimes it forms composite grains (crystals), locally corroded on their boundaries. Płonczyńska (2000) described slight dynamic deformations in the quartz in granitoids from the Małopolska Block (MB). In the samples studied, quartz crystals show undulatory extinction (Fig. 9) and contain small inclusions of biotite and plagioclase. Large

quartz crystals are rarely broken into numerous subgrains (consertal/mortar textures) and show deformed/cataclastic features.

Alkali feldspars

The amount of alkali feldspar in the rocks studied is different in various samples (5-20vol% – Table 1). Similarly varying proportions in the modal composition of alkali feldspar crystals from the Dolina Będowska valley granodiorites were described by Markiewicz (2006 vide Żelaźniewicz et al. 2008). In the rocks studied, these minerals form anhedral, small crystals (up to 3 mm) which occur in interstices between other minerals (Fig. 10). They often occur as small inclusions or veinlets in ‘old cores’ of boxy cellular plagioclase megacrysts as well as in outer zones/rims of tabular plagioclase crystals. Their chemical formula: $Or_{97-87} Ab_{13-2} An_{2-1}$ corresponds to K-feldspar/orthoclase. According to a study by Żelaźniewicz et al. (2008), alkali feldspars from the Dolina Będowska valley granodiorite were occasionally replaced by kaolinite.

On the other hand, secondary K-feldspar occurs only in the contact host granites (cHG) where it forms replacement (interlocking or interpenetrating) perthites and veinlets in strongly altered primary crystals of plagioclases (Fig. 8), which was determined during the present studies.

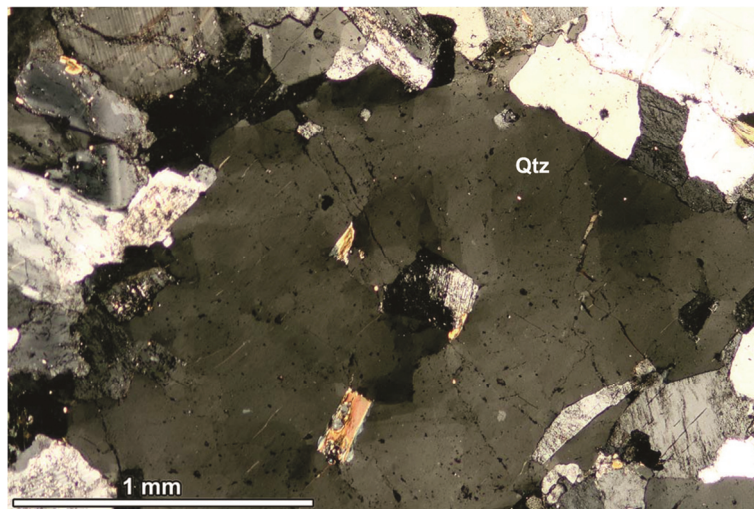


Fig. 9. Undulose extinction of large quartz crystal (Qtz) – pale grey host granites (sample no. KH1/7). Crossed polars.

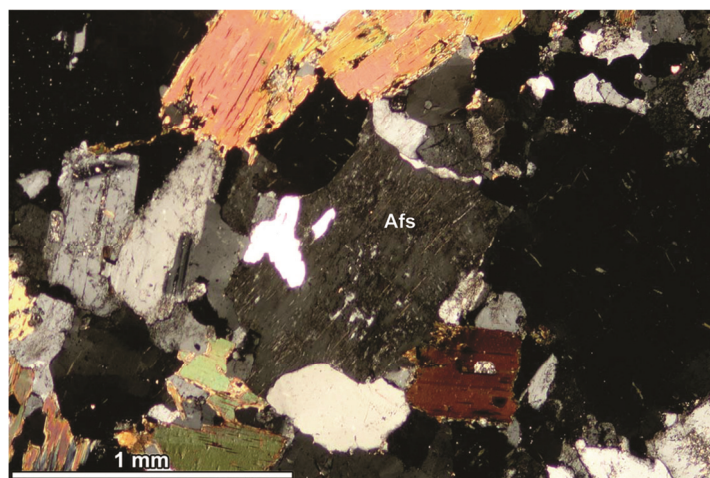


Fig. 10. Small alkali feldspar (perthitic) crystal (Afs) – pale grey host granites (sample no. KH1/7). Crossed polars.

Biotite

In the studied rocks biotite (0.7-11vol% – Table 1) occurs as large (up to 5 mm in size) euhedral/subhedral plates containing small inclusions of zircon, apatite and opaque minerals (Fig. 11). It is strongly pleochroic from pale straw yellow (α) to reddish brown (γ) in colours. As reported by Żelaźniewicz et al. (2008) biotite is rarely chloritized. Sometimes in the samples studied, biotite is altered by various degrees into pale green chlorite. It is characterized by medium #Mg number (0.40-0.52), high amount of Al^{IV} (2.05-2.35 apfu), FeO (20-22wt%), and TiO_2 (3.5-5.0wt%), and variable content of MnO (0.0-0.6wt%) respectively. In the classification diagram its composition is plotted in the phlogopite-annite field very close to the annite end member (Fig. 12).

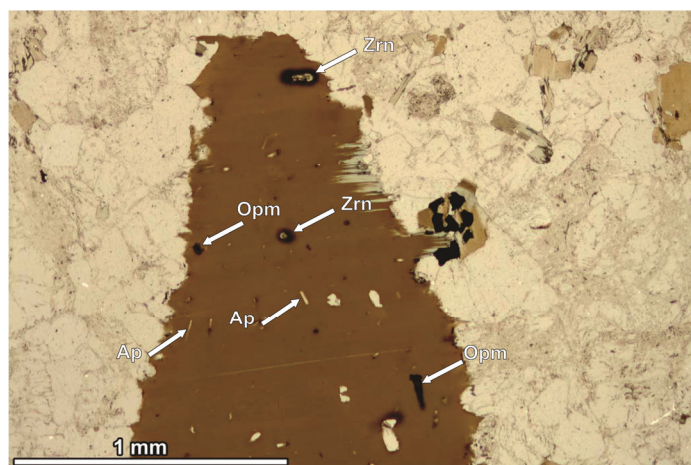


Fig. 11. Large biotite plate containing small inclusions of zircon (Zrn), apatite (Ap) and opaque minerals (Opm) – pale grey host granites (sample no. WB102A/2). Plain-polarized light.

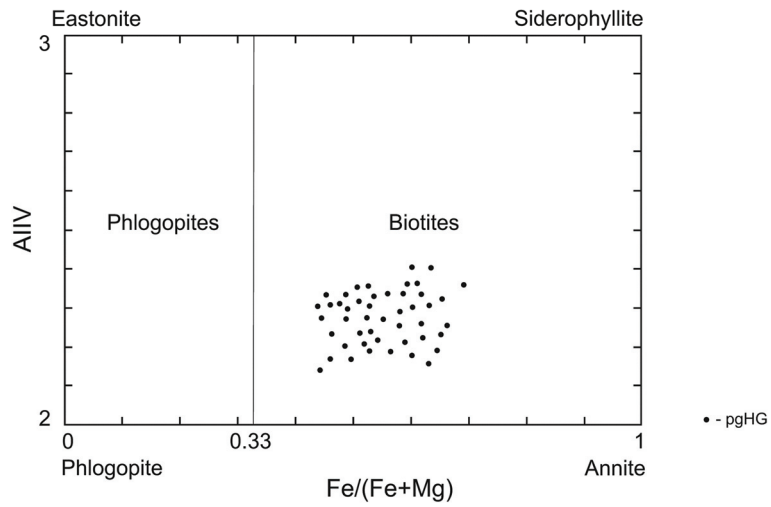


Fig. 12. Composition of biotites from pale grey host granites studied on the $\text{Fe}/(\text{Fe}+\text{Mg})$ vs Al^{IV} diagram. Symbol: pgHG - pale grey host granites.

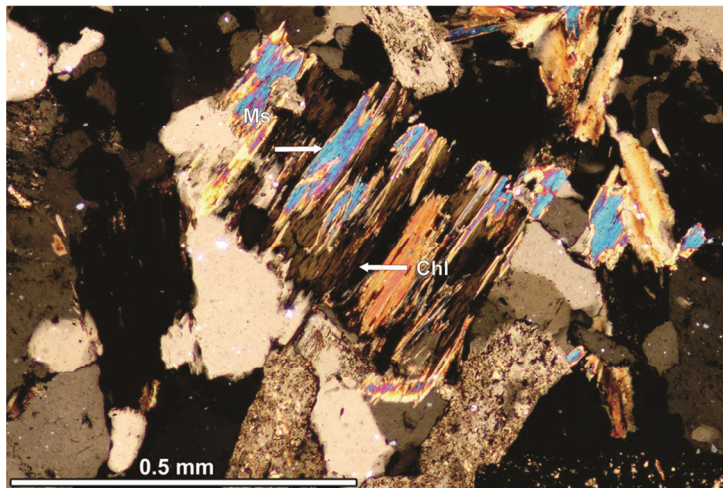


Fig. 13. Pseudomorph after biotite filled with chlorite (Chl) and white mica (muscovite Ms) – contact host granites (sample no. KH1/1). Crossed polars.

In the contact host granites (cHG), fresh biotite plates occur sporadically and are generally strongly altered. Pseudomorphs after biotite are often present in the rocks studied (Fig.13). They are commonly filled with chlorite and opaque minerals and overgrown by white mica.

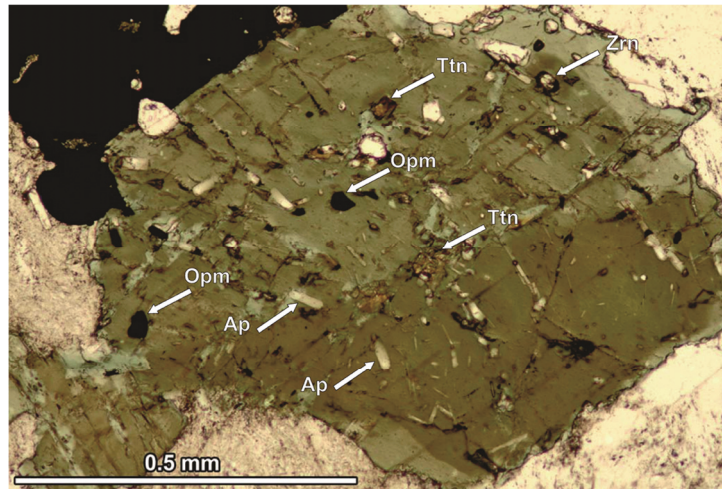


Fig. 14. Individual, euhedral amphibole crystal containing small inclusions of zircon (Zrn), apatite (Ap), titanite (Ttn) and opaque minerals (Opm) – pale grey host granites (sample no. KH1/7). Plain-polarized light.

Amphiboles

Amphibole occurs as minor component (up to 3vol%) in the rocks studied (Table 1). Similar modal content of amphiboles from the Dolina Będkowska valley granodiorite was described by Markiewicz (2006 vide Żelaźniewicz et al. 2008). In the samples studied, amphiboles commonly form aggregates/glomerocrysts of small diversely oriented clots (Fig. 15) and occasionally large (up to 3 mm in size) individual euhedral crystals (Fig. 14)

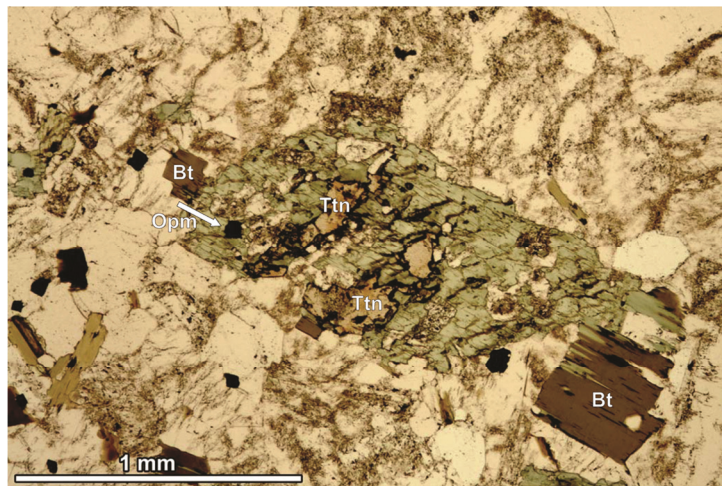


Fig. 15. Amphibole aggregate/glomerocryst containing titanite (Ttn) and opaque minerals (Opm) and overgrown by biotite (Bt) – pale grey host granite (sample no. KH3/5a). Plain-polarized light.

green, olive brown and pale bluish green in colour. It seems that individual amphibole crystals are detached clots that originated from aggregates or glomerocrysts. In the host granites studied, very rare amphibole megacrysts (acicular crystals 9 mm x 3 mm in size) also occur, showing irregular (sutured and corroded) boundaries – Fig. 16). They likely formed in the same way.

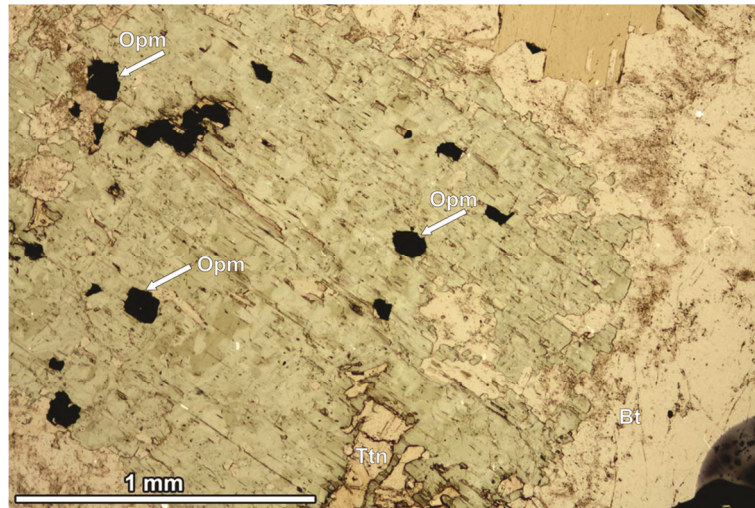


Fig. 16. Individual amphibole crystal with opaque minerals (Opm) and titanite (Ttn) inclusions showing irregular corroded boundaries – pale grey host granites (sample no. WB102A/1a). Plain-polarized light.

Amphibole crystals are altered to various degrees. The pseudomorphs after amphiboles commonly contain chlorite, titanite, epidote and opaque minerals. Sometimes, the biotitization process is overprinted on amphibole grains (Fig. 15). In the rocks studied, rare aggregates of amphibole, titanite, epidote and opaque minerals can be observed. They are probably the pseudomorphs after primary minerals: amphiboles or pyroxenes (?). Amphiboles show moderate to strong pleochroism from pale yellow (α) to pale bluish green/olive green (γ) colours, the angle $z/\gamma \sim 21^\circ$, showing simple twinning and inclusions of small, acicular apatite (needle-shaped crystals). The occurrence of only Mg-hornblende in the Dolina Będkowska valley granodiorite was described by Markiewicz (2006 vide Żelaźniewicz et al. 2008). The present study provides information that amphiboles are calcic in composition: $Ca_B \geq 1.50$, $Ca_A < 0.50$, $(Na + K) < 0.50$ – according to the classification of Leake et al. (1997). They are represented by two types of hornblendes, showing different #Mg numbers (Fig. 17 – the Leake et al. 1997 classification diagram). In general, two types of this mineral occur in different proportions both in the amphibole aggregates/glomerocrysts and in the individual crystals. The olive brown hornblende, rare in the granites studied, have low #Mg = 0.46-0.48 and higher admixture of TiO_2 (1.3-1.9wt%) and MnO (0.6-0.9 wt%). On the other hand, the pale green hornblende, which is common in the granites studied, shows a higher #Mg (0.51-0.62) number but is also lower in TiO_2 (0.1-0.4wt%) and MnO (0.4-0.6wt%) contents. In both hornblende varieties, the sum of Na

+ K (0.45-0.50 apfu) is similar. Also, the occurrence of amphibole crystals or clots showing a higher proportion of Na + K > 0.50 (up to 0.65 apfu.) – probably edenite/ferroedenite – was also noted. Unlike hornblendes, the secondary actinolite (#Mg = 0.50-0.69) is poorer in Al₂O₃, FeO and TiO₂ (0.0-0.4wt%) but has similar MnO content (0.4-0.8wt%) and the Na+K sum (0.45 apfu). The weak zonation in amphibole grains is only observed in individual crystals (Fig. 14), whilst in aggregates/glomerocrysts it is more complicated because of the occurrence of patches of secondary actinolite apparently irregularly scattered and overgrowing them.

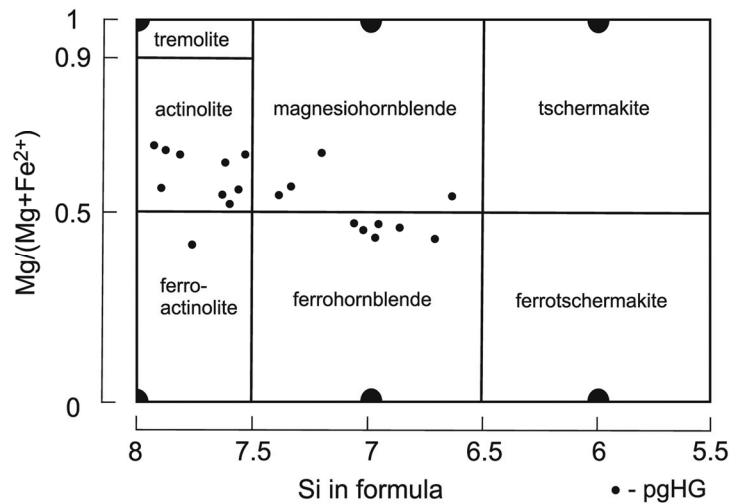


Fig. 17. Composition of amphiboles from host granites studied on the classification diagram (Leake et al. 1997). Symbol: pgHG - pale grey host granites.

In the contact host granites (cHG), amphibole crystals are lacking, but pseudomorphs after amphiboles filled with chlorite, titanite, epidote and opaque minerals are often observed.

Accessory minerals

Płoczyńska (2000) defined the accessory minerals composition (titanite, apatite, zircon, rutile, pyrrhoite and magnetite) in granitoids from the Malopolska Block (MB). On the other hand, the occurrence of zircon, apatite and titanite in the Dolina Będowska valley granodiorite was described by Markiewicz (2006 – vide Żelaźniewicz et al. 2008).

Accessory minerals in the samples studied (Table 1) are represented by opaque minerals (up to 3vol%), titanite (up to 2vol%) and epidote (< 1vol%). Opaque minerals (up to 3vol%) are mainly represented by pure magnetite, and rarely by magnetite grains with ilmenite intergrowths in individual amphibole crystals (Fig. 16). Titanite (up to 2vol%) commonly occurs in individual amphibole crystals (Fig. 15) and amphibole aggregates/glomerocrysts as well as in pseudomorphs after amphibole (or pyroxene?). On the other hand, epidote/zoisite (< 1vol%) and zircon and apatite are very rare in the host granites described. They form very small crystals (< 0.01 mm in size) and occur as

inclusions in amphibole crystals (Fig. 14) and biotite (Fig. 11). Zircon crystals show the admixture of Hf (1-2wt%). Zircon crystals from the Dolina Będkowska valley granodiorite are described in detail by Żelaźniewicz et al. (2008) as euhedral, short- and normal-prismatic forms with markedly visible oscillatory zoning which have moderate U and Th contents (Th/U ratio of 0.28-1.00). The occurrence of allanite in the Małopolska granites is described in the present monograph, for the first time. Allanite (< 1vol%) occurs sporadically in the contact host granites (Fig. 18), and in the host granites (pgHG) in which the enclaves of hornfels are observed.

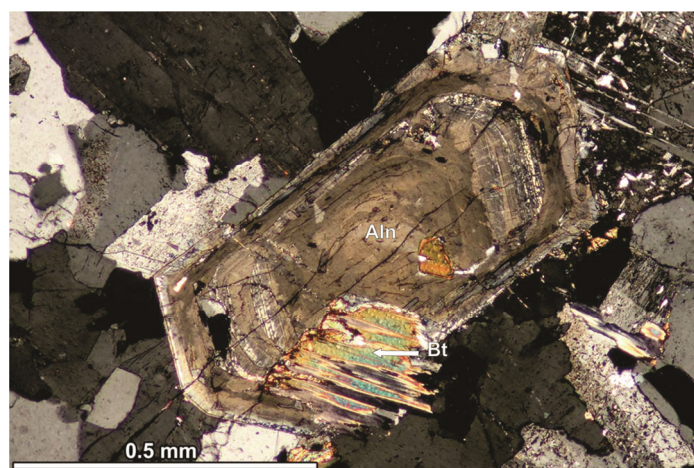


Fig. 18. Allanite zoned crystal with biotite (Bt) overgrowth – contact host granites (sample no. KH2/1). Crossed polars.

5.2. Petrography of mafic microgranular enclaves (MME)

For the first time, the occurrence of dark enclaves (to 15 cm in size and larger) is described in the pale grey host granites. Their shapes and character of the contact margins with the pale grey host granites are mostly sharp amoeboidal, semioval to oval (Fig. 19). The dark enclaves (MME) are mainly represented by two subtypes: dark grey (Fig. 20) and rarely by pale grey (Fig. 21). The localization of the MME samples in the boreholes is presented on Figure 22.

The MME studied have variable colour (from dark grey to pale grey) and massive texture, holocrystalline but with distinctly inequigranular structure. Thus, the size of rock-forming minerals is different and the rocks exhibit 'porphyritic' texture (according to Didier (1973) terminology). Relatively large crystals (phenocrysts or xenocrysts – 5-20 mm in size) are randomly embedded in the fine-grained groundmass which shows affinities to pseudo-doleritic textures. The MME exhibit variable contents of megacrysts (phenocrysts/xenocrysts) (2-23vol% – Table 2). Two subtypes of MME are distinguished based on their macroscopic features and general appearance of the samples – the different colour of the groundmass as well as the larger amount of quartz megacrysts/xenocrysts, and

especially the pink alkali feldspar megacrysts/xenocrysts compared to plagioclase megacrysts/xenocrysts (Table 2).

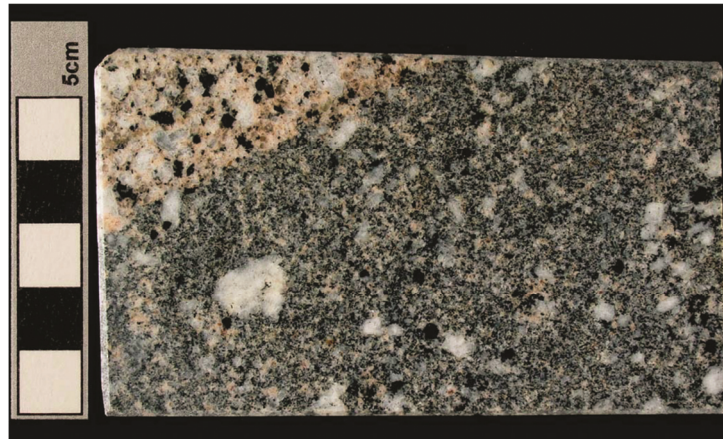


Fig. 19. Sharp contact margin of dark grey MME (right) with pale grey host granites (left). Both rock types show lower degree hydrothermal alteration (sample no. WB 102A/7).

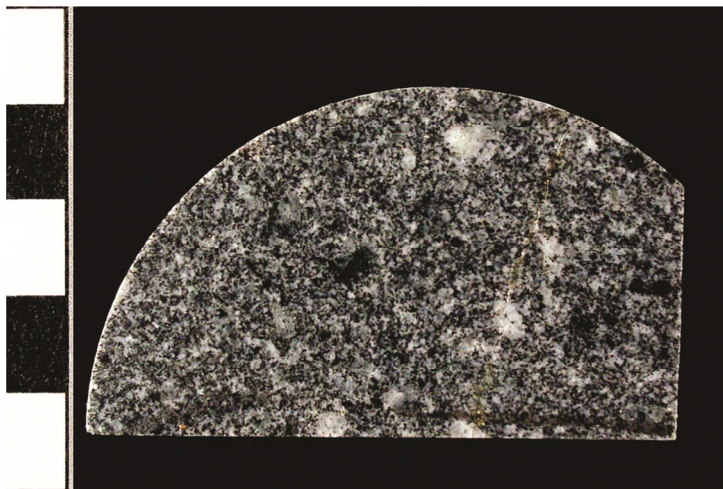


Fig. 20. Dark grey MME (sample no. KH1/10).

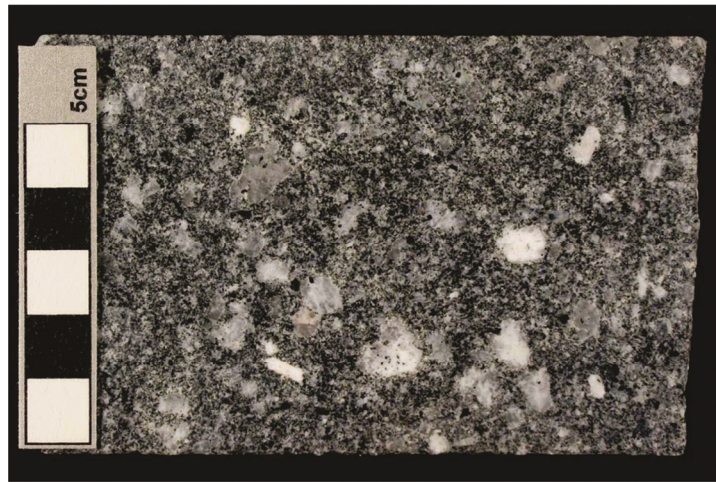


Fig. 21. Pale grey MME (sample no. KH3/2).

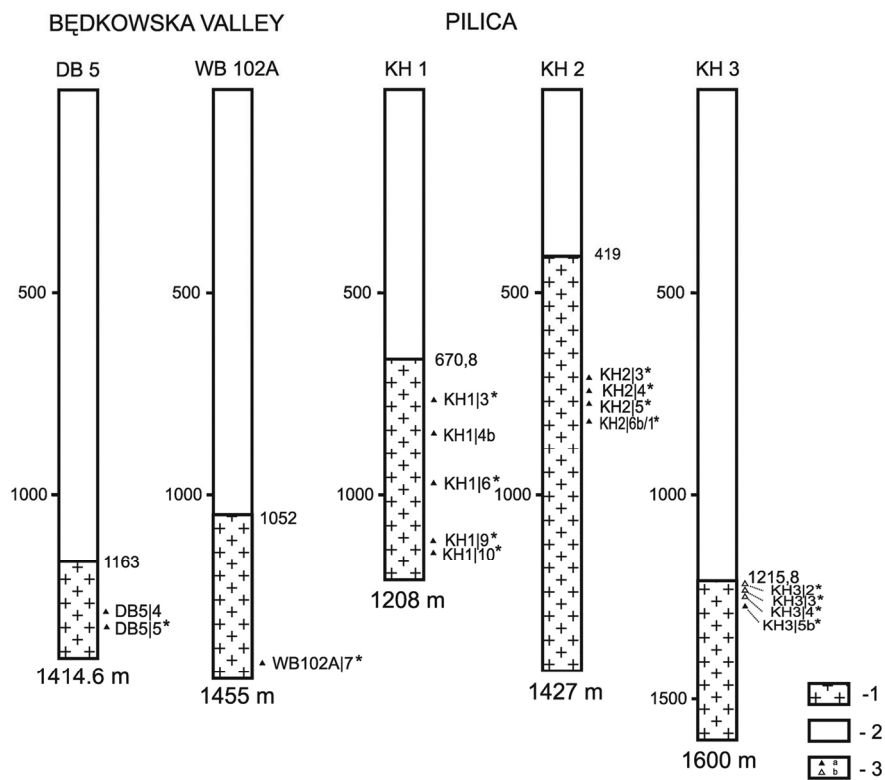


Fig. 22. Localization of the MME samples in the sections of the boreholes: Dolina Będkowska valley (DB5, WB102A) and Pilica (KH1, KH2, KH3) after Harańczyk (1984), Harańczyk et al. (1995). 1 – granites, 2 – other rocks, 3 – sampling sites (symbols of samples); a – dark grey MME samples; b – pale grey MME samples.

5.2.1. Modal composition of mafic microgranular enclaves (MME)

Both subtypes of MME, dark grey (dgMME) and pale grey (pgMME), consist of plagioclase, quartz, biotite, hornblende, K-feldspar and accessory minerals (opaque minerals, titanite, epidote/zoisite, apatite) in various proportions (Table 2). Chlorite, sericite and calcite are secondary minerals. Modal compositions of the MME are presented in Table 2.

On the IUGS classification diagram, the dark grey enclave (dgMME) samples plot in Q-diorite and tonalite fields (Fig. 23) because they have different Q and P modal contents. In Q-diorites, the Q and P modal contents vary from 14 to 20vol% and from 77 to 84vol%, respectively. On the other hand, the contents of these minerals in the tonalites are from 23 to 35vol% and from 61 to 75vol%, respectively. In the classification diagram of plutonic rocks (according to Le Maitre 1989), Q-diorites are generally characterized by the following amounts of modal minerals Q in the range 5-20vol%, the P' index ($100 \times P/(A+P)$) in the range 90-100% and the colour index ($M' > 20\text{vol}\%$). On the other hand, tonalites are characterized by the higher amount of the Q modal content (20-60vol%), the P' index (90-100) and the M' index ($> 10\text{vol}\%$). In the samples of dark grey (dgMME) enclaves studied, the M' index for tonalites ranges from 9 to 21vol% while this index for Q-diorites ranges from 13 to 28vol%. The samples of tonalites studied showing M' index below 10% are classified as leuco-tonalites. On the other hand, the samples of Q-diorites studied displaying the M' index of $< 20\%$ are leuco-Q-diorites.

All the samples of pale grey (pgMME) enclaves studied plot on the IUGS classification diagram in the tonalite field (Fig. 23). These rocks have lower P modal contents (57-69vol%) and the P' index (89-96%) but higher Q modal contents (28-38vol%). They are characterized by lower M' index (6-12vol%) and, according to the IUGS classification, represent leuco-tonalites as well as tonalites.

TABLE 2

Modal composition of mafic microgranular enclaves (MME).

Sample	KH1/3	KH1/4b	KH1/6	KH1/9	KH1/10	KH2/3	KH2/4	KH2/5	KH2/6b	KH3/5b	DB5/4	DB5/5	WB102A	KH3/2	KH3/3	KH3/4
	dark grey enclaves (dgMME)										pale grey enclaves (pgMME)					
plagioclase	0.0	4.2	22.7	14.7	6.2	2.5	1.8	4.0	5.7	3.2	6.4	2.5	3.8	7.4	11.1	8.1
megacrysts																
quartz megacrysts	0.0	3.2	0.0	0.0	0.0	0.0	0.5	2.5	1.5	0.6	0.4	1.0	0.6	3.7	1.5	3.0
plagioclases	48.3	52.2	46.0	48.0	51.2	52.5	60.6	54.2	51.8	54.0	54.7	56.5	56.6	57.5	44.4	44.3
quartz	27.8	23.3	17.6	21.8	22.0	16.4	9.9	15.9	12.3	18.3	21.4	28.5	14.7	22.2	24.9	31.4
hornblende	2.1	0.3	2.6	3.8	5.8	6.2	7.7	8.7	1.9	4.5	0.0	0.0	5.7	0.9	0.0	0.3
biotite	2.3	0.0	7.7	7.5	12.7	14.4	14.7	10.5	16.4	10.7	8.7	4.5	12.7	2.8	6.4	3.5
titanite	2.2	1.3	0.4	0.2	0.1	1.3	0.8	0.8	1.1	0.8	0.7	0.4	0.7	0.0	0.8	0.4
chlorite	10.8	11.3	1.0	0.8	0.1	2.6	0.8	0.4	0.6	3.0	2.4	2.2	0.2	0.9	2.0	2.8
K-feldspar	3.5	0.9	1.1	2.3	1.3	1.2	1.6	2.1	1.3	1.3	1.5	1.8	2.6	2.8	6.5	4.1
sercite	0.2	1.6	0.2	0.3	0.0	1.0	0.5	0.3	0.4	1.4	1.9	1.5	1.2	0.9	1.5	1.1
opaque minerals	1.7	1.2	0.6	0.3	0.5	2.0	0.5	0.7	6.4	1.3	2.0	0.4	0.9	0.9	0.6	0.5
apatite	0.0	0.0	0.0	0.1	0.1	0.0	0.6	0.0	0.7	0.0	0.0	0.0	0.3	0.0	0.2	0.0
epidote/zoisite	1.2	0.6	0.1	0.2	0.0	0.0	0.0	0.0	0.0	1.0	0.0	0.0	0.0	0.0	0.0	0.4
myrmekite	0.0	0.0	0.0	0.0	0.0	0.0	0.0	0.0	0.0	0.0	0.0	0.0	0.0	0.0	0.2	0.1
calcite	0.0	0.0	0.0	0.0	0.0	0.0	0.0	0.0	0.0	0.0	0.0	0.7	0.0	0.0	0.0	0.0
Total	100.1	100.1	100.0	100.0	100.0	100.1	100.0	100.1	100.0	100.1	100.1	100.0	100.0	100.0	100.1	100.0
P' index	93.2	98.4	98.4	96.4	97.8	97.8	98.1	96.4	97.7	97.7	97.3	96.9	95.8	95.7	89.4	92.6
M' index	20.5	16.3	12.6	13.2	19.3	27.5	25.9	21.4	27.4	22.8	15.7	9.0	21.7	6.4	11.5	9.0

P' index – 100xP/A+P (in%); M' index – the colour index

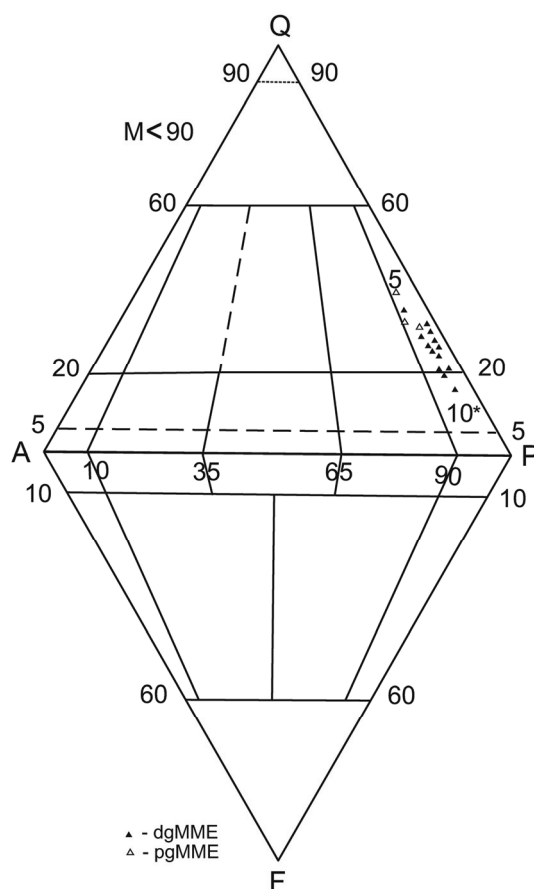


Fig. 23. Modal composition of MME studied on the IUGS classification diagram. Symbols: dgMME – dark grey MME, pg MME – pale grey MME; (5) – tonalite; (10*) – quartz diorite/quartz gabbro.

5.2.2. Mineral characteristics of mafic microgranular enclaves (MME)

Plagioclases

Plagioclases in dark grey MME (dgMME) occur both as megacrysts/xenocrysts (2-23vol%) and as small euhedral laths (61vol%) in the groundmass. In pale grey MME (pgMME), the amount of plagioclase megacrysts/xenocrysts varies from 7 to 11vol%, whereas in the groundmass the amount of plagioclase laths is up to 58vol% (Table 2). Heterogeneous mantled plagioclase megacrysts/xenocrysts are common in two subtypes of the MME studied. They occur locally as single larger megacrysts/xenocrysts (Fig. 24) and/or glomerocrysts. In the dark grey MME (dgMME) the plagioclase mantled megacrysts/xenocrysts exhibit multiple twinning (albite, pericline or rare Carlsbad law). These megacrysts/xenocrysts are represented by boxy cellular plagioclase containing 'old core' overgrown by several inner and outer zones. The resorption zone between 'old cores' and the rim is markedly visible. In the inner and outer zones, combinations of

discontinuous/continuous, oscillatory and convolute zoning of different widths can be seen (Fig. 24). Plagioclase megacrysts/xenocrysts are fresh but sometimes show some alteration in various degrees, thus the presence of secondary sericite and zoisite is observed. These megacrysts/xenocrysts exhibit inner textural features related to complex magma evolution.

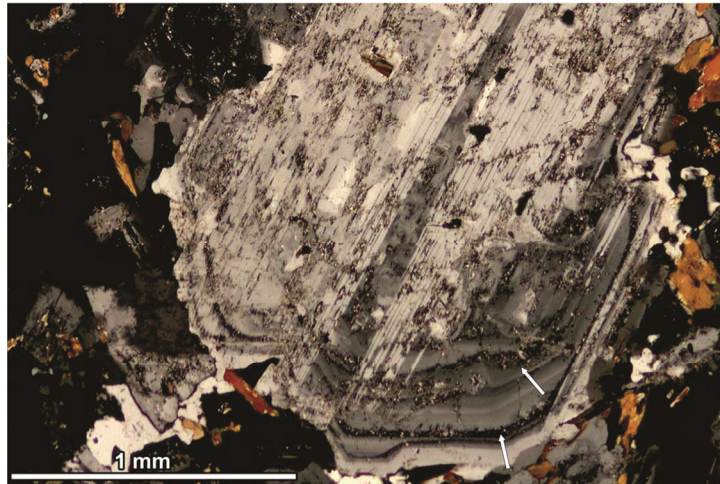


Fig. 24. Fragment of plagioclase megacryst containing ‘old core’ and overgrown by multiple zoning rims (arrows - resorption surface) – dark grey MME (sample no. KH2/5). Crossed polars.

The chemical composition of the plagioclase mantled megacrysts/xenocrysts range from labradorite (‘old core’) through andesine (inner rim) to oligoclase (outer rim). The megacryst/xenocryst cores showing labradorite composition ($Ab_{39-47} An_{60-51} Or_1$) are not homogenous and show a spike zone boundary and melting/regrowth? features. The veinlets and/or interlocking/interpenetrating K-feldspar perthite ($Or_{94} Ab_{9-6} An_{0.3}$) are commonly observed in the megacryst/xenocryst cores. They are mainly filled with inclusions of short prismatic amphiboles and opaque minerals (Fe-oxides, commonly magnetite). The inner rim consists of andesine ($Ab_{67-53} An_{46-31} Or_{2-1}$) and may even be composed of a few zones (up to 5) – Ab_{53} , Ab_{57} , Ab_{62} , Ab_{65} , Ab_{67} . While the oligoclase ($Ab_{71-81} An_{27-18} Or_{2-1}$) forming outer rims of the plagioclase mantled megacrysts/xenocrysts is always broad and consists of two or three zones ($Ab_{71}, Ab_{75}, Ab_{81}$) markedly visible (Fig. 24). The resorption zone between the inner and outer rim (Fig. 24) as well as numerous inclusions of biotite and quartz in the outer rim are commonly observed.

The mantled plagioclase megacrysts/xenocrysts in the pale grey MME (pgMME) exhibit similar composition and the inner textural characteristics. The composition of the plagioclases studied is presented in the Ab-An-Or diagram (Fig. 25a, b).

On the other hand, small plagioclase laths (0.2-0.4 mm in size) that form the groundmass of dark grey (dgMME) and pale grey (pgMME) enclaves show multiple twinning and simple continuous, convolute and oscillatory zoning (Fig. 26). Their cores are homogenous and show labradorite ($Ab_{39} An_{61-51} Or_1$) composition. The Ab content increases in laths from the inner to the outer rims – from the andesine ($Ab_{52} An_{47} Or_1$) to the oligoclase ($Ab_{78} An_{21} Or_2$) composition.

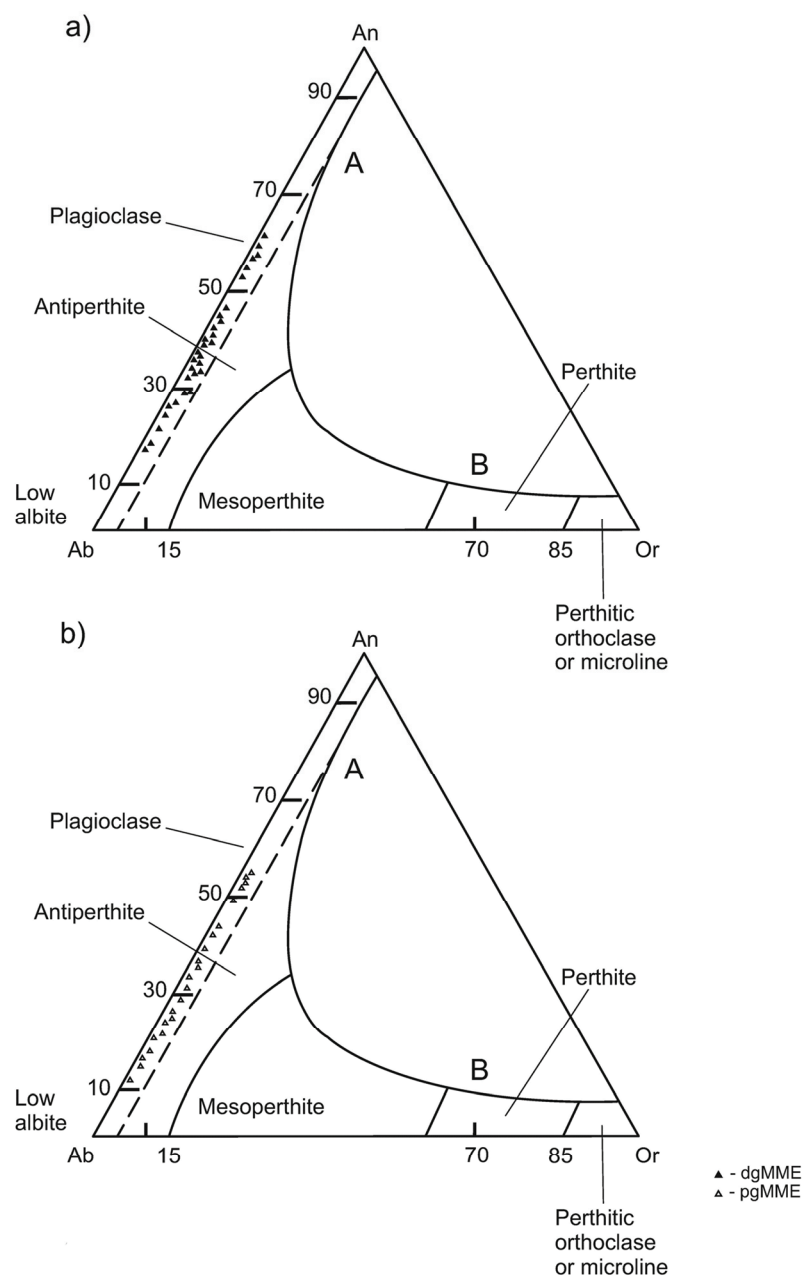


Fig. 25. Composition of plagioclases from MME studied on the Ab-An-Or classification diagram. a. – pale grey MME, b. – dark grey MME. Symbols: dgMME – dark grey MME, pg MME – pale grey MME.

Quartz

Quartz is unequally scattered in the fine-grained groundmass between plagioclase laths and occurs in variable amounts (Table 2), 29-10vol% in the dark grey MME (dgMME) samples and 31-22vol% in the pale grey MME (pgMME) samples (Fig 26). It forms small anhedral crystals that show no visible deformation or fragmentation. All crystals exhibit normal extinction. Small inclusions and veinlets of quartz are often observed in the plagioclase megacrysts/xenocrysts.

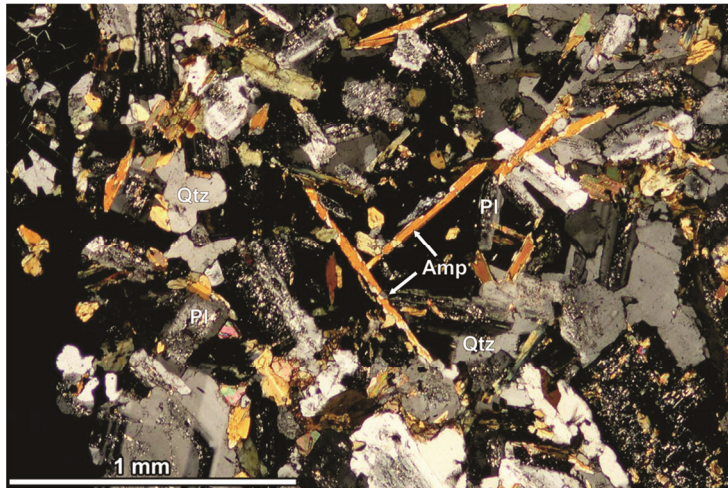


Fig. 26. Unevenly scattered quartz (Qtz) crystals between zoned plagioclase (Pl) laths and needle-shaped amphibole (Amp) crystals in the groundmass of dark grey MME (sample no. KH2/4). Crossed polars.

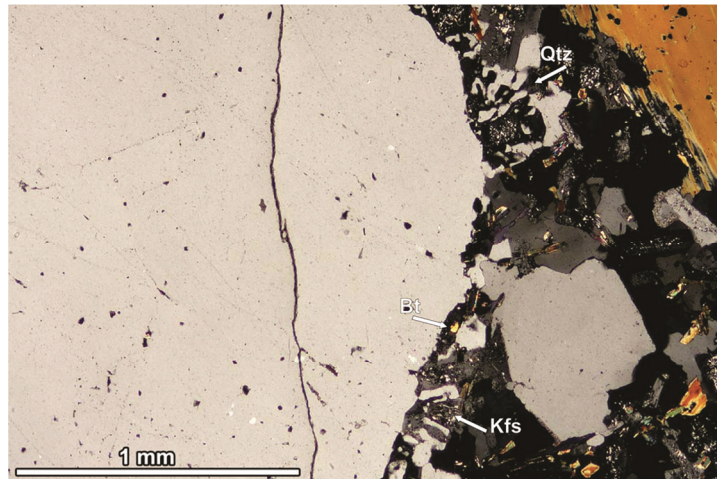


Fig. 27. Fragment of quartz megacryst/xenocryst ('ocelli') showing reaction rim (quartz-Qtz, biotite-Bt and feldspars-Kfs) at the contact with the fine-grained groundmass – pale grey MME (sample no. KH3/4). Crossed polars.

Moreover, quartz rarely forms very large megacrysts/xenocrysts (up to 5-6 mm in size). The amount of quartz in the rocks studied is up to 3vol% in the dark grey MME (dgMME) samples and up to 4vol% in the pale grey MME (pgMME) samples (Table 2). Strong undulose extinction and granulation of grain boundaries is observed.

Quartz crystals are usually broken into several subgrains, causing mortar/consertal texture. These megacrysts/xenocrysts are called ‘ocelli’ (Fig. 27) because they are of heterogeneous origin. They have characteristic reaction rims (coronas) and amoeboidal shape at the contact with the fine-grained matrix. These reaction rims (coronas) consist of a symplectite intergrowth of quartz, oligoclase ($\text{Ab}_{79-77} \text{An}_{23-16} \text{Or}_{2-4}$), K-feldspar ($\text{Or}_{89-87} \text{Ab}_{11-10} \text{An}_1$) and zoisite. They are surrounded by tangentially oriented biotite and plagioclase laths. In the outer rims of quartz ‘ocelli’, several biotite and amphibole inclusions are observed.

Amphiboles

Amphiboles (up to 9vol% – Table 2) form crystals of variable size (from 0.1 to 3 mm). Apart from aggregates/glomerocrysts of small crystals/clots showing lobate outlines, there are also subhedral, individual large crystals (Fig. 28). Moreover, needle-shaped crystals (Fig. 26) and small anhedral crystals occur in interstices between plagioclase laths. In pale grey MME (pgMME), amphibole aggregates/glomerocrysts and individual crystals are rare (up to 1vol%). In dark grey MME (dgMME), very large ‘relic’ crystals (up to 2-3 mm in grain size) are sometimes observed. They are columnar and/or acicular in shape, and their outer margins are corroded to various degrees (Fig. 29), even forming skeletal forms. Some large amphibole crystals and aggregates/glomerocrysts of small clots (Fig. 30) with considerable amounts of needle-shaped apatite and opaque mineral inclusions enclosed are common in the rocks studied. Moreover, pseudomorphs that are probably after higher temperature amphiboles or pyroxenes (of metamorphic origin) can be observed. Amphiboles apparently tend to form clots associated with biotite and titanite. They show strong pleochroism in various colours: from (α) dark yellow to (γ) olive brown through (α) pale yellow, (γ) green, (α) pale yellow to (γ) pale bluish green. The maximum extinction angle (z/γ) is 21-23°. In general, all amphiboles represent calcic group ($\text{Ca}_B \geq 1.50$, $\text{Ca}_A < 0.50$, $(\text{Na}+\text{K}) < 0.50$) according to the classification of Leake et al. (1997) but exhibit considerable compositional variation. Actinolite is poorer in Al_2O_3 and TiO_2 and richer in MgO. The #Mg number ranges from 0.52 to 69, while the TiO_2 and MnO contents vary from 0.0 to 0.4wt% and from 0.3 to 1.0wt%, respectively. The amount of Na+K is < 0.50 (up to 0.30 apfu). Moreover, very rare ferroactinolite (#Mg = 0.40-0.41) has a similar content of TiO_2 (0.02-0.2wt%) and MnO (0.5-1.0wt%) but a lower amount of Na + K (< 0.15 apfu).

In the dark grey MME (dgMME), Mg-hornblende (#Mg = 0.50-0.54) is commonly richer in MgO and has medium amounts of Al_2O_3 and TiO_2 (0.5-1.4wt%) and a higher proportion of Na+K (0.45 apfu). On the other hand, Fe-hornblende (#Mg = 0.41-0.49), rare in the rocks studied, is generally richer in Al_2O_3 and TiO_2 (0.8-1.8wt%) and poorer in SiO_2 and MgO, but has a similar content of MnO (0.7-1.0wt%) and the Na+K sum (0.48 apfu).

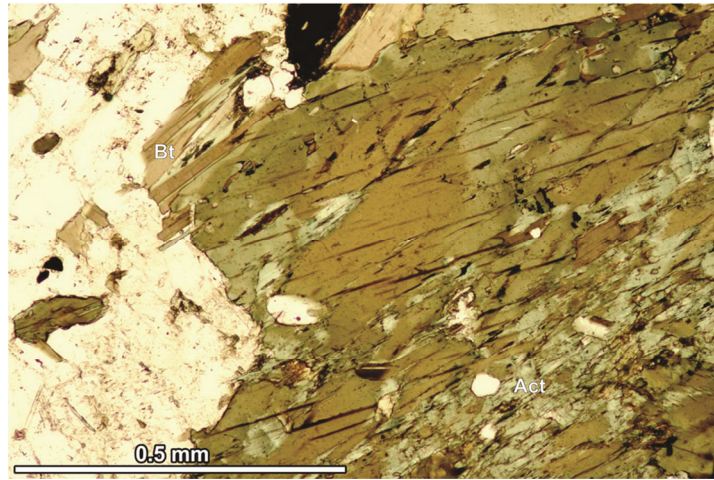


Fig. 28. Fragment of amphibole crystals filled by secondary actinolite (Act) and overgrown by biotite (Bt) – dark grey MME (sample no. KH2/4). Plain-polarized light.

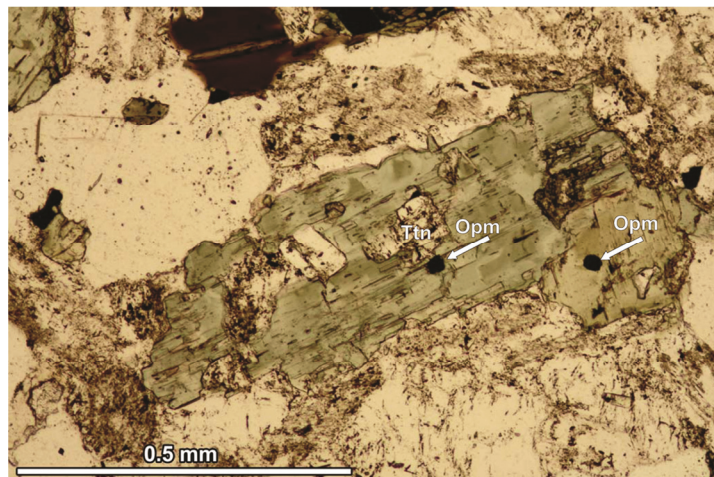


Fig. 29. Corroded columnar amphibole crystal containing inclusions of titanite (Ttn) and opaque minerals (Opm) – dark grey MME (sample no. KH3/5b). Plain-polarized light.

In the dark grey MME (dgMME), the occurrence of ferroedenite, characterized by the sum of Na+K > 0.50 (up to 0.65 apfu) is sporadically noted. The zonation in large amphibole crystals is difficult to observe. It is apparent that actinolite, and rarely ferroactinolite, are probably secondary minerals that formed during alteration processes of primary amphiboles. They occur within amphibole crystals as irregular scattered patchy-like forms, spots and veinlets. In the enclaves studied, the pseudomorphs after amphibole or pyroxene (?) filled by titanite, epidote, opaque minerals and chlorite, are noted.

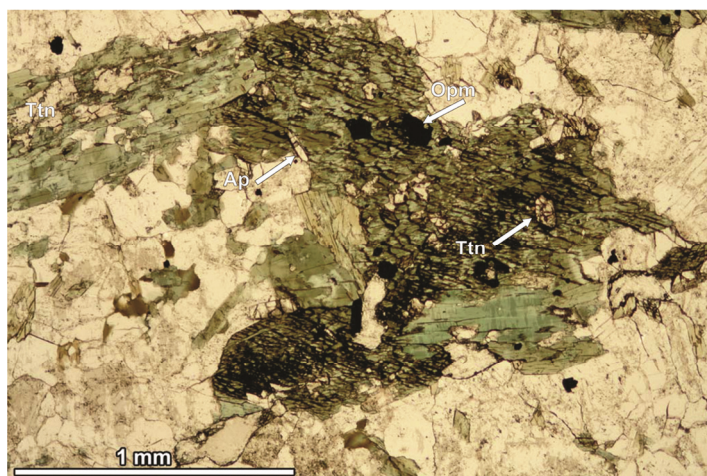


Fig. 30. Fragment of amphibole aggregates/glomerocrysts filled by apatite (Ap), titanite (Ttn) and opaque minerals (Opm) – dark grey MME (sample no. KH2/5). Plain-polarized light.

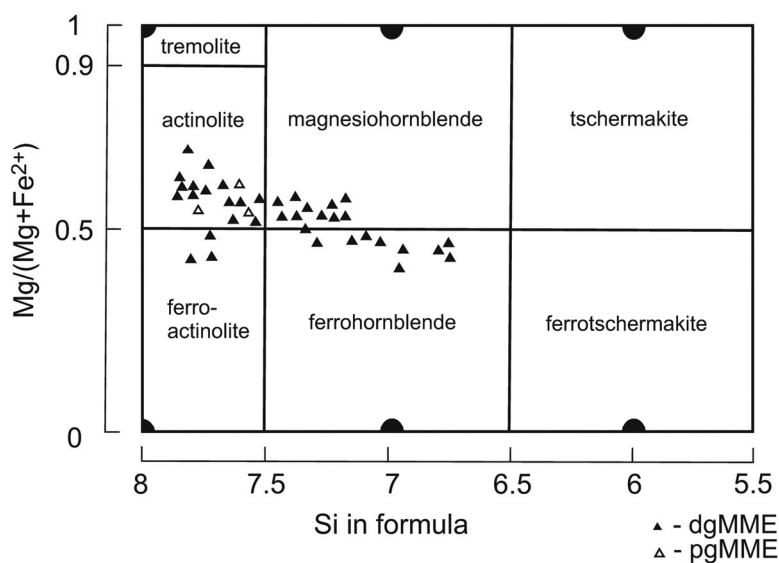


Fig. 31. Composition of amphiboles from MME studied on the classification diagram (Leake et al., 1997). Symbols: dgMME – dark grey MME; pgMME – pale grey MME.

In the pale grey MME (pgMME), amphibole crystals are rare (up to 1vol% – Table 2). They are generally represented by Mg-hornblende and secondary actinolite. Mg-hornblende and actinolite have a similar #Mg number (0.52-0.54). Actinolite is characterized by similar amounts of TiO_2 (0.8-1.4wt%), MnO (up to 1.0wt%) and the lower sum of Na + K (up to 0.25 apfu) as actinolites from the dark grey variety of MME. Furthermore, Mg-hornblende has a similar composition to the minerals in dark grey MME (dgMME). The compositional variation of the amphibole studied is presented on the classification diagram (Fig. 31). The

similar chemical composition of amphibole clots from aggregates/glomerocrysts, as well as individual crystals, in both MME subtypes suggests their similar origin. Individual amphibole crystals probably represent detached large fragments from amphibole aggregates/glomerocrysts.

Biotite

The amount of biotite (Table 2) varies from 16 to 2vol% in the samples of dark grey MME (dgMME) and from 6 to 3vol% in the pale grey MME (pgMME) (Table 2). Biotite forms large platy crystals (0.2-0.3 mm in size). It is often overgrowing large amphibole crystals (Fig. 28) and forms lobate flakes in amphibole crystals. Biotite exhibits strong pleochroism in colours from (α) pale straw yellow to (γ) dark reddish brown and is often, to various degrees, altered to chlorite. The #Mg number ranges from 0.36 to 0.52, and the TiO₂ content (2.9-4.3wt%) is higher but the MnO content (0.3-0.6wt%) is medium. It is characterized by high Al^{IV} and Fe_{tot.} contents ranging between 2.1-2.3 apfu and 2.4-2.5 apfu, respectively. Thus, the composition of biotite exhibits the predominance of the annite end member in the annite-phlogopite series (Fig. 32). In the rocks studied, the pseudomorphs after biotite, filled with chlorites and opaque minerals, are often observed. Biotite forms relatively small inclusions in the megacrysts/xenocrysts of plagioclase and quartz.

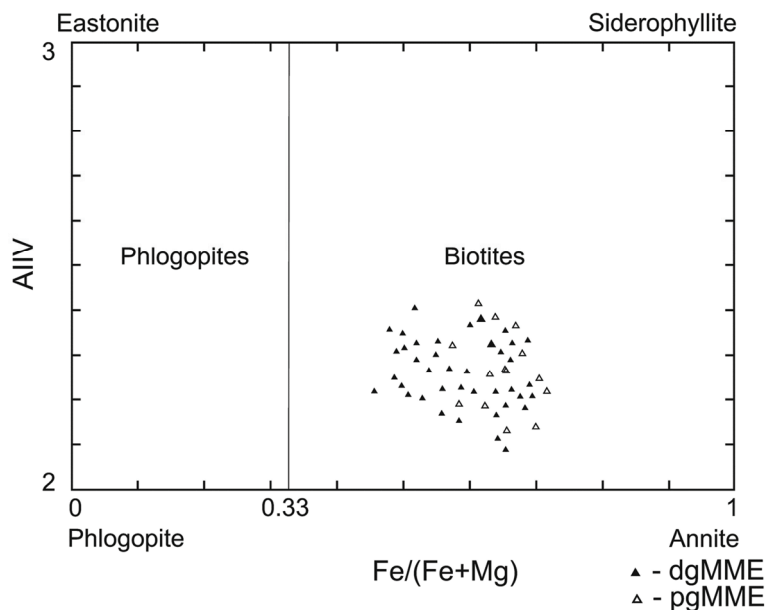


Fig. 32. Composition of biotites from MME studied on the Fe/(Fe + Mg) vs Al^{IV} diagram. Symbols: dgMME – dark grey MME; pgMME - pale grey MME.

Alkali feldspars

These minerals are rare in the studied rocks (Table 2). Their contents in two of the subtypes of MME amount to 3-1vol% in dark grey (dgMME) and 7-3vol% in pale grey

(pgMME). Small anhedral crystals of alkali feldspar (perthitic orthoclase: $\text{Or}_{95-94} \text{Ab}_{6-5} \text{An}_{0.3}$) are unequally distributed in the matrix, mainly in the interstices between plagioclase laths. These minerals are also present in the plagioclase boxy cellular megacrysts/xenocrysts that form inclusions, poikilitic intergrowths and irregular veinlets, interlocking/interpenetrating perthite in their ‘old cores’.

On the other hand, in the pale grey (pgMME) enclaves, rare megacrysts/xenocrysts (up to 5 mm in size) of alkali feldspar ($\text{Or}_{89-88} \text{Ab}_{11-10} \text{An}_1$) with broad reaction rims (myrmekite-like) are observed (Fig. 33). The reaction rims (coronas), at the boundary with the plagioclase laths, consist of symplectite intergrowths of andesine ($\text{Ab}_{69} \text{An}_{29} \text{Or}_1$) and oligoclase ($\text{Ab}_{79} \text{An}_{20} \text{Or}_2$).

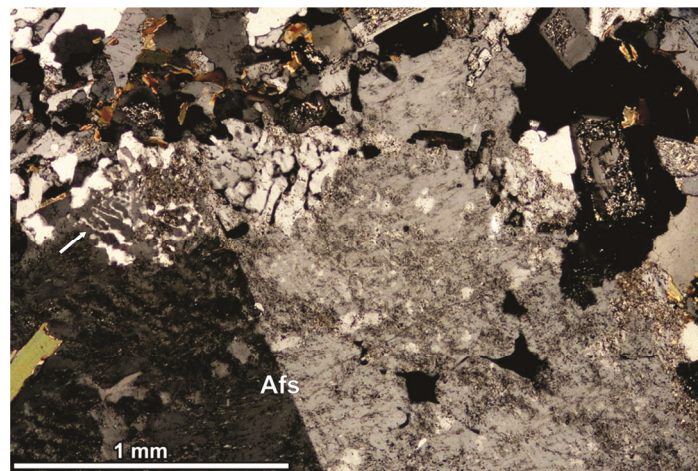


Fig. 33. Fragment of alkali feldspar megacryst/xenocryst with reaction rim (arrow) at the contact with the groundmass – pale grey MME (sample no. KH3/3). Crossed polars.

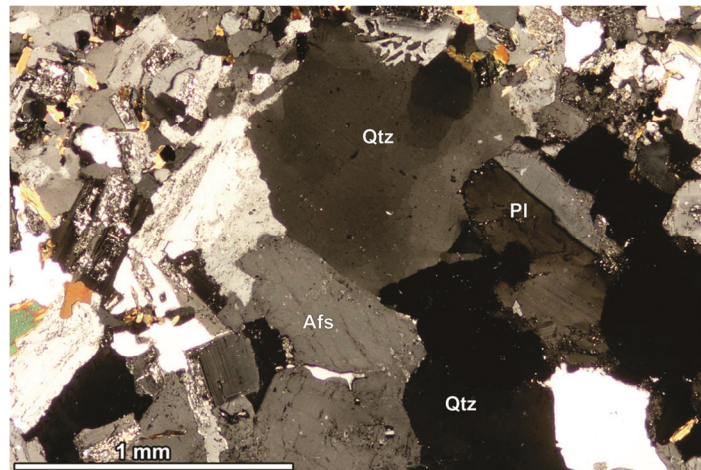


Fig. 34. Fragment of a granitic clast (probably host granites containing quartz-Qtz, alkali feldspar-Afs and plagioclase-Pl crystals) – pale grey MME (sample no. KH3/2). Crossed polars.

Moreover, a few enclaves composed of quartz and feldspar (Fig. 34) are sporadically observed in the rocks studied. They are relics of igneous rocks and probably originated from the host granites (HG).

Accessory minerals

Apatite (up to 1vol%) is a common accessory mineral, occurring in long prismatic crystals in the matrix of the rocks studied (Fig. 35). Frequently, acicular (needle-shaped) apatite crystals occur in individual amphibole crystals (Fig. 28) and in amphibole aggregates/glomerocrysts (Fig. 30) as well as in boxy cellular plagioclase megacrysts/xenocrysts, mostly in their ‘old cores’.

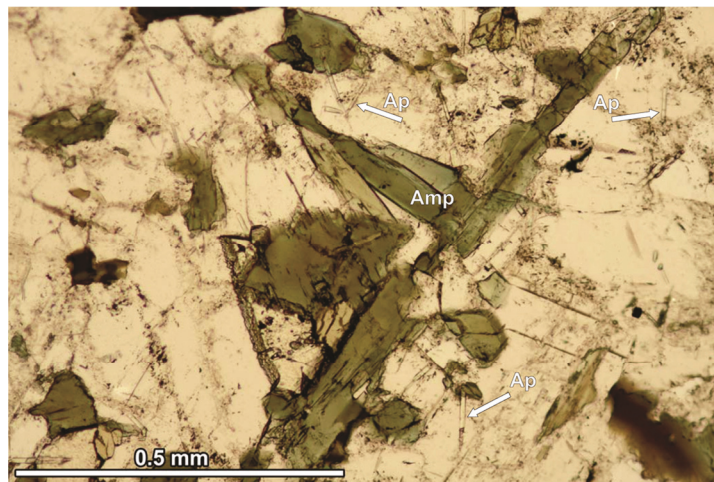


Fig. 35. Acicular-shaped apatite (Ap) crystals in the groundmass – dark grey MME (sample no. KH2/3). Plain-polarized light.

Small zircon crystals are enclosed within larger individual amphibole crystals, the amphibole aggregates/glomerocrysts and the biotite plates. Zircon crystals are euhedral and show short-prismatic morphology with commonly visible oscillatory zoning. This mineral exhibits the admixture of Hf (up to 1.7wt%) and trace amounts of U and Th.

Moreover, epidote/zoisite (up to 1vol%) sometimes occurs in altered ‘old cores’ of plagioclase megacrysts/xenocrysts and is rarely noted in pseudomorphs after amphiboles. Titanite occurs in individual amphibole crystals (Fig. 29) and amphibole aggregates/glomerocrysts (Fig. 30), as well as in pseudomorphs after amphibole or pyroxene (?).

Opaque minerals (up to 6vol%) are commonly represented by magnetite, and rarely by ilmenite. They occur as inclusions in large individual amphibole crystals (Fig. 28), amphibole aggregates/glomerocrysts/clots (Fig. 30) and in biotite plates.

Secondary calcite (up to 2vol%) forms veinlets and patches in plagioclase megacrysts/xenocrysts. In central or marginal parts of altered plagioclase megacrysts/xenocrysts, small flakes of secondary sericite are observed.

5.3. Geochemistry of pale grey host granites (HG)

In granitoid intrusions from the Małopolska Block (MB), zones of hydrothermal alteration connected with Cu-Mo porphyry type deposits mineralization were commonly described (see Chapter 3: Magmatic rock investigations). The host granite samples provided for analysis were carefully selected by eliminating the samples showing distinct effects of hydrothermal alteration. For geochemical investigations, only a few samples were assigned which have pale grey colouration, sometimes (rare) with a pale pinkish shade. The content of major and trace elements in the whole-rock samples is presented in Table 3.

TABLE 3

Chemical composition of pale grey host granites (HG).

Sample	KH1/2	KH2/2	KH2/6a/1	KH2/6a/2	KH3/6	KH3/5a	DB5/1	DB5/2	DB5/6	WB/102A/2	WB102A/6	WB102A/7	WB 115/1	KH1/1	KH2/1	KH3/1
pale grey host granites (pgHG)														contact host granites (cHG)		
wt%																
SiO ₂	68.66	70.37	69.10	69.45	67.55	68.39	69.62	68.47	67.11	70.26	67.88	68.80	69.38	70.96	75.88	75.50
TiO ₂	0.56	0.55	0.59	0.59	0.55	0.59	0.51	0.55	0.76	0.49	0.54	0.54	0.57	0.49	0.13	0.27
Al ₂ O ₃	15.14	13.64	14.14	14.11	15.81	15.18	14.40	15.52	15.17	15.13	16.08	15.60	14.37	14.81	12.81	13.20
Fe ₂ O ₃ *	3.45	3.28	3.50	3.57	3.25	3.37	2.94	3.36	4.16	2.34	3.00	3.27	3.45	2.04	0.58	0.66
MnO	0.08	0.06	0.08	0.08	0.04	0.04	0.05	0.05	0.07	0.04	0.03	0.04	0.05	0.05	0.01	0.02
MgO	1.24	1.11	1.34	1.34	1.30	1.28	1.05	1.26	1.71	1.10	1.20	1.19	1.42	1.01	0.23	0.54
CaO	2.57	2.41	2.44	2.46	3.16	2.98	3.13	3.17	2.82	2.54	3.25	3.49	2.31	1.96	0.78	0.79
Na ₂ O	3.31	2.95	3.09	3.04	3.93	3.87	3.86	4.04	3.93	3.69	4.33	4.14	3.16	3.11	2.05	3.60
K ₂ O	3.97	4.33	4.51	4.53	3.38	3.67	2.65	2.97	3.24	3.30	3.00	2.73	4.27	4.47	6.78	4.60
P ₂ O ₅	0.12	0.11	0.13	0.14	0.12	0.11	0.10	0.11	0.13	0.11	0.11	0.13	0.13	0.13	0.05	0.06
C _{tot.}	0.07	0.06	0.06	0.07	0.07	0.07	0.06	0.07	0.10	0.08	0.05	0.05	0.05	0.07	0.10	0.06
S _{tot.}	0.32	0.40	0.69	0.73	0.61	0.01	0.01	0.01	0.01	0.21	0.07	0.01	0.32	0.32	0.08	0.04
LOI	1.32	1.10	1.00	0.60	0.80	0.40	1.60	0.40	0.80	0.90	0.20	0.45	0.80	0.90	0.20	0.70
Total	100.42	99.91	99.92	99.91	99.89	99.88	99.92	90.90	99.90	99.90	99.80	100.46	99.91	99.92	99.50	99.94
ppm																
Ba	708.0	664.3	657.3	641.5	810.4	833.9	764.4	729.7	822.1	680.1	718.8	734.0	745.2	656.3	587.4	686.4
Cs	6.0	3.9	4.6	4.4	3.8	3.1	3.2	3.0	3.4	4.8	2.2	2.6	5.4	7.0	2.1	5.3
Ga	19.0	16.0	15.6	15.5	18.9	16.5	19.1	18.6	16.7	16.5	17.4	19.0	17.6	14.4	10.8	11.1
Hf	3.4	4.0	4.5	5.0	4.6	4.1	3.8	4.6	4.1	3.6	3.5	3.2	5.3	3.3	2.2	4.3
Nb	13.0	16.7	15.9	15.7	8.7	11.5	10.4	10.4	11.8	9.4	9.4	10.0	13.5	10.7	4.4	14.6
Rb	141.0	119.8	139.2	141.4	111.1	109.6	103.3	101.8	101.8	105.6	91.1	93.0	136.3	136.1	136.8	154.2
Sc	6.9	7.0	10.0	10.0	7.0	7.0	7.0	7.0	9.0	7.0	7.0	7.6	9.0	7.0	2.0	6.0
Sr	314.0	244.2	312.2	318.6	449.0	392.2	462.7	419.3	373.7	366.0	441.6	400.0	298.1	248.1	265.8	171.9
Ta	1.0	1.3	1.4	1.3	0.7	0.9	0.7	0.7	0.7	0.5	0.7	0.9	1.1	0.5	0.6	1.3
Th	8.8	14.0	14.8	10.8	12.5	12.2	8.9	15.3	8.1	10.6	6.7	7.0	12.2	12.7	5.7	17.5

cont. TAB. 3

U	2.2	4.4	3.7	3.8	2.7	3.3	3.3	4.2	2.5	2.4	2.8	1.9	4.2	2.8	2.7	5.3
V	54.0	71.0	63.0	65.0	64.0	67.0	65.0	61.0	77.0	45.0	58.0	60.0	67.0	52.0	12.0	25.0
Zr	153.0	154.1	163.8	185.1	150.2	150.1	146.1	154.7	147.8	129.9	123.9	136.0	186.3	134.6	68.6	133.4
Co	8.0	6.8	8.3	7.3	5.6	6.1	7.5	8.0	10.0	9.0	7.5	8.0	7.0	3.6	1.3	1.8
Cr	10.0	20.0	20.0	20.0	20.0	20.0	10.0	20.0	30.0	20.0	10.0	5.0	30.0	20.0	10.0	20.0
Ni	3.0	2.9	4.5	4.7	4.9	4.7	4.6	4.8	7.2	5.0	4.2	3.0	4.7	6.2	1.1	3.7
Cu	51.0	155.0	13.9	14.7	22.1	4.3	5.4	5.6	6.0	2.4	3.6	9.0	66.6	45.7	8.9	2.2
Mo	<5	0.1	0.1	<0.1	0.3	0.1	0.1	0.1	0.1	0.1	0.4	<5	0.1	0.3	0.8	275.5
Pb	24.0	16.1	18.9	19.5	3.6	3.3	3.2	3.6	2.5	6.4	2.6	9.0	9.5	7.8	6.9	12.3
Zn	79.0	93.0	31.0	32.0	24.0	18.0	22.0	29.0	34.0	30.0	56.0	33.0	44.0	38.0	17.0	18.0
Y	22.0	24.7	25.5	26.0	13.8	19.2	16.5	16.3	17.2	16.3	12.6	16.0	21.7	18.8	6.4	38.8
La	31.6	38.0	26.4	28.2	37.9	27.3	25.8	28.6	22.5	18.0	19.3	37.4	26.8	18.3	7.8	28.5
Ce	48.0	75.3	56.7	60.6	70.8	56.8	52.9	56.2	48.3	37.0	43.4	51.1	56.8	39.7	15.2	63.1
Pr	n.d.	8.75	6.70	7.39	7.46	6.65	6.06	6.27	5.88	4.21	4.98	n.d.	6.51	4.86	1.66	7.84
Nd	17.0	29.3	24.2	26.4	23.6	23.9	20.8	21.6	21.7	14.4	18.0	16.0	22.8	16.9	6.7	27.1
Sm	4.30	5.39	4.84	5.00	2.35	4.51	3.65	3.83	4.17	2.86	2.89	3.80	4.13	3.63	1.19	5.95
Eu	1.00	1.10	0.96	0.98	0.88	0.92	0.98	0.90	0.85	0.69	0.84	1.00	0.84	0.77	1.07	0.83
Gd	n.d.	4.37	4.58	4.51	2.70	3.69	3.32	2.92	3.51	2.61	2.28	n.d.	3.75	3.46	1.15	5.36
Tb	0.50	0.86	0.85	0.92	0.52	0.66	0.62	0.53	0.64	0.52	0.47	0.50	0.67	0.62	0.20	1.14
Dy	n.d.	3.99	4.24	4.37	2.33	3.18	2.69	2.51	3.05	2.75	2.02	n.d.	3.33	3.21	1.04	5.94
Ho	n.d.	0.84	0.85	0.86	0.45	0.64	0.55	0.51	0.58	0.50	0.45	n.d.	0.70	0.67	0.22	1.19
Er	n.d.	2.32	2.27	2.23	1.21	1.67	1.47	1.43	1.50	1.39	1.16	n.d.	1.85	1.81	0.55	3.43
Tm	n.d.	0.59	0.42	0.38	0.20	0.27	0.25	0.23	0.24	0.24	0.22	n.d.	0.29	0.29	0.13	0.62
Yb	2.60	2.38	2.30	2.33	1.24	1.68	1.42	1.45	1.36	1.40	1.13	1.60	1.81	1.60	0.63	5.48
Lu	0.40	0.39	0.37	0.39	0.20	0.27	0.25	0.23	0.23	0.21	0.18	0.24	0.32	0.27	0.14	0.58

n.d. – not determined

5.3.1. Major element geochemistry of pale grey host granites (HG)

The pale grey host granites (pgHG) and the contact host granites (cHG) show some marked similarities and differences in the content of major and trace elements (Table 3).

In the pale grey host granites studied (pgHG), the amount of SiO₂ is especially high and varies from 67.1 to 70.4wt%. Słaby et al. (2010) mentioned that granitoids from the Małopolska Block show a relatively narrow range of SiO₂ content (64.9-78.9wt%). On the other hand, the amount of Al₂O₃, in the granites studied is moderate and varies from 13.6 to 16.1wt%. The pale grey host granite (pgHG) samples display low Fe₂O₃ and MgO contents ranging from 2.3 to 4.2wt% and from 1.1 to 1.7wt%, respectively.

The abundance of CaO and alkalis (Na₂O and K₂O) varies from 2.4 to 3.5wt%, from 3.0 to 4.3wt% and from 2.7 to 4.5wt%, respectively. Finally, the amount of TiO₂, MnO and P₂O₅ ranges from 0.5 to 0.8wt%, from 0.03 to 0.08wt% and from 0.10 to 0.14wt%, respectively.

As is shown in Table 3, the content of LOI (0.2-1.6wt%) and S (0.01-0.7wt%), in the samples of the pale grey host granites (pgHG), is very low. It is suggested that the samples

studied display a low degree of hydrothermal alteration and ore mineralization. Therefore, some of them show the following contents of Cu (up to 155.0 ppm), Mo (up to 275.5 ppm), Zn (up to 93 ppm) and Pb (up to 24.0 ppm).

The samples of the host granites from contact with host sedimentary rocks (cHG) are distinctly enriched in SiO_2 (71.0-75.9wt%) and K_2O (4.5-6.8wt%), and depleted in Al_2O_3 (12.8-14.8wt%), Fe_2O_3 (0.6-2.0wt%), MgO (0.2-1.0wt%), CaO (0.8-2.0wt%), Na_2O (2.1-3.6wt%) and TiO_2 (0.1-0.5wt%), compared to the pale grey host granites (pgHG) from inner part of the pluton.

The amounts of MnO and P_2O_5 (0.01-0.05wt% and 0.05-0.13wt%, respectively) is the same as in the pale grey host granite samples. The contents of LOI (0.2-0.9wt%) and S (0.04-0.3wt%) show that these samples exhibit a low degree of assimilation and hydrothermal alteration.

The plots of major elements in the Harker diagram (Fig. 36) show negative correlation for Fe_2O_3 , TiO_2 , MgO , MnO , P_2O_5 , CaO , Na_2O with SiO_2 , and positive correlation for K_2O . These variations and continuous trends on the Harker diagrams apparently indicate that during fractional crystallization of the host granites studied, the precipitation of Mg-Fe silicates (hornblende and biotite), plagioclases and opaque minerals played an important role. The variable correlation and the increasing trend of K_2O vs SiO_2 is connected with a small effect of hydrothermal alteration which is only observed in the pale pinkish samples studied.

5.3.2. Trace element geochemistry of pale grey host granites (HG)

Pale grey host granites (pgHG) are characterized by a high content of Ba (833.9-641.5 ppm) and Sr (462.7-244.2 ppm), and low Rb content (141.4-91.1 ppm). Moreover, the amount of LIL elements (especially Cs) and HFS elements (Nb, Ta, Zr) is not high – 6.0-2.2 ppm, 16.7-8.7 ppm, 1.4-0.5 ppm and 186.3-123.9 ppm, respectively. On the other hand, transition elements display rather high contents: Ni (7.2-2.9 ppm), Co (10.0-5.6 ppm), Cr (30-5 ppm) and V (77-45 ppm).

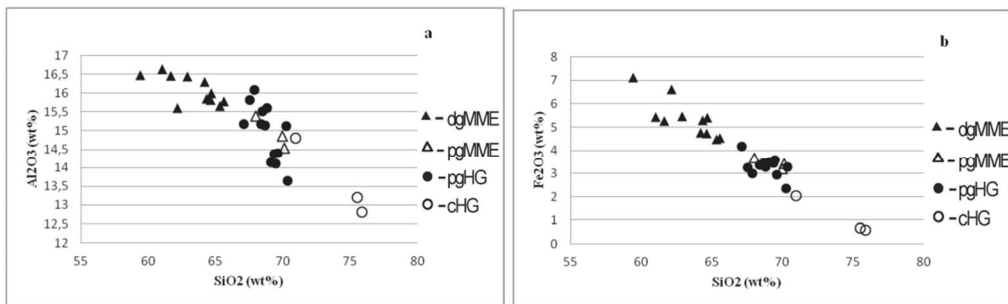


Fig. 36a-b. Harker diagrams for major oxide correlations of the studied granite samples. Symbols: dgMME – dark grey MME; pgMME – pale grey MME; pgHG – pale grey host granites; cHG – contact host granites.

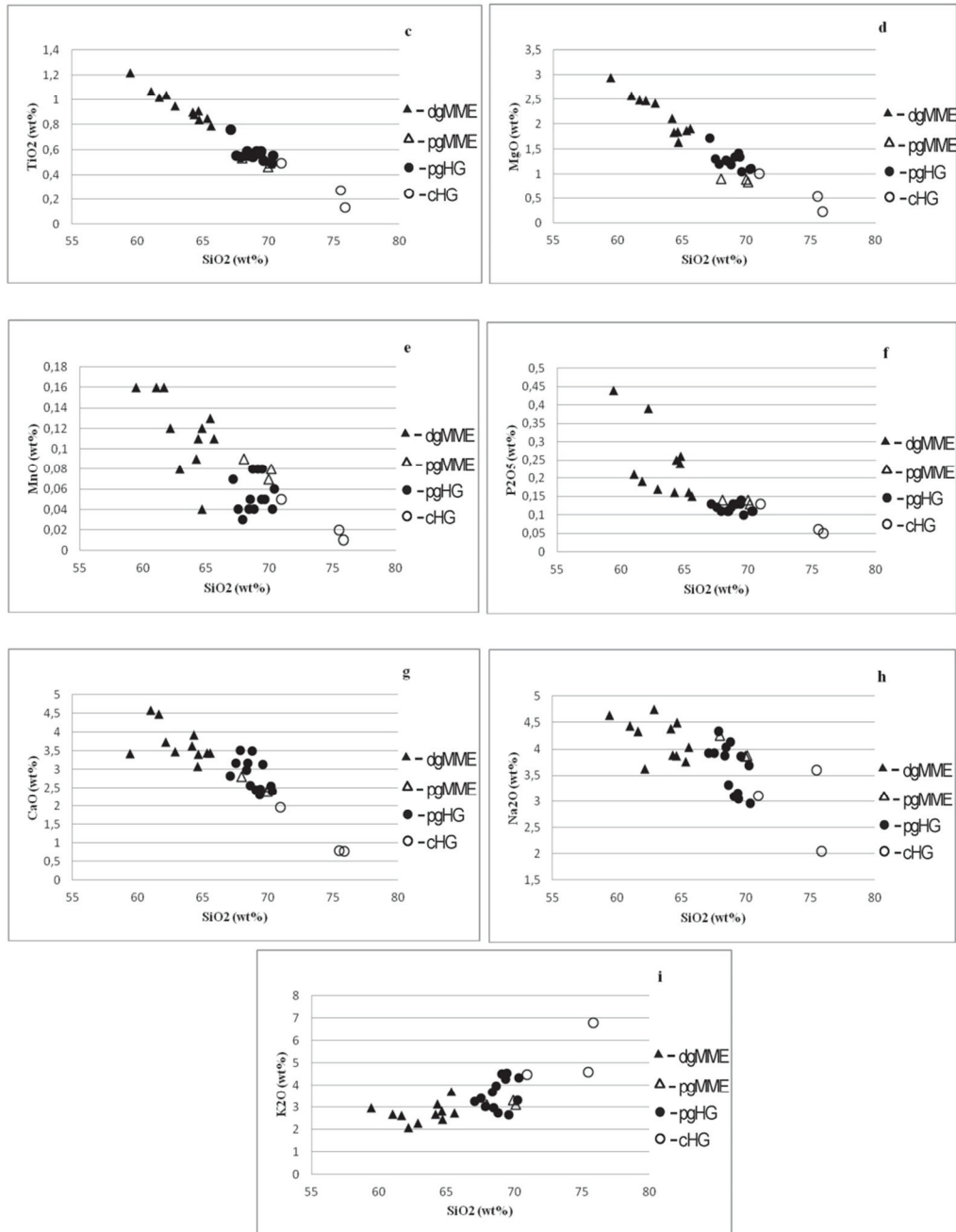


Fig. 36c-i. Harker diagrams for major oxide correlations of the studied granite samples. Symbols: dgMME – dark grey MME; pgMME – pale grey MME; pgHG – pale grey host granites; cHG – contact host granites.

On the contrary, the samples of contact host granites (cHG) are enriched in Rb (154.2-136.1 ppm) and depleted both in LIL elements: Ba (686.4-587.4 ppm), Sr (265.8-171.9 ppm), and transition elements Ni (6.2-1.1 ppm), Co (3.6-1.3 ppm), Cr (20-5 ppm) and V (52-12 ppm), compared to the pale grey host granites (pgHG). Nevertheless, it is noted that the content of Cs is a similar (7.0-2.1 ppm) and HFSEs show some depletion in Nb (14.6-4.4 ppm), Ta (1.3-0.5 ppm), Zr (134.6-68.6 ppm) compared to the former granites.

As shown on bivariate plots (Fig. 37), no simple correlation between these elements (LILE, HFSE and transition elements – mentioned above) and silica is observed.

5.3.3. Normative composition of pale grey host granites (HG)

The normative composition of the host granites studied, recalculated according to the Barth method (1962), is presented in Table 4. The majority of samples of the pale grey host granites (pgHG) contain normative diopside (*di* up to 1%), while in only a few samples, instead of normative *di*, a small amount of normative corundum (*C* up to 1%) is noted. On the other hand, the contact host granite samples (cHG) are characterized by a high amount of normative *C* (1-2%) and a lack of samples with normative diopside (*di*). The amount of normative hypersthene (*hy*) is variable and ranges from 10 to 6% (in the pale grey host granites) to 5-1% (in the contact host granites).

At any rate, according to the classification based on normative composition, the host granites studied show different names in the following petrochemical diagrams. In the Q'-ANOR diagram (Fig. 38) the pale grey host granite samples (pgHG) plot in the granodiorite or monzonite (monzogranite) fields, whilst the contact host granites (cHG) plot not only in the monzonite (monzogranite) fields but also in the granite fields.

The position of host granites in the IUGS diagram is as follows: the pale grey host granite samples (pgHG) plot in the granodiorite field, whereas the contact host granite samples (cHG) plot in the granite field (Fig. 39).

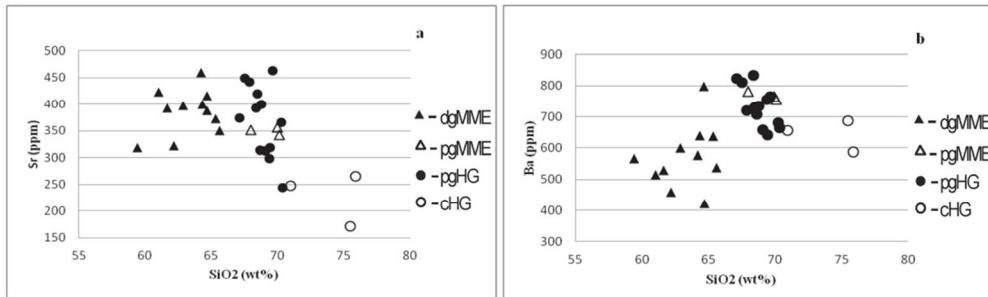


Fig. 37a-b. Chemical variation diagrams for trace element correlations of the granites studied. Symbols: dgMME – dark grey MME; pgMME – pale grey MME; pgHG – pale grey host granites; cHG – contact host granites.

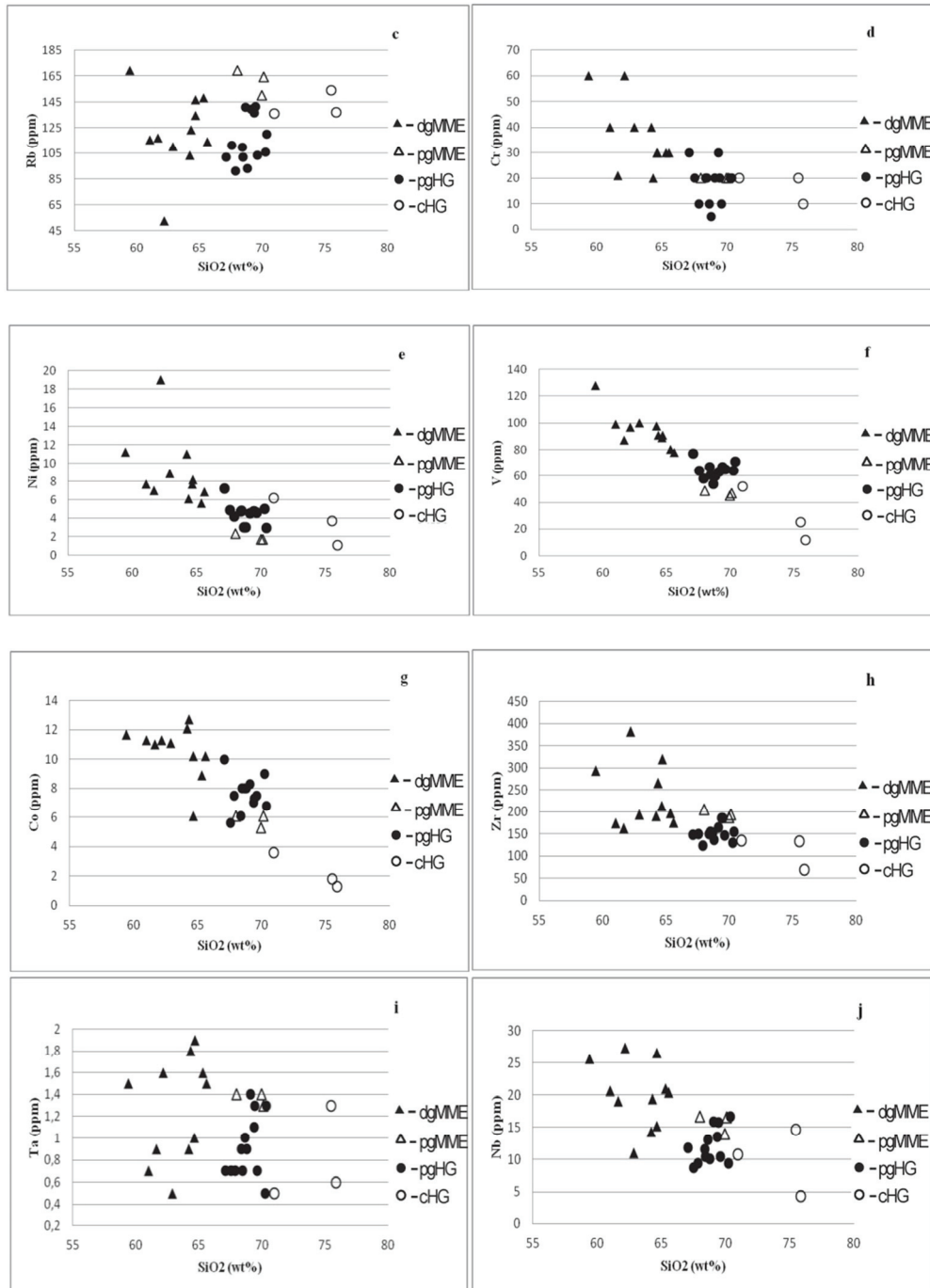


Fig. 37c-j. Chemical variation diagrams for trace element correlations of the granites studied. Symbols: dgMME – dark grey MME; pgMME – pale grey MME; pgHG – pale grey host granites; chHG – contact host granites.

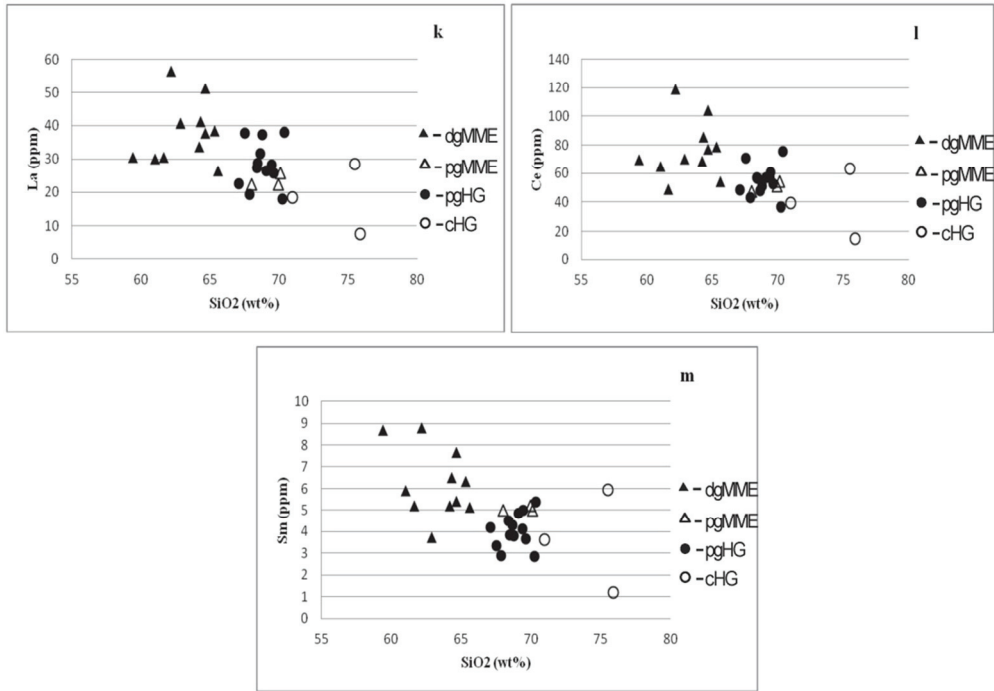


Fig. 37k-m. Chemical variation diagrams for trace element correlations of the granites studied. Symbols: dgMME – dark grey MME; pgMME – pale grey MME; pgHG – pale grey host granites; cHG – contact host granites.

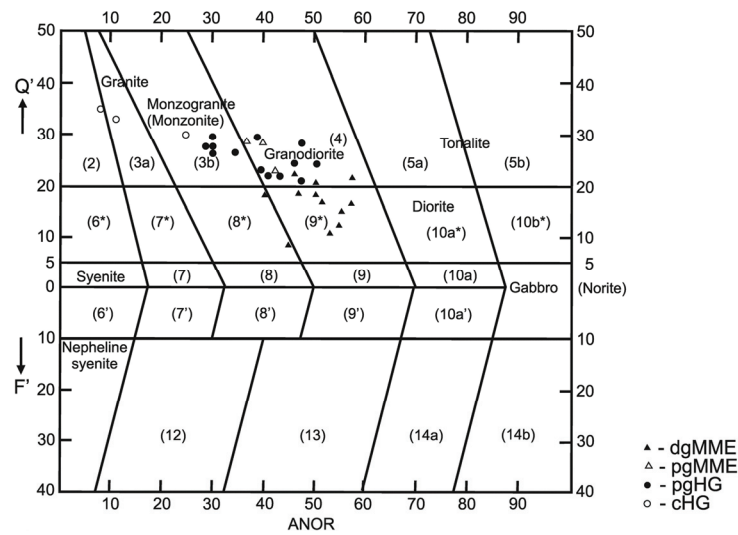


Fig. 38. Normative composition of the granites studied on the Q'-ANOR diagram (according to Streckeisen, Le Maitre 1979). Symbols: dgMME – dark grey MME; pgMME – pale grey MME; pgHG – pale grey host granites; cHG – contact host granites; (3a) granite; (3b) monzonite (monzogranite); (4) granodiorite; (8*) quartz monzonite; (9*) quartz monzodiorite/quartz monzogabbro.

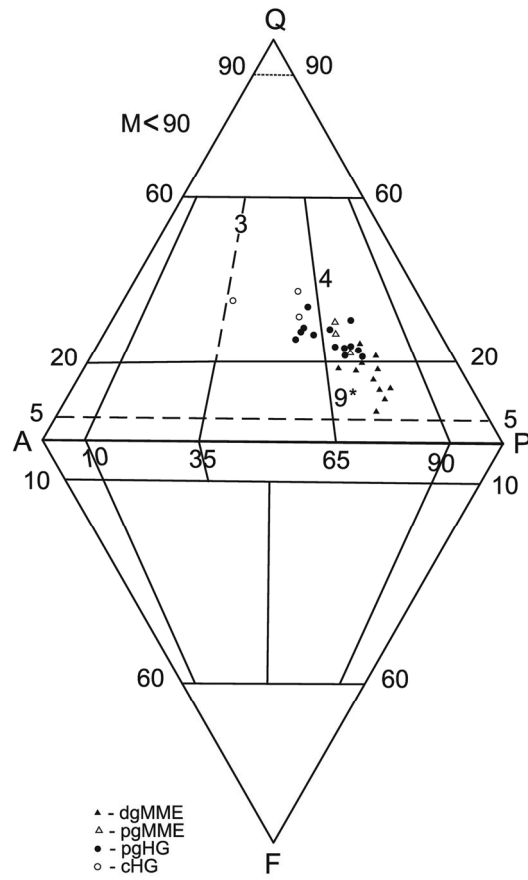


Fig. 39. Normative composition of the granites studied on the IUGS classification diagram. Symbols: dgMME – dark grey MME; pgMME – pale grey MME; pgHG – pale grey host granites; cHG – contact host granites; (3) granite; (4) granodiorite; (9*) quartz monzodiorite/quartz monzogabbro.

In the Ab-An-Or diagram (after O'Connor, 1965 and modified by Barker, 1979) the pale grey host granite samples (pgHG) plot in the granodiorite field, while the contact host granite samples (cHG) plot in the Q-monzonite and granite fields (Fig.40).

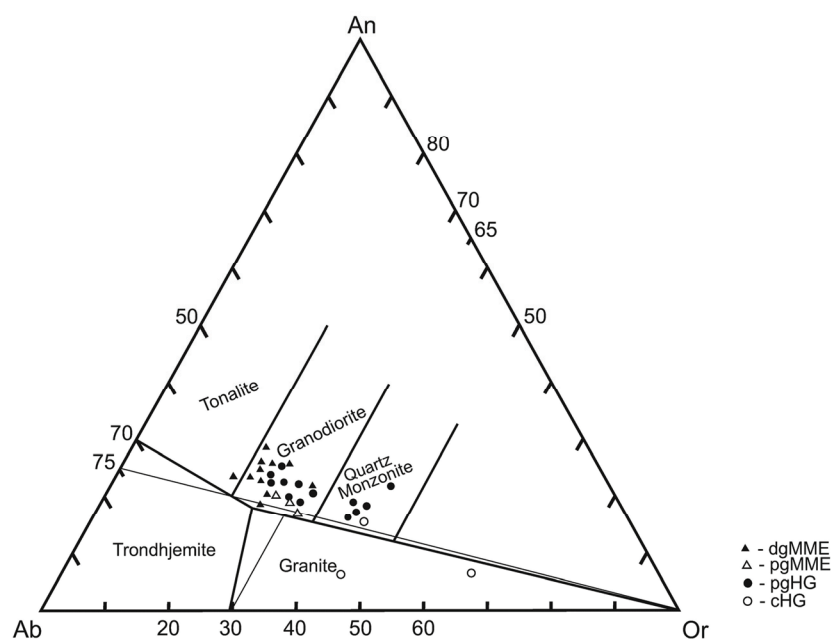


Fig. 40. Normative composition of the granites studied on the Ab-An-Or diagram (according to O'Connor 1965, modified by Barker 1979). Symbols: dgMME – dark grey MME; pgMME – pale grey MME; pgHG – pale grey host granites; cHG – contact host granites.

TABLE 4

Normative composition of pale grey host granites (HG) (is calculated using Barth's (1962) petrochemical method).

Sample	KH1/2	KH2/2	KH2/6a/1	KH2/6a/2	KH3/6	KH3/5a	DB5/1	DB5/2	DB5/6	WB/102A/2	WB/102A/6	WB/102A/7	WB/115/1	KH1/1	KH2/1	KH3/1
	pale grey host granites (pgHG)										contact host granites (cHG)					
<i>ap</i>	0.24	0.24	0.27	0.29	0.24	0.24	0.21	0.24	0.27	0.24	0.08	0.27	0.27	0.27	0.13	0.13
<i>il</i>	0.80	0.80	0.84	0.84	0.78	0.84	0.74	0.78	1.08	0.70	0.76	0.76	0.80	0.70	0.18	0.38
<i>or</i>	23.90	26.35	27.30	27.35	20.25	21.95	16.05	17.75	19.45	19.85	17.80	16.25	25.75	26.95	41.05	27.60
<i>ab</i>	30.35	27.25	28.45	27.85	35.80	35.15	35.60	36.70	35.90	33.70	39.15	37.45	29.00	28.50	18.90	32.85
<i>an</i>	12.25	11.50	11.55	11.60	15.15	13.38	14.55	15.15	13.40	12.10	15.68	16.03	10.85	9.10	3.55	3.60
<i>C</i>	1.12	0.0	0.05	0.05	0.24	0.0	0.0	0.19	0.41	1.26	0.0	0.0	0.74	1.77	0.92	1.11
<i>di</i>	0.0	0.03	0.0	0.0	0.0	0.64	0.60	0.0	0.0	0.0	1.32	0.44	0.0	0.0	0.0	0.0
<i>hy</i>	7.74	7.12	8.08	8.14	7.52	7.24	6.24	7.54	9.74	5.80	6.16	6.96	8.20	5.14	1.32	2.10
<i>Q</i>	23.59	26.71	23.46	23.87	20.01	20.55	26.01	21.65	19.76	26.36	19.05	21.86	24.38	27.57	33.97	32.24
Total	99.99	100.00	100.00	99.99	99.99	99.99	100.00	100.00	100.00	100.01	100.00	100.02	99.99	100.00	100.02	100.01

5.3.4. Petrochemical characteristics of pale grey host granites (HG)

The nomenclature of the pale grey host granites studied (pgHG), as well as of the contact host granites (cHG) and their position in various petrochemical classification diagrams, is clearly connected with their chemical composition, generally with the amount of major elements especially alkalis (mainly Na_2O and K_2O), rarely CaO and SiO_2 . It determines their classification as different granitic types. Commonly, the pale grey host granite samples (pgHG) plot mostly in the granodiorite field, while the contact host granite samples (cHG) plot in the granite field.

In the majority of papers regarding mineralogical-geochemical characteristics of granitoids, petrochemical diagrams are commonly used in the same way as IUGS diagrams (modal and normative) for classification, even of coarse-grained, holocrystalline magmatic rocks. The presentation of different positions of magmatic rocks on the modal as well as the normative and petrochemical diagrams may clearly explain some geochemical processes that were acted on the rocks studied. The position of the host granites studied in the petrochemical diagrams is described in detail below as follows.

The petrographic nomenclature of the host granites studied is presented below. The data on the R1-R2 multicationic diagram (Fig. 41) shows that the pale grey host granite samples (pgHG) plot in the granodiorite field. Only the projection points of contact host granite samples (cHG) plot in the syenogranite field.

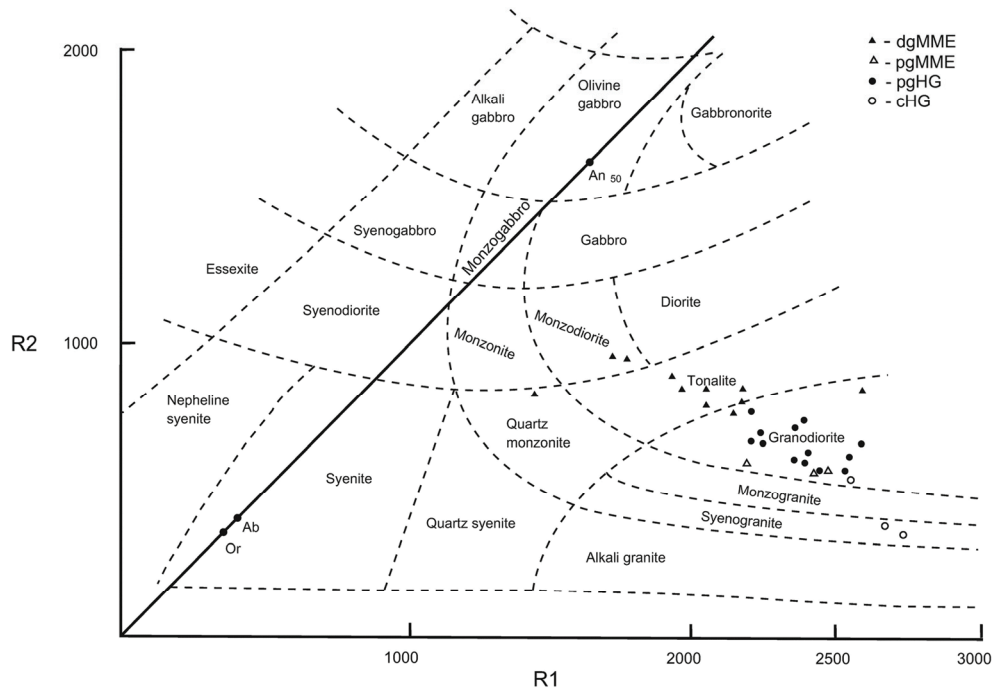


Fig. 41. Geochemical characteristics of the granites studied on the R1-R2 multicationic diagram (according to de la Roche et al. 1980). Symbols: dgMME – dark grey MME; pgMME – pale grey MME; pgHG – pale grey host granites; cHG – contact host granites.

On the other hand, in the $\text{Na}_2\text{O} + \text{K}_2\text{O}$ vs SiO_2 diagram after Middlemost (1994), the pale grey host granite samples (pgHG) plot in the granodiorite field, whereas the contact host granite samples (cHG) plot in the granite field. This relationship may reflect different amounts of alkalis, especially the K_2O content in the contact host granite samples (Fig. 42). In contrast, the similar $\text{Na}_2\text{O} + \text{K}_2\text{O}$ vs SiO_2 diagram for plutonic rocks but according to Cox et al. (1979) and modified by Wilson (1989), the pale grey host granite samples (pgHG) plot in the Q-diorite (granodiorite) as well as the granite fields, but the contact host granite samples (cHG) plot mainly in the alkali granite field (Fig. 43).

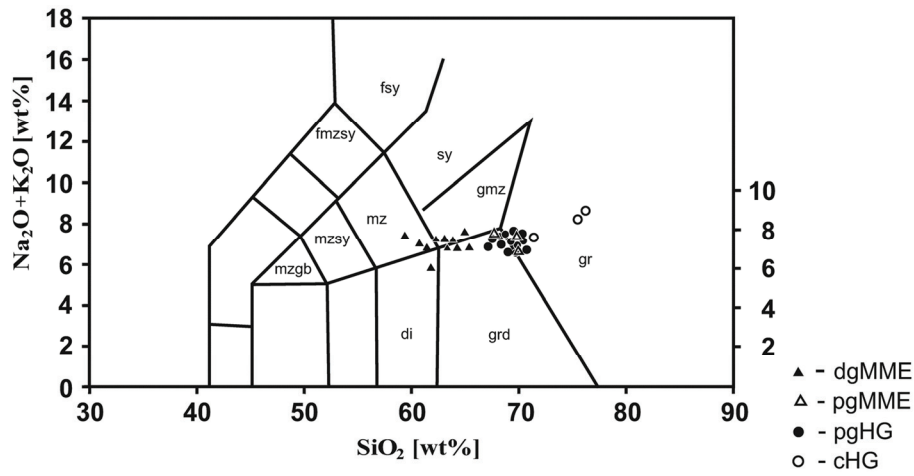


Fig. 42. Geochemical characteristics of the granites studied on the $\text{Na}_2\text{O} + \text{K}_2\text{O}$ vs SiO_2 diagram (after Middlemost 1994). Symbols: dgMME – dark grey MME; pgMME – pale grey MME; pgHG – pale grey host granites; cHG – contact host granites. Abbreviations: mz – monzonite; di – diorite; qmz – quartz monzonite; grd – granodiorite; gr – granite.

According to the Q-P diagram (after Debon, Le Fort, 1988), the pale grey host granite samples (pgHG) plot generally in the granodiorite (2) field, sometimes at the boundary of the granodiorite (2) adamellite (3) fields and in the granite (4) field, but the contact host granite samples (cHG) plot in the adamellite (3) field (Fig. 44).

The clear correlation between the content of alkalis (K_2O and Na_2O) and petrochemical character of the host granites is markedly visible in Fig. 45 where the pale grey host granite samples (pgHG) plot in the granodiorite field and in the Qtz-monzonite field, and the contact host granites (cHG) in the Qtz-monzonite and the granite field. It is connected to increased amounts of K_2O during assimilation processes, which is especially visible in the contact host granites.

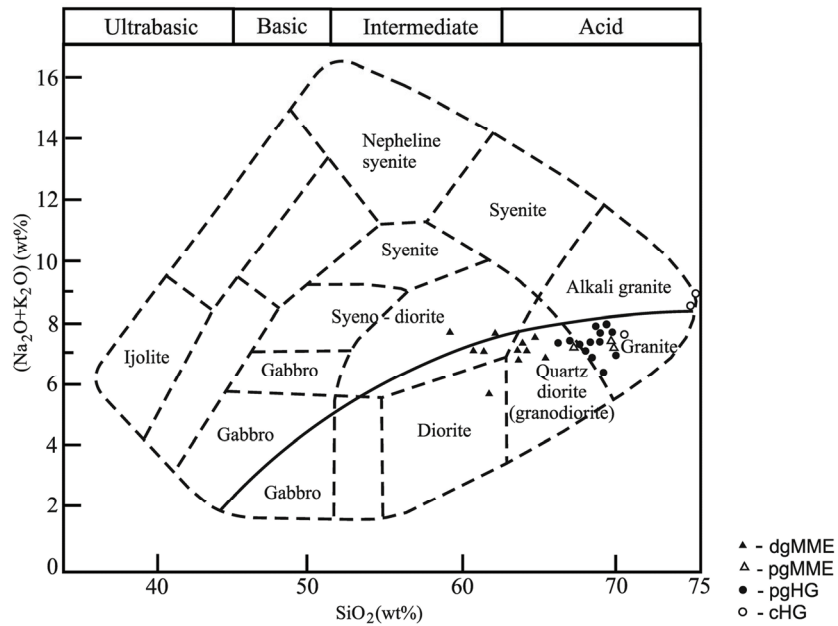


Fig. 43. Geochemical characteristics of the granites studied on the $\text{Na}_2\text{O}+\text{K}_2\text{O}$ vs SiO_2 diagram (according to Cox et al. 1979 and modified by Wilson 1989). Symbols: dgMME – dark grey MME; pgMME – pale grey MME; pgHG – pale grey host granites; cHG – contact host granites.

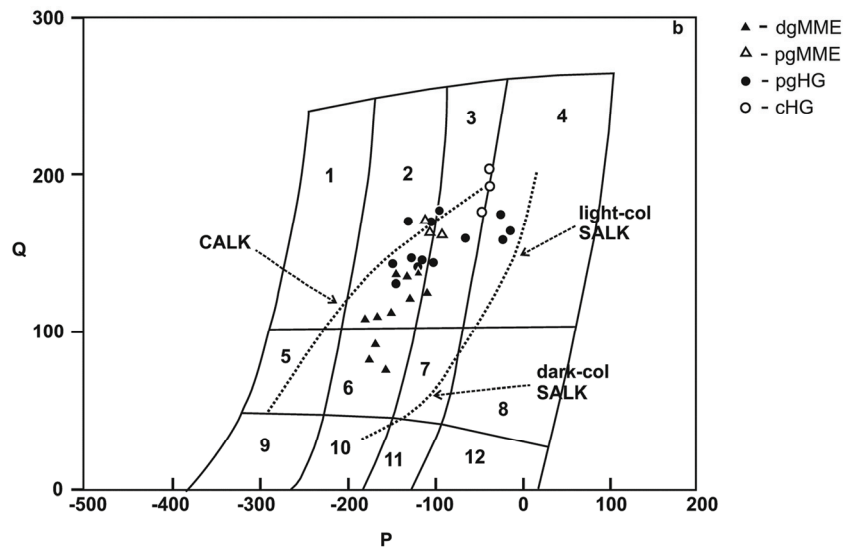


Fig. 44. Geochemical characteristics of the granites studied on the Q-P chemical nomenclature diagram (after Debon, Le Fort 1988). Symbols: dgMME – dark grey MME; pgMME – pale grey MME; pgHG – pale grey host granites; cHG – contact host granites; (2) granodiorite; (3) adamellite; (4) granite; (6) quartz monzodiorite; $Q = \text{Si}/3 - (\text{K} + \text{Na} + 2\text{Ca}/3)$; $P = \text{K} - (\text{Na} + \text{Ca})$; CALK – calc-alkaline trend; SALK – subalkaline trend: dark coloured and light coloured rocks.

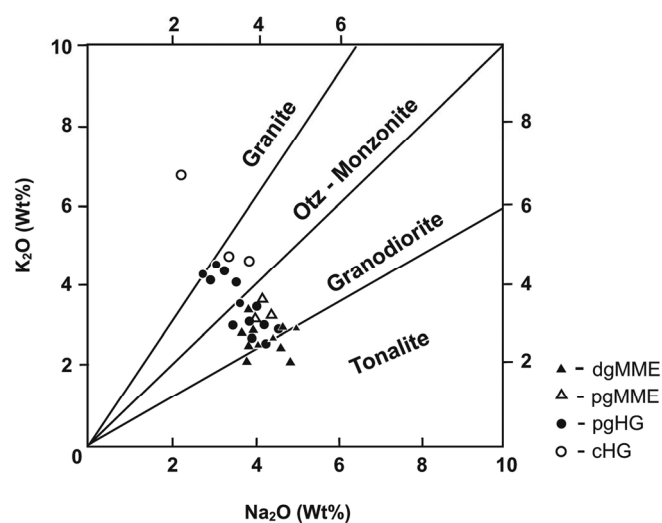


Fig. 45. Geochemical characteristics of the granites studied on the K_2O vs Na_2O diagram. Symbols: dgMME – dark grey MME; pgMME – pale grey MME; pgHG – pale grey host granites; cHG – contact host granites.

All the samples of the host granites studied show a typical calc-alkaline trend on the $Na_2O + K_2O - CaO$ vs SiO_2 diagram (Fig. 46), and have high-K character, although two samples of the pale grey host granites have medium-K character (Fig. 47). Żelaźniewicz et al. (2008) mentioned that the Dolina Będowska valley granodiorite exhibits K-rich, calc-alkaline characteristics.

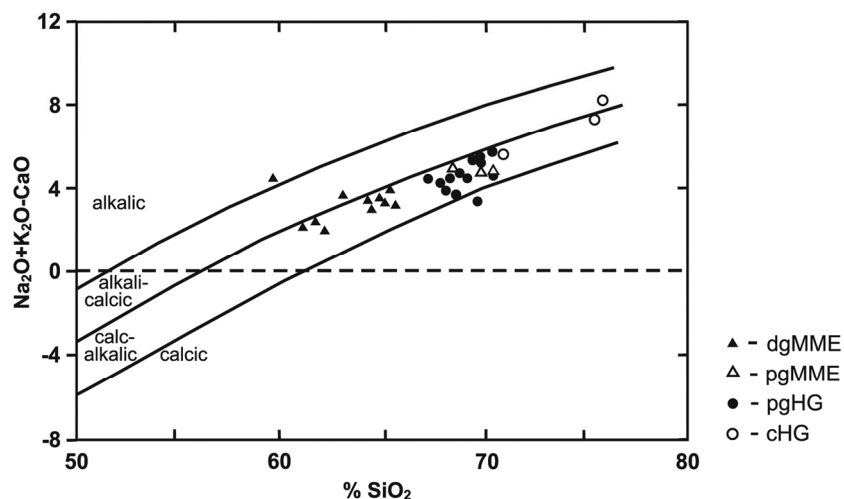


Fig. 46. Geochemical characteristics of the granites studied on the $Na_2O + K_2O - CaO$ vs SiO_2 diagram (according to Frost et al. 2001). Symbols: dgMME – dark grey MME; pgMME – pale grey MME; pgHG – pale grey host granites; cHG – contact host granites.

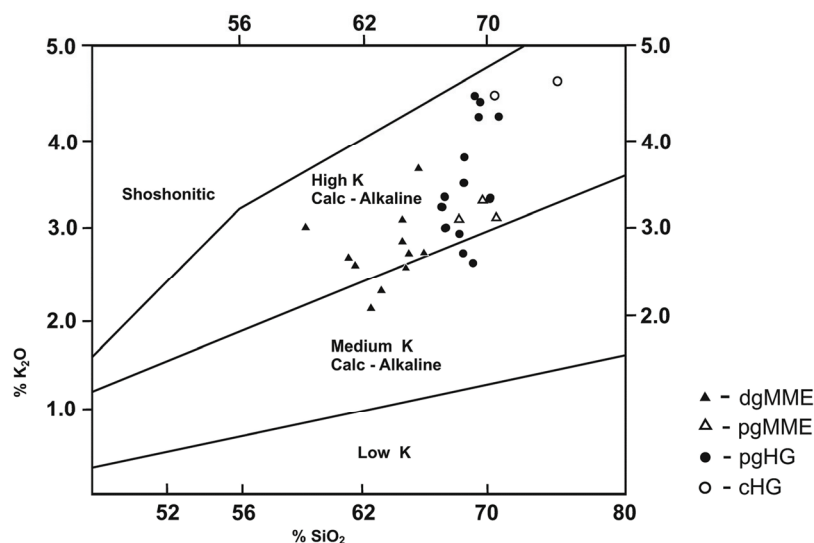


Fig. 47. Geochemical characteristics of the granites studied on the K_2O vs SiO_2 diagram (according to Peccerillo, Taylor 1976). Symbols: dgMME – dark grey MME enclaves; pgMME – pale grey MME; pgHG – pale grey host granites; cHG – contact host granites.

The agpaitic index (molar $(Na + K)/Al$ after Liégeois, Black 1987) of all the samples of the host granites studied is < 0.87 . In the pale grey host granites (pgHG) it ranges from 0.63 to 0.71 and in the contact host granites (cHG) from 0.67 to 0.83.

The MALI value (after Frost et al. 2001) of the pale grey host granites (pgHG) ranges from 3.4 to 5.2, and of the contact host granites (cHG) from 5.6 to 8.1. The host granites studied are mainly metaluminous and slightly peraluminous (the ASI vs SiO_2 diagram – Fig. 48). The classification based on the aluminium saturation (after Shand 1943; Zen 1986) indicates that the majority of these granite samples are metaluminous ($ASI = 0.96-1.07$ for the pale grey host granites) and only some of them peraluminous. Only the contact host granites have peraluminous character ($ASI = 1.06-1.12$). According to Płoczyńska (2000), granitoids from the Małopolska Block (MB) are strongly peraluminous ($ASI = 1.24-1.72$). Meanwhile, Żelaźniewicz et al. (2008) suggested that the Dolina Będowska valley granodiorite have metaluminous character (A/CNK index ~ 0.9). Słaby et al. (2010) define that granitoids are both metaluminous and peraluminous (A/CNK up to 1.29).

Finally, all the samples of host granites studied represent magnesian series, which is distinctly visible both in the $Mg/(Mg + Fe)$ vs $Fe + Mg + Ti$ diagram according to Debon and Le Fort (1988) (Fig. 49) and the $FeO_t/(FeO_t + MgO)$ vs SiO_2 diagram after Frost et al. (2001) (Fig. 50). The Fe^* number of the pale grey host granites (pgHG) ranges from 0.68 to 0.75, and for the contact host granite samples it is similar (0.55 to 0.72). The #Mg number ($MgO/(MgO + 0.9FeO_t)$) in the pale grey host granites is moderate (0.40-0.30), but in the contact host granites (cHG) it is distinctly higher (up to 0.50). These data are very close values presented by Słaby et al. (2010 – #Mg number of granitoids ranges from 0.31 to 0.60).

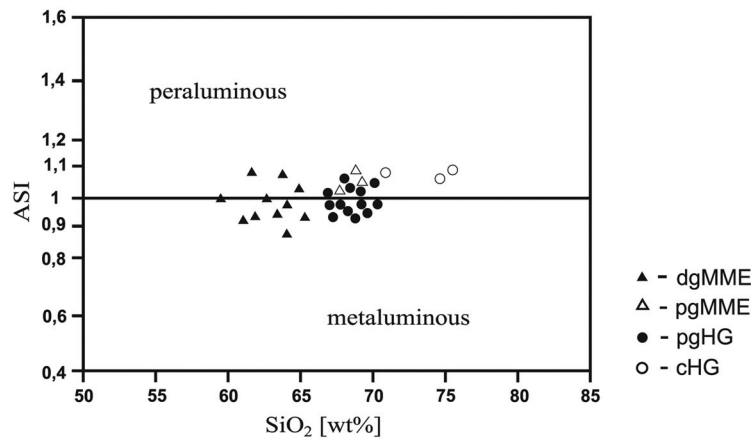


Fig. 48. Geochemical characteristics of the granites studied on the ASI vs SiO_2 diagram. Symbols: dgMME – dark grey MME; pgMME – pale grey MME; pgHG – pale grey host granites; cHG – contact host granites.

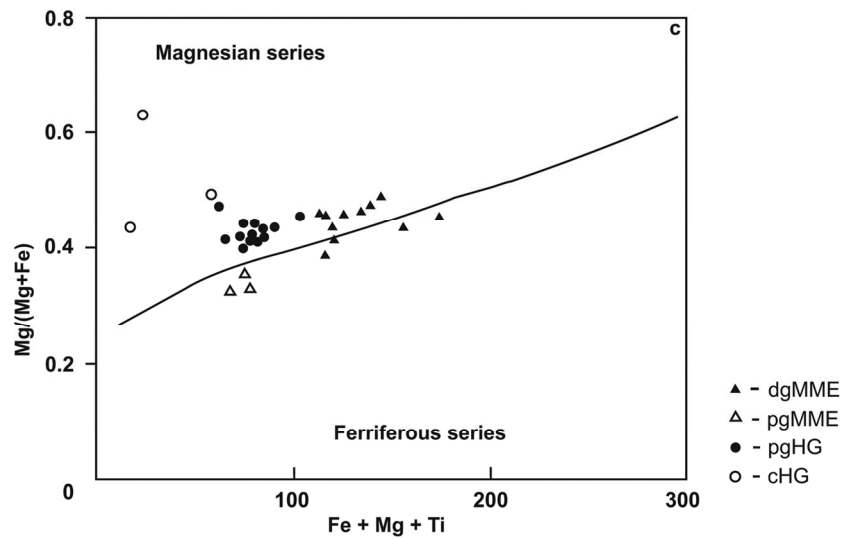


Fig. 49. Geochemical characteristics of the granites studied on the $\text{Mg}/(\text{Mg} + \text{Fe})$ vs $\text{Fe} + \text{Mg} + \text{Ti}$ diagram (according to Debon, Le Fort 1988). Symbols: dgMME – dark grey MME; pgMME – pale grey MME; pgHG – pale grey host granites; cHG – contact host granites.

According to the A-B multicationic diagram (after Debon, Le Fort 1983), where the A parameter represent the Al saturation index and the B parameter the sum of $\text{Fe} + \text{Mg} + \text{Ti}$, the host granite samples mainly represent the IV hbl (occasionally the III bt) mineralogical type of granites which contain mainly hornblende or biotite as ferromagnesian minerals (Fig. 51). On the other hand, the contact host granites (cHG) represent the III bt type of granites (Fig. 51).

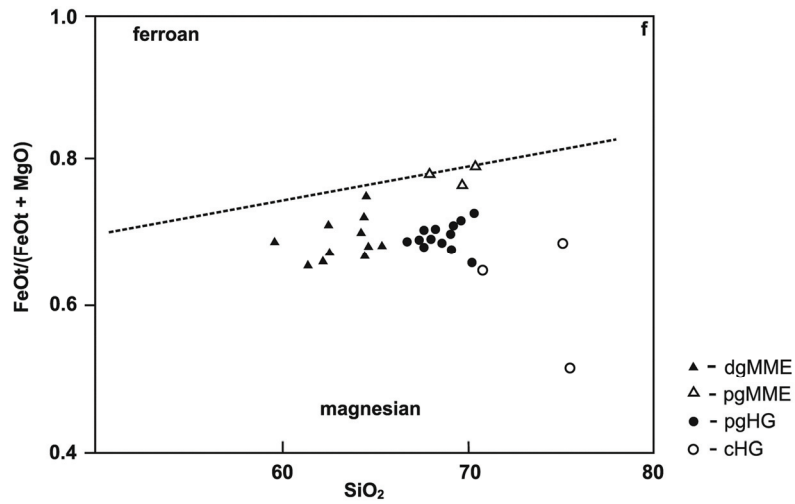


Fig. 50. Geochemical characteristics of the granites studied on the FeOt/(FeOt + MgO) vs SiO₂ diagram (after Frost et al. 2001). Symbols: dgMME – dark grey MME; pgMME – pale grey MME; pgHG – pale grey host granites; cHG – contact host granites.

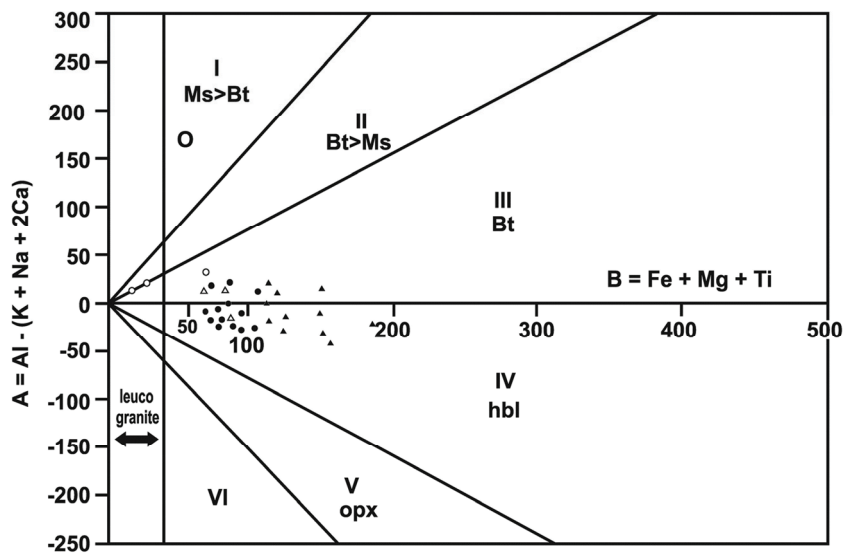


Fig. 51. Petrological characteristics of the granites studied on the A-B multicatic diagram (according to Debon, Le Fort 1983). Symbols: dgMME – dark grey MME; pgMME – pale grey MME; pgHG – pale grey host granites; cHG – contact host granites.

The pale grey host granite samples (pgHG) are demonstrably poorly evolved, and only the contact host granite samples (cHG) show moderate evolution that is clearly shown on the Rb-Ba-Sr ternary discrimination diagram (Fig. 52 – according to El Bouseily, Sokkary 1975). The host granites belong to both the HiBaSr (> 300 ppm Sr, especially the pale grey

host granites) and the LoBaSr (< 300 ppm Sr, mainly the contact host granites) types (Fig. 53), which is clearly shown by the Sr vs Ba diagram (Hawkesworth et al. 1991).

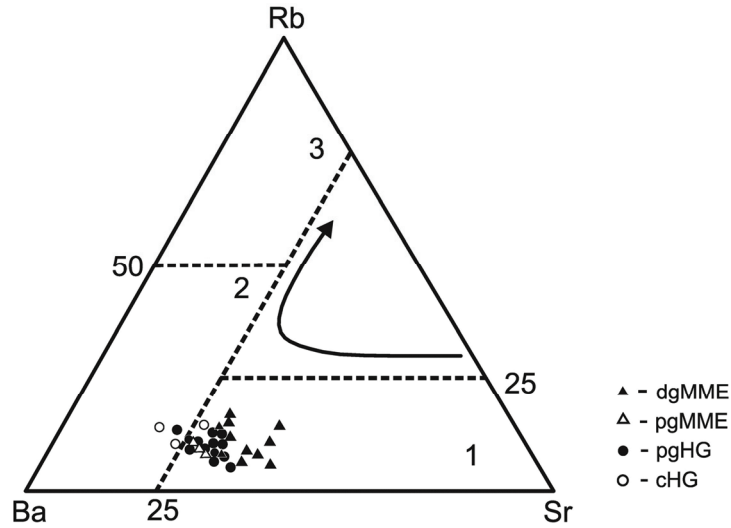


Fig. 52. Geochemical characteristics of the granites studied on the Rb-Ba-Sr ternary diagram (El Bouseily, Sokkary 1975). Symbols: dgMME – dark grey MME; pgMME – pale grey MME; pgHG – pale grey host granites; cHG – contact host granites; (1) poorly evolved granites; (2) mildly evolved granites; (3) highly evolved granites.

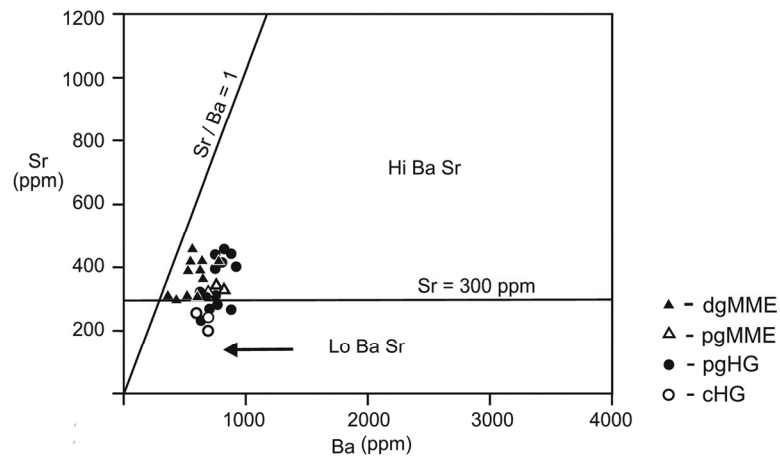


Fig. 53. Geochemical characteristics of the HG granites studied on the Sr vs Ba diagram (Hawkesworth et al. 1991). Symbols: dgMME – dark grey MME; pgMME – pale grey MME; pgHG – pale grey host granites; cHG – contact host granites.

5.3.5. Tectonic setting characteristics of pale grey host granites (HG)

All the host granite samples apparently belong to the I-type granites (Na_2O vs K_2O diagram after White, Chappell 1983 – Fig. 54) which not only confirms their geochemical characteristics (the Na_2O content above 3.2wt%, $\text{A/CNK} < 1.1$) but also their petrographic characteristics (the occurrence of hornblende, biotite and titanite as well as apatite inclusions in biotite and hornblende). In contrast, Płoczyńska (2000) classified granitoids from the Małopolska Block (MB) as S-type, whereas Żelaźniewicz et al. (2008) classified them as I-type based on the Dolina Będkowska valley granodiorite study.

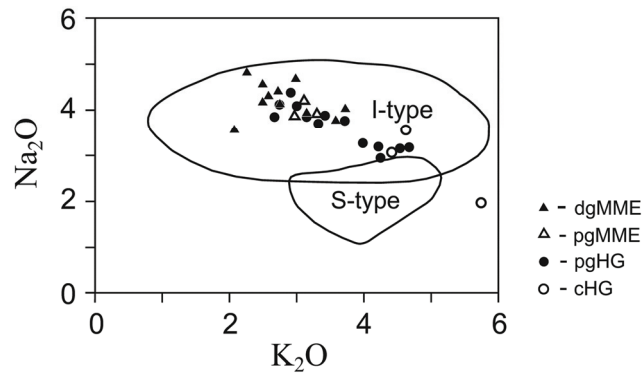


Fig. 54. Geochemical characteristics of the granites studied on the Na_2O vs K_2O diagram (after White, Chappell 1983). Symbols: dgMME – dark grey MME; pgMME – pale grey MME; pgHG – pale grey host granites; cHG – contact host granites.

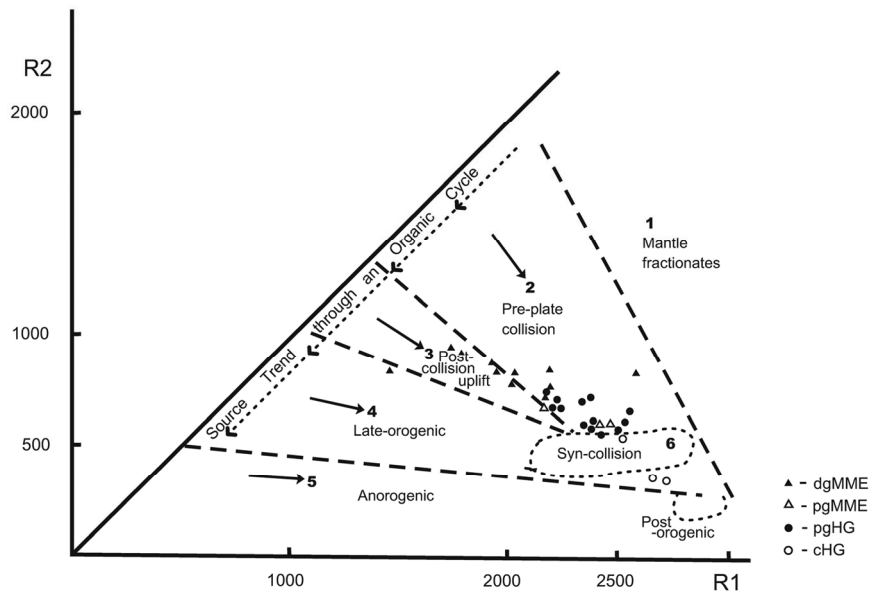


Fig. 55. Tectonic characteristics of the granites studied according to the R1-R2 diagram (Batchelor, Bowden 1985). Symbols: dgMME – dark grey MME; pgMME – pale grey MME; pgHG – pale grey host granites; cHG – contact host granites.

The host granites exhibit distinct differences in their tectonic characteristics, according to their position in the Batchelor and Bowden (1985) R1-R2 tectonic discrimination diagram. The pale grey host granites (pgHG) plot in the pre-plate collision granite field, and less commonly (only three samples) in the syn-collision granite field (Fig. 55). The contact host granite samples nearly plot in the syn-collision granite field (Fig. 55). According to Żelaźniewicz et al. (2008), the Dolina Będowska valley granodiorites plot close to the border between the pre-plate collision and post-collisional uplift fields.

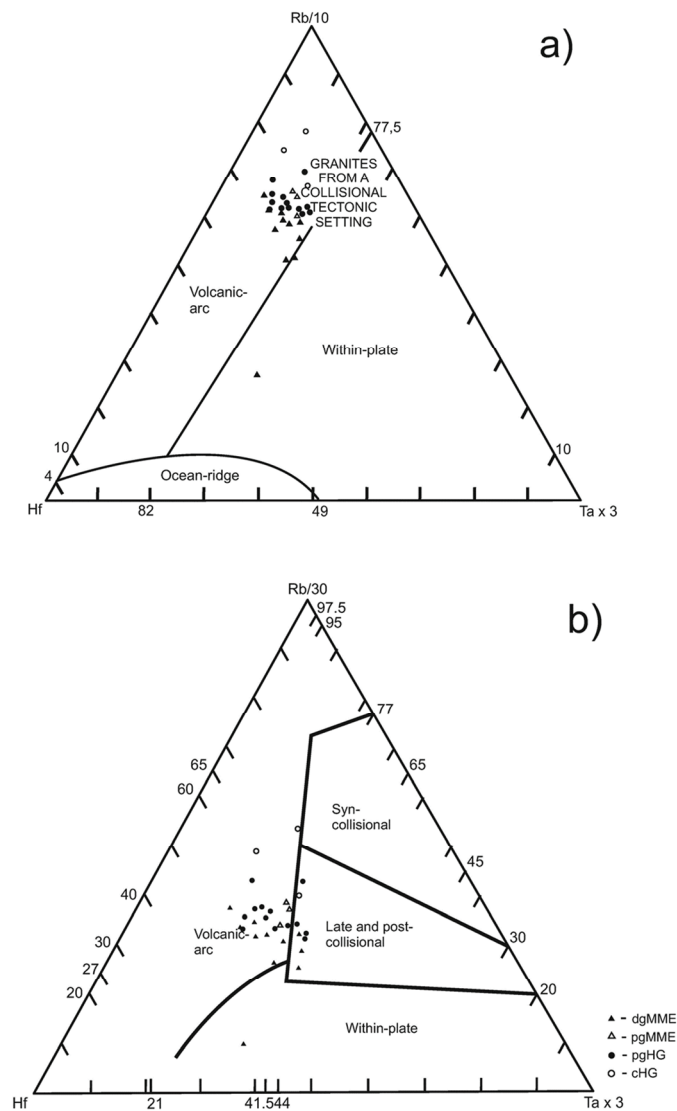


Fig. 56. Tectonic characteristics of the granites studied: a. – Hf-(Rb/10)-Tax3 diagram (Harris et al. 1986); b. – Hf-(Rb/30)-Tax3 diagram (Harris et al. 1986). Symbols: dgMME – dark grey MME; pgMME – pale grey MME; pgHG – pale grey host granites; cHG – contact host granites.

In the Hf-(Rb/10)-Tax3 diagram (Harris et al. 1986), the host granite samples (pgHG) plot in the volcanic arc granite but also as granites from collisional tectonic setting fields (Fig. 56a). On the other hand, based on the Hf-(Rb/30)-Tax3 diagram, they can be classified as volcanic arc granites with some affinities toward late- and post-collisional granites (Fig. 56b). The latter position is typical for all the samples of the contact host granites and some samples of pale grey MME (Fig. 56b).

According to the Maniar and Piccoli (1989) classification, based on the major element ratios ($\text{MgO}/\text{FeO}_{\text{tot}}$, $\text{Na}_2\text{O}/\text{K}_2\text{O}$ and MgO/MnO), the host granites studied belong to CAG (continental arc granitoids) and IAG (island arc granitoids), and the contact host granites to CCG (continental collision granitoids) (Fig. 57).

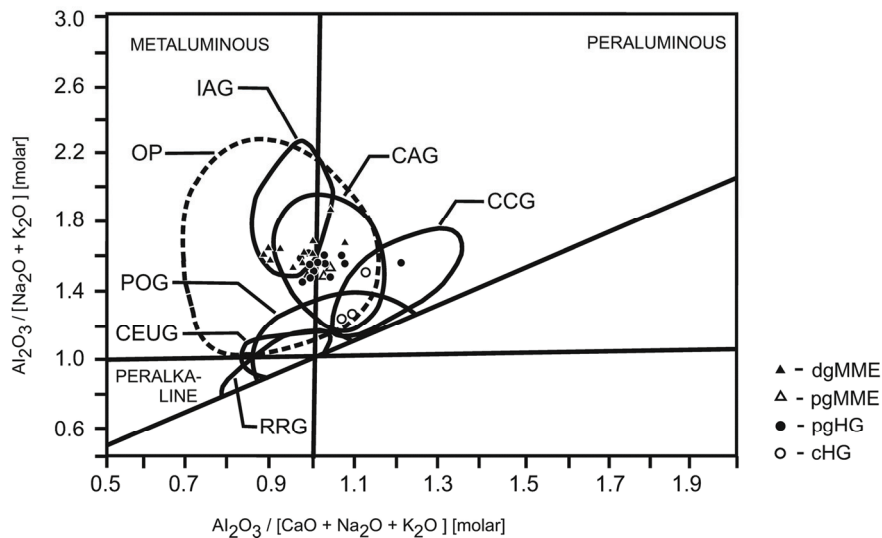


Fig. 57. Geochemical characteristics of the granites studied in A/(N+K) vs A/(C+N+K) Shand's diagram (1943) modified by Maniar, Piccoli (1989). Symbols: dgMME – dark grey MME; pgMME – pale grey MME; pgHG – pale grey host granites; cHG – contact host granites. Abbreviations: CCG – continental collision granitoids; CAG – continental arc granitoids; IAG – island arc granitoids; OP – oceanic plagiogranites; POG – post-orogenic granitoids; CEUG – continental epeirogenic uplift granitoids; RRG – rift-related granitoids.

Instead, based on the trace elements data – in the Nb vs Y and Ta vs Yb diagrams, all the samples of the host granites plot in the VAG + syn COLG granites field (Fig. 58a, b), and in the Rb vs Y+Nb and the Rb vs Yb + Ta diagrams – in the VAG granites field (Fig. 58c, d)(Pearce et al. 1984). Similar tectonic setting features for the Dolina Będowska valley granodiorite were described by Żelaźniewicz et al. (2008). According to Brown et al. (1984), all the host granite samples represent 'the N-arc' – the normal continental arc granites (the Rb/Zr vs Nb and Rb/Zr vs Y diagrams – Fig. 59).

On the Rb vs Y + Nb diagram modified by Pearce (1996), all the host granite samples fall into the post-collision granite field (Fig. 60). The Dolina Będowska valley granodiorites were similarly determined by Żelaźniewicz et al. (2008). But the position of the host granites studied on the (Rb/100)-Tb-Ta diagram (Thiéblemont, Cabanis 1990)

indicates the post-collisional and syn-subductional characteristics of the pale grey host granites (pgHG), whereas the contact host granite samples (cHG) apparently have no clear relation to the anorogenic alkaline granites or the syn-collisional granites (Fig. 61).

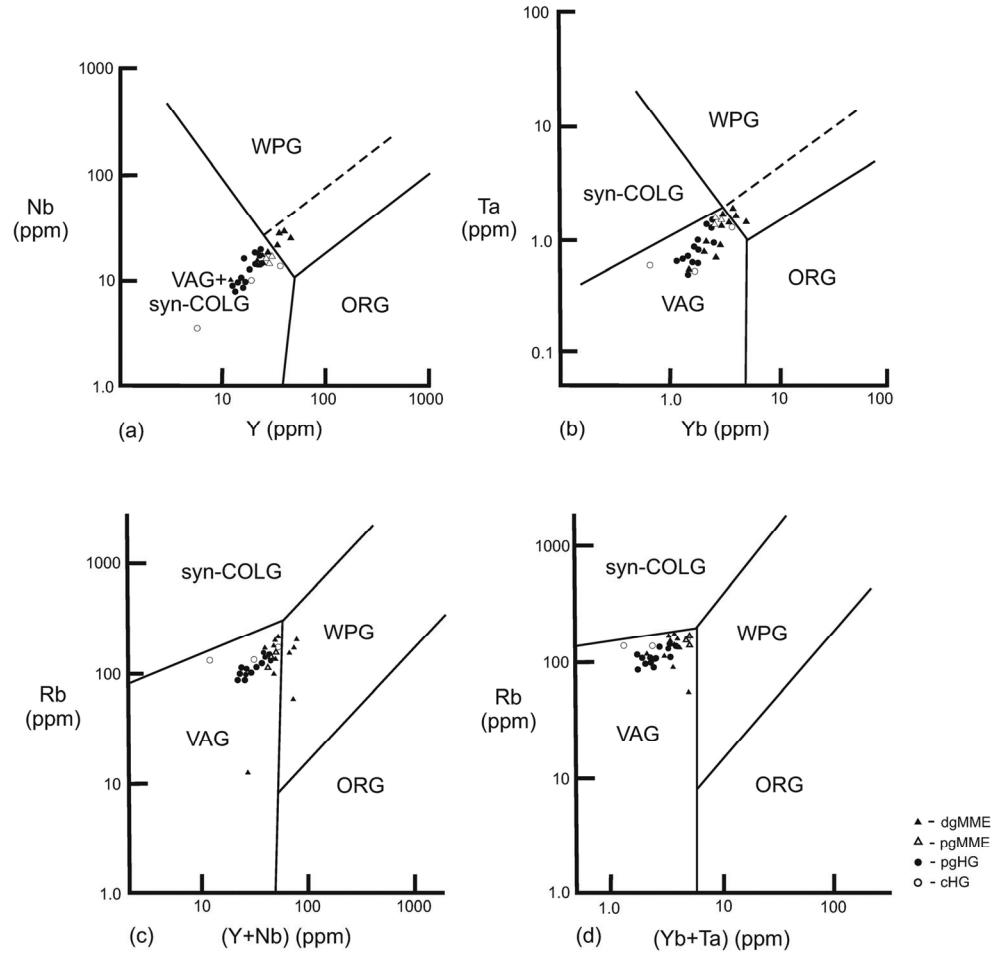


Fig. 58. Tectonic characteristics of the granites studied according to: a. – Nb vs Y; b. – Ta vs Yb; c. – Rb vs Y + Nb and d. – Rb vs Yb + Ta (after Pearce et al. 1984). Symbols: dgMME – dark grey MME; pgMME – pale grey MME; pgHG – pale grey host granites; cHG – contact host granites. Abbreviations: WPG – within-plate granites; ORG – ocean ridge granites; syn-COLG – syn-collision granites; VAG – volcanic arc granites.

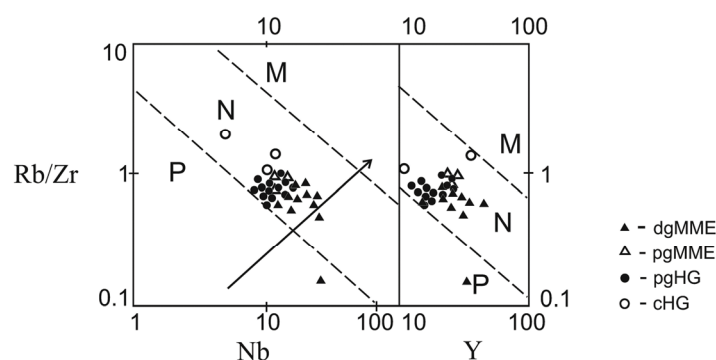


Fig. 59. Tectonic characteristics of the granites studied according to Rb/Zr vs Nb and Rb/Zr vs Y diagram (Brown et al. 1984). Symbols: dgMME – dark grey MME; pgMME – pale grey MME; pgHG – pale grey host granites; cHG – contact host granites. Abbreviations: P – primitive island arcs and continental arcs; N – normal continental arcs; M – mature continental arcs; arrow – increasing maturity.

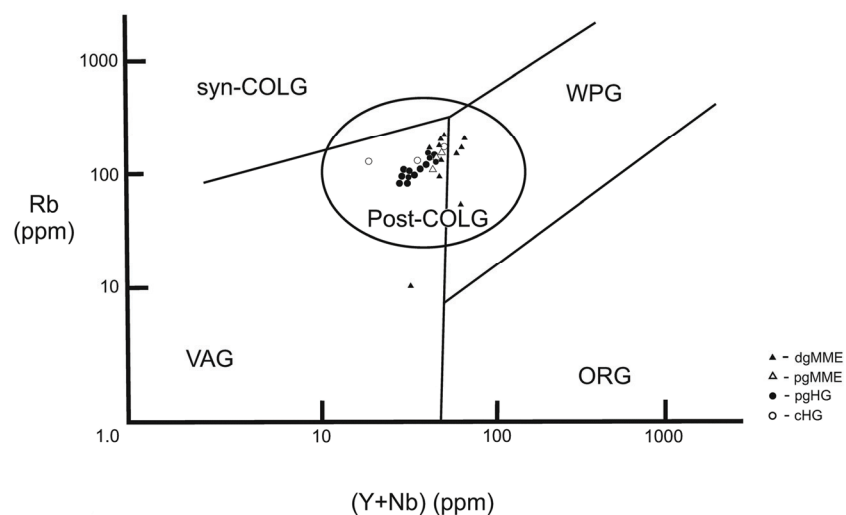


Fig. 60. Tectonic characteristics of the granites studied according to the Rb vs Y + Nb diagram (modified by Pearce 1996). Symbols: dgMME – dark grey MME; pgMME – pale grey MME; pgHG – pale grey host granites; cHG – contact host granites. Abbreviations: WPG – within-plate granites; ORG – ocean ridge granites; syn-COLG – syn-collision granites; VAG – volcanic arc granites; post-COLG – post-collision granites.

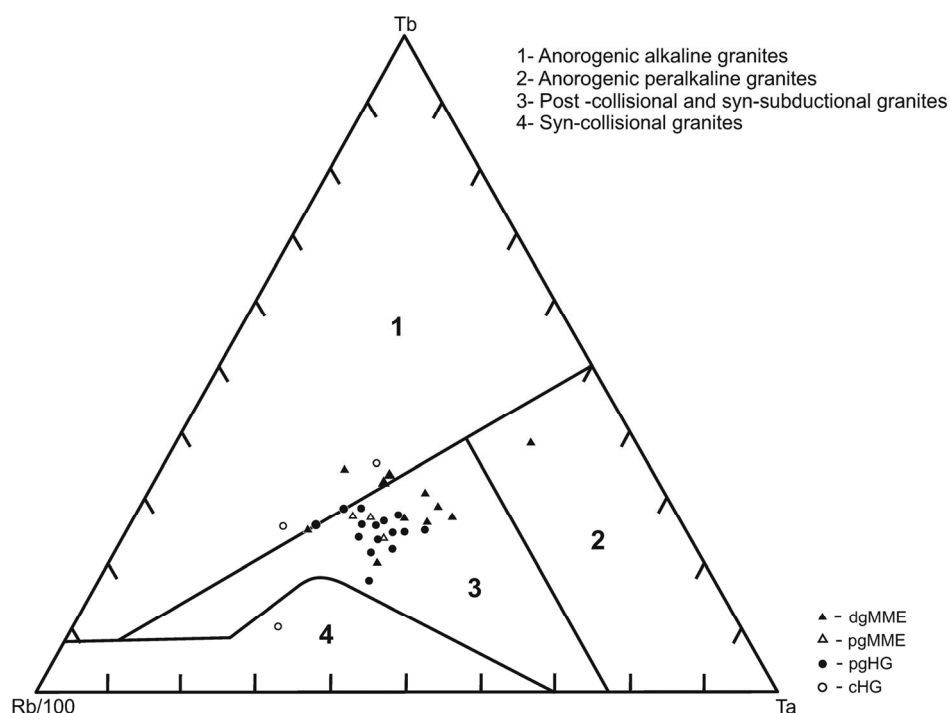


Fig. 61. Tectonic characteristics of the granites according to the (Rb/100)-Tb-Ta diagram after Thiéblemont, Cabanis (1990). Symbols: dgMME – dark grey MME; pgMME – pale grey MME; pgHG – pale grey host granites; cHG – contact host granites.

5.3.6. Geochemical patterns: chondrite-normalized spider diagrams of pale grey host granites (HG)

In Figure 62, the chondrite-normalized trace element patterns of the pale grey host granites is presented, along with the contact host granite samples. Normalization calculation factors are after Sun and McDonough (1989). These spider diagrams indicate that the trace element concentrations of the pale grey host granite samples (pgHG) show regular variation. Their geochemical patterns reveal the enrichment in some of the LIL (Rb, K), Nd and HFS (La, Zr, Hf and Tb) elements relative to the LIL (Ba, Sr), HFS (Nb, Ta, Ti) and P elements. The samples of the contact host granites (cHG) show similar geochemical patterns. These diagrams point out the higher level LIL elements relative to HFS elements and the geochemical patterns indicate a smooth slope down to the right.

The REE chondrite normalized patterns (Fig. 63a, b) display Eu negative anomaly ($\text{Eu}/\text{Eu}^* = 0.62-1.0$) or $\text{Eu} = \text{Eu}_N/(\text{Sm}_N + \text{Gd}_N)/2$ is 0.61-0.97, markedly lower slopes and the HREE depletion (especially Yb) in the samples of pale grey host granites. In the contact host granites (cHG) the Eu/Eu^* ratio ranges from 0.5 to 2.8. The samples of the host granite indicate low LREE/HREE fractionation $(\text{La}/\text{Yb})_N = 5.5-20.7$ e.g. 7.8-20.7 for pale grey host granite samples, and $(\text{La}/\text{Yb})_N = 5.5-8.4$ for the contact host granite samples, respectively. Their chondrite-normalized patterns show a smoothly declining slope toward the right

(Fig. 63a, b). The low content values of Y (12.6-26.0 ppm) and Yb (1.1-2.6 ppm) show the samples of pale grey host granites (pgHG). The contact host granites (cHG) are markedly enriched in Y and Yb – 6.4-38.0 ppm and 0.6-3.5 ppm, respectively. All the samples of the pale grey host granites (pgHG) studied display very distinct variation of $\sum \text{REE} = 103\text{-}198 \text{ ppm}$. On the other hand, the contact host granite samples (cHG) show a marked depletion in REE ($\sum \text{REE} = 44\text{-}194 \text{ ppm}$).

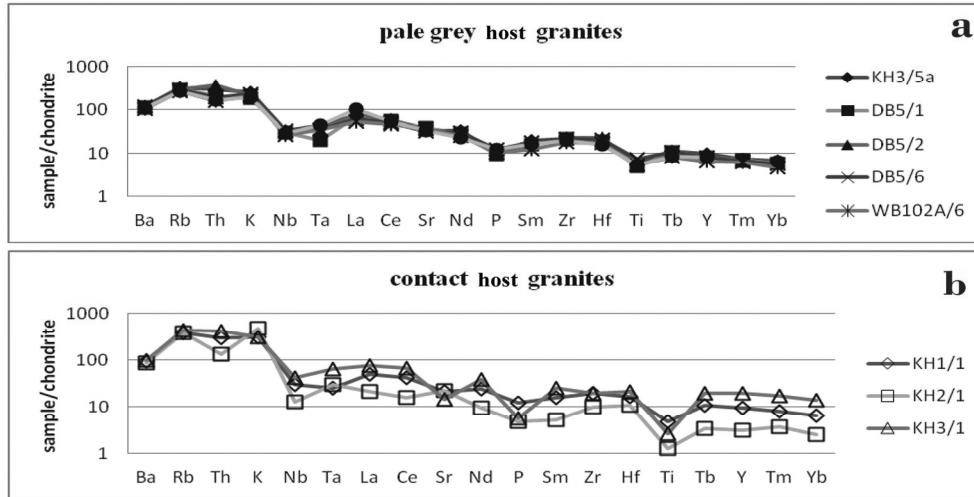


Fig. 62. The chondrite-normalized trace element patterns for the selected samples of the HG granites: a. – pale grey host granites; b. – contact host granites.

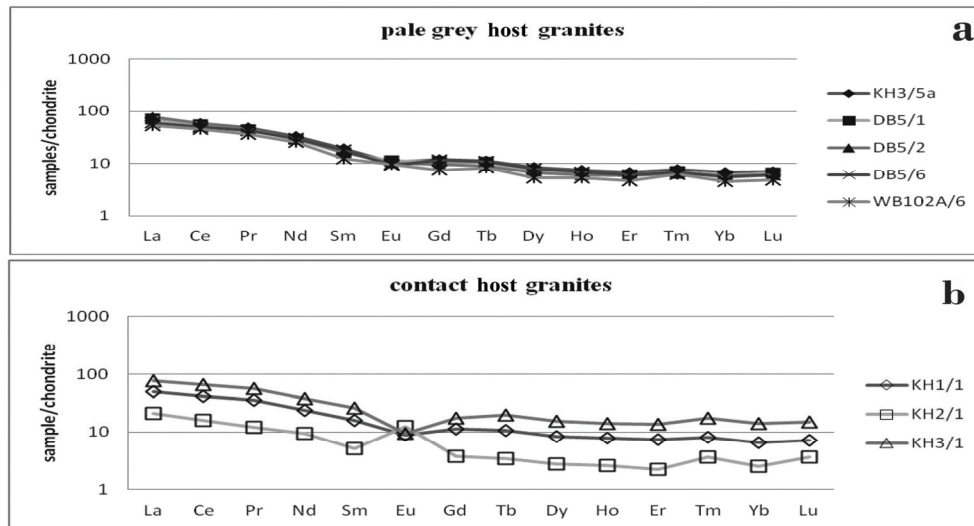


Fig. 63. The chondrite-normalized rare earth element patterns for the selected samples of the host granites: a. – pale grey host granites; b. – contact host granites.

Płonczyńska (2000) displayed the $(La/Yb)_N$ fractionation granitoids data as follows: for the Dolina Będkowska valley – 8.0-13.0 and the Pilica area – 13.2. Żelaźniewicz et al (2008) mentioned that the REE pattern of the Dolina Będkowska valley granodiorite is moderately fractionated and LREE contents are 60-100 times chondrite value.

5.3.7. Isotope data of pale grey host granites (HG)

The Sr-Nd isotopic data for the pale grey host granites are presented in Table 5. In Figure 64 their plots occur between the continental crust field and the 'orogenic mantle array' field. The value of $^{86}Sr/^{87}Sr_{(i)}$ varies from 0.709375 to 0.710426 while $\epsilon Nd_{(i)}$ exhibit values from -4.1 to -3.8. The isotopic data are recalculated to the time of granite formation (300 Ma) according to the data reported by Jarmołowicz-Szulc (1984, 1985), Żelaźniewicz et al. (2008), and Nawrocki et al. (2008). On the $^{86}Sr/^{87}Sr$ vs SiO_2 and $^{143}Nd/^{144}Nd$ vs SiO_2 diagrams, all the samples of the host granites studied plot close the crust composition field (Fig. 65a, b).

TABLE 5

Pale grey host granites (HG) – Sm-Nd isotope data.

Sample	DB5/2	DB5/6	WB102A/6
pale grey host granites (pgHG)			
Sm(ppm)	4.203000	3.260000	2.696070
Nd(ppm)	21.01900	18.76700	27.87960
$^{147}Nd/^{144}Nd$	0.120900	0.105000	0.058460
$^{143}Nd/^{144}Nd$	0.512272	0.512243	0.512315
2 σ	0.000007	0.000006	0.000004
$^{87}Sr/^{86}Sr$	0.710426	0.709988	0.709375
2 σ	0.000013	0.000010	0.000016
CHUR $\epsilon Nd_{(0)}$	-7.1	-7.7	-6.3
CHUR $\epsilon Nd_{(300)}$	-4.1	-4.1	-3.8

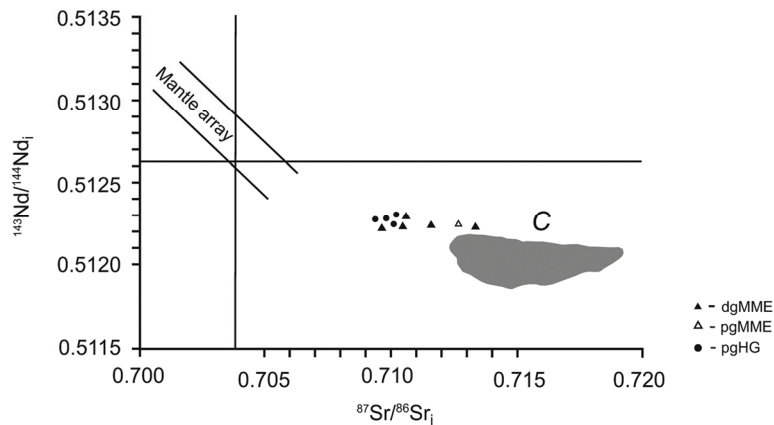


Fig. 64. Isotopic characteristics of the granites studied on the $^{143}Nd/^{144}Nd$ vs $^{86}Sr/^{87}Sr$ diagram (after Ilbeyli et al. 2004). Symbols: dgMME – dark grey MME; pgMME – pale grey MME; pgHG – pale grey host granites. Abbreviation: C – crust composition of Central European metamorphic rocks (Voshage et al. 1990).

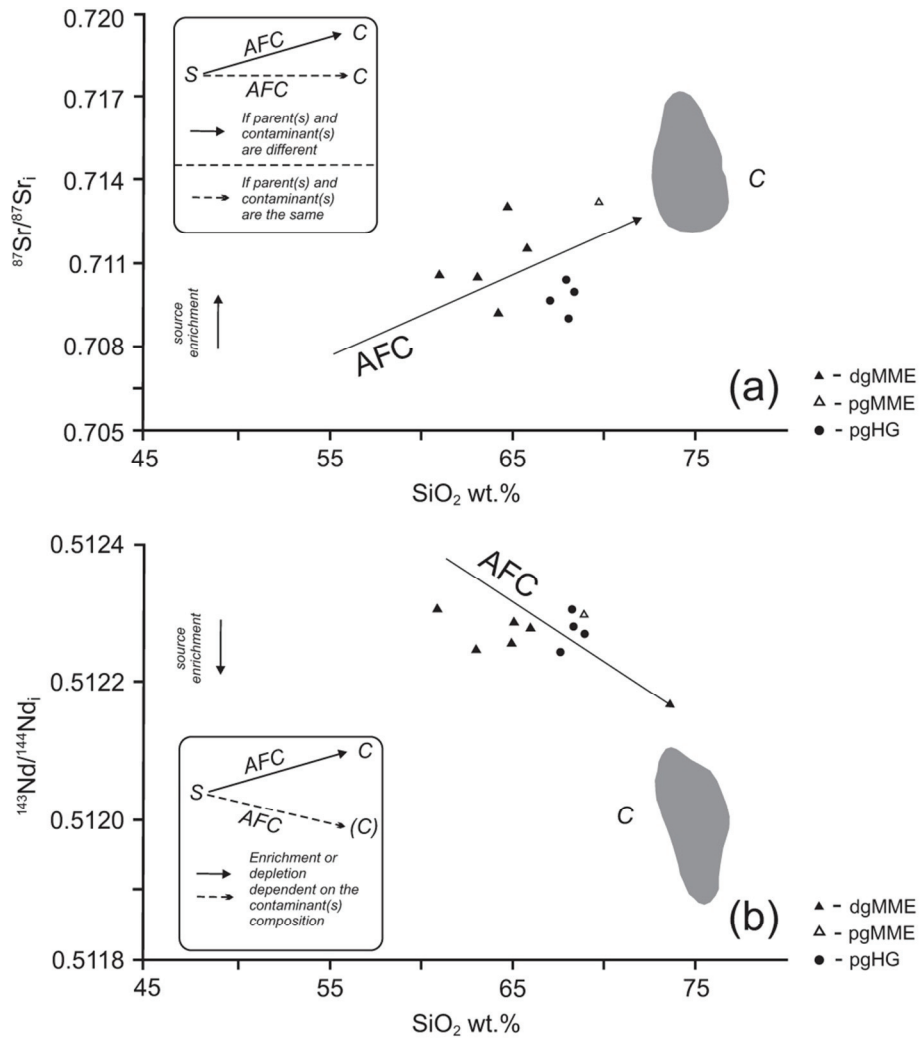


Fig. 65. Isotopic characteristics of the granites studied on: a. – the $^{86}\text{Sr}/^{87}\text{Sr}$ vs SiO_2 diagram and b. – the $^{143}\text{Nd}/^{144}\text{Nd}$ vs SiO_2 diagram (after Ilbeyli et al. 2004). Symbols: dgMME – dark grey MME; pgMME – pale grey MME; pgHG – pale grey host granites. Abbreviation: C – crust composition of metamorphic rocks from Central European (Voshage et al. 1990).

5.4. Geochemistry of mafic microgranular enclaves (MME)

Chemical analyses of dark grey and pale grey MME are presented in Table 6. For geochemical investigations, fresh, unaltered rock samples or those showing less distinct hydrothermal alteration were selected. The feldspatization process in some samples of dark grey MME (dgMME) is manifested by the overprint of a pale pinkish shades on pale grey colour unaltered rocks.

TABLE 6

Chemical composition of mafic microgranular enclaves (MME).

Sample	KH1/3	KH1/6	KH1/9	KH1/10	KH2/3	KH2/4	KH2/5	KH2/6b	KH3/5b	DB5/5	WB102A/7	KH3/2	KH3/3	KH3/4
dark grey enclaves (dgMME)												pale grey enclaves (pgMME)		
wt%														
SiO ₂	62.18	64.69	65.60	64.34	61.03	61.66	65.34	59.43	62.89	64.65	64.21	68.00	70.12	69.96
TiO ₂	1.04	0.84	0.79	0.88	1.07	1.02	0.85	1.22	0.95	0.91	0.90	0.53	0.49	0.46
Al ₂ O ₃	15.61	15.99	15.79	15.85	16.64	16.46	15.66	16.47	16.45	15.81	16.30	15.39	14.54	14.86
Fe ₂ O ₃ *	6.62	5.42	4.54	5.29	5.43	5.26	4.47	7.13	5.45	4.72	4.76	3.67	3.41	3.19
MnO	0.12	0.12	0.11	0.11	0.16	0.16	0.13	0.16	0.08	0.04	0.09	0.09	0.08	0.07
MgO	2.47	1.64	1.91	1.83	2.57	2.48	1.87	2.94	2.42	1.84	2.11	0.91	0.84	0.87
CaO	3.74	3.40	3.44	3.92	4.58	4.48	3.45	3.42	3.48	3.08	3.64	2.80	2.53	2.40
Na ₂ O	3.63	4.50	4.04	3.89	4.44	4.33	3.77	4.64	4.75	3.87	4.39	4.26	3.88	3.86
K ₂ O	2.07	2.45	2.73	3.12	2.68	2.60	3.71	2.95	2.28	2.80	2.66	3.11	3.10	3.29
P ₂ O ₅	0.39	0.26	0.15	0.25	0.21	0.19	0.16	0.44	0.17	0.24	0.16	0.14	0.13	0.14
C _{tot.}	0.07	0.08	0.06	0.08	0.09	0.0	0.05	0.05	0.09	0.14	0.07	0.05	0.08	0.05
S _{tot.}	0.51	0.08	0.06	0.01	0.03	0.04	0.03	0.82	0.01	0.69	0.01	0.01	0.01	0.01
LOI	2.00	0.60	0.80	0.40	1.10	1.30	0.50	1.40	1.00	1.90	0.70	1.00	0.80	0.80
Total	99.87	99.92	99.90	99.88	99.92	99.92	99.91	99.91	99.92	99.87	99.92	99.90	99.92	99.92
ppm														
Ba	459.1	421.0	537.2	638.5	514.1	530.0	637.6	566.2	599.2	798.1	576.1	782.1	755.2	764.9
Cs	4.3	6.4	5.0	3.3	7.8	7.3	8.1	9.4	5.2	9.6	5.1	3.9	4.2	3.8
Ga	21.5	21.9	17.9	20.2	20.2	21.0	18.9	23.7	20.9	21.4	18.6	19.1	18.1	19.9
Hf	9.0	8.4	4.9	6.4	5.0	3.8	5.7	7.2	4.4	5.6	4.9	5.4	5.1	5.8
Nb	27.3	26.5	20.4	19.4	20.6	19.0	21.0	25.6	10.9	15.2	14.2	16.6	16.5	13.9
Rb	52.7	146.9	114.1	123.5	115.6	117.0	148.1	169.3	110.3	134.6	103.1	169.2	164.2	150.2
Sc	11.0	11.0	11.0	11.0	13.0	11.6	10.0	18.0	12.0	11.0	13.0	8.0	8.0	7.0
Sr	322.0	387.8	349.7	400.0	423.0	393.0	372.1	318.3	397.2	416.0	460.1	350.9	341.6	356.3
Ta	1.6	1.9	1.5	1.8	0.7	0.9	1.6	1.5	0.5	1.0	0.9	1.4	1.3	1.4
Th	11.6	21.2	11.3	15.5	6.7	5.5	14.8	13.8	11.7	8.0	9.4	9.3	10.7	11.6
U	2.6	6.3	4.1	3.8	2.9	2.3	3.8	3.6	3.0	2.8	3.0	2.9	3.3	4.6
V	97.0	91.0	78.0	91.0	99.0	87.0	80.0	128.0	100.0	89.0	98.0	49.0	47.0	45.0
Zr	381.6	319.6	175.9	266.6	174.2	162.0	197.0	294.4	194.0	214.0	190.9	205.9	193.2	186.8

Co	11.3	10.2	10.2	12.7	11.3	11.0	8.9	11.7	11.1	6.1	12.1	6.1	6.1	5.3
Cr	60.0	30.0	30.0	20.0	40.0	21.0	30.0	60.0	40.0	30.0	40.0	20.0	20.0	20.0
Ni	19.0	8.2	6.9	6.1	7.7	7.0	5.6	11.2	8.9	7.7	11.0	2.3	1.7	1.7
Cu	250.0	23.2	187.0	17.8	3.5	13.0	5.4	23.6	5.4	99.1	16.9	6.4	3.7	4.9
Mo	0.1	0.1	1.0	0.4	<0.1	<5.0	0.1	0.1	0.1	<0.1	0.6	0.2	0.2	0.2
Pb	5.0	3.1	5.3	3.2	6.0	17.0	5.0	20.6	3.7	2.4	3.4	5.8	5.0	5.0
Zn	51.0	56.0	45.0	58.0	44.0	69.0	48.0	71.0	32.0	90.0	27.0	41.0	47.0	28.0
Y	36.1	36.8	30.2	31.1	25.7	22.0	36.9	47.9	15.6	22.3	23.5	29.6	27.4	28.9
La	56.5	51.3	26.5	41.3	30.1	30.6	38.5	30.5	40.7	37.9	33.7	22.2	25.7	22.3
Ce	118.9	104.0	54.3	85.9	65.1	49.0	78.9	69.8	70.3	77.4	68.6	47.6	54.3	50.9
Pr	14.23	12.17	6.49	9.93	8.08	n.d.	9.08	9.36	7.21	8.74	7.91	6.02	6.51	6.28
Nd	51.2	42.1	24.0	34.3	27.5	22.0	31.5	38.4	23.8	29.6	27.5	22.2	23.8	24.6
Sm	8.80	7.67	5.15	6.52	5.90	5.20	6.33	8.67	3.74	5.41	5.19	4.98	4.98	5.20
Eu	1.60	1.07	0.95	1.28	1.15	1.20	1.07	0.98	0.81	1.23	0.96	1.09	1.06	1.07
Gd	7.68	6.74	5.07	5.69	5.01	n.d.	5.83	8.79	3.38	4.30	4.41	4.90	4.64	4.84
Tb	1.36	1.29	1.03	1.08	0.97	0.50	1.17	1.58	0.60	0.86	0.87	0.98	0.95	0.99
Dy	5.97	6.18	4.63	5.05	4.81	n.d.	5.77	7.78	2.54	3.84	3.91	4.52	4.14	4.83
Ho	1.19	1.26	1.00	1.04	0.94	n.d.	1.18	1.55	0.51	0.82	0.76	0.96	0.83	0.99
Er	3.21	3.37	2.95	2.89	2.47	n.d.	3.26	4.17	1.40	2.03	2.18	2.62	2.34	2.71
Tm	0.56	0.58	0.47	0.51	0.44	n.d.	0.55	0.66	0.22	0.36	0.37	0.43	0.44	0.43
Yb	3.21	3.51	2.93	2.86	2.38	2.60	3.52	4.09	1.55	1.89	1.94	2.65	2.39	2.53
Lu	0.50	0.61	0.48	0.47	0.39	0.39	0.57	0.65	0.25	0.30	0.32	0.45	0.36	0.41

n.d. – not determined

5.4.1. Major element geochemistry of mafic microgranular enclaves (MME)

Dark grey and pale grey MME, as in the host granites, exhibit both similarities and differences in the amount of major, trace and rare earth element composition (Table 6).

The samples of dark grey MME (dgMME) are generally characterized by low content of SiO₂ (65.6-59.4.0wt%), moderate Al₂O₃ content (16.6-15.8wt%) and high content of both Fe₂O₃ (7.1-4.5wt%) and MgO (2.9-1.6wt%) compared to the pale grey host granites (pgHG). Furthermore, the dark grey MME contain demonstrably higher amounts of CaO (4.6-3.1wt%), Na₂O (4.8-3.6wt%) and lower K₂O content (3.7-2.3wt%). These granites reveal also a higher amount of TiO₂ (1.2-0.9wt%), MnO (0.2-0.04wt%) and P₂O₅ (0.44-0.15wt%).

The LOI (2.0-0.4wt%) value and S_{tot} (1.1-0.01wt%) content are relatively low, and point to a low degree of hydrothermal alteration connected with ore mineralization. However, in some samples, increased contents of Cu (up to 250 ppm), Zn (up to 90 ppm) and Pb (to up 21 ppm) were determined.

Pale grey MME (pgMME) samples have markedly higher content of SiO₂ (70.1-68.0wt%) and lower of Al₂O₃ (15.4-14.5wt%), Fe₂O₃ (3.7-3.2wt%), and especially MgO (0.9-0.8wt%) in comparison with the dark grey MME (dgMME). Furthermore, in the studied pale grey MME (pgMME) both CaO (2.8-2.4wt%) and Na₂O (4.3-3.9wt%) contents are lower than in the dark grey MME (dgMME). On the other hand, the pale grey MME samples are slightly enriched in K₂O (3.2-3.1wt%). The amounts of TiO₂ (0.5wt%) as well as of P₂O₅ (0.1wt%) and MnO (0.1wt%) are somewhat lower than in the dark grey MME samples (dgMME). Generally, the pale grey MME samples exhibit no hydrothermal alteration what is demonstrated by lower LOI and S_{tot.} contents, but some of them show low degree of hydrothermal ore mineralization.

On the Harker variation diagrams (major oxides vs silica diagrams – Fig. 36), Al₂O₃, Fe₂O₃, MgO, CaO, Na₂O, TiO₂, P₂O₅ and MnO show continuous trends and exhibit negative correlations whilst K₂O shows positive correlations.

5.4.2. Trace element geochemistry of mafic microgranular enclaves (MME)

The dark grey MME samples (dgMME), compared to the pale grey host granites (pgHG), are characterized by high content of Ba (798.1-421.0 ppm) as well as Sr (460.1-318.3 ppm), whereas the content of Rb (169.3-52.7 ppm) is low.

The contents of both LIL (Cs 9.6-3.3 ppm) and HFS elements: Nb (27.3-10.9 ppm), as well as of Ta (1.9-0.5 ppm) and Zr (381.6-162.0 ppm) are variable. In comparison with the pale grey host granites (pgHG), the samples of dark grey MME are enriched in transition elements as: Ni (19.0-5.6 ppm), Co (12.7-6.1 ppm), Cr (60-20 ppm) and V (128-78 ppm).

On the other hand, the pale grey MME samples (pgMME), when compared to the dark grey MME samples (dgMME), exhibit strong enrichment in Ba (782.1-755.2 ppm), moderate enrichment in Rb (169.2-150.2 ppm) and are slightly depleted in Sr (356.3-341.6 ppm). The amounts of Cs (LILE) – 4.2-3.8 ppm as well as of Nb (HFSE) – 16.6-13.9 ppm, Ta (1.4-1.3 ppm), Zr (205.9-186.8 ppm) are variable. These samples are strongly depleted in transition elements: Ni (2.3-1.7 ppm), Co (6.1-5.3 ppm), Cr (20 ppm) and V (49-45 ppm) compared to the former granite subtype.

In general, the MME reveal no simple correlation between LIL, HFS and transition elements versus silica (SiO₂wt%), which is evident on the bivariate plots (Fig. 37).

5.4.3. Normative composition of mafic microgranular enclaves (MME)

The normative composition of the MME studied (Table 7) is calculated using Barth's (1962) petrochemical method. Some dark grey MME samples (dgMME) contain variable amounts of normative *C* (up to 2%) and show lack of normative *di* whereas the majority of them exhibit the occurrence of normative *di* (up to 3%) as well as lack of normative *C*. Furthermore, the amount of normative *hy* is very high and ranges from 11 to 17%. On the other hand, the pale grey MME samples (pgMME) contain normative *C* (up to 1%) and show lack of normative *di*. The content of normative *hy* is lower (up to 7%) than in the former rocks.

Normative composition MME, especially the differences in the content of normative *Q*, *ab*, *an* and *or* is related to the occurrence of the granites studied in different fields on

various classification diagrams. So, in the IUGS classification diagram the dark grey MME samples (dgMME) plot in the Q-monzodiorite/Q-monzogabbro field, whilst the pale grey MME (pgMME) plot in the granodiorite field (Fig. 39).

TABLE 7

Normative composition of mafic microgranular enclaves (MME) (is calculated using Barth's (1962) petrochemical method).

Sample	KH1/3	KH1/6	KH1/9	KH1/10	KH2/3	KH2/4	KH2/5	KH2/6b	KH3/5b	DB5/5	WB102A/7	KH3/2	KH3/3	KH3/4
	dark grey enclaves (dgMME)											pale grey enclaves (pgMME)		
<i>ap</i>	0.83	0.53	0.32	0.53	0.45	0.40	0.32	0.93	0.37	0.51	0.32	0.29	0.27	0.29
<i>il</i>	1.50	1.18	1.14	1.24	1.52	1.44	1.20	1.72	1.34	1.30	1.28	0.74	0.70	0.66
<i>or</i>	12.70	14.65	16.40	18.70	16.05	15.60	22.20	17.65	13.60	17.00	15.85	18.70	18.70	19.80
<i>ab</i>	33.80	40.95	36.85	35.45	40.35	39.50	34.30	42.30	43.10	35.75	39.80	38.90	35.55	35.30
<i>an</i>	16.55	15.45	16.30	16.83	17.78	18.08	15.05	14.30	16.35	14.15	17.15	13.25	11.95	11.25
<i>C</i>	1.71	0.39	0.34	0.0	0.0	0.0	0.0	0.52	0.28	1.56	0.0	0.28	0.57	1.00
<i>di</i>	0.0	0.0	0.0	1.00	3.04	2.60	1.04	0.0	0.0	0.0	0.08	0.0	0.0	0.0
<i>hy</i>	15.36	11.28	10.84	11.04	12.10	11.92	10.02	16.88	13.22	10.78	11.42	7.16	6.64	6.48
<i>Q</i>	17.46	15.56	17.84	15.21	8.71	10.46	15.87	5.70	11.74	18.94	14.10	20.67	25.62	25.21
Total	100.10	99.99	100.00	100.00	100.00	100.00	100.00	100.00	100.00	99.99	100.00	99.99	100.00	99.99

On the other hand, on the Q'-ANOR diagram (according to Streckeisen, Le Maitre, 1979) the dark grey MME (dgMME) plot in the Q-monzodiorite/Q-monzogabbro field, similar to in the former classification diagram but also on the boundary of the Q-monzodiorite/Q-monzogabbro with the monzonite field (Fig. 38). The pale grey MME samples (pgMME) plot in granodiorite field (Fig. 38), as in the former classification diagram.

The pale grey MME (pgMME) plot in the Ab-An-Or diagram (after O'Connor (1965) modified by Barker (1979)) fall invariably into the granodiorite field (Fig. 40). Only some samples of the dark grey MME (dgMME) plot in the granodiorite/tonalite and in tonalite fields (Fig. 40).

5.4.5. Petrochemical characteristics of mafic microgranular enclaves (MME)

The petrographic characters of both the dark grey and pale grey MME and their positions on various petrochemical classification diagrams are strictly connected to their compositional differences. Generally, the chemical compositions of the dark grey MME (dgMME), reveal their affinities to intermediate/basic plutonic rocks. On the other hand, the pale grey MME (pgMME) exhibit some features resembling the pale grey granite (their host rock). Actually, the weak hydrothermal alteration observed in the dark grey MME

(dgMME) has caused both their different positions in various fields of classification diagrams and variable formal nomenclature of the granites studied compared to their modal classification (see: Chapter 5.2. Petrography of mafic microgranular enclaves (MME)). It is related to the variable contents of alkali elements (Na_2O and K_2O) and to lesser amount to the CaO in the dark grey and the pale grey MME subtypes.

In the R1-R2 multicaticonic diagram, the dark grey MME samples (dgMME) plot in the monzodiorite and tonalite field, whereas the pale grey MME samples (pgMME) plot in the granodiorite field (Fig. 41).

On the other hand, in the $\text{Na}_2\text{O}+\text{K}_2\text{O}$ vs SiO_2 diagram after Middlemost (1994), the dark grey MME samples (dgMME) fall into several fields from diorite and granodiorite through monzonite to quartz monzonite (Fig. 42), whereas the pale grey MME samples (pgMME) plot in both the granodiorite and the granite fields. In contrast, in the similar $\text{Na}_2\text{O} + \text{K}_2\text{O}$ vs SiO_2 diagram after Cox et al. (1979) and modified by Wilson (1989), the MME samples fall in several fields. For example, the dark grey MME (dgMME) in the Q-diorite (granodiorite) or syenodiorite fields, and the pale grey MME (pgMME) in the Q-diorite (granodiorite) or granite fields (Fig. 43). These differences are due to relationships between the content of alkalis, especially K_2O , and to lesser degree to the Na_2O content in all the samples of the MME studied.

In the Q-P diagram (Debon, Le Fort 1988), the dark grey MME samples (dgMME) are situated in the granodiorite and Qtz-monzodiorite fields, but the pale grey MME samples (pg MME) are situated in the granodiorite/adamellite fields (Fig. 44).

Futhermore, the projection points on the K_2O vs Na_2O diagram (Fig. 45) fall into different fields: tonalite, granodiorite (dark grey MME) and granodiorite fields (pale grey MME).

All of the MME, like the host granite samples, commonly exhibit calc-alkaline trend on the $\text{Na}_2\text{O} + \text{K}_2\text{O}-\text{CaO}$ vs SiO_2 diagram (Frost et al. 2001) (Fig. 46).

The pale grey and dark grey MME samples exhibit generally high-K characteristic (Fig. 47). However, some samples of the MME are also medium-K. The agpaite index (the molar $\text{Na}+\text{K}/\text{Al}$ ratio after Liégeois, Black 1987) is < 0.87 for all the MME samples, e.g. in the dark grey it is 63-0.53 and in the pale grey samples 0.68-0.66.

The MALI value (according to Frost et al. 2001) slightly increases with the increase of SiO_2 content and ranges in the dark grey MME (dgMME) from 2.0 to 4.2 and in the pale grey MME (pgMME) from 4.5 to 4.8. In general, the MME samples are mainly metaluminous to slightly peraluminous (Fig. 48). Consequently, the ASI index (after Zen 1986) is varying in the dark grey MME (dgMME) from 0.89 to 1.08, whilst in the pale grey MME samples (pgMME) it is somewhat higher (1.01-1.06).

On the $\text{FeO}_t/(\text{FeO}_t + \text{MgO})$ vs SiO_2 diagram (Debon, Le Fort 1988 – Fig.50) as well as on the $\text{Mg}/\text{Mg}+\text{Fe}$ vs $\text{Fe}+\text{Mg}+\text{Ti}$ cationic diagram (Frost et al. 2001– Fig. 49), the majority of the samples of the MME fall into the magnesian series field. Nevertheless, on the latter diagram the pale grey MME samples plot in the ferriferous series field (Fig.49). The #Mg number ($\text{\#Mg} = \text{MgO}/(\text{MgO} + 0.9\text{FeO}_t)$) is moderate (0.40-0.30) in the dark grey MME (dgMME) and low (0.20-0.30) in the pale grey MME (pg MME). The Fe^* number ($\text{Fe}^* = \text{FeO}_{\text{tot}}/(\text{FeO}_{\text{tot}} + \text{MgO})$) of the dark grey MME samples (dgMME) is high (0.68-0.77) whereas in the pale grey MME enclave samples (pgMME) increases to 0.80.

The mineral character of the MME studied is apparently clearly characterized based on the A-B multicationic diagram (after Debon, Le Fort 1983). All the samples show mixed characteristics of IV hbl and III bt granite types, containing hornblende and/or biotite as the main ferromagnesian minerals (Fig. 51).

The MME studied are characterized by different contents of CaO, Na₂O, K₂O, Ba, Sr and Rb. Nevertheless, on the ternary Ba-Rb-Sr diagram (according to El Bouseily, Sokkary 1975), all the samples of MME plot in the field of poorly evolved granites (Fig. 52). On the Sr vs Ba diagram (Hawkesworth et al. 1991), both the dark grey MME samples (dg MME) and the pale grey MME samples (pg MME) exhibit mixed character and belong to HiBaSr granites (Sr > 300 ppm) (Fig. 53).

5.4.6. Tectonic setting characteristics of mafic microgranular enclaves (MME)

The MME samples fall on several diagrams of tectonic classifications in various fields. Therefore, it is difficult to characterize their paleotectonic setting based only on geochemical data. As already mentioned, distinct differences in the contents of CaO, Na₂O and K₂O in the MME also renders it difficult to indicate their precise setting. Consequently, this problem calls for a more general discussion.

All the samples of MME belong to I types granites (Fig. 54). They not only have a mineral composition which is characteristic of these types of granites (rock-forming minerals: hornblende, biotite and accessory minerals: titanite and apatite as inclusions in hornblende and biotite) but also geochemical features (Na₂O > 3.2wt%, the A/CNK ratio < 1.1) (Chappell, White 1974).

On the R1-R2 diagram (Batchelor, Bowden 1985 – Fig. 55), the samples of dark grey MME (dgMME) exhibit distinct differences, indicating a tectonic setting. They are plotting partly in the post-collision uplift and also in the pre-plate collision granite fields. The pale grey MME samples (pgMME) plot in the pre-plate collision granite field.

However, in the Hf-(Rb/10)-Tax3 diagram (Harris et al. 1986), the MME samples are grouped both in the volcanic arc and collisional granites fields (Fig. 56a). On the other hand, in the Hf-(Rb/30)-Tax3 diagram, the MME samples plot mainly in the volcanic arc granite field and some samples of the dark grey MME (dgMME) also plot in the late and post-collisional granite field (Fig. 56b).

According to Maniar and Piccoli's (1989) classification, based merely of major elements (MgO/FeO_{tot}, Na₂O/K₂O and MgO/MnO ratios), the MME samples exhibit mixed/composite geotectonical character of the island arc (IAG), continental arc (CAG) and continental collision granites (CCG) (Fig. 57).

On the grounds of classical geotectonic diagrams, based on more or less immobile trace elements (Pearce et al. 1984): Nb vs Y and Ta vs Yb (Fig. 58a, b), Rb vs Nb + Y, Rb vs Yb + Ta (Fig. 58c, d), the pale grey MME studied (pgMME) generally show geochemical characteristics of VAG granites (VAG + synCOLG granites), whereas the dark grey MME (dgMME) mainly have similar geochemical characteristics to the former (the VAG granites and the VAG + syn COLG granites, respectively), but some samples have the WPG granite characteristics. Nevertheless, on the Rb/Zr vs Nb and Rb/Zr vs Y diagrams (Fig. 59) all the samples are plotted in 'the N-arc' – the normal continental arc granites field (according to Brown et al. 1984).

On the other hand, in the modified Rb vs Y+Nb diagram (Pearce 1996), all the samples of MME plot in the field of post-collision granites (Fig. 60). However, on the (Rb/100)-Tb-Ta diagram (Thiéblemont, Cabanis 1990), all the MME samples fall mainly in the post-collisional and syn-subductional granite field (Fig. 61).

5.4.7. Geochemical patterns: chondrite-normalized spider diagrams of mafic microgranular enclaves (MME)

The chondrite-normalized trace element patterns of the dark grey (a) and pale grey MME studied (b) are presented in Figure 66. These diagrams indicate that both subtypes of the MME have similar regular geochemical patterns. The dark grey MME show the enrichment in LILEs (Rb, K), Nd, and HFSEs (La, Zr, Hf, Tb) relative to LILEs (Ba, Sr), HFSEs (Nb, Ta, Ti) and P. Similar geochemical patterns have the pale grey MME samples but exhibit Th negative anomaly and lack of Ta negative anomaly. These diagrams are evidence of the higher level of LIL elements relative to the HFS elements and the geochemical patterns characterized by a smooth slope down to the right.

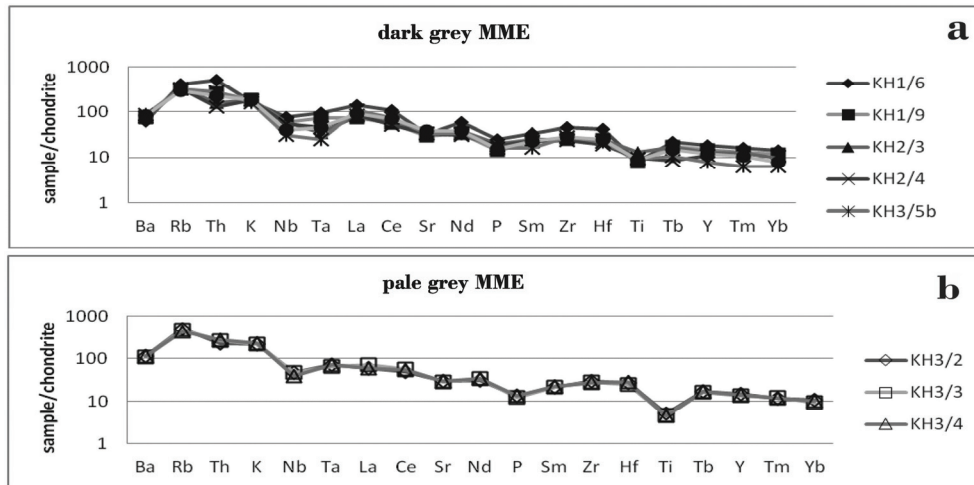


Fig. 66. The chondrite-normalized trace element patterns for selected samples of the PG granites: a. – dark grey MME; b. – pale grey MME.

The chondrite normalized REE patterns (Fig. 67) exhibit an Eu negative anomaly ($Eu/Eu^* = 0.34-0.78$) or $Eu = Eu_N / (Sm_N + Gd_N) / 2$ is 0.34-0.76, and a depletion in HREE (especially Yb) in the samples of both the dark grey and pale grey MME. The MME are characterized by low LREE/HREE fractionation ($(La/Yb)_N = 5.0-17.7$). For the dark grey MME (dgMME) it is 5.0-17.7, and for the pale grey MME (pgMME) it is 5.5-7.3. In the dark grey MME (dgMME), the content of Y amounts to 15.6-47.9 ppm and of Yb to 1.6-4.1 ppm. The samples of the pale grey MME (pgMME) contain similar amounts of Y and Yb. All the samples of the dark grey MME (dgMME) display very distinct variations of $\sum REE$ (155.2-274.9 ppm) but the pale grey MME samples (pgMME) exhibit lower $\sum REE$ (121.6-132.4 ppm).

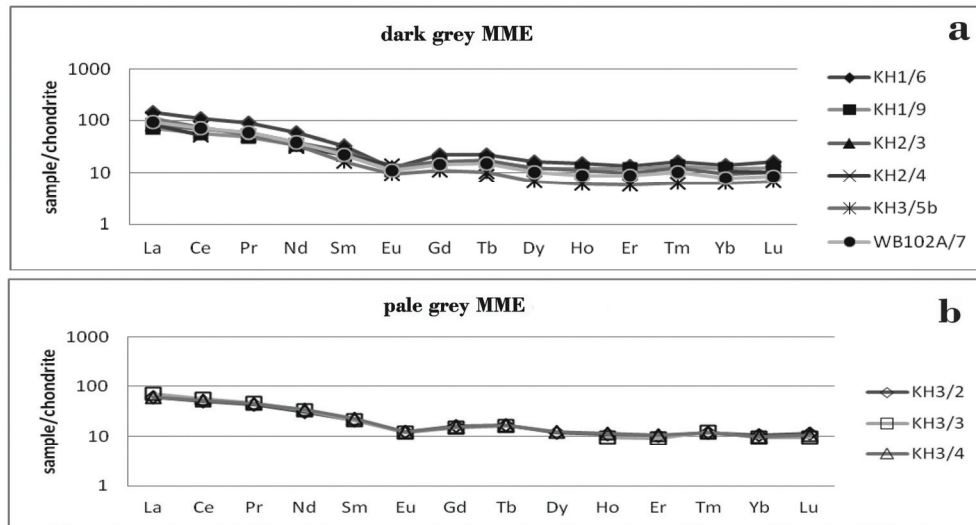


Fig. 67. The chondrite-normalized REE patterns for selected samples of the PG granites: a. – dark grey MME; b. – pale grey MME.

5.4.8. Isotope data of mafic microgranular enclaves (MME)

The Sr-Nd isotopic data for the dark grey and the pale grey MME are presented in Table 8. These samples are scattered and plot more closely the continental crust field, but also on the 'orogenic mantle array' trend (Fig. 64). The values of $^{86}\text{Sr}/^{87}\text{Sr}_{(i)}$ vary from 0.709593 to 0.713297, whereas $\varepsilon\text{Nd}_{(i)}$ shows values from -3.4 to -4.2. The isotopic data was recalculated to the granites age (300 Ma), which was determined by Jarmolowicz-Szulc

TABLE 8

Mafic microgranular enclaves (MME) – Sm-Nd isotope data.

Samples	KH1/6	KH1/10	KH2/3	KH3/5b	WB102A/7	KH3/4
	dark grey enclaves (dgMME)			pale grey enclaves (pgMME)		
Sm(ppm)	7.198972	6.116991	5.658843	3.925000	4.171721	0.734751
Nd(ppm)	36.87254	31.76352	27.87844	22.822981	20.83199	43.88444
$^{147}\text{Nd}/^{144}\text{Nd}$	0.118025	0.116418	0.122708	0.103931	0.121058	0.134099
$^{143}\text{Nd}/^{144}\text{Nd}$	0.512261	0.512283	0.512315	0.512257	0.512284	0.512301
2σ	0.000007	0.000007	0.000004	0.000007	0.000003	0.000004
$^{87}\text{Sr}/^{86}\text{Sr}$	0.713135	0.711624	0.710688	0.710444	0.709593	0.713297
2σ	0.000017	0.000016	0.000011	0.000008	0.000011	0.000012
CHUR $\varepsilon\text{Nd}_{(0)}$	-7.4	-6.9	-6.3	-7.4	-6.9	-6.6
CHUR $\varepsilon\text{Nd}_{(300)}$	-4.2	-3.7	-3.4	-3.7	-3.9	-4.1

(1984, 1985), Żelaźniewicz et al. (2008) and Nawrocki et al. (2008). The samples of both the dark grey MME and the pale grey enclaves plot on the $^{86}\text{Sr}/^{87}\text{Sr}$ vs SiO_2 and the $^{143}\text{Nd}/^{144}\text{Nd}$ vs SiO_2 diagrams near the field of crust composition (Fig. 65a, b).

6. Discussion

6.1. Variscan volcano-plutonic magmatic activity

In the broad tectonic zone (the Kraków-Lubliniec Fault Zone) separating the Upper Silesian Block (USB) and the Małopolska Block (MB), a manifestation of the Variscan magmatism episode (Carboniferous/Permian age) is well documented. Several generations of investigators determined mineral and geochemical characteristics of both volcanic and plutonic magmatic rocks (see Chapter 3: Magmatic rock investigations). The Variscan volcano-plutonic magmatic activity is related to the development of not only volcanic rocks on the surface in the Krzeszowice area but also the granitoid pluton and/or batholith in the deeper levels of the Małopolska Block (MB) basement. The occurrence of plutonic as well as volcanic rocks may be connected to continued incremental input of magma in this region during long-lived magmatic activity of the Carboniferous/Permian age (Żelaźniewicz et al. 2008; Słaby et al. 2010).

The plutonic rocks (granitoids) were founded in several boreholes in four areas of the Małopolska Block (MB): Dolina Będkowska valley, Pilica, Zawiercie and Myszków-Mrzygłód. In many papers (see Chapter 3: Magmatic rock investigations), their similar petrographic features, mineral features and textural characteristics were described. According to geophysical investigations, the conclusion that these granodiorites are an apical part (hypabyssal level) of a deeper seated large batholith (Żaba 1999; Żelaźniewicz et al. 2008) was accepted. They are represented by a pale grey granodiorite that is coarse- to medium-grained, equigranular and has a holocrystalline structure. Sometimes, the inequigranular variety of granodiorites that is characterized by 'porphyritic' textures (Płonczyńska 2000; Harańczyk et al. 1995) was also mentioned. The spatial correlation between equigranular and inequigranular textural varieties is difficult to define because the geometry and architecture of granodioritic intrusions were only determined by deeper boreholes (Harańczyk 1984, Harańczyk et al. 1995) and geophysical investigations (Królikowski, Petecki 1995; Podemski 2001).

New investigations of granitic batholiths, easily accessible on the surface (e.g. Sierra Nevada, see Mahan et al. 2003), provide information about their formation and accumulation. Large plutons may commonly be formed, in a manner analogous to the growth of crack-seal veins (Ramsay 1980), by amalgamation of numerous small intrusions (sheet intrusions according to Mahan et al. 2003) similar in composition and origin that exhibit internal cryptic contacts – the occurrence of inner porphyritic facies and no evidence of chilling at any contacts (Glazner et al. 2004). In the large granite plutons, the rock textures were homogenized by post-emplacement annealing that obscured internal contacts (Glazner et al. 2004). It makes it more difficult to recognize and describe their prevalence and abundance. A similar scenario for the formation and accumulation of a granitoid batholith in the Małopolska Block (MB) basement during the Variscan magmatic activity was not excluded.

6.2. Petrography of contrasted rocks – MME and host granites

The mineralogy and structures/textures of the Małopolska granitoids reflect a complex history and different conditions of magmatic crystallization in high-level magma chambers (Harańczyk et al. 1995; Żaba 1999; Płonczyńska 2000; Żelaźniewicz et al. 2008). Based on the present investigations, these magmatic rocks may be subdivided into two types on the grounds of different structural/textural and mineralogical features – host pale grey granites (HG) and mafic microgranular enclaves (MME).

The first type (HG) commonly form large magmatic plutons (Fig.1). They are represented by pale grey, coarse- to medium-grained, equigranular, homogenous granodiorites (pgHG) (Fig. 3). Their inequigranular varieties are rarely observed. Though nearly all minerals are of a similar size in host granites, some of them, especially plagioclases and less frequently quartz, form larger crystals and may be called ‘megacrysts’. In this case, the host granites display a distinct ‘porphyritic’ structure. In contrast, amphiboles commonly occur as large aggregates/glomerocrysts of small clots and rarely as simple crystals. The latter formed during disruption and penetration of amphibole aggregates/glomerocrysts by magmatic melt.

On the other hand, the granites of contact zones with sedimentary rocks (cHG) have a greyish white or pale pink colour (Fig. 4). It is caused by alteration of primary plagioclases and dark minerals (amphiboles and biotite) in outer parts of the pluton. The contact host granites (cHG) exhibit similar structures, textures and grain size to the pale grey host granites (pgHG).

The second type is represented by dark enclaves (resembling MME with characteristic ‘porphyritic’ textures described by Didier 1973; Didier, Barbarin 1991) in the pale grey host granites. They differ from those described above in colour and structural and textural features. The contacts between these enclaves and the host magmatic rocks (the pale grey granites) are sharp (Fig. 19). The MME are represented by ‘porphyritic’ Q-diorites and tonalites, characterized by variable shades from dark to pale grey (Fig. 20 and 21). It is connected to a different content of felsic minerals in the enclaves studied, compared to the amount of femic minerals (mainly amphiboles and biotites). The original composition of the MME (former blobs of mafic magma) were likely modified by interaction with felsic magma (the host granites) in a similar way as described by Waight et al. (1998). The ‘porphyritic’ MME have typical inequigranular structure in which the large individual megacrysts/xenocrysts of plagioclases (Fig. 24) and the aggregates/glomerocrysts of amphiboles (Fig. 28), rarely alkali feldspar or quartz megacrysts/xenocrysts, occur in fine-grained groundmass that shows pseudo-doleritic structure, manifested by characteristic arrangement of plagioclase plate-laths and needle-shaped crystals of amphibole and acicular-shaped apatite (Fig. 26).

The mineral composition of both the MME and host granites studied is similar but varies in modal proportion of plagioclase, quartz, alkali feldspar, biotite, amphibole and accessory minerals (titanite, epidote/zoisite, zircon, apatite and opaque minerals, allanite)(Tables 1 and 2). The occurrence of two different types of feldspars (plagioclases and alkali feldspar), corrosion and regrowth of quartz grains and sericite patches in plagioclase crystals – all of these features suggest the formation of these rocks under conditions of high P_{H_2O} and activity of O_2 in subsolvus environment (Clarke 1992; Shelly

1993). The presence of different primary and secondary minerals (amphibole, biotite and chlorite) is related to their growth as subsolidus minerals during the interaction of solid rocks with high-temperature hydrothermal fluids (Wilson 1989).

In the samples from the contact of the host granites, the plagioclases show distinct replacement by perthite, inclusion and veinlets of K-feldspar, whereas the dark minerals are completely altered to chlorite. Allanite occurs as accessory minerals mainly in the contact host granites (Fig. 18). The occurrence of allanite in highly differentiated granites was defined by Hoshino et al. (2007).

Differences in the modal composition of both host granites and MME are illustrated in the IUGS classification diagram, where their projection points are scattered in several fields: from Q-diorites through tonalites to granodiorites/granites (Fig. 5, 23). The M' index (the colour index) is variable and increased in some samples. Consequently, the rocks in question are subdivided partly into 'leuco varieties', e.g. leuco-Q-diorites, leuco-tonalites and leuco-granodiorites. Contact host granites (cHG) have low M' index (< 2.5) and obviously belong to leuco-granodiorites.

Inner textures in rock-forming minerals

The inner textures in rock-forming minerals of the Małopolska granites as well as in the MME are described for the first time. The characteristic texture in rock-forming minerals of granitic rocks from various granitic batholiths was described by Hibbard (1991), Vernon (1990, 1991), Barbarin (1990), Baxter and Feely (2002), Janoušek et al. (2004), Słaby and Martin (2008), Pietranik and Koepke (2009) and Catlos et al. (2011) as evidence of mafic/felsic magma mixing, and by Catlos et al. (2011) as evidence of tectonomagmatic history.

Plagioclase megacrysts - mantled boxy cellular crystals

The composition of plagioclase of the rocks studied is presented on the triangular classification diagram (Ab-An-Or) (Fig. 7, 25). In the MME, the plagioclase megacrysts/xenocrysts (Fig. 24) are frequent (up to 23vol%), especially in the dark grey MME samples (Table 2). In the pale grey MME, their content is lower (up to 11vol%). In the host granites showing 'porphyritic' structure, the occurrence of larger plagioclase crystals is also observed (Fig. 6). In both rock types (the MME and the host granites), the mantled boxy cellular plagioclase megacrysts/xenocrysts are present. Plagioclase mantled megacrysts/xenocrysts have composite inner textures of 'old cores' and combinations of several discontinuous/continuous, oscillatory and convolute zones in outer zones (Fig. 24). The inner textures of 'old cores', frequently observed in both subtypes of MME and in the host granites, are unhomogenous 'patchy', and show boxy cellular growth/regrowth textures, spike zones and spongy cellular dissolution/melting zones (Fig. 24). The 'old cores' consist of labradorite (Ab₃₉₋₄₇) with irregular intergrowths of andesine and oligoclase. According to Hibbard (1991), the occurrence of the resorption-regrowth textures (mixing textures) in 'old cores' may be connected with the superheating of felsic magma, and a generation of processes of partial melting or dissolution or growth/regrowth of pre-mixing crystals during mafic/felsic magma mixing. Inner zones of other plagioclase crystals commonly consist of andesine (Ab₅₃₋₆₇), whilst outer zones display oligoclase (Ab₇₁₋₈₁) composition.

In the host granites, the occurrence of larger plagioclase crystals is also observed. Plagioclases exhibit similar inner textures of their cores to plagioclase megacrysts/xenocrysts in the MME. They also have unhomogenous, patchy 'old cores' of labradorite composition (Fig. 6) surrounded by intergrowths of more Na plagioclases which form simple, continuous and concordant zoning. In the host granites, plagioclase crystals commonly exhibit andesine-oligoclase composition and simple, concordant zoning that was described earlier by Płonczyńska (2000) and Żelaźniewicz et al. (2008) in granodiorites from the Małopolska Block (MB). In both rocks studied, the occurrence of resorption zones between the inner and outer rim of plagioclase megacrysts/xenocrysts is observed (Fig. 6, 24).

The mantled boxy cellular plagioclase megacrysts/xenocrysts may be of different origin e.g. from: host granites, primary mafic magma, differentiated and assimilated mafic magma, palinogenetic felsic magma or continental crust metamorphic rocks. Castro and Stephens (1992) described the occurrence of similar 'relic' An-rich cores in plagioclases from granodiorites, and suggested their origin as xenocrysts incorporated to granodiorite magma from lower continental crust rocks. Meanwhile, Wiebe (1968) suggested that calcic cores with anorthite-rich 'spike' zones in the plagioclase crystals derived from the mafic magma. In contrast, White and Chappell (1977) interpreted similar plagioclase Ca-rich cores as remnants of restite. Based on the studies of Clemens et al. (2011), it may be accepted opinion that plagioclase 'old cores' represent either restitic phases (residual primary crystals) or peritectic phases (minerals generated by the melting reactions in the early stages of fractional crystallization).

Słaby and Götze (2004) and Wnorowska (2006 vide Słaby, Martin 2008), based on the cathodoluminescence study of the Karkonosze granites, provided information that the plagioclase megacrysts migrated between mixed mafic and felsic environments during crystallization. More extensive mixing in the magma chamber caused the transfer of plagioclase phenocrysts from felsic magma to the MME (Waight et al. 2000; Słaby, Martin 2008). Similar episodes of resorption and regrowth in plagioclase crystals as a result of rapid changes in magma composition related to magma mixing were described in the Karkonosze granitic pluton by Słaby and Götze (2004) and Słaby and Martin (2008). The occurrence of similar plagioclase megacrysts/xenocrysts in the MME and in the host granites studied imply that they are peritectic minerals (according to the terminology of Clemens et al. 2011) and may be originated from the granodioritic magma chamber.

The resorption zones in the plagioclase megacrysts were generated by rapid magma decompression during ascent, as described by Nelson and Montana (1992). In the rocks studied, internal resorption surfaces in the plagioclase megacrysts/xenocrysts at the boundary between 'old cores' and outer simple zoning suggested a decompression process related to mixing between mafic and felsic magmas. Pietranik and Koepke (2009) implied that plagioclase megacrysts (the Gęsiniec Intrusion) preserve a record of mixing between felsic and mafic magmas, and that their compositional zoning patterns are related to fractional crystallization in closed system and interrupted by resorption, probably induced by decompression. Numerous resorption zones in plagioclase megacrysts were defined by Hattori and Sato (1996), Tepley et al. (2000), Waight et al. (2000) as formed during injections of mafic magma into the felsic magma chamber with subsequent homogenization and hybridisation. Catlos et al. (2011) suggested that plagioclase crystals are useful in

recording the tectonomagmatic evolution of granites because they preserve compositional zoning and microcracks features in Ca-rich cores. Microcracks are commonly indicators of the deformation history of rocks and minerals and form due to thermal contraction during cooling, tectonic stress and relaxation at uplift conditions (Wang et al. 1989; Åkesson et al. 2004). Microcracks in 'old cores', and at the boundary between 'old cores' and outer zoned rim in the plagioclase megacrysts/xenocrysts of both types of rocks studied, are observed. It is likely that they developed during magma mixing and during later tectonic deformation related to uplift, in a similar way to that described by Janoušek et al. (2004). In the studied rocks, microcracks in the plagioclase megacrysts are also connected to decompression related to granitic magma ascend to the surface. Similar mechanism of microcracks formation was defined by Pietranik and Waight (2008).

Plagioclase megacrysts with biotite/hornblende zones

In the megacrysts/xenocrysts of plagioclases that occur both in the MME and host granites, the texture of concentric zones of biotite/hornblende inclusions is observed (Fig. 6, 24). They are similar to the 'biotite/hornblende zone' within larger plagioclase crystals described by Hibbard (1991). This texture can only be formed when plagioclases are in a relatively early crystallizing phase in the more felsic melt and are compatible with processes of felsic/mafic magma mixing.

Plagioclase lath-shaped crystals in the groundmass

The fine-grained groundmass is only observed in MME (both the dark and pale grey subtypes). It is composed of small lath-shaped plagioclases (Fig. 26) which are characterized by simple normal zoning: more calcic core (labradorite composition) and more sodic rim (oligoclase composition). These crystals were formed during fast crystallization, favoured by a high nucleation rate (Brandeis et al. 1984). As described by Hibbard (1991), the cores are related to an early stage of crystallization of more mafic primary magma, whereas the more sodic rims reflect late-stage 'equilibration' of the hybrid system. The presence of various sizes of plagioclase crystals (megacrysts/xenocrysts as well as lath-shaped plagioclases) in the MME studied may be dependent on cooling rate and their thermal history above the liquidus in igneous systems (Pupier et al. 2008a, b), and indicate the presence of a magma mixing process (Salisbury et al. 2008).

Quartz megacrysts/xenocrysts

Quartz megacrysts/xenocrysts ('ocelli') occur in both pale grey and dark grey MME. They show strong undulose extinction, granulation and mortar texture. The quartz megacrysts/xenocrysts have characteristic rims (coronas) with symplectite intergrowth of quartz, oligoclase and K-feldspar – myrmekite like intergrowth (Fig. 27), resembling Vernon's 'ocellus' (1991) and Hibbard's 'ocellar rims' (1991). They are surrounded by tangentially oriented mafic mineral (biotite plates) and plagioclase laths. This process is related to crystallization of fine-grained aggregates of mafic minerals at magma saturation condition (Vernon 1991). As postulated by Hibbard (1991), these textures developed in a second phase of mixing with more felsic magma and are connected with epitaxial growth of small K-feldspar, oligoclase and biotite crystals on original quartz megacrysts/xenocrysts. These megacrysts/xenocrysts probably originated from the host granites or

came from continental crust metamorphic rocks. According to Elburg (1996), Waight et al. (2000), Słaby et al. (2008), Vernon and Paterson (2008), such quartz megacrysts/xenocrysts, typical of the more felsic magma, occur within the mafic enclaves due to mechanical transfer of these crystals between two contrasting magmas.

The host granites also contain large quartz crystals that, similar to the MME, show cataclastic and deformed features. However, they are rare in these rocks. There are quartz crystals in the Małopolska Block granitoids which show slight dynamic deformations, as mentioned by Płoczyńska (2000). These characteristic features in the quartz crystals from the granites studied suggest their tectonomagmatic evolution.

Quartz crystals in the groundmass

Small anhedral quartz crystals, which occupy interstices between other rock-forming minerals, occur in the groundmass of the MME (Fig. 26). They were probably formed after the magma mixing episode due to infiltration of the leucocratic residual granitic melt, either during the later stage of mafic microgranular enclaves crystallization or shortly after their complete solidification. Pietranik and Koepke (2009) described a similar mechanism of hybridisation in diorites in the Gęsiniec intrusion by leucocratic melt squeezed from the granodiorite at solidus or subsolidus conditions.

Alkali feldspar megacrysts/xenocrysts

Rare alkali feldspar megacrysts/xenocrysts ($\text{Or}_{89-88}\text{Ab}_{11-10}\text{An}_1$) with reaction rims of a symplectite intergrowth of andesine and oligoclase are described in pale grey MME (Fig. 33). These rims may resemble rapakivi textures described by Hibbard (1991) in hybrid granitic rocks. It is thought that these textures developed during mixing processes of mafic/felsic magma when alkali feldspar megacrysts from felsic magma reacted with mafic magma to form plagioclase rims. In the pale grey MME, the alkali feldspar crystals originated from metamorphic wall rocks rather than a granodioritic host. According to studies by Vernon (1991), Elburg (1996), Waight et al. (2000), Słaby and Götze (2004) and Vernon and Paterson (2008), the occurrence of the alkali feldspar megacrysts/xenocrysts in mafic enclaves suggests mechanical transfer of these crystals from the more felsic host magma. It is postulated that the reaction of the mafic melt with these heterogeneous minerals, which probably originated from metamorphic rocks of continental crust rather than from the host host granites, took place in the formation process of the pale grey MME.

Alkali feldspar crystals in the groundmass

Small crystals of alkali feldspars ($\text{Or}_{95-94}\text{Ab}_{6-5}\text{An}_{<1}$) in the interstices between minerals in the groundmass of dark grey MME are rarely observed. They are similar to those observed in the pale grey MME. These alkali feldspars are characterized by larger Or content compared to the composition of the alkali feldspar megacrysts/xenocrysts. In the host granites, alkali feldspars ($\text{Or}_{97-87}\text{Ab}_{13-2}\text{An}_{2-1}$) form medium-sized subhedral and anhedral crystals (Fig. 10). In host granites, alkali feldspars were formed during late-stage differentiation of more-or-less homogenous mixed magma (after a felsic/mafic magma mixing episode). In the MME, small alkali feldspar crystals, similar to quartz crystals, crystallized in the interstices of the groundmass during infiltration of leucocratic residual granitic melt in the late-stage of hybridisation process.

Amphiboles

Amphiboles commonly form aggregates/glomerocrysts of numerous small clots (Fig. 30) and rare individual crystals (Fig. 28, 29), as well as needle-shaped small crystals occurring in the groundmass (Fig. 26).

Amphibole aggregates/glomerocrysts and individual crystals

In both types of granites studied, amphibole crystals are common but occur in variable amounts (Table 1 and 2). In some samples, especially of pale grey enclaves (pgMME) and in the contact host granites (cHG), amphibole crystals are lacking. In both MME and host granites, the margins of amphibole crystals are irregular and corroded (Fig. 16, 29). The biotitization process is overprinted on them (Fig. 15, 28). These features suggest a disequilibrium state of these minerals with magmatic melt. Amphiboles (aggregates/glomerocrysts as well as individual crystals) in both types of rocks studied have similar composition (Fig. 17, 31). They are calcic amphiboles with $Ca_B \geq 1.50$, $Ca_A < 0.50$ and $Na + K < 0.50$ (according to the classification of Leake et al. 1997) and represent hornblendes showing variable #Mg number – from 0.41 to 0.62, corresponding to magnesio- and ferro-hornblendes enriched in Al and Ti to various degrees. Magnesio-hornblende is common in the rocks studied compared to ferro-hornblende, which occurs in the former as inclusions of small clots. The occurrence of two types of hornblende reflects the change in chemical composition of the melt (e.g. decreasing content of TiO_2 and Al_2O_3), not only during differentiation process but also during the mixing of felsic and mafic magmas, or it may be also related to later alteration processes (biotitization). It seems that the latter scenario connected to biotitization processes of amphiboles is more likely in the rocks studied.

Secondary amphiboles in the rocks studied are represented by actinolite (#Mg number 0.52-0.69) and ferroactinolite (in MME). This mineral is poorer in Ti and Al and lower in the sum $Na + K$ (decreasing to 0.25 apfu) and forms irregular patches and veinlets within zoned primary amphibole (Fig. 28).

Some features of amphibole crystals, such as corrosion of margins (Fig. 29), variable composition (Fig. 28), inclusions of frequently acicular apatite and opaque minerals and overprinting on the two stage alteration processes (formation of secondary actinolite and biotite overgrowth) may suggest a long history of their origin and evolution. It seems that the formation of amphiboles (magnesio- and ferro-hornblendes) in the host granites took place during an early stage of magmatic differentiation (probably before mixing) in deeper levels of the lower continental crust or at the crust/mantle boundary. Amphiboles in the host granites, according to Clemens et al. (2011), may represent restitic phases (residual primary minerals) or peritectic phases (mafic minerals formed by the melting reactions in differentiated mafic melt). The second possibility may be more probable. Both rocks studied (host granites and MME) contain aggregates/glomerocrysts of clots, consisting of amphibole, titanite, epidote and opaque minerals (Fig. 15 and 30). This indicates them to be pseudomorphs after primary amphibole and pyroxene (?), as suggested Barbarin and Didier (1991a). It is not obvious because the presence of pyroxene relics was not observed in the granites studied. In the Krzeszowice area, Sutowicz (1982) described the occurrence of relics of clinopyroxene in some amphiboles in volcanic rocks (the Zalas rhyolites). In the rocks studied, amphibole aggregates/glomerocrysts consist of small clots and do not exhibit

marked zoning. It cannot be excluded that their origin may be related to metamorphic rocks. In this case, they may represent relics of amphibolites that occur in deeper parts of lower continental crust. In an Archaean basement of the Upper Silesian Block (USB) amphibolites occurs in the Rzeszotary Block (Żelaźniewicz et al. 2009). Słaby et al. (2010) implied that amphibolites may have contributed to the generation of granodioritic magma within the Kraków-Lubliniec Fault Zone (KLFZ)

The type of fine-grained amphibole aggregates/clots was described by Mason (1990) as the product of metamorphic processes (e.g. cataclasis) in the lower part of the continental crust, where replacing of primary amphibole crystals in protolithic granitic rocks may have taken place. Castro and Stephens (1992) interpreted the occurrence of amphibole clots in granodiorites and associated granitic enclaves as a product of px-melt reaction or solid material (opx) dragged by magmatic melt due to extraction from continental crust metamorphic rocks. According to Clemens et al. (2011), amphibole aggregates in granites may be restitic or peritectic mineral phases. Similarly, Donaire et al. (2005) provide information that clots consisting of late amphibole and biotite may be interpreted as pseudomorphs after earlier magmatic orthopyroxenes. It is more probable that amphibole aggregates in the rocks studied are peritectic minerals which formed in the mafic magma due differentiation processes rather than residual primary minerals from metamorphic protholith.

Amphibole blade-shaped crystals (acicular, needle-shaped) in the groundmass

Characteristic blade-shaped (acicular, needle-shaped) amphibole crystals occur in the groundmass of dark grey MME (Fig. 26, 35). Their characteristic distribution in the rocks studied is connected to the growth processes during the undercooling of mafic melt under conditions of relatively higher nucleation and crystallization rates (Hibbard 1991). Based on experimental studies, Naney and Swanson (1980) suggested that dark minerals nucleate more quickly than feldspars and quartz when temperature decrease to sub-liquidus values during the earliest crystallization phases of magmatic melt. In this case, dark rock-forming minerals coexist with the early crystallized accessory minerals (apatite and opaque minerals). A similar mechanism, described by Donaire et al. (2005), took place in the MME during local interaction between granitic and mafic melt.

Biotite blade-shaped crystals

Biotite in both MME and host granites forms large platy crystals (blade-shaped crystals according to Hibbard, 1991) altered to various degrees (Fig.11). The content of biotite in the rocks studied varies from 16vol% (in dark grey MME), through 11vol% (in host granites) to 6vol% (in pale grey MME). In both rocks studied, biotite represents a late sequence of fractional crystallization after a mixing episode, as indicated by the occurrence of overgrown individual amphibole crystals (Fig. 28) and differently oriented patches/flakes within amphibole aggregates/glomerocrysts (Fig. 15). Biotite is characterized by a high TiO₂ content (up to 5.0wt % in the host granites). The #Mg number ranges from 0.36 to 0.52, and similar values of this ratio were found in both rocks studied. Moreover, in both rocks biotite has high Al^{IV} and Fe_{tot} contents (2.1-2.3 apfu and 2.4-2.5 apfu., respectively). In the composition of biotite in both rocks, the predominance of annite end member (annite-phlogopite series) is markedly visible (Fig. 12, 32). The

occurrence of blade-shaped biotite (so called ‘hydrogenic biotite’ – Hibbard 1991) is observed (Fig.11). It is related to the mixing of an aluminosilicate melt rich in magnesium and iron with a felsic melt rich in potassium (Hibbard 1991).

Biotite crystals are often altered to chlorite as a consequence of interactions with hydrothermal fluids during late stage alteration processes. These processes may be connected with Cu-Mo porphyry deposit mineralization of the Małopolska Block granitoids (see Chapter 3: Magmatic rock investigations).

Accessory minerals

Euhedral morphologies of accessory minerals, and their inclusion in major rock-forming minerals of felsic plutonic rocks, are markedly petrographic criteria that are useful to the interpretation of their early crystallization in melt (Gromet, Silver 1983; Sawka 1988; Shannon et al. 1997; Warner et al. 1998; Hoskin et al. 2000).

Opaque minerals are represented by magnetite, and less commonly by Ti-magnetite and ilmenite. These minerals occur as small inclusions in individual crystals (Fig. 14, 29), in aggregates/glomerocrysts of amphibole (Fig. 15, 30) and rarely in plagioclases. It is postulated that magnetite precipitates simultaneously with/or after amphibole and plagioclase. Hornblende crystals with magnetite inclusions in the rocks studied may be peritectic minerals – products of primary pyroxene (?) or amphibole breakdown (Fig. 15, 30). Magnetite forms homogenous crystals and grains with ilmenite exsolution lamellae. The latter crystals are related to the oxidizing evolution of primary spinels in magmatic melt close to its sub-solidus re-equilibration (Hoskin et al. 2000). The presence of magnetite and ilmenite in granites was also discussed by Ishihara (1977). Clemens et al. (2011) defined the occurrence of ilmenite in granites as one with the peritectic mineral assemblage ($\text{Opx} + \text{Cpx} + \text{Pl} + \text{Ilm} \pm \text{Grt}$) which formed during melting reactions produced during combined biotite-hornblende incongruent melting. Probable source rocks for the host granites studied contain hornblende or biotite (?) (the Rzeszotary amphibolites), and are located in a deeper part of the continental crust – in the basement of the Upper Silesian Block (USB) – as suggested by Żelaźniewicz et al. (2008) and Słaby et al. (2010).

Euhedral zircon crystals, short-and normal- prismatic in shape, formed inclusions in the amphibole (Fig. 14) and biotite (Fig. 11) and rarely in the plagioclase in the two rocks studied (MME and host granites). They are characterized by a similar amount of a Hf admixture (up to 2wt%) in the host granites as well as the MME subtypes. Żelaźniewicz et al. (2008) defined two possible stages of their growth, based on the determined ages of zircons from the Dolina Będkowska valley granodiorite (according to U-Pb SHRIMP II data between 311 Ma and 278 Ma). No old components surviving in the zircon population from the Dolina Będkowska valley granodiorite were observed (Żelaźniewicz et al. 2008). The zircon crystallized at earlier stages of fractional crystallization, in higher temperatures related to the greater degree saturation of a parent magma. The zircon saturation temperature was estimated by Hoskin et al. (2000) to be close to $\sim 700^\circ\text{C}$.

Apatite forms acicular-shaped crystals in most major rock-forming minerals from the groundmass of MME (Fig. 35). The specific shape of the apatite studied is characteristic of mixing textures (Didier 1973; Reid et al. 1983). The apatite shape is considered to be the result of rapid growth of this mineral in a quenched magma (Wyllie et al. 1962) in the mixed mafic/felsic system (Hibbard 1991). Bacon (1989) suggested that these acicular

shaped inclusions of apatite probably formed by local saturation during mineral growth related to crystal-melt interface. In the rocks studied, acicular-shaped apatite crystals occur as inclusions in amphibole (Fig. 14, 28), biotite (Fig. 11) and plagioclase crystals (Fig. 24). Apatite was an early crystallizing mineral in the rocks studied because its estimated saturation temperature is relatively high ($> 800^{\circ}\text{C}$ after Harrison, Watson 1984).

Allanite crystals with repeated oscillatory zones (Fig. 18) occur in the host granites from the contact with metasedimentary rocks. Hoshino et al. (2007) described the occurrence of this mineral in highly differentiated granites. Allanite may crystallize below the critical temperature of about 800°C (Chesner, Ettlinger 1989) in a late stage of magma differentiation.

In the rocks studied, titanite occurs with epidote and opaque minerals in the amphibole aggregates/glomerocrysts (Fig. 15, 30). Secondary titanite formed by partial breakdown of early crystallized minerals (hornblende or pyroxene ?) is related to an increase in f_{O_2} according to Hoskin et al. (2000). It is more likely that the secondary titanite formed in the rocks studied on the similar way.

Late stage of differentiation of more-or-less homogeneous mixed melt

In both types of rocks studied, concentric zones in the outer parts of plagioclase megacrysts/xenocrysts have an andesine-oligoclase composition (Fig. 6, 24). In the MME subtypes, the concentric zones in both the outer parts of plagioclase megacrysts/xenocrysts (Fig. 24) and in the outer zones of the lath-shaped plagioclases dispersed in the groundmass (Fig. 26) have a similar andesine-oligoclase composition. This fact is evidence of late-stage 'equilibration' of hybridic melt, accompanied by normal fractional crystallization in the more-or-less homogenous melt.

Problem of magmatic corrosion

It is supposed that some plagioclase as well as K-feldspar and quartz megacrysts/xenocrysts occurring in the MME subtypes were mechanically transferred from the host magma (probably from hybrid host granitic magma) to the mafic magma blobs during the hybridisation process (Barbarin, Didier 1992; Słaby, Martin 2008).

In the MME samples, plagioclase (Fig. 24) megacrysts/xenocrysts, alkali feldspars (Fig. 33), quartz (Fig. 27) megacrysts/xenocrysts as well as individual amphibole crystals (Fig. 29) and aggregates/glomerocrysts, have corroded outer margins. This process is related to the corrosion/interaction of hot mafic magma with the margins of early crystallized minerals (of different composition and origin) during the late-stage of magma mixing related to normal fractional crystallization in a locked crystal mush. Similar corrosion processes can be observed on the outer margins of individual amphibole crystals (Fig. 16) and amphibole aggregates/glomerocrysts in the host granites.

Post-magmatic episode

The occurrence of secondary actinolite and chlorite in amphibole aggregates/glomerocrysts and simple crystals (Fig. 28), as well as the occurrence of secondary sericite in plagioclase megacrysts/xenocrysts and lath-shaped plagioclases (Fig. 26) dispersed in the groundmass, is related to post-magmatic processes. The second stage of alteration and formation of biotite overgrowing individual amphibole crystals (Fig. 28) and aggregates/

glomerocrysts (Fig. 30) can be connected to the late-stage of fractional crystallization or post-magmatic alteration of rock-forming minerals related to hydrothermal processes.

Hybridisation process

According to Fernandez and Barbarin (1991), the multiple injections of mafic magma into granitoid systems (parent magma chamber) at different stages of the fractional crystallization of felsic magma were evidence of many granitoid plutons. In this case, the different types of interactions of mafic/felsic magma can be generated. They depend on: (1) the stages of the crystallization of felsic magma and (2) the time of mafic magma injection (3) and/or rate of a chemical exchange (mutual diffusion according to Debon 1991) between contrasting magmas.

On the grounds of structural/textural and mineralogical features, the Małopolska Block granites studied were subjected to a hybridisation process.

Some features of the rocks studied, as variations of the chemical composition of minerals, suggest that their formation was accompanied by changes in equilibrium conditions during the differentiation of magma and fractional crystallization. Moreover, these features (described above) are evidence of local mixing between granitic and mafic magmas (mafic blobs). It is postulated that this process played an important role in the origin of the Małopolska Block granites during magmatic crystallization. Similar magmatic evolution of the Karkonosze pluton and complexity of mixing processes between a felsic and mafic magma were described in detail by Slaby and Martin (2008).

The host granites exhibit typical magmatic disordered textures (Fig. 3) and represent magmatic rocks formed during local mixing between mafic magma (mafic blobs), and peritectic minerals and granitic magma under conditions of diffusion, thermal equilibration and crystallization of more-or-less homogenous melt (Hibbard 1991). Their features indicate on equilibrated hybrid system (EHS) after Hibbard (1991), or homogenous hybrid magmas (Fernandez, Barbarin 1991), formed during introduction of mafic melt (mafic blobs) into slightly crystallized granitic magma, and generated during local mixing processes and/or chemical exchange (interdiffusion-mutual diffusion according to Debon 1991). As described by Sparks and Marshall (1986), the large voluminous proportions between mafic and felsic magma, and local thermal equilibration, favour mixing processes. According to Hallot et al. (1994, 1996), a small difference in viscosity between the felsic and mafic melt can favour more complete local mixing. Repeated injections of mafic magma (blobs) into a crystallizing granodioritic pluton may proceed at deeper levels (e.g. mantle/lower continental crust boundary) of the Małopolska Block (MB). Consequently, it is postulated that host granites are crystallization products of more-homogenized or completely homogenized hybrid magma.

On the other hand, the occurrence of abundant MME (dark and pale grey MME – Q-diorites and tonalites) in the host host granites (pale grey granodiorites) indicates the important role of magma mingling processes.

The common interpretation of the occurrence of MME in granitoid host implies that both magmatic rocks represent the products of mixing and mingling mafic and felsic magmas derived from the mantle and crust (Vernon 1983, 1984, 1991; Reid et al. 1983; Didier 1987; Huppert, Sparks 1988; Dorais et al. 1990; Castro et al. 1990; Barbarin, Didier 1991b). MME represent ‘chilled pillows’ (Blake et al. 1965; Vogel, Wilband 1978),

‘quenched globules’ (Vernon 1984), or ‘blobs’ (Zorpi et al. 1989) of mafic magma in a granitic magma host. In contrast, there are opinions that enclaves in granites have a restitic origin and represent solid residues of partial melting or samples of unmelted, refractory minerals from the source region (White, Chappell 1977; Chen et al. 1989; Chappell 1996; White et al. 1999). Instead, many scientists (Phillips et al. 1981; Clemens, Wall 1988; Dodge, Kistler 1990; Fershtater, Borodina 1991; Dahlquist 2002; Donaire et al. 2005) suggested that MME are disrupted fine-grained borders which were generated by crystal-liquid differentiation within a single parental granitoid magma, at the border zones of magma conduits. Later, these zones were incorporated into the host granitoid as totally or partially solidified bodies where they have reworked and mingled (Donaire et al. 2005). In this case, both MME and the granitic host may have obtained very similar mineral, chemical and isotopic compositions related to thermal and chemical/isotopic equilibration between coeval, but contrasted magmas (Dorais et al. 1990; Eberz, Nicholls 1990; Allen 1991).

Based on present investigations, it may be suggested that the MME do not represent an initial chemistry of ‘primary mafic magma’ but exhibit re-equilibrated chemical composition of less hybridised mafic magma (less hybridised dark grey subtype, more pale grey subtype – Fig. 20, 21). They may be formed, following the opinion of Fernandez and Barbarin (1991), when mafic magma (hot) was introduced into felsic magma (cooler) when the effective viscosity of the latter was still significantly low, but sufficiently high to permit mingling process. In contrast, high magma viscosity influenced the differentiation degree (e.g. increasing polymerization and crystal load – Hallot et al. 1994, 1996). Blobs of mafic magma have produced the MME (Q-diorites and tonalites), introduced into felsic magma (the host granites). The MME show textural evidence of rapid crystallization and local quenching (the ‘pseudo-doleritic’ textures of the groundmass, lath-shaped plagioclases, blade-shaped amphiboles and acicular shaped apatite). Plagioclase megacrysts/xenocrysts show resorption and regrowth zones as evidence of rapid changes in magma composition (see Chapter 5.1: Petrography of pale grey host granites (HG) and Chapter 5.2: Petrography of mafic microgranular enclaves (MME)). A large proportion of the felsic magma and temperature contrast (Sparks, Marshall 1986) and a higher viscosity contrast (Hallot et al. 1994, 1996) favoured mingling. This process could operate before and during the emplacement of granodioritic pluton (e.g. in the upper level of continental crust) in to Ediacaran/Paleozoic basement of the Małopolska Block (MB). Donaire et al. (2005) suggested that the occurrence of microgranular enclaves (MME) is a typical feature of epizonal granitoids.

To sum up, based on the above petrographic investigations it is postulated that the MME studied represent no primary mafic magma but probably more-or-less homogenized (analogically: from dark to pale grey MME subtypes) hybrid magmas, whereas the host granites more or completely homogenized hybrid magma.

Rare enclaves of hornfels and restites, which occur in peripheral zones of the granitic pluton (Wolska 2004, 2009), are evidence of mechanical crushing of metasedimentary wall-rocks during the uprise of the granodioritic pluton. The distribution of these enclaves in the Małopolska granitoid pluton is difficult to describe, because its architecture is still poorly known, and because only a few deeper boreholes reached granodioritic plutons. Enclaves of

hornfels and restites probably occur at the border zones of the pluton and metasedimentary wall-rocks but at different levels.

6.3. Geochemistry of contrasted rocks – MME and host granites

Major elements

Both rocks studied exhibit marked differences in chemical composition, in both the content of major and trace elements. Namely, the pale grey host granite samples (granodiorites according to the modal composition – Fig. 5) are characterized by a high amount of SiO_2 (67-70wt%), and significant values of CaO (2.4-3.5wt%) and Na_2O (3.0-4.3wt%). The Na_2O content (Table 3) is important in these rocks and corresponds to a high abundance of plagioclase in their mineral (modal) composition (Table 1). On the other hand, the diversity of the K_2O content in various host granite samples (2.7-4.5wt%) and its increase to 4.5wt% suggests a lower degree of hydrothermal alteration. The diversity in K_2O is the cause of displacing these granites in different fields from granodiorite through Qtz-monzonite (monzogranite) to granite in the classification diagrams based on the normative composition and the content of major elements (Fig. 38, 41, 42, 43, 44, 45 – see Chapter 5.3: Geochemistry of pale grey host granites (HG)). In particular, the contact host granite samples plot in the granite field in all the discrimination diagrams because they are distinctly enriched in K_2O (~ 6.7wt%). It is related to the assimilation processes of metasedimentary wall-rocks by magmatic melt in the outer part of the intrusion (pluton), or more likely metasomatic (hydrothermal fluids) interaction with their metasedimentary wall-rocks.

The dark grey MME samples (Q-diorites and tonalites according to the modal composition – Fig. 23) exhibit lower content of SiO_2 (~59-66wt%) and are more enriched in CaO (3.1-4.6wt%) than the former. The K_2O content (2.3-3.7wt%) is slightly lower and the Na_2O content (3.6-4.8wt%) a little higher compared to the host granites (Table 6). On the other hand, the pale grey MME samples (according to modal composition: tonalites – Fig. 23) generally have a higher content of SiO_2 (~68-70wt%) and a lower content of CaO (2.4-2.8wt%) and Na_2O (3.9-4.3wt%) similar to the host granites. The K_2O values (~3.0wt%) in the pale grey MME are similar, as in both dark grey MME and host granites. The dark grey MME plot in several classification diagrams in various fields: diorite, Q-monzodiorite/Q-monzogabbro, monzodiorite, syenodiorite, tonalite, granodiorite, monzonite and quartz monzonite (Fig. 38, 41, 42, 43, 44, 45 – and see Chapter 5.4: Geochemistry of mafic microgranular enclaves (MME)). The pale grey MME often plot in the granodiorite field, less often in the granite and adamellite fields (Fig. 38, 41, 42, 43, 44, 45, and see Chapter 5.4: Geochemistry of mafic microgranular enclaves (MME)). These differences in petrochemical classification of two subtypes of the MME is largely connected to the hybridisation process and their variable mineral composition, particularly the occurrence of different amount of megacrysts/xenocrysts of minerals: plagioclase, quartz, alkali feldspar (Table 2) compared to mafic minerals. Apparently, it refers to pale grey rather than dark grey MME samples.

As in the case of major elements, the both rock types, in particular, differ in the TiO_2 as well as P_2O_5 contents (see Chapter 5.3: Geochemistry of pale grey host granites (HG) and Chapter 5.4: Geochemistry of mafic microgranular enclaves (MME)). The low TiO_2 content

shows the host granites (0.76-0.49wt%), and the pale grey MME (0.53-0.46wt%). In contrast, the dark grey MME display a markedly higher TiO_2 content (1.22-0.79wt%). Analogically, the host granites (0.14-0.10wt%) and the pale grey MME (0.13-0.14wt%) have a similar level of the P_2O_5 value. Only the dark grey MME (0.44-0.15wt%) are especially enriched in this element. The enrichment of the dark grey MME in TiO_2 and in P_2O_5 is related to their more mafic character (higher contents of mafic components from enriched mantle and/or lower continental crust). The lower abundances of P_2O_5 and TiO_2 in the host granites studied are caused by early fractionation of Fe-Mg silicates, Fe-Ti oxides and other accessory minerals (Osborn 1959).

On the other hand, both the rocks types studied show similar geochemical features. The MME as well as the host granites belong to I-type granites (Fig. 54) as defined by Chappell and White (1974), White and Chappell (1983). The rocks studied are characterized by typical mineral composition (the occurrence of titanite and apatite) and high Na_2O content $> 3.2\text{wt}\%$ (up to $4.8\text{wt}\%$), $\text{ASI} < 1.1$ and the occurrence of normative diopside. The content of normative corundum generally ranges $< 1\%$. The presence of early magmatic accessory minerals (Fe-Ti oxides) defines the rocks studied as connected to magnetite granites series (Ishihara 1977). All the samples of the MME and host granites commonly exhibit a calc-alkaline trend (Fig. 46). In Didier and Barbarin (1991) opinion calc-alkaline granitoids are of mixed origin and involve both crustal and mantle materials. Despite the fact that the rocks studied have high Na_2O content, all the samples show low a agpaitic index < 0.87 (Table 9) and have a medium-K to high-K character (Fig. 47). Their high-K character may reflect the increasing degree of crustal contamination as suggested by Wilson (1989) for granitic rocks formed in active continental margin. In the rocks studied, a marked increase of K relative to Rb (diagram K vs Rb – Fig. 68) is observed. The K/Rb ratio is usually

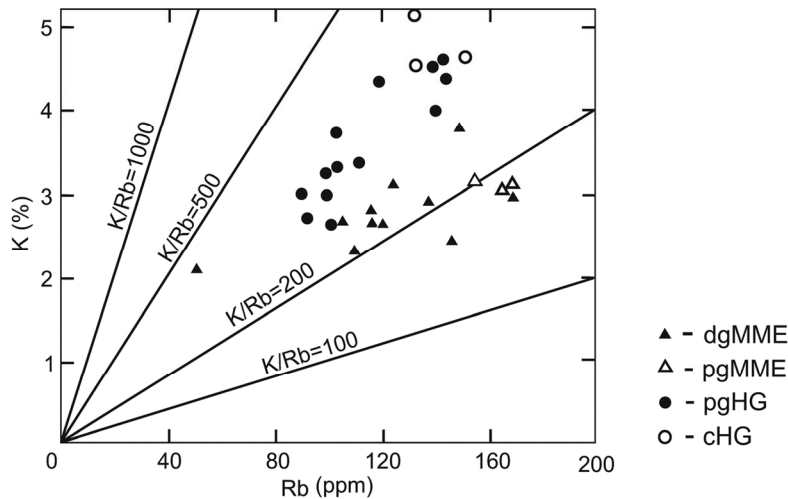


Fig. 68. Geochemical characteristics of the granites studied on the K vs Rb correlation diagram. Symbols: dgMME – dark grey MME; pgMME – pale grey MME; pgHG – pale grey host granites; cHG – contact host granites.

attributed to crustal contamination (assimilation) during fractional crystallization processes (Davidson et al. 1987). The K/Rb ratio may also be commonly used to explain the evolution of granitic melt. The Rb content increases due to fractional crystallization (differentiation process), because Rb prefers to remain in residual melts and/or during assimilation of continental crust (Wilson 1989). The K/Rb ratio is variable in the granites studied (Fig. 68), and ranges from 138 to 326 in the dark grey MME, from 153 to 182 in the pale grey MME, from 213 to 330 in the host granites, which is characteristic of slightly evolved granites (Fig. 52) and is consistent with correlation of these elements on chemical variation diagrams (Fig. 37). Shaw (1968) provided information that the K/Rb ratio decreases below 50 in highly evolved magmatic melts. In the case of the contact host granites, the K/Rb ratio varies from 411 to 248, which indicates a possibility of interaction of the parent magma of the host granites studied with metasedimentary wall-rocks and/or post-magmatic hydrothermal activity. The latter scenario of interactions with hydrothermal fluids is possible in little degree, because in Clarke's (1992) opinion the K/Rb ratios < 100 may indicate an interaction with aqueous fluids or mineral growth in the presence of an aqueous phase (Shearer et al. 1985) under hydrothermal conditions.

TABLE 9

Petrochemical indices and element ratios of pale grey host granites (HG) and mafic microgranular enclaves (MME).

	Mafic microgranular enclaves (MME)		Host granites (HG)	
	dark grey	pale grey	pale grey	contact
Aqpaitic index	0.65-0.53	0.68-0.66	0.71-0.63	0.83-0.67
K ₂ O/Na ₂ O	0.98-0.48	0.85-0.73	1.49-0.66	3.31-1.28
MALI	4.17-1.96	4.84-4.45	5.16-3.38	8.05-5.62
CaO/Na ₂ O	1.03-0.73	0.66-0.62	0.82-0.69	0.63-0.21
ASI	0.89-1.08	1.01-1.06	0.96-1.07	1.06-1.12
Ba/Sr	1.92-1.09	2.23-2.15	2.72-1.63	3.99-2.21
Ba/Rb	8.71-2.87	5.09-4.60	9.29-4.54	4.82-4.29
#Mg	0.40-0.30	0.30-0.20	0.40-0.30	0.50-0.30
Rb/Zr	0.75-0.14	0.85-0.80	0.92-0.66	1.99-1.01
Yb/Sr	0.013-0.004	0.008-0.007	0.010-0.003	0.020-0.002
Eu*	0.76-0.34	0.67-0.64	0.97-0.61	2.76-0.44
ΣREE	274.9-155.2	132.4-121.6	198.1-103.1	127.5-44.1
Ba/Nb	54.97-15.89	55.03-45.77	93.15-39.78	133.50-47.01
(Ce/Yb) _N	10.51-4.42	5.89-5.21	14.80-4.79	6.43-4.70
Ba/La	21.06-8.13	35.23-29.38	37.78-17.48	75.31-24.08
La/Ta	43.0-17.7	19.8-15.9	54.1-18.9	36.6-13.0
La/Sm	10.88-3.52	5.16-4.29	11.31-5.40	6.55-4.79
Sm/Yb	2.74-1.76	2.08-1.88	2.70-1.65	2.27-1.71
(La/Yb) _N	17.74-5.04	7.26-5.66	20.65-7.76	8.37-5.54

The relatively low/medium content of Rb as well as K in the rocks studied (especially in some samples of dark grey MME) are not connected with the intense assimilation of felsic magmas and in this case is rather impossible. It seems that the K-high character of the rocks studied may be connected with shoshonitic affinities and influence of mantle components (probably from enriched mantle). In the Kraków-Lubliniec Fault Zone (KLFZ), the occurrence of lamprophyre (minettes and kersantites) dykes was described (Ryka 1974; Heflik et al. 1985; Heflik et al. 1989; Heflik et al. 1992; Czerny, Muszyński 1998) in numerous boreholes localized near Lubliniec, Siewierz, Zawiercie, Strzegowa, Opatkowice and Zabierzów. As suggested by their geological/tectonic position, they are related to a late episode of the Variscan magmatic cycle (Harańczyk 1985, 1989, 1994; Żaba 1999). The lamprophyre series related to Variscan granite plutons are very common and known from many localities in Western and Central Europe (vide Słaby, Martin 2008). These rocks are mainly associated with postorogenic granitoid complexes in orogenic belts (Rock 1987). The lamprophyre series are represented by mafic melt which generated in an anomalous sub-Hercynian mantle and later modified by interactions with crustal rocks (Sabatier 1991). Sisson et al. (2005) defined that hydrous, medium- to high-K mafic magmas may fractionate to produce 12-25vol% of granitic melt.

The K_2O/Na_2O ratio increases during fractional crystallization. In the rocks studied, the ratio markedly ranges from 0.5 to 1.0 (MME), from 0.7 to 1.5 (host granites) and suddenly increases up to 3.3 in the contact host granites (Table 9). The ratio values are likely to exhibit the various degrees of the mixing process between mafic and granodioritic magmas more than simple fractional crystallization. The higher ratio in the contact host granites is perhaps a result not only of these complex processes but also of the overprint of K-rich hydrothermal fluid action in a later stage of the granite's development.

Summing up, the different K_2O contents in the granites studied is commonly related to variable degrees of magma fractionation, mixing and homogenization and/or assimilation of continental crust metamorphic rocks, rather than shoshonitic affinities and the occurrence of a large abundance of components from enriched mantle. It cannot be excluded that the K_2O contents are connected to mobilization of potassium during hydrothermal processes related to the Cu porphyry type deposits mineralization (Meyer, Hemley 1967).

As described by Frost et al. (2001), the MALI is an indicator of a mantle contribution. This index in the rocks studied is variable (Table 9). In the host granite samples, the MALI value ranges from 3 to 5. The dark grey MME samples exhibit the lower range of the MALI value (2-4), suggesting some influence of mantle component. The pale grey MME have a higher MALI (~5), similar to the host granites. This MALI value can be related to their higher degree of fractional crystallization. In the contact host granite samples, the MALI is somewhat higher (~6-8) and may reflect an interaction between the magmatic melt and metasedimentary wall-rocks in the outer parts of the pluton (assimilation and contamination processes) during the variation of water pressure (Holtz, Johannes 1991; Patiño Douce, Harris 1998) related to hydrothermal processes.

The CaO/Na_2O ratio is lowered during the differentiation of magma. Jung and Pfänder (2007) suggested that the CaO/Na_2O ratio also reflects a kind of source rock for the granitic melts. The CaO/Na_2O ratio (Table 9) is higher in the dark MME (0.7- 1.0) and successively decreases in the pale grey host granites (0.7-0.8) through the pale grey MME (0.6-0.7) to

the contact host granites (0.2-0.6). However, the latter values may rather be connected with wall-rock assimilation process or metasomatic processes related to hydrothermal interactions. This trend is distinctly visible in the CaO-K₂O-Na₂O diagram (Fig. 69), but only for the samples of pale grey MME and pale grey host granites. This relationship may be explained by assuming that both types of the rocks studied did not originate from the same source, but it is more likely that the advanced hybridisation process of the host granodioritic magma overprinted on mingled mafic magma blobs. The dark grey MME preserve more mafic components from the enriched mantle because they exhibit a less degree of hybridisation.

The ASI number is considered to indicate the composition of the source area and the nature of melting process (Frost et al. 2001). This index in the rocks studied is lower than 1.1 (Table 9). The samples of the host granites are metaluminous to slightly peraluminous (Fig. 48) and the values of their ASI vary between 0.96 and 1.07. Both the dark grey MME (ASI = 0.89-1.08) and the pale grey MME (ASI=1.01-1.06) are also metaluminous to slightly peraluminous and have similar values of ASI as the former (Fig. 48). Only the contact host granites have a slightly peraluminous to peraluminous character (ASI = 1.06-1.12) (Fig. 48). In the rocks studied, the value of the ASI < 1 is connected to the presence of normative *di* in several samples (Table 4 and 7). Based on petrographical observations, these samples are characterized by the occurrence of aggregates of hornblende with Fe-oxides, titanite, chlorite and biotite, and are probably pseudomorphs after pyroxenes (see Chapter 6.2: Petrographic features of contrasted rocks – MME and host granites). The peraluminous character (the ASI >1) is related to the presence of normative *C* in few samples (Tables 4 and 7). The peraluminous character of rocks may be attributed to the differentiation of hornblende (Zen 1986, 1988), the water content in the protolith (Waight et al. 1998) or pelitic rock assimilation (Clarke 1992). According to some authors' data, some I-type granites have moderately peraluminous character related to high degrees of fractionation and/or assimilation of large volumes of crustal material by basaltic melts (e.g. Atherton, Sanderson 1987, Castro et al. 1999). In contrast, Clemens et al. (2011) suggested that entrained peritectic solids (minerals), either clinopyroxene or a much larger amount of hornblende into granitic magma, caused the decrease in ASI in I-type granites. Moreover, Clemens et al. (2011) provide information that the mixing of mantle and crustal material occurred in the arc tectonic setting, therefore the sources for metaluminous I-types granites can be commonly related to the crustal rocks (metamorphosed series of ancient volcanic and sedimentary sequences of the arc tectonic setting).

According to the A-B multicationic diagram (Debon, Le Fort 1983) showing the trends of evolution – in particular, the content of dark minerals (ferromagnesian phases) relative to the Al saturation index, the majority of the samples of both MME and host granites (Fig. 51), contain hornblende (the IV hbl field) as the main primary dark mineral. Only few samples exclusively contain biotite (the III bt field), which probably replaced primary hornblende. In the contact host granites, both biotite and biotite with muscovite occur (III bt and IIbt > mt fields). This geochemical classification was confirmed by petrographical investigation (see Chapter 6.2: Petrographic features of contrasted rocks – MME and host granites).

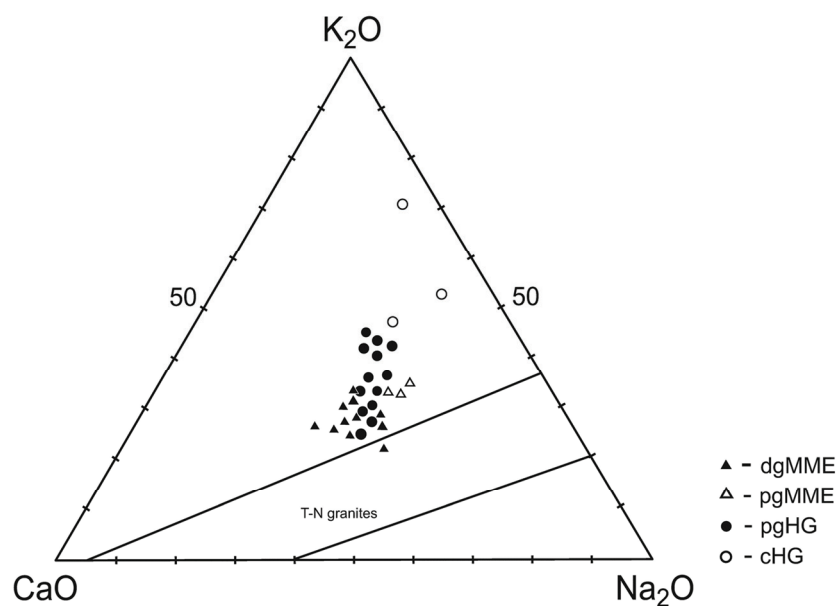


Fig. 69. Geochemical characteristics of the granites studied on the CaO-K₂O-Na₂O ternary diagram. Symbols: dgMME – dark grey MME; pgMME - pale grey MME; pgHG – pale grey host granites; cHG – contact host granites; T-N (the Tanzawa-Nijima granites – typical oceanic crust granites after Ishihara et al. 1976).

Trace elements

As suggested by Frost et al. (2001), trace element composition in granitoids may be a function of the sources and crystallization history of the melt.

Based on geochemical studies, the rocks studied are mainly weakly evolved (Fig. 52). The Ba/Sr and Ba/Rb ratios of the both rock types do not vary markedly (Table 9). The host granites show low values (2-3 and 5-9, respectively) similar to the dark grey MME (1-2 and 3-9, respectively). The pale grey MME have average values (~2 and ~5, respectively) analogous to both former types. These values are also similar to VA-granites (Pearce et al. 1984). The high Sr concentration (460-318 ppm) is a characteristic feature of the MME well as of the host granites (463- 244 ppm). The contact host granites are strongly depleted in Sr (up to ~172 ppm). The high Sr concentration, both in the dark grey MME and host granites, and the small Eu negative anomaly (already presented in Chapter 5.3: Geochemistry of pale grey host granites (HG) as well as in the Chapter 5.4: Geochemistry of mafic microgranular enclaves (MME)) is probably related to the presence (to various degrees) of mafic components in the rocks studied. The origin of these components is probably connected to the melting of mafic rocks of lower continental crust (Duchnese et al. 1998) in the case of the host granites, and fractionation of mafic magmas (Emslie 1980) in the case of the MME (mafic blobs).

This suggestion may be confirmed by the content of transition elements in the rocks studied. The dark grey MME exhibit a high content of Ni (up to 19.0 ppm), Cr (up to 60 ppm), Co (up to 12.7 ppm) and V (up to 128 ppm). On the other hand, the host granites

have moderate Ni contents (up to 7.2 ppm), Cr (up to 30 ppm), Co (up to 10 ppm) and V (up to 77 ppm) compared to the former. This relationship may be evidence of significant hybridisation (contamination) of primary mafic melts (mafic blobs) by the granodioritic melt generated in lower continental crust. The pale grey MME are depleted in these elements compared with the dark grey MME as well as host granites, what may suggest their higher degree of hybridisation and also contamination by crustal metamorphic rocks (the occurrence of alkali feldspar megacrysts/xenocrysts in the pale grey MME). Relatively low Ni contents related to Cr contents are characteristic of the rocks studied.

The host granites studied are magnesian ($\#Mg = MgO/(MgO + 0.9FeO_t)$ amounts to 0.30), show no iron enrichment (Fig. 49 and 50). The $\#Mg$ number of the dark grey MME is higher (0.40-0.30), whereas the pale grey MME have lower $\#Mg$ number (0.30-0.20) and sometimes these rocks have ferriferous character (Fig. 49). In Osborn's (1959) opinion, the early crystallization of magnetite inhibits Fe enrichment during differentiation of magma. It is now accepted that magnesian granitoids are probably related to island arc magmas which show oxidizing differentiation trends (Frost et al. 2001) and reflect a close affinity to relatively hydrous magmas (Frost, Lindsley 1991).

The Zr content in the host granites ranges from 123.9 to 186.3 ppm, whilst the contact host granites are depleted in this element (68.6-134.6 ppm). In contrast, the MME are enriched in Zr (dark grey MME: 162.0-381.6 ppm and pale grey MME: 186.8-205.9 ppm) compared to the host granites. This relation may be explained by the more advanced assimilation processes of mafic magma by lower crust metamorphic rocks during its rise through thickening continental crust, probably in the late stage of collision of two blocks.

The Rb/Zr ratio is below 1 in all the samples of the rocks studied (Table 9). The Rb/Zr ratio indicates a degree of fractionation because Rb generally behaves as an incompatible element during increasing silica content, whereas Zr conversely behaves as a compatible element. This ratio in the dark grey MME is the lowest (0.1-0.8) and increases in the host granites (0.7-0.9) as well as in the pale grey MME (0.8-0.9). However, in only the contact host granites this ratio is higher (1.0-2.0). This relationship is mainly related to granitic magma hybridisation and to a lesser degree of fractional crystallization and metasedimentary wall-rocks assimilation. This refers especially to the pale grey MME and (to a lesser degree) to the pale grey host granites.

The Yb/Sr ratio can be used as an assimilation index of granites (Tindle 1991). The ratio value for the rocks studied varies in a broad range (Table 9). Namely, in the MME this ratio ranges from 0.004 to 0.013 (for two subtypes). In the host granites it is slightly lower and ranges from 0.003 to 0.010. In only the contact host granites, it increases up to 0.020, which may be due to medium-scale contamination and assimilation of metasedimentary wall-rocks and/or related to hydrothermal processes. Some samples of both rock types, in which the Yb/Sr ratio is < 0.005 , show predominance of mafic components and a complete lack of assimilation signs.

HFS elements characteristics

The rocks studied are depleted in HFS elements (Nb and Ta), because their chondrite-normalized patterns exhibit distinct Nb and Ta negative anomalies. The content of Ta in the host granites is low (1.4-0.5) and similar as in both subtypes of the MME (1.9-0.5 ppm), evidence of low degree of crustal assimilation. The abundance of Nb (16.7-8.7 ppm) and Y

(26.0-12.6 ppm) in the host granites is also evidence of a relatively low degree of fractional crystallization. It is supposed that the later processes of hydrothermal alteration and/or metasedimentary wall-rocks assimilation (mainly in the contact host granites) caused mobilization of these elements – some decrease of Nb (14.6-4.4 ppm) and a distinct increase of Y (38.8-6.4 ppm) contents. The dark grey MME exhibit some enrichment in Nb (27.3-10.9 ppm) and Y (47.9-15.6 ppm) compared to the pale grey MME (Nb 16.6-13.9 ppm, Y 27.4-29.6 ppm), what may suggest a more effective influence of the mantle component. The Hf content in the host granites is low (5.0-3.2 ppm) and similar to the pale grey MME (up to 5.8 ppm) or in the contact host granites (4.3-2.2 ppm). Some of dark grey MME samples display enrichment of the Hf content (3.8-9.0 ppm) relative to the former granites, suggesting a higher degree of participation of mafic component from enriched mantle source or assimilation of crustal rocks enriched in this elements.

Tarney and Saunders (1979) and Brown et al. (1984) defined that the concentration of HFS elements (Ta, Nb, Y and Hf) in granitic rocks may reflect a degree of their contribution from enriched mantle sources. On the other hand, Brown et al. (1984) suggested that these elements have a trend to be enriched in granitic rocks that originated in more ‘mature’ arcs. It is related to the increasing distance from the active trench and the generation of magmas from the laterally heterogeneous mantle. In contrast, the depletion in HFS elements is characteristic of subduction related regimes (primitive and normal volcanic arc – Brown et al. 1984). Żelaźniewicz et al. (2008) described, for the Dolina Będkowska valley granodiorite, negative anomalies of Nb and Ti that strongly indicate a supra-subduction affinity. Similarly, based on Nb and Ti anomalies in the normalized patterns for the volcanic rocks from the Krzeszowice area, Słaby et al. (2010) suggested the possibility of an island arc-related environment. Hence, it may be supposed that the host granites originated from the metamorphic rock source and inherited the geochemical signature of the ancient volcanic arc. On the other hand, the MME of mafic rocks originated from mantle preserve its geochemical signature, despite strong hybridisation by granodioritic melt.

REE pattern characteristics

The REE patterns of the MME and host granites studied show similar trends. All the granite samples display fractionation of LREE and flat HREE patterns (Fig. 63, 67), which is characteristic of calc-alkaline series (Wilson 1989). The rocks studied exhibit high $(La/Yb)_N$ ratios (host granites 7.8-20.7, contact host granites 5.5-8.4, dark grey MME 5.0-17.7, and pale grey MME 5.7-7.3 – Table 9).

The rocks studied also exhibit an enrichment of LREEs (La, Ce, Sm). It is related to the fractionation of REE in accessory minerals e.g. zircon, apatite, titanite and allanite (Hoskin et al. 2000) but this process is not evident in some granitoids (Brown et al. 1984). The rocks studied show regular variations (negative correlations) of these elements vs SiO_2 on bivariate plots (Fig. 37). In the host granites, the content of La ranges from 37.4 to 18.0 ppm, Ce from 75.3 to 37.0 ppm and Sm from 5.39 to 2.86 ppm. The pale grey MME have a similar content of La, Ce and Sm (25.7-22.2 ppm and 54.3-47.6 ppm and 5.20-4.98 ppm, respectively) to the former. On the other hand, the dark grey MME exhibit a higher value of La (56.5-30.1 ppm), and especially of Ce (118.9-49.0 ppm) and Sm (8.80-3.74 ppm). The contact host granites show a lower La value (28.5-7.8 ppm) as well as Ce

(63.1-15.2 ppm) and a similar Sm value (5.95-1.19 ppm). The chondrite-normalized patterns of all the samples of the rocks studied show a lack of strong depletion in Yb. Low $(\text{Ce/Yb})_N$ ratio can be the result of biotite fractionation, especially in the host granites and pale grey MME (Table 9).

The host host granites exhibit a small negative Eu anomaly (0.61-0.97) that is related to the minor fractional crystallization of plagioclases. In contrast, the both subtypes of the MME show marked differentiation in the value of a negative Eu anomaly (0.34-0.76), which may be explain both the advanced, to various degrees, fractional crystallization of plagioclases from small to larger, or more likely the complex mixing processes of mafic/felsic magma than simple fractional crystallization.

Distinct enrichment in LREE and high-K calc-alkaline character (as already mentioned) means that the rocks studied reveal some shoshonitic affinities (according to Foley, Percerillo 1992).

The very flat REE pattern on the chondrite-normalized diagrams (Fig. 63 and 67) combined with medium tREE content (100- 270 ppm in both rock types – Table 9) is a characteristic feature of the rocks studied. Such a flat pattern could be generated by the specific origin of the granitoids in question as fractionates of mafic magma, as suggested by Stone (1995).

Isotope geochemistry

The $^{87}\text{Sr}/^{86}\text{Sr}$ data for the host granites studied shows lower values (0.709375-0.710426) compared to the values which were determined for the MME (0.709593-0.713297). On the other hand, the $^{143}\text{Nd}/^{144}\text{Nd}$ ratios and $\epsilon_{\text{Nd}(t)}$ are very similar in both rock types (Table 5 and 8). These isotopic values may suggest that the MME may be comagmatic with their host granites. It is possible that the large primary differences in isotopic signatures between the MME and the host granites were erased by the re-equilibration process during the occurrence of mafic magma blobs in the large hot granodioritic chamber. The isotopic data plots between those characteristic of upper crust and mantle array (Fig. 64, 65) in the discrimination diagrams. These data indicate a contamination of mantle-derived magmas by elements of the continental crust (McCulloch, Perfit 1981; Hawkesworth 1982; James 1982; Harmon et al. 1984; Thorpe et al. 1984). In many authors' opinions (mentioned above), the isotopic ratios are not significantly changed by partial melting or differentiation. Consequently, granites produced by the partial melting of the upper mantle still have a lower initial $^{87}\text{Sr}/^{86}\text{Sr}$ ratio compared to other rocks generated in the continental crust. Magmatic rocks derived by partial melting of the upper mantle (e.g. basalt) have low initial $^{87}\text{Sr}/^{86}\text{Sr}$ ratios (0.702-0.706), whereas the crust is enriched in radiogenic ^{87}Rb (which decays to ^{87}Sr) and show a high initial $^{87}\text{Sr}/^{86}\text{Sr}$ ratio (0.730). The rocks studied have a markedly lower $^{87}\text{Sr}/^{86}\text{Sr}$ ratio (0.709-0.713) compared to ratios of rocks from the continental crust. Low Nd ratios and higher Sr ratios of the rocks studied indicate a lower crustal source, with a minor contribution of mafic component from enriched mantle source. These isotopic signatures are also thought to be connected either to the assimilation of subducted sediment by the upper mantle wedge (Tatsumi, Hanyu 2003) or to wall-rock assimilation during AFC processes (DePaolo et al. 1992) when the parent granitic magma was rising through thickened continental crust.

However, it cannot be excluded that, in the case of both rocks studied, the hybridisation process as well as crustal contamination has also influenced their isotopic characteristics. On the other hand, it seems that the MME studied do not retain their primary isotopic signatures during their residence in the host granites, especially at high-temperature conditions. It seems that they are isotopically equilibrated with their host because they exhibit similar the $^{143}\text{Nd}/^{144}\text{Nd}$ ratios when compared to the host granites. As defined by Leshner (1990), enclaves occurred in granitic plutons are frequently isotopically equilibrated with their host because isotopic equilibrium proceeds much more quickly than chemical exchanges. These processes are clearly related to dimensions of the enclaves, and Pin et al. (1990) suggested that large enclaves commonly show isotopic equilibration with their host whereas smaller enclaves exhibit large isotopic differences. In the case of all samples of the host granites studied, their isotopic signatures display similar isotopic ratios (homogenous) which prevent (to some extent) precise information about their petrogenetic history, hybrid nature and evolution in the continental crust. The MME isotopic data are slightly different and simultaneously similar to the host granites' isotopic signatures, which may be related to fast isotopic equilibration processes during local hybridisation in the granodioritic magma chamber.

Ślaby et al. (2010) provided information on the isotopic ratios of volcanic rocks from the Krzeszowice area. On the basis of determined values of $^{87}\text{Sr}/^{86}\text{Sr}$ ratios (0.709858 for intermediate rocks and 0.712192 for acid rocks) and $^{143}\text{Nd}/^{144}\text{Nd}$ ratios (0.512224 and 0.512219, respectively), they suggested that the signatures of intermediate and acid volcanic rocks are inherited from old lower crust (Ślaby et al. 2010). The isotopic data of the host granites studied are similar or slightly higher, which may imply their similar source.

It seems that the Sr and Nd isotope data for the rocks studied may suggest that in the origin of their parent magma participated material from continental lower crust as well as overlying upper mantle in several granitic plutons, as described by White and Patchett (1984), White and Dupré (1986), Davidson et al. (1987).

Tectonic setting problem

In the tectonic discrimination diagrams (see Chapter 5.3: Geochemistry of pale grey host granites (HG) and Chapter 5.4: Geochemistry of mafic microgranular enclaves (MME)), the samples of the host granites as well as the MME plot mainly in the VAG-granites field. Żelaźniewicz et al. (2008) drew similar conclusions, that the Małopolska granites have geochemical characteristics of the VAG granites. In the diagrams Nb-Y and Rb-(Nb+Y) (Pearce et al., 1984), only a few samples plot in the within-plate granites field (Fig. 58a). On the other hand, in the Hf-Rb/10-Tax3 and Hf-Rb/30-Tax3 (Harris et al., 1986) the samples of both rock types occur in the field of granites from a collisional tectonic setting (Fig. 56a) and the late- and post-collisional granite field (Fig. 56b), respectively. Płonczyńska (2000) defined the geochemical character for the Małopolska granites related to the VAG as well as syn-COLL granites. Pearce et al. (1984) implied that the discrimination diagrams based on trace elements Rb, Nb, Ta, Y and Yb tend to indicate the characteristics of source regions, melting and crystallization histories rather than tectonic regimes. In the R1-R2 diagram (Batchelor, Bowden 1985) the rocks studied commonly plotted in the pre-plate collision granite field (Fig. 55) similar to the studies of

Żelaźniewicz et al. (2008) but also in the field of post-collisional uplift (Fig. 55). In Gill's (1981) opinion, Ba/Nb ratio > 30 is related to subduction magmas. The rocks studied exhibit variable values of this ratio, but generally it is above 30 (Table 9). The ratio is more variable only in the dark grey MME (15.9-55.0), which may be explained by the more advanced contribution of mafic magma/mafic components in the collision regime. According to Kay et al. (1992) and Gill (1981), the Ba/La ratio > 30 and La/Ta ratio > 25 may be evidence of arc magmas. The magmatic arc signature of the host granites studied does not reflect the tectonic setting during the Carboniferous period (Żaba 1999). In a case of the host host granites (Table 9), their arc signature and also geochemical data indicate that the source rocks for the parent magma originated from an ancient Ediacaran/Cambrian subduction zone (Żelaźniewicz et al. 2009). But the granodioritic magma is probably enriched by components from the lower crust, which may have taken place during contamination/assimilation processes at the Carboniferous/Permian collision stage (Żelaźniewicz et al. 2008; Słaby et al. 2010).

In the rocks studied, both the host granites and the MME are characterized by high levels of LIL elements (K, Rb, Th, U) on the chondrite-normalized diagrams and low HFS/LIL ratio (Ta, Nb)/(K, Rb, La) ratio that Brown et al. (1984) defined as typical to normal calc-alkaline continental arc granitoids that are connected to subduction zone enrichment and/or crustal contamination. Żelaźniewicz et al. (2008) suggested a supra-subduction geochemical signature of the Dolina Będkowska valley granodiorite (negative Nb and Ti anomalies and relatively low Th content) as inherited from the source rocks which formed in the ancient subduction zone. Similar tectonic characteristics are exhibited in the rocks studied, based on the Rb/100-Tb-Ta diagram (Thiéblamont, Cabanis 1990) where they plot in the field of post-collisional and syn-subductional granites (Fig. 61). In Western and Central Europe, during the Late Devonian-Early Carboniferous period, several subduction zones existed between Saxo-Thuringia and Bohemian Massif (Matte 1998; Altherr et al. 1999; Matte 2002; Schaltegger 2000). In contrast, between the Upper Silesian Block (USB) and the Małopolska Block (MB), the occurrence of no subduction zone was described by (Żelaźniewicz 1998; Żaba 1999; Nawrocki et al. 2008; Żelaźniewicz et al. 2008; Słaby et al. 2010). In the KLFZ, only the presence of a remnant of oceanic plate related to processes of amalgamation terranes during Variscan tectonic events was mentioned by Berthelsen (1998), Żelaźniewicz et al. (2008), Słaby et al. (2010).

On the other hand, the enrichment of the rocks studied in K, Ba, Th and LREE is also similar to the geochemical characteristics of granites from the post-collisional setting, as substantiated by Harris et al. (1986). In the modified Rb-(Y+Nb) discrimination diagram (Pearce 1996), all samples of the rocks studied plot in the post-collisional field (Fig. 60), similar to the Dolina Będkowska valley granodiorite described by Żelaźniewicz et al. (2008). The consensus is that the Małopolska granites are a 'stitching intrusion' (Harańczyk et al. 1995) emplaced after collision between the Upper Silesian Block (USB) and the Małopolska Block (MB). In this setting batholiths are generated, extending parallel to the continental margins as well as to the deeper fault zone (suture) in the collisional tectonic regime, as described by Pitcher (1983, 1993). This mechanism may be confirmed by the geological context of the Małopolska granite plutons and their occurrence at the boundary of the Małopolska Block (MB), near the deeper suture zone between the Małopolska Block (MB) and the Upper Silesian Block (USB) (see Chapter 2: Geological setting).

According to Frost et al. (2001), post-collisional granitoids can be derived from a number of different sources, depending on the composition of the continental crust thickened during orogenesis and/or the composition of the oceanic slab (basalts+oceanic sediments) and/or mantle wedge from ancient subduction and collision events in the regime of active continental margins, according to the Wilson cycle (1966).

Variscan magmatism with inherited geochemical characteristics which are not correlated to the tectonic setting was described in several regions of the Variscan orogen (e.g. the Halle Volcanic Complex – Romer et al. 2001; NW Iberia – Fernández-Suárez et al. 2011). Its inherited geochemistry is connected to the underlying amalgamated different blocks, which have a composition and history that are related to ancient tectonomagmatic events.

Żelaźniewicz et al. (2008) proposed a hypothesis that the parent melts for the Małopolska and Upper Silesian granitoids were derived from the thickened lower crust (orogenic root with remnant subduction zone) of the Variscan orogenic belt. They generated in an extensional decompressional regime near the crust/mantle boundary. The granitic magma intruded outside the orogenic belt towards the foreland – in the crust of the Małopolska Block (MB) (Żelaźniewicz et al. 2008). In the light of this hypothesis, the granitic melt with ‘memory’ of the supra-subduction geochemical signatures was derived from below the Variscan orogen that underwent thermal relaxation. The granitic magma had a high temperature and migrated as a crystal mush, but magmatic flow was turbulent (Żelaźniewicz et al. 2008). In contrast, Słaby et al. (2010) suggested that the melts generated in situ in the KLFZ and migrated to the surface through the fractured basement. Mechanic deformation related to strike-slip activity formed in a regime of recurring dextral transpression and transtension on the boundary zone between the Upper Silesian Block (USB) and the Małopolska Block (MB) (Żaba 1999).

As postulated by Bonin (2004), medium-K to high-K calc-alkaline magma can be generated during slab break-off. The Małopolska granites have similar geochemical characteristics inherited from ancient Ediacaran magmatism (Finger et al. 1999; Finger et al. 2000; Murphy et al. 2004) but their geological context and the occurrence of the Małopolska Block (MB) at the boundary suggests another mechanism of magma generation, development and evolution during the Carboniferous/Permian period.

Słaby et al. (2010) described the mechanism of the formation of magma in the KLFZ according to the delamination model (Jull, Keleman 2001; Lustrino 2005). The delamination model is commonly used for the Variscan fold belt (Zulauf 1997; Schott, Schmeling 1998; Arnold et al. 2001; Massonne 2005; Medaris et al. 2005; Finger et al. 2009; Fernández-Suárez et al. 2011), because it may explain the formation and fast exhumation of HP-HT metamorphic rocks in the Variscan basement and also their re-sedimentation in foreland basins. According to Słaby et al. (2010), in the KLFZ during the transpressional tectonic regime, thickened continental lithosphere was created as a result of thrusting and faulting. In this regime, the bottom layer of the continental lithosphere (lower crust) became denser due to metamorphic processes (formation of amphibolites/eclogites – HT-HP metamorphic rocks) and was delaminated, detached and sank into the mantle (asthenospheric mantle). The lower crustal melts generated in the bottom part of the sinking, and remaining continental lithosphere migrated to the crust and transported heat (Słaby et al. 2010). During the delamination processes, mantle-derived mafic melts mixed with and

were assimilated by the lower crustal melts to form 'hybrid' intermediate melts (Finger et al. 2009). Delamination led to (in a few million years) lithospheric thinning (Black, Liégeois 1993, Bonin 2004) and a change of the geochemical characteristics of magmatic suites from high-K calc-alkaline to alkaline (Liégeois, Black 1987; Bonin 1990). In the KLFZ, the occurrence of no alkaline magmatic suite was observed (Żelaźniewicz et al. 2008) because the Early Permian period came at marked change of tectonic regime, and magmatic activity generated in conditions of subhorizontal extension (Żaba 1999).

Source of magma

The generation of granitic magma is related to the processes of crustal growth and recycling during Earth's evolution (Fernández-Suárez et al. 2011). Calc-alkaline I-type granites that formed in collisional environments had complex crustal sources and a complex history of their tectonomagmatic processes (Fernández-Suárez et al. 2011), therefore is difficult to explain their source, because it is really a 'source problem' (Castro 2004).

The determination of source rocks for the granitic rocks studied is difficult because the geological setting of the Kraków-Lubliniec Fault Zone (KLFZ) and the vicinity of large blocks (the Małopolska and the Upper Silesian Blocks) in this part of collision zone has complicated its geological setting (see Chapter 2: Geological setting).

The tectonic evolution and paleogeography of this part of southern Poland is connected to the amalgamation process of different mosaic composite blocks during the Variscan orogeny. According to Unrug et al. (1999), in the Kraków-Lubliniec Fault Zone (KLFZ) the Lubliniec-Zawiercie-Wieluń Terrane has a crystalline basement that is characteristic of the Gondwana continent. Similarly, in the light of previous investigations, the Upper Silesian Block (USB) may have Gondwana affinity (Buła et al. 1997a) and is a sector of the Brunovistulia composite Terrane (BVT) – Bukowy (1964), Herlich (1981) and Kotas (1982). The occurrence of amphibolites in the Archean basement of the Brunovistulian Block (BVB) was described by Żelaźniewicz et al. (2009). They formed a convergent plate margin called the Rzeszotary Block (Żelaźniewicz et al. 2009). Słaby et al. (2009) suggested that the Kraków-Lubliniec Fault Zone (KLFZ) is a fragment of an oceanic plate, the occurrence of which between microterranes is a result of a number of collisions from Late Silurian through Late Devonian to Carboniferous periods. On the other hand, Berthelsen (1998) identified the Kraków-Lubliniec Fault Zone (KLFZ) as a remnant part of the Tornquist Sea. Based on the petrography studies of the Ludlow deposits on the Małopolska Terrane (MT), Kozłowski et al. (2004) suggested that they did not originate from the Brunovistulian Terrane (BVT) but from an island arc material. Consequently, Kozłowski et al. (2004) assumed the existence of an island arc which, according to the opinion of Nawrocki et al. (2007b), was located west of the Małopolska Terrane (MT) in the place now occupied by the Brunovistulian Terrane (BVT).

As suggested by Frost et al. (2001), geochemical classifications are not able to precisely distinguish the parent magma source of granitoids that formed in a subduction setting from other granites formed from metamorphic rocks which generated in an earlier subduction-related setting.

The occurrence of the MME which represent intermediate magmatic rocks (Q-diorites/tonalites) in the host granites studied confirms the previous hypothesis by Słaby

et al. (2010) that interactions of the mantle/crust were possible during the Carboniferous/Permian period in the KLFZ.

At any rate, it cannot be excluded that volcanic rocks from the Krzeszowice area (the USB or the KLFZ) and the Małopolska granites (granites from the boundary of the Małopolska Block basement) likely belong to one volcano-plutonic magmatic system. Although the granites studied are strongly related to ore-bearing mineralization (Harańczyk et al. 1995), on the contrary the volcanic rocks from the Krzeszowice area are not (Harańczyk 1988, 1989). Słaby et al. (2010) described that the chemical composition of the granitoids overlap with the felsic extrusive rocks from the Krzeszowice area, but precursors for these rocks had more mafic character.

The low contents of Rb and high of Sr as well as low of Cs and Nb (Table 3, 6) in the rocks studied can be related to the generation of magmas in lower part of continental crust (Altherr et al. 1999).

The calc-alkaline host granites and MME studied have medium but also high-K character. As described by Wilson (1989), increasing degrees of crustal contamination of calc-alkaline granites caused their high-K character.

Moreover, the MME and host granite samples display a negative Nb anomaly (Fig. 62, 66), which is considered to be connected to crustal contamination processes of basic/intermediate magmas (Dupuy, Dostal 1984; Dostal et al. 1998), inherited from metasomatized lithospheric mantle (Brown et al. 1984; Coish, Sinton 1992) or can be related to a metamafic magma source (Foley et al. 2002; Rapp et al. 2003). A similar Nb negative anomaly exhibited in extrusive and intrusive magmatic rocks from the Krzeszowice area (the KLFZ) was described by Słaby et al. (2010).

According to Jung and Pfänder (2007), the $\text{Al}_2\text{O}_3/\text{TiO}_2$ ratio depends on the amount of fractionating minerals and the nature of the contamination process, whilst the $\text{CaO}/\text{Na}_2\text{O}$ ratio may indicate the source of melt. In the rocks studied, the values of the $\text{Al}_2\text{O}_3/\text{TiO}_2$ and $\text{CaO}/\text{Na}_2\text{O}$ ratios reflect this kind of parent melt which derived from mafic igneous rocks (metabasites?) rather than greywackes sources. On the other hand, Żelaźniewicz et al. (2008) show that the $\text{CaO}/\text{Na}_2\text{O}$ ratio (0.8) of the Dolina Będkowska valley granodiorite may suggest its generation by partial melting of metapsammitic or granodioritic to tonalitic rather than pelitic rocks.

Based on the major element ratios (Fig. 70) obtained in experimental studies (vide Altherr et al. 1999), it may be concluded that the host granites studied can be generated during partial melt of metabasaltic to metatonalitic sources or, to a lesser degree, of metagreywackes. These mafic source rocks likely represented metamorphic rocks (amphibolites) of an ancient subducted slab (oceanic sediments + basalt plate). These source rocks may occur in the KLFZ as an orogenic root with a remnant subduction zone in thickened lower crust of the Variscan orogenic belt of this region, which was described by Żelaźniewicz et al. (2008). In contrast, the MME exhibit a more mafic character, which may suggest their origin from parental basaltic magmas from enriched mantle.

Similarly, according to the petrogenetic model of Green and Leshner (1987), moderate values of Sr/Yb and Zr/Sm ratios in the both rocks studied suggest that these rocks could have originated from a mafic source (amphibolitic source of middle-to-lower continental crust – Fig. 71). This model confirms the occurrence of restite enclaves in the host granites (Wolska 2004), representing a refractory residuum after partial melting of magma that is

evidence of the possibility of generation of granodioritic magma from mafic or intermediate metamorphic rocks (amphibolites, gneisses – Beard, Lofgren 1990; Patiño Douce, Beard 1995; Clemens et al. 2011) which built deeper levels of the old basement of amalgamated Brunovistulian Terrane (BVT) – the Rzeszotary Block (Żelaźniewicz et al. 2009).

Burham (1979) noted the development of porphyry copper deposits in the I-type granitoids and they are strictly related to granitoid source rocks – metamorphosed basalt originated from oceanic plate or lower crustal amphibolites enriched in Cu. The Małopolska Block granites exhibit the occurrence of classical porphyry copper deposits (Cu-Mo) – see Chapter 3: Magmatic rock investigations.

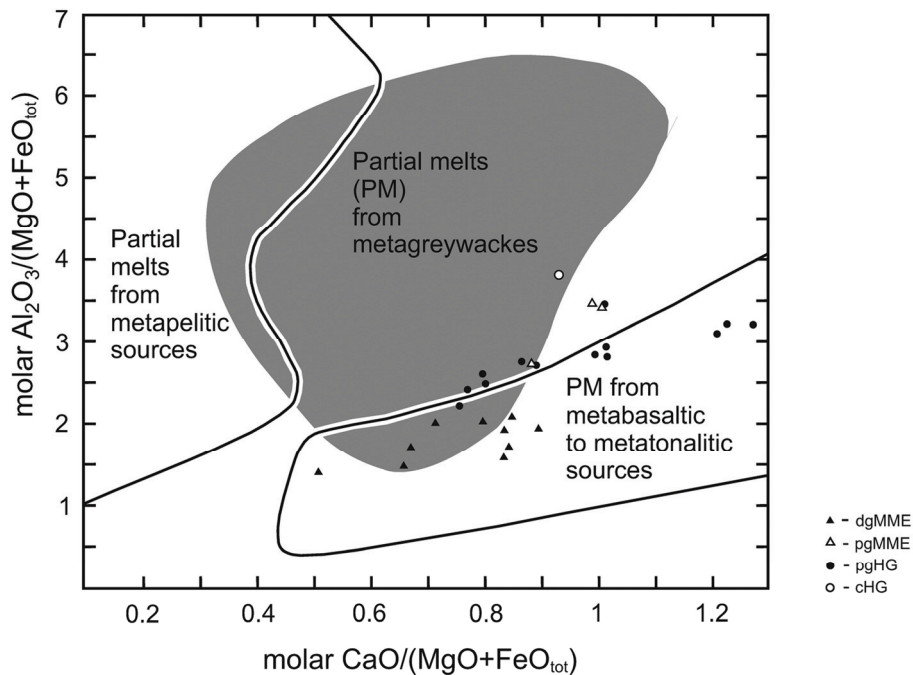


Fig. 70. Chemical composition of the granites studied on the molar $\text{Al}_2\text{O}_3/(\text{MgO} + \text{FeO}_t)$ vs molar $\text{CaO}/(\text{MgO} + \text{FeO}_t)$ diagram (fields obtained on the base of experimental studies of several authors vide Altherr et al. 1999). Symbols: dgMME – dark grey MME; pgMME – pale grey MME; pgHG – pale grey host granites; cHG – contact host granites.

The values of the La/Sm and Sm/Yb (Table 9) ratios in the rocks studied indicate negligible influence of the mantle component. The La/Sm ratio for the MME ranges from 3.5 to 10.9 (for the pale grey MME 4.3-5.2) but for the host host granites they are slightly higher at 5.4-11.3 (for the contact host granites 4.8-6.6). The Sm/Yb ratio in the MME varies from 1.8 to 2.9 (in pale grey MME 1.9-2.1) and in the host granites 1.7-2.7 (in the contact host granites 1.7-2.3). These values suggest that the mafic component presented in the MME (especially in the dark grey MME) may have originated from spinel peridotite according to the opinion of Green and Leshner (1987). These data confirm previous

investigations (Słaby et al. 2010) respecting source rocks and generation magmas in the KLFZ zone.

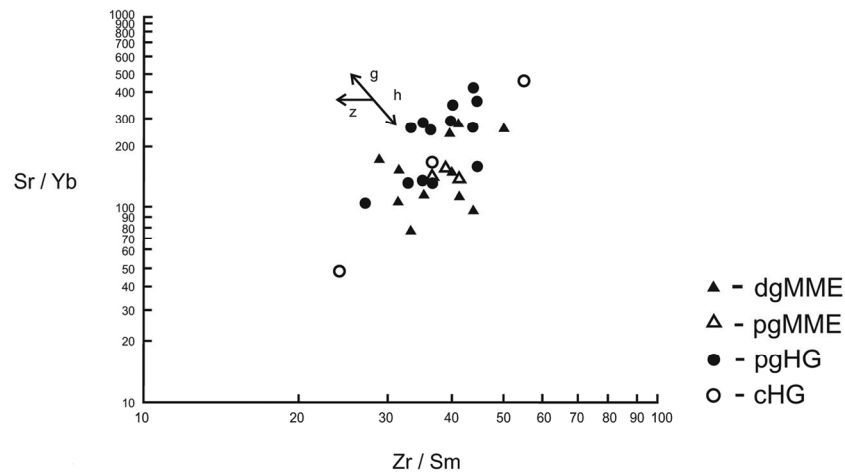


Fig. 71. Geochemical characteristics of the granites studied on the Sr/Yb vs Zr/Sm diagram (according to Green, Leshner 1987). Symbols: dgMME – dark grey MME; pgMME – pale grey MME; pgHG – pale grey host granites; cHG - contact host granites. Abbreviations: z – zircon; g – garnet; h – hornblende

Słaby et al. (2010) defined that volcanic rocks from the Krzeszowice area have high Zr/Sm and low Nb/Ta ratios that show on amphibolite melting. Słaby et al. (2010) assumed that granodioritic magma may be generated from the amphibolitic source (likely from the Rzeszotary Block amphibolites).

Previous studies (Płonczyńska 2000; Żelaźniewicz et al. 2008) and the present data state that the Małopolska Block granites exhibit calc-alkaline and medium-K to high-K geochemical signatures inherited from source rocks. The Rzeszotary amphibolites represent ancient magmas which were generated during Late Ediacaran/Early Cambrian (560-550 Ma – Żelaźniewicz et al. 2009) when the Rzeszotary terrane collided with the Małopolska Block (MB). Mafic magmas formed in the subduction setting from two sources (the mantle and the crust) and have calc-alkaline character (Żelaźniewicz et al. 2009). According to Słaby et al. (2010), the subduction ‘memory’ of the KLFZ volcanic rocks can be correlated to the Ediacaran/Cambrian reorganization.

Based on the modelling data (the inverse model – Słaby et al. 2010), the volcanic rocks from the Krzeszowice area exhibit calculated composition of a source related to peridotite enriched in hydrous minerals (garnet-, spinel- or even plagioclase- bearing peridotites).

The results of modelling the amphibolites’ partial melting (Słaby et al. 2010) represent a garnet-bearing and garnet-free residue after amphibolites melting. This is according to Rapp and Watson’s (1995) experiment of low-degree dehydration melting of metabasalt at low/medium pressures. Consequently, Słaby et al. (2010) emphasized that a model without garnet is more realistic for this type of formation of mafic/intermediate melts in the KLFZ, but melt generation may be more complex. This scenario is compatible with the numerous

data of present geochemical characteristics of the host granites studied, which is described above. The present chemical study of the rocks studied implies that they probably generated close to partial melting of the mafic rocks which gave a garnet-free residual melt, according to modelling by Słaby et al. (2010).

The investigations of Clemens et al. (2011) also confirm this conclusion. The capacity of granitic magmas to dissolve, react with and recrystallise entrained solids during ascent, cooling and emplacement has been described by Clemens et al. (1997). The addition of an aluminous peritectic phase as garnet in a source produced more strongly peraluminous magmas (Clemens et al. 1997). The rocks studied represented metaluminous to slightly peraluminous I-type granites. According to the opinion of Clemens et al. (2011), only the addition of peritectic phases as hornblende and clinopyroxene to the source rocks produced metaluminous to slightly peraluminous I-types magmatic rocks during partial melting. This scenario is more likely for the development and evolution of the host granites which have similar mineralogical and geochemical characteristics.

The lack of distinct depletion in Yb of the rocks studied (Fig. 63, 67) was evidently related to the lack of relic garnets in the magma source (Sun, Stern 2001).

As described above, the Małopolska Block granites belong to medium-K to high-K calc-alkaline granitoid suites. Based on Bonin's (2004) suggestions, this type of granitoid suite may originate from the partial melting of amphibole-spinel (garnet-free) peridotite metasomatized by a lithospheric source.

The lack of garnets in the restite enclaves that occur in the host granites (Wolska 2004) suggests, and is substantiated by Harris et al. (1994), that the parent melt of the Małopolska Block granites could be generated during melting of the mafic source (metamorphic rocks).

The negative Eu (Eu/Eu^*) anomaly was found to be characteristic of both the host granites (61-97) and MME (34-76), as well as distinct LREE-enrichment relative to HREE – for the host granites $(\text{La}/\text{Yb})_N = 7.8\text{-}20.7$; for the MME $(\text{La}/\text{Yb})_N = 5.0\text{-}17.7$ (Table 9). These REE patterns suggest a certain role of plagioclase and/or hornblende in the source of the rocks studied or plagioclase fractionation due their removal from the melt (Rollison 1993). Both types of the rocks studied show a small/more pronounced negative Eu anomaly (Fig. 67), which substantiated a slight degree of fractional crystallization of plagioclases during the evolution of the magma.

Żelaźniewicz et al. (2008) implied that the Dolina Będowska valley granodiorite shows a small Eu anomaly, relatively high contents of Sr and Ba, and undepleted Rb and Cs amounts that caused that plagioclase not to be left at the source. The moderate fractionation in the Dolina Będowska valley granodiorite was also mentioned by Żelaźniewicz et al. (2008), based on the high Ba content and relatively low Rb in the granitic rocks according to Blevin and Chappell's (1992) study.

The geochemical and isotopic data (described above) have confirmed the influence of mixing mafic and crustal components to form a homogenous, hybrid parent magma of the pale grey host granites in the basement of the Małopolska Block (MB).

The high-K character of calc-alkaline Małopolska Block granites may also reflect increasing degrees of crustal contamination, as described by Wilson (1989).

According to Taylor and McLennan (1985), the continental crust material is characterized by high abundances of K, Rb, Ba, Ta and La (LILE/HFSE ratios > 10) and by

the relative depletion of Nb in the chondrite-normalized diagram. The rocks studied show approximate patterns (Fig. 62, 63, 66, 67).

Following on from the position of the rocks studied in the Th/Yb vs Nb/Yb diagrams (Fig. 72), the MME originated from mantle-derived magmas (enriched OIB mantle sources) and were hybridized (contaminated) by voluminous granodioritic magmas that originated in the continental crust (UC). Analogically, Słaby et al. (2010) assumed OIB – E-MORB as well as LCC signatures for the intermediate volcanic rocks from the Krzeszowice area. According to the data of Słaby et al. (2010), it may be supposed that parental mafic magmas of the MME originated from a metasomatized mantle source but also exhibit the presence of crustal components related to the hybridisation process in the granodioritic magma chamber.

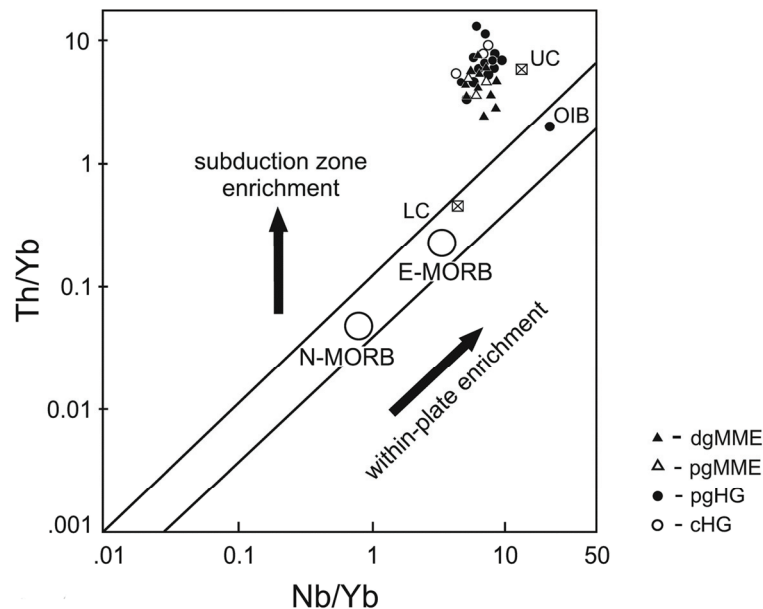


Fig. 72. Geochemical characteristics of the granites studied in the Th/Yb vs Nb/Yb diagram (after Pearce, Pete 1995). Symbols: dgMME – dark grey MME; pgMME – pale grey MME; pgHG – pale grey host granites; cHG – contact host granites. OIB value – after Pearce, Pete (1995), N-MORB and E-MORB values – after Sun, McDonough (1989), LC (lower crust) value – after Weaver, Tarney (1984), UC (upper crust) value – after Taylor et al. (1981).

Model of magma generation (mingling mixing) and its emplacement

Based on the petrographical, geochemical and isotope investigations, the following scenario of the formation of the rocks studied may be defined.

In the Late Carboniferous period, the collision of the Upper Silesian Block (USB) and the Małopolska Block (MB), caused lithospheric crust thickening in the KLFZ (Słaby et al. 2010). This process formed in tectonic regime of recurred stages of dextral transpression and dextral transtension (Żaba 1999). As postulated by Żelaźniewicz et al. (2008), granitic magmas in the Małopolska Block (MB) were derived from the thickened lower crust of the

Variscan orogenic belt. At the depth near the crust/mantle boundary, felsic melt was generated under conditions of extension and decompression (Żelaźniewicz et al. 2008). Due to advanced thickening and increased pressure, the lower crust rocks (with remnant oceanic plate – basalt+oceanic sediments of ancient subduction regime) were transformed to medium/high grade metamorphic rocks (probably amphibolites without garnet – the Rzeszotary amphibolite block. see Chapter 2: Geological setting). During increasing density, the lower crust underwent delamination and detachment and next sank into the upper mantle (according to Jull, Keleman 2001; Lustrino 2005).

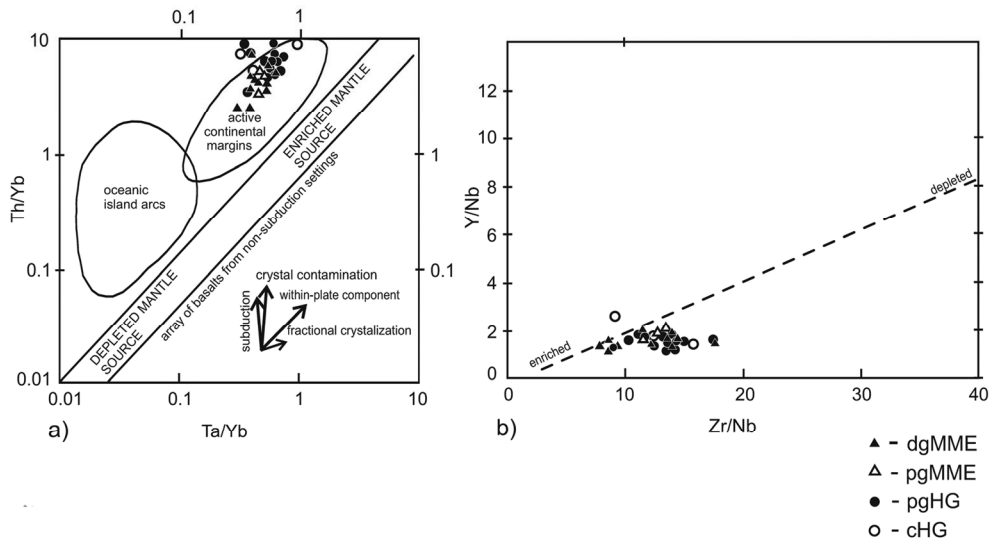


Fig. 73. Geochemical characteristics of the granites studied in a. – the Th/Yb vs Ta/Yb diagram (after Pearce 1983), b. – the Y/Nb vs Zr/Nb diagram; the dashed line indicates a mixing trend between enriched and depleted sources (Wilson 1989). Symbols: dgMME – dark grey MME; pgMME – pale grey MME; pgHG – pale grey host granites; cHG – contact host granites

The mafic lower crust (amphibolites, gneisses) dipped into the upper mantle, and during probably dehydration-melting processes (water-undersaturated) may have yielded mildly peraluminous to metaluminous granodioritic melts with coexisting anhydrous solid assemblage (Pl + Opx + Cpx + Mgt ± Il – according to Beard, Lofgren, 1990; Patiño Douce, Beard 1995; Clemens et al. 2011). Next, granodioritic melts mixed with residual solids/peritectic minerals and differentiated. During normal fractional crystallization, normal oscillatory zoning in plagioclase crystals (andesine-oligoclase) was formed and biotite overgrew amphibolites aggregates (represented as peritectic minerals rather than residual refractory solids). At a later stage of fractional crystallization, alkali feldspars and quartz were formed. Some plagioclase crystals show in the core of relic of peritectic minerals/residual solids of labradorite composition ('old cores'). The host granites studied formed during the solidification of crustal granodioritic melt. These granites exhibit less hybridisation by peritectic minerals/residual solids, and in a late stage of fractional crystallization they became completely homogenized magmatic rocks. According to Żaba

(1996), the generation of host granites took place (1996) during the D3 deformation phase (the pre-intrusive Namurian A stage) in deep levels of Paleozoic basement of the Małopolska Block (MB).

According to a study of magmatism in the Krzeszowice area and geochemical characteristics of volcanic rocks in this region by Słaby et al. (2010), it may be supposed that the basaltic melt originated from a metasomatized mantle source (Słaby et al. 2010) that inputs into the lower crust of the KLFZ. It seems that the mantle source consists of ultramafic rocks (likely spinel-amphibole garnet free peridotite) and was possibly enriched (metasomatized) by an earlier subduction process (Jayananda et al. 2000; Moyen et al. 2001; Słaby, Martin 2008) or by delaminated and remelted continental crust (Lustrino 2005).

In the case of the KLFZ basement, is difficult to determine a precise source and chronology of the mafic magma input/injection. It cannot be excluded that the mafic magma that originated from the upper mantle may have formed a magma chamber in a deeper part of the lower crust, and injected episodically into the granodioritic pluton at different stages of granodioritic magma crystallization rather than a continuous flux from mantle. A similar mechanism of mafic magma generation in an independent magma chamber and injection was described in the Karkonosze granitic pluton (Słaby, Martin 2008) and the Gęsiniec intrusion (Pietranik, Koepke 2009). In the KLFZ basement, two magma chambers (mafic and granodioritic) coexisted and evolved independently by fractional crystallization. Granodioritic magma differentiated independently in an early stage of fractional crystallization into a magma chamber before the mafic magma injection.

During its ascent into the lower crust, the basaltic melt (dyke) probably assimilated in lower degree by crustal wall rocks (the occurrence of alkali feldspar xenocrysts with reaction rim in the MME studied). Later, the basaltic melt intruded into the magma chamber and mingled with the granodioritic melt, which consists of crystal mush of partially crystallized rock-forming minerals and peritectic minerals/residual solids. As suggested by Solgadi et al. (2007), the mingling and also the mixing processes formed more easily into a magma chamber which filled by a well-stirred magma. The MME may be formed by mingling and mixing processes during contemporaneous ascent or emplacement of mafic and granitic magma, as described in detail by Collins et al. (2000) and Barbarin, (2005).

Basaltic melt formed blobs in the granodioritic host because of a large proportion of felsic magma, as well as the temperature and viscosity contrast caused by the mingling process (Sparks, Marshall 1986; Hallot et al. 1994, 1996). Next, the mixing process was generated locally in magma chamber during local interaction between the basaltic and granodioritic melts. In addition, diffusion between the granodioritic and basaltic melts caused the exchange of chemical components (Vernon 1990) both in the host magma (host granites) and the blobs (MME). The mixing process is related to the early stage of fractional crystallization. The induced reaction between the primary minerals and modified basaltic melt and the pseudo-doleritic texture of a fine-grained groundmass in the hybridized basaltic melt was formed in the enclave due to fast cooling. The compositional similarity of minerals in enclaves may be observed as in the granodioritic host – plagioclase and quartz megacrysts, and also amphibole aggregates, but also inner mixing textures in rock-forming minerals. The megacrysts of the plagioclases show resorption zones that

formed in response to the injection of mafic magma. Later, leucocratic granitic melt ($\text{SiO}_2 > 70\text{wt}\%$ – Wiebe et al. 2004) squeezed from the granodioritic host, infiltrated into the MME and formed quartz and alkali feldspar crystals in interstices in the fine-grained groundmass. All the processes described above caused hybridisation of basaltic blobs by the granodioritic host and the formation of the MME close to the composition of Q-diorites and tonalites. According to Janoušek et al. (2004) and Barbarin (2005) studies, may analogically ascertain that the MME studied represent different stages of interaction between mafic and felsic magmas. Their composition does not reflect their primary magmatic chemistry because their parental mafic magma bodies were chemically re-equilibrated with their granodioritic host.

Next, the hybrid, homogenous magma of host granites containing enclaves (the MME subtypes exhibit various degrees of mixing and hybridisation) rose up to the level of the Ediacaran/Paleozoic basement of the Małopolska Block (MB). During the Westphalian B-Stephanian stage (Żaba 1996, 1999) or close to the Carboniferous/Permian boundary (Nawrocki et al. 2008; Żelaźniewicz et al. 2008), the emplacement of the host granites containing MME to the upper crustal levels took place (near 10-15 km in depth). This part of the upper crust was probably warmer and more ductile therefore, as described by Jellinek and DePaolo (2003), in such conditions granitic plutons favour accumulation over eruption. Based on the study of oscillatory zoning in plagioclase crystals (Kośnik, Muszyński 1990) and melt inclusion in quartz, apatite and zircon (Karwowski 1988), the depth of solidification of granodioritic melt was estimated to be 5-6 km (Żaba 1999).

Broad zones of contact aureoles and specific mineral paragenesis cordierite + andalusite (Koszowska, Wolska 2000a, b) suggest high temperature gradients between the wall sedimentary rocks and calc-alkaline granodioritic magmas and the large size of the granodioritic pluton which formed at a deeper level of the Ediacaran/Paleozoic basement of the Małopolska Block (MB).

In the post-magmatic episode, hydrothermal processes developed and connected with the formation of Cu-Mo porphyry deposits within the Małopolska granitoids (see Chapter 3: Magmatic rock investigations).

7. Conclusions

1. In the pale grey host granites (granodiorites), mafic microgranular enclaves (MME) of the Q-dioritic and tonalitic composition occur.
2. The occurrence of MME is evidence of mingling processes which formed during injection of hot mafic magma into the granodioritic magma chamber in the deeper levels of the Małopolska Block (MB). The mafic magma was not dispersed into granodioritic mush but formed relatively large blobs of various sizes.
3. The host granites (granodiorites) and MME (Q-diorites and tonalites) consist of similar rock-forming minerals (in various modal proportions), but they exhibit different structural and textural features.
4. Mantled boxy cellular plagioclase crystals with 'old cores' of the labradorite composition and amphibole aggregates with titanite and opaque minerals represent peritectic minerals produced by melting reactions rather than primary refractory residual minerals.

5. The later interaction processes between mafic blobs and granodioritic host magmas are related to the local mixing process.
6. In the host granites (granodiorites), inner textures of rock-forming minerals (the spike and spongy cellular zones as well as biotite/amphibole zones in plagioclase crystals) are connected to subtle, local mixing of granodioritic and mafic magmas, whereas normal zoning in the outer parts of plagioclase crystals is connected to fractional crystallization more homogenized granodioritic magma, after the mixing episode.
7. The MME (Q-diorites and tonalites) were strongly hybridized by a granodioritic host magma. The occurrence in the MME megacrysts of plagioclases (mantled boxy cellular crystals) and quartz is evidence for a mechanical transfer of these minerals from the granodioritic host. Leucocratic residual melt squeezed from the granodioritic host caused crystallization of small quartz and alkali feldspar crystals in interstices of fine-grained groundmass of the MME.
8. The presence of lath-shaped plagioclases, blade-shaped amphiboles/biotite and acicular-shaped apatites in the groundmass of the MME is evidence for undercooling of hot mafic melt blobs in cold granodioritic magma chamber.
9. The host granites (granodiorites) and the MME (Q-diorites and tonalites) are characterized by various amounts of major elements (SiO_2 , Na_2O and K_2O), trace elements (especially transition metals Ni, Cr, V, Ti and P), #Mg and MALI that is evidently related to their origins from different sources.
10. Both rocks studied have similar chondrite-normalized patterns, LIL elements (Sr, Ba and Rb), ASI and isotopic signatures (markedly lower than for continental crust) that is connected with strong hybridisation of the mafic melt blobs by the granodioritic host magma.
11. The entrainment of peritectic minerals into granodioritic magma, which originated during dehydration melting of amphibolites (remnants of the subducted slab consist of basalt + oceanic sediments of ancient arc tectonic setting), caused its transformation to metaluminous-slightly peraluminous I-type granitic melt, which at a later stage formed the pale grey host granites (granodiorites).
12. During the hybridisation process by the granodioritic host magma, the MME obtained geochemical characteristics typical for calc-alkaline, metaluminous slightly peraluminous, medium- to high-K magmatic rocks.
13. Based on geochemical data, it may be supposed that parental magma of both rocks studied have mafic signatures (characteristic of metamorphic rocks such as metabasalts, metatonalites, amphibolites or amphibole-spinel garnet free peridotite), whereas they were generated from different sources: the host granites (granodiorites) in lower continental crust, while the MME (primary mafic basaltic melt) is enriched (metasomatized) upper mantle.
14. The MME represent rocks which crystallized from less homogenized (to various degrees – an examples of dark grey and pale grey subtypes of MME probably related to dimensions of mafic blobs) strongly hybridized magma of intermediate compositions (Q-diorites and tonalites) rather than from primary mafic magma.
15. The pale grey host granites (granodiorites) crystallized from completely homogenized granodioritic crustal magma only in small degree hybridized by peritectic minerals and by local interaction with mafic blobs.

Acknowledgements. This study has been supported by several grants from the Jagiellonian University (project number: DS. 802, WRBW/BiNoZ/ING/53/2007, DSP K/ZDŚ/00 1675). I would like to thank Jadwiga Faber M.Sc. (the Laboratory of Scanning Electron Microscopy of the Institute Zoology, Jagiellonian University) and Anna Łatkiewicz M.Sc. (Laboratory of Field Emission Scanning Electron Microscopy and Microanalysis at the Institute of Geological Sciences, Jagiellonian University) for help and assistance during microprobe analytical sessions, and Waldemar Obcowski M. Sc. for professional photographs of rock specimens.

The author is also grateful to three anonymous reviewers for constructive suggestions and thorough, critical comments on the manuscript.

8. References

- Allen, C. M. (1991). Local equilibrium of mafic enclaves and granitoids of the Turtle pluton, southeast California: mineral, chemical, and isotopic evidence. *American Mineralogists*, 76(3-4), 574-588.
- Altherr, R., Henes-Klaiber, U., Hegner, E., Satir, M., & Langer, C. (1999). Plutonism in the Variscan Odenwald (Germany): from subduction to collision. *International Journal of Earth Sciences*, 88(3), 422-443. DOI: 10.1007/s005310050276.
- Altherton, M. P., & Sanderson, L. M. (1987). The Cordillera Blanca Batholith: a study of granite intrusion and the relation of crustal thickening to peraluminosity. *Geologische Rundschau*, 76(1), 231-232. DOI: 10.1007/BF01820584
- Arnold, J., Jacoby, W. R., Schmeling, H., & Schott, B. (2001). Continental collision and the dynamic and thermal evolution of the Variscan orogenic crustal root – numerical models. *Journal of Geodynamics*, 31(3), 273-291.
- Åkesson, U., Hansson, J., & Stigh, J. (2004). Characterisation of microcracks in the Bohus granite, western Sweden, caused by uniaxial cyclic loading. *Engineering Geology*, 72(1-2), 131-142. DOI:10.1016/j.enggeo.2003.07.001
- Bacon, C. R. (1989). Crystallisation of accessory phases in magmas by local saturation adjacent to phenocrysts. *Geochimica et Cosmochimica Acta*, 53(5), 1055-1066.
- Baldwin, A. J., & Pearce, J. A. (1982). Discrimination of productive and non productive porphyritic intrusions in the Chilean Andes. *Economic Geology*, 77(3), 664-674.
- Banaś, M., Paulo, A., & Piekarski, K. (1972). O mineralizacji miedziowej i molibdenowej w rejonie Mrzygłodu. *Rudy i Metale Nieżelazne*, 17(1), 3-7 (in Polish).
- Barbarin, B. (1990). Plagioclase xenocrysts and mafic magmatic enclaves in some granitoids of the Sierra Nevada Batholith, California. *Journal of Geophysical Research*, 95(B11), 17747-17756. DOI: 10.1029/JB095iB11p17747.
- Barbarin, B. (2005). Mafic magmatic enclaves and mafic rocks associated with some granitoids of the central Sierra Nevada batholiths, California: nature, origin, and relations with the hosts. *Lithos*, 80(1-4), 155-177. DOI:10.1016/j.lithos.2004.05.010.
- Barbarin, B., & Didier, J. (1991a). Microscopic features of mafic microgranular enclaves. In J. Didier & B. Barbarin (Eds.), *Enclaves and Granite Petrology* (pp. 253-262). Amsterdam-Oxford-New York-Tokyo: Elsevier.
- Barbarin, B., & Didier, J. (1991b). Conclusions: enclaves and granite petrology. In J. Didier & B. Barbarin (Eds.), *Enclaves and Granite Petrology* (pp. 545-549). Amsterdam-New York-Tokyo: Elsevier.
- Barbarin, B., & Didier, J. (1992). Genesis and evolution of mafic microgranular enclaves through various types of interaction between coexisting felsic and mafic magmas. *Transactions of the Royal Society of Edinburgh, Earth Sciences*, 83(1-2), 145-153. DOI:10.1017/S0263593300007835.
- Barker, F. (1979). Trondhjemites: definition, environment and hypothesis of origin. In F. Baker (Ed.), *Trondhjemites, Dacites and Related Rocks* (pp.1-12). Amsterdam, New York: Elsevier.
- Barth, T. F. W. (1962). *Theoretical Petrology*. New York: Wiley. 416pp.
- Batchelor, R. A., & Bowden, P. (1985). Petrologic interpretation of granitoid rock series using multicationic parameters. *Chemical Geology*, 48(1-4), 43-55.
- Baxter, S., & Feely, M. (2002). Magma mixing and mingling textures in granitoids: examples from the Galway Granite, Ireland. *Contributions to Mineralogy and Petrology* 76(1), 63-74.

- Beard, J. S., & Lofgren, G. E. (1990). Dehydration melting and water-saturated melting of basaltic and andesitic greenstones and amphibolites at 1.3 and 6.9 kb. *Journal of Petrology*, 32(2), 365-401. DOI: 10.1093/petrology/32.2.365.
- Belka, Z., Valverde-Vaquero, P., Dörr, W., Ahrendt, H., Wemmer, K., Franke, W., & Schäffer, H. J. (2002). Accretion of first Gondwana-derived terranes at the margin of Baltica. In J. A. Winchester, J. Verniers & T. C. Pharaoh (Eds.), (pp. 19-36). *Geological Society of London Special Publications* 201.
- Berthelsen, A. (1998). The Tornquist Zone northwest of the Carpathians: An interplate pseudosuture. *Geologiska Föreningens i Stockholm Föreläsningar*, 120(2), 223-230. DOI: 10.1080/11035899801202223.
- Black, R., & Liégeois, J. P. (1993). Cratons, mobile belts, alkaline rocks and continental lithospheric mantle: the Pan-African testimony. *Journal of the Geological Society of London*, 150(1), 89-98.
- Blake, D. H., Elwell, R. W. D., Gibson, I. L., Skelhorn, R. R., & Walker, G. P. L. (1965). Some relationships resulting from the intimate association of acid and basic magmas. *Journal of the Geological Society of London*, 121(1), 31-50.
- Blevin, P. L., & Chappell, B. W. (1992). The role of magma sources, oxidation states and fractionation in determining the granite metallogeny of eastern Australia. *Transactions of the Royal Society of Edinburgh, Earth Sciences*, 83(1-2), 305-316.
- Bogacz, K. (1980). Budowa geologiczna paleozoiku dębnickiego. *Roczniki Polskiego Towarzystwa Geologicznego*, 50(2), 183-208 (in Polish).
- Bogacz, W., & Krokowski, J. (1981). Rotation of the basement of the Upper Silesian Coal Basin. *Annales Societatis Geologorum Poloniae*, 51(3-4), 361-381.
- Bolewski, A. (1939). Zagadnienie "kalifikacji" krakowskich skał magmowych. *Rocznik Polskiego Towarzystwa Geologicznego*, 15(1), 42-85 (in Polish).
- Bonin, B. (1990). From orogenic to anorogenic settings: evolution of granitoid suites after a major orogenesis. *The Journal of Geology*, 25(3-4), 261-270.
- Bonin, B. (2004). Do coeval mafic and felsic magmas in post-collisional to within-plate regimes necessarily imply two contrasting, mantle and crustal, sources? A review. *Lithos*, 78(1-2), 1-24.
- Brandeis, G., Jaupart, C., & Allègre, C.J. (1984). Nucleation, crystal growth and thermal regime of cooling magmas. *Journal of Geophysical Research*, 89(B12), 10161-10177. DOI:10.1029/JBO89iB12p10161.
- Brochwic-Lewiński, W., Pożaryski, W., & Tomczyk, H. (1983). Ruchy przesuwcze południowej Polsce w paleozoiku. *Przegląd Geologiczny*, 31(12), 651-658 (in Polish).
- Brochwic-Lewiński, W., Vidal, G., Pożaryski, W., Tomczyk, H., & Zajac, R. (1986). Pre-Permian tectonic position of the Upper Silesian Massif (S Poland) in the light of studies on the Cambrian. *Comptes Rendus de l'Académie des Sciences, Paris, Série II*, 303(16), 1493-1496.
- Broder, J. (1931). Diabase von Niedzwiedzia Góra bei Krzeszowice und die begleitenden Gebilde. *Bulletin de l'Académie Polonaise des Sciences et des Lettres, Classe des Sciences Mathématiques et Naturelles, Ser. A, Cracovie*, 546-569.
- Brown, G. C., Thrope, R. S., & Webb, P. C. (1984). The geochemical characteristics of granitoids in contrasting arcs and comments on magma sources. *Journal of the Geological Society of London*, 141(5), 413-426.
- Bukowy S. (1964). Nowe poglądy na budowę północno-wschodniego obrzeżenia Górnośląskiego Zagłębia Węglowego. *Biuletyn Instytutu Geologicznego*, 184(7), 5-19 (in Polish).
- Bukowy, S. (1984). Struktury waryscyjskie regionu śląsko-krakowskiego. Sosnowiec: *Prace Naukowe Uniwersytetu Śląskiego, Geologia*, 691, 1-75 (in Polish).
- Bukowy, S. (1994). Zarys budowy paleozoiku północno-wschodniego obrzeżenia Górnośląskiego Zagłębia Węglowego. In A. Rózkowski, J. Ślósarz & J. Żaba (Eds.), *Przewodnik 65. Zjazdu Polskiego Towarzystwa Geologicznego, Sosnowiec 22-24 września 1994* (pp. 14-30). *Prace Naukowe Uniwersytetu Śląskiego w Katowicach*, 1431. Katowice: Wydawnictwa Uniwersytetu Śląskiego (in Polish).
- Bukowy, S., & Cebulak, S. (1964). Nowe dane o magmatyzmie antyklinorium śląsko-krakowskiego. *Biuletyn Instytutu Geologicznego*, 184(7), 41-94 (in Polish).
- Bukowy, S., & Ślósarz, J. (1968). Wyniki wiercenia Bębło. *Biuletyn Instytutu Geologicznego* 212(9), 7-38 (in Polish).
- Buła, Z. (1994). Problemy stratygrafii i wykształcenie osadów starszego paleozoiku północno-wschodniego obrzeżenia Górnośląskiego Zagłębia Węglowego. In A. Rózkowski, J. Ślósarz & J. Żaba (Eds.), *Przewodnik 65. Zjazdu Polskiego Towarzystwa Geologicznego, Sosnowiec 22-24 września 1994* (pp. 31-57). *Prace Naukowe Uniwersytetu Śląskiego* 1431. Katowice: Wydawnictwa Uniwersytetu Śląskiego (in Polish).
- Buła, Z. (2000). The Lower Palaeozoic of Upper Silesia and West Małopolska. *Prace Państwowego Instytutu Geologicznego*, 171, 1-89.

- Buła, Z., & Jachowicz, M. (1996). The Lower Palaeozoic sediments in the Upper Silesian Block. *Geological Quarterly*, 40(3), 299-336.
- Buła, Z., Jachowicz, M., & Přichstál, A. (1997a). Lower Palaeozoic deposits of the Brunovistulikum. *Terra Nostra*, 11, 32-38.
- Buła, Z., Jachowicz, M., & Żaba, J. (1997b). Principal characteristics of the Upper Silesian Block and Małopolska Block border zone (southern Poland). *Geological Magazine*, 134(5), 669-677.
- Buła, Z., & Żaba, J. (2005). Pozycja tektoniczna Górnośląskiego Zagłębia Węglowego na tle prekambryjskiego i dolno paleozoicznego podłoża. In J. Jureczka, Z. Buła & J. Żaba (Eds.), *Geologia i zagadnienia ochrony środowiska w rejonie górnośląskim* (pp. 14-42). Warszawa: Państwowy Instytut Geologiczny, Polskie Towarzystwo Geologiczne (in Polish).
- Buła, Z., & Żaba, J. (2008). Struktura prekambryjskiego podłoża wschodniej części bloku górnośląskiego (Brunovistulikum). *Przegląd Geologiczny*, 56(6), 473-480 (in Polish).
- Buła, Z., & Habryn, R. (Eds.) (2008). *Geological-structural atlas of the Palaeozoic basement of the Outer Carpathians and Carpathian Foredeep*. Warszawa: Państwowy Instytut Geologiczny.
- Buła, Z., Żaba, J., & Habryn, R. (2008). Regionalizacja tektoniczna Polski – Polska Południowa (blok górnośląski i blok małopolski). *Przegląd Geologiczny*, 56(10), 912-920 (in Polish).
- Buła, Z., & Habryn, R. (2010). Precambrian and Paleozoic geology of Cracow region. In M. Jachowicz-Zdanowska & Z. Buła (Eds.), *Prekambr i Paleozoik Regionu Krakowskiego-model budowy geologicznej-jego aspekt uptylarny, Kraków 19 listopada 2010* (pp. 7-39). Warszawa: Państwowy Instytut Geologiczny-Państwowy Instytut Badawczy. (in Polish, English summary).
- Burnham, C. W. (1979). Magmas and hydrothermal fluids. In H.L. Barnes (Ed.), *Geochemistry of Hydrothermal Ore Deposits* (pp. 71-136), 2nd. Ed, New York: John Wiley & Sons.
- Bylina, P., Żelaźniewicz, A., & Dörr, W. (2000). Archean basement in the Upper Silesian Block: U-Pb zircon age from amphibolites of the Rzeszotary horst. *Abstracts, Joint Meeting EUROPROBE and PACE projects, Zakopane* (pp. 11-12).
- Castro, A. (2004). The source of granites: inferences from the Lewisian complex. *Scottish Journal of Geology*, 40(1), 49-65.
- Castro, A., Moreno-Ventas, I., & De la Rosa, J. D. (1990). Microgranular enclaves as indicators of hybridization processes in granitoid rocks, Hercynian Belt, Spain. *The Journal of Geology*, 25(3-4), 391-404.
- Castro, A., & Stephens, W. E. (1992). Amphibole-rich polycrystalline clots in calc-alkaline granitic rocks and their enclaves. *Canadian Mineralogist*, 30(4), 1093-1112.
- Castro, A., Patiño Douce, A. E., Corretgé, L. G., De la Rosa, J. D., El-Biad, M., & El-Hamidi, H. (1999). Origin of peraluminous granites and granodiorites, Iberian massif, Spain: an experimental test of granite petrogenesis. *Contributions to Mineralogy and Petrology*, 135(2-3), 255-276. DOI:10.1007/s004100050511.
- Çatlos, E. J., Baker, C. B., Sorensen, S. S., Jacob, L., & Çemen, I. (2011). Linking microcracks and mineral zoning of detachment-exhumed granites to their tectonomagnetic history: Evidence from the Salihli and Turgutlu plutons in western Turkey (Menderes Massif). *Journal of Structural Geology*, 33(5), 951-969. DOI: 10.1016/j.jsg.2011.02.005.
- Cebulak, S., & Kotas, A. (1982). Profil utworów intruzywnych i prekambryjskich w otworze Goczałkowice IG-1. In A. Rózkowski & J. Ślósarz (Eds.), *Przewodnik 54 Zjazdu Polskiego Towarzystwa Geologicznego, Sosnowiec 23-25 września 1982* (pp. 205-210). Warszawa: Wydawnictwa Geologiczne (in Polish).
- Chappell, B. W. (1996). Magma mixing and the production of compositional variation within granite suites: evidence from the granites of Southeastern Australia. *Journal of Petrology*, 37(3), 449-470.
- Chappell, B. W., & White, A. J. R. (1974). Two contrasting granite types. *Pacific Geology*, 8, 173-174.
- Chen, Y. D., Price, R. C., & White, A. J. R. (1989). Inclusions in three S-type granites from southeastern Australia. *Journal of Petrology*, 30(5), 1181-1218.
- Chesner, C. A., & Ettlinger, A. D. (1989). Composition of volcanic allanite from the Toba Tuffs, Sumatra, Indonesia. *American Mineralogist*, 74(7-8), 750-758.
- Clarke, B. (1992). The mineralogy of peraluminous granites: A review. *Canadian Mineralogist*, 19(1), 3-17.
- Clemens, J. D., & Wall, V. J. (1988). Controls on the mineralogy of S-type volcanic and plutonic rocks. *Lithos*, 21(1), 53-66.
- Clemens, J. D., Petford, N., & Mawer, C. K. (1997). Ascent mechanisms of granitic magmas: causes and consequences. In M. Holness (Ed.), *Deformation-enhanced Fluid Transport in the Earth's Crust and Mantle* (pp. 144-171). London: Chapman & Hall.
- Clemens, J. D., Stevens, G., & Farina, F. (2011). The enigmatic sources of I-type granites: The peritectic connexion. *Lithos* 126(3-4), 174-181. DOI: 10.1016/j.lithos.2011.07.004.

- Cohen, A. S., O'Nions, R. K., Siegenthaler, R., & Griffin, W. L. (1988). Chronology of the pressure-temperature history recorded by granulite terrain. *Contributions to Mineralogy and Petrology*, 98(3), 303-311.
- Coish, R. A., & Sinton, C. W. (1992). Geochemistry of mantle dikes in the Adirondack Mountains: implications for Late Proterozoic continental rifting. *Contributions to Mineralogy and Petrology*, 110(4), 500-514. DOI:10.1007/BFO0344084.
- Collins, W.J., Richards, S. R., Healy, B. E., & Ellison, P.I. (2000). Origin of heterogeneous mafic enclaves by two-stage hybridisation in magma conduits (dykes) below and in granite magma chambers. *Transactions of the Royal Society of Edinburgh, Earth Sciences*, 91(1-2), 27-45.
- Cox, K. G., Bell, J. D., & Pankhurst, R. J. (1979). *The Interpretation of Igneous Rocks*. London: Allen & Unwin.
- Czerny, J., & Muszyński, M. (1997). Co-magmatism of the Permian Vulcanite of the Krzeszowice area in the light of petrochemical data. *Mineralogia Polonica*, 28(2), 3-25.
- Czerny, J., & Muszyński, M. (1998). New petrochemical data on lamprophyres from the NE margin of the Upper Silesian Coal Basin. *Mineralogia Polonica*, 29(1), 67-75.
- Czerny, J., & Muszyński, M. (2000). The current state of recognition of Upper Paleozoic volcanites of the Cracow area. *Mineralogical Society of Poland Special Papers*, 17, 13-17.
- Czerny, J., Heflik, W., & Muszyński, M. (2000). Granitoid and dioritic enclaves in the porphyries of the Cracow area. *Polish Mineralogical Society Special Papers*, 17, 18-19.
- Czerny, J., & Muszyński, M. (2002). Enclaves of microgranodiorites and micromonzodiorites in the rhyodacitic porphyries from Miękinia near Krzeszowice. *Mineralogia Polonica*, 33(2) 49-59.
- Dadlez, R. (1995). Debates about the pre-Variscan tectonics of Poland. *Studia Geophysica et Geodaetica*, 39(3), 227-234.
- Dadlez, R., Kowalczewski, Z., & Znosko, J. (1994). Some key problems of the pre-Permian tectonics of Poland. *Geological Quarterly*, 38(2), 169-190.
- Dahlquist, J. A. (2002). Mafic microgranular enclaves: early segregation from metaluminous magma (Sierra de Chepes), Pampean Ranges, NW Argentina. *Journal of South American Earth Sciences*, 15(6), 643-655.
- Davidson, J. P., Dungan, M. A., Ferguson, K. M., & Colucci, M. T. (1987). Crust-magma interactions and the evolution of arc magmas: The San Pedro-Pellado volcanic complex, southern Chilean Andes. *Geology*, 15(5), 443-446.
- Debon, F. (1991). Comparative major element chemistry in various "microgranular enclave-plutonic host" pairs. In J. Didier & B. Barbarin (Eds.), *Enclaves and Granite Petrology*. (pp. 293-310). Amsterdam-Oxford-New York-Tokyo: Elsevier.
- Debon, F., & Le Fort, P. (1983). A chemical-mineralogical classification of common plutonic rocks and associations. *Transactions of the Royal Society of Edinburgh, Earth Sciences*, 73(3), 135-149.
- Debon, F., & Le Fort, P. (1988). A cationic classification of common plutonic rocks and their magmatic associations: principles, method application. *Bulletin de Minéralogie*, 111(5), 493-510.
- De la Roche, H., Leterrier, J., Grandclaude, P., & Marchal, M. (1980). A classification of volcanic and plutonic rocks using R1, R2-diagrams and major element analysis-its relationships with current nomenclature. *Chemical Geology*, 29(1-4), 183-210.
- DePaolo, D. J., Perry, F. V., & Baldrige, W. S. (1992). Crustal vs. mantle sources of granitic magmas: A two parameter model based on Nd isotopic studies. In P. E. Brown & B. W. Chappell (Eds.), *Second Hutton Symposium: The Origin of Granites and Related Rocks* (pp.439-446). *Transactions of the Royal Society of Edinburgh, Earth Sciences*, 83(1-2). DOI: 10.1017/S02635933000008.
- Depciuch, T. (1971). Oznaczenie wieku bezwzględnego za pomocą wolumetrycznej odmiany metody K-Ar, stosowanej w Instytucie Geologicznym. *Kwartalnik Geologiczny*, 15(3), 483-496 (in Polish).
- Didier, J. (1973). *Granites and their enclaves*. Amsterdam-London-New York: Elsevier, 393pp.
- Didier, J. (1987). Contributions of enclaves studies to the understanding of origin and evolution of granitic magmas. *Geologische Rundschau*, 76(1), 41-50.
- Didier, J., & Barbarin, B. (1991). *Enclaves and Granite Petrology*. Amsterdam-Oxford-New York-Tokyo: Elsevier, 625pp.
- Dodge, F. C. W., & Kistler, R. W., (1990). Some additional observations on inclusions in the granitic rocks of the Sierra Nevada. *Journal of Geophysical Research*, 95(B11), 17841-17848.
- Donaire, T., Pascual, E., Pin, C., & Duthou, J-L. (2005). Micogranular enclaves as evidence of rapid cooling in granitoid rocks: the case of the Los Pedroches granodiorite, Iberian Massif, Spain. *Contribution to Mineralogy and Petrology*, 149(3), 247-265.
- Dorais, M. J., Whitney, J. A., & Roden, M. (1990). Origin of mafic enclaves in the Dinkey Creek Pluton, Central Sierra Nevada batholiths, California. *Journal of Petrology*, 31(4), 853-881.

- Dostal, J., Cousens, B., & Dupuy, C. (1998). The incompatible element characteristics of an ancient subducted sedimentary component in ocean islands basalt from French Polynesia. *Journal of Petrology*, 39(5), 937-952.
- Duchnese, J.-C., Berza, T., Liégeois, J.-P., & Auwera, J. V. (1998). Shoshonitic liquid line of descent from diorite to granite: the Late Precambrian post-collisional Tismana pluton (South Carpathians, Romania). *Lithos*, 45(1), 281-303.
- Dudek, A. (1980). The crystalline basement Block of the Outer Carpathians in Moravia: Bruno-Vistulicum. *Rozprawy Česká Akademie Věd a Umění Řada Matematicko-Přirodovědecká Věd*, 90, 1-85.
- Dupuy, C., & Dostal, J. (1984). Trace element of some continental tholeiites. *Earth Planetary Science Letters*, 67(1), 61-69.
- Dzik, J. (1983). Early Ordovician conodonts from the Barrandian and Bohemian-Baltic faunal relationships. *Acta Palaeontologica Polonica*, 28(3-4), 327-368.
- Eberz, G. W., & Nicholls, I. A. (1990). Chemical modification of enclave magma by post-emplacement crystal fractionation, diffusion and metasomatism. *Contribution to Mineralogy and Petrology*, 104(1), 47-55.
- El Bouseily, A. M., & Sokkary, A. A. (1975). The relation between Rb, Ba and Sr in granitic rocks. *Chemical Geology*, 16(3), 207-219. DOI: 10.16/0009-2541(75)90029-7.
- Elburg, M. A. (1996). Evidence of isotopic equilibration between microgranitoid enclaves and host granodiorite, Warburton Granodiorite, Lachlan Fold Belt, Australia. *Lithos*, 38(1-2), 1-22.
- Emslie, R. F. (1980). Geology and petrology of the Harp Lake Complex, Central Labrador: an example of Elsonian magmatism. *Geological Survey of Canada Bulletin*, 293, 236pp.
- Fernandez, A. N., & Barbarin, B. (1991). Relative rheology of coeval mafic and felsic magmas: Nature of resulting interaction processes. Shape and mineral fabrics of mafic microgranular enclaves. In J. Didier & B. Barbarin (Eds.), *Enclaves and Granite Petrology* (pp. 263-275). Amsterdam-Oxford-New York-Tokyo: Elsevier.
- Fernández-Suárez, J., Gutierrez-Alonso, G., Johnston, S. T., Jeffries, T. E., Pastor-Galán, D., Jenner, G. A., & Murphy, J. B. (2011). Iberian late-Variscan granitoids: some considerations on crustal sources and the significance of "mantle extraction ages". *Lithos*, 123(1-4), 121-132.
- Fershtater, G. B., & Borodina, N. S. (1991). Enclaves in the Hercynian granitoids of the Ural Mountains, USSR. In J. Didier & B. Barbarin (Eds.), *Enclaves and Granite Petrology* (pp. 83-94). Amsterdam-New York-Tokyo: Elsevier.
- Finger, F., Schitter, F., Riegler, G., & Krenn, E. (1999). The history of the Brunovistulian total-Pb monazite ages from the metamorphic complex. *Geolines*, 8, 21-23.
- Finger, F., Hanzl, P., Pin, C., Von Quadt, A., & Steyrer, H. P. (2000). The Brunovistulian: Avalonian Precambrian sequence at the eastern end of the Central European Variscides? In W. Franke, O. Haak, O. Oncken & D. Tanner, (Eds.), *Orogenic Processes: Quantification and Modelling in the Variscan Belt* (pp.103-112). Geological Society London Special Publications, 179.
- Finger, F., Gedres, A., Rene, M., & Riegler, G. (2009). The Saxo-Danubian Granite Belt: magmatic response to post-collisional delamination of mantle lithosphere below the south-western sector of the Bohemian Massif (Variscan orogen). *Geologica Carpathica*, 60(3), 205-212.
- Foley, S., & Peccerillo, A. (1992). Potassic and ultrapotassic magmas and their origin. *Lithos*, 28(3-6), 181-185. DOI:10.1016/0024-4937(92)900005-J.
- Foley, S. F., Tiepolo, M., & Vannucci, R. (2002). Growth of early continental crust controlled by melting of amphibole in subduction zones. *Nature*, 417(6889), 637-640.
- Frost, B. R., & Lindsley, D. H. (1991). The occurrence of Fe-Ti oxides in igneous rocks. In D. H. Lindsley (Ed.), *Oxide Minerals: Petrologic and Magmatic Significance* (pp.433-486). Mineralogical Society of America, Reviews in Mineralogy 25.
- Frost, B. R., Barnes, C. G., Collins, W. J., Arculus, R. J., Ellis, D. J., & Frost, C. D. (2001). A geochemical classification for granitic rocks. *Journal of Petrology*, 42(11), 2033-2048.
- Gawel, A., (1955). Xenolith of plutonic rock in the porphyry of Siedlec near Krzeszowice. *Biuletyn Instytutu Geologicznego*, 97(1), 102-113.
- Gill, J. B. (1981). *Orogenic Andesites and Plate Tectonics*. New York: Springer, 390pp.
- Glazner, A. F., Bartley, J. M., Coleman, D. S., Gray, W., & Taylor, R. Z. (2004). Are plutons assembled over millions years by amalgamation from small magma chambers ?. *GSA Today*, 14(4-5), 4-9. DOI: 10.1130/1052-5173(2004)014<0004:APAOMO>2.0.CO;2.
- Green, N. L., & Lesher, C. M. (1987). Mineralogy and geochemistry of the Hog Mountain pluton, Northern Alabama Piedmont. In M. S. Drummond, N. L. Green & M. J. Neilson (Eds.), *The Granites of Alabama*, 24th Annual Field Trip Guidebook (pp. 1-12). Alabama Geological Society.

- Gromet, L. P., & Silver, L. T. (1983). Rare earth element distributions among minerals in a granodiorite and their petrogenetic implications. *Geochimica et Cosmochimica Acta*, 47(5), 925-939.
- Górecka, E. (1972). Mineralizacja kruszcowa w utworach paleozoicznych północno-wschodniej części obszaru śląsko-krakowskiego. *Acta Geologica Polonica*, 22(2) 275-326 (in Polish).
- Hallot, E., Auvray, B., de Bremond d'Ars, J., Davy, P., & Martin, H. (1994). New injection experiments in non-Newtonian fluids. *Terra Nova*, 6, 274-281.
- Hallot, E., Davy, P., de Bremond d'Ars, J., Auvray, B., Martin, H., & van Damme, H. (1996). Non-Newtonian effects during injection in partially crystallized magmas. *Journal of Volcanology and Geothermal Research*, 71(1), 31-44.
- Harańczyk, C. (1978). Mineralizacja polimetaliczna w utworach paleozoicznych wschodniego obrzeżenia Górnośląskiego Zagłębia Węglowego. *Prace Instytutu Geologicznego*, 83, 171-182 (in Polish).
- Harańczyk, C. (1982). Krakowidy jako orogen kaledoński. *Przegląd Geologiczny*, 30(11), 575-582 (in Polish).
- Harańczyk, C. (1984). Utwory kambry strefy krakowskiej. Materiały niepublikowane. Sosnowiec: Archiwum Państwowego Instytutu Geologicznego (in Polish).
- Harańczyk, C. (1985). Paragenezy mineralne w złożach Krakowidów i ich pokrywy. *Annales Societatis Geologorum Poloniae*, 53(1-4), 91-126 (in Polish).
- Harańczyk, C. (1988). Znaczenie suturalnego rozłamu wgłębnego Zawiercie-Rzeszotary dla powstania i rozmieszczenia mineralizacji paleozoicznej i złóż Zn-Pb. *Przegląd Geologiczny*, 36(7), 379-381 (in Polish).
- Harańczyk, C. (1989). Wulkanizm rejonu Krzeszowic. In J. Rutkowski (Ed.), *Rozwój wulkanizmu krakowskiego. Przewodnik LX Zjazdu PTG, Kraków 14-15 września 1989* (pp. 51-58). Kraków: Wydawnictwa AGH, Państwowy Instytut Geologiczny (in Polish).
- Harańczyk C. (1994). Kaledońskie Krakowidy jako górotwór transpresyjny. *Przegląd Geologiczny*, 42(11), 893-901 (in Polish).
- Harańczyk, C., Małkiewicz, T., Szostek, L., Kurek, S., & Rogoż, S. (1980). Porfirowa i skarnowa mineralizacja Cu-Mo z Zawiercia. Cz. 1. Budowa geologiczna. *Rudy i Metale Nieżelazne*, 25(11), 484-490 (in Polish).
- Harańczyk, C., & Wala, A. (1982). Profile proterozoiku i paleozoiku: mineralizacja kruszcowa. In A. Rózkowski & J. Ślósarz (Eds.), *Przewodnik LIV Zjazdu Polskiego Towarzystwa Geologicznego*, Sosnowiec, 23-25 września 1982 (pp. 127-132). Warszawa: Wydawnictwa Geologiczne (in Polish).
- Harańczyk, C., McKinnaird, J., & Sawłowicz, Z. (1988). Inkluzje ciekło-gazowe w żyłach kwarcowych Krakowidów (wstępne dane). *Rudy i Metale Nieżelazne*, 33(11), 412-415 (in Polish).
- Harańczyk, C., Lankosz, M., & Wolska, A. (1995). Granodioryt Jerzmanowicki, porfiry i kruszce Cu i Mo. *Rudy i Metale Nieżelazne*, 40(9), 334-341 (in Polish).
- Harańczyk, C., Koszowska, E., & Wolska, A. (1996). Przeobrażone tufity ze skał dolno-kambryjskich z wierceń w Dolinie Będkowskiej. *Polskie Towarzystwo Mineralogiczne-Prace Specjalne*, 9, 46-48 (in Polish).
- Harmon, R. S., Halliday, A. N., Clayburn, J. A. P., & Stephens, W. E. (1984). Chemical and isotopic systematic of the Caledonian intrusion of Scotland and Northern England: a guide to magma source region and magma-crust interaction. *Philosophical Transactions of the Royal Society, London A*, 310(1514), 709-742.
- Harris, N. B. W., Pearce, J. A., & Tindle, A. G. (1986). Geochemical characteristics of collision-zone magmatism. In M. P. Coward & A. C. Ries (Eds.), *Collision Tectonics* (pp. 67-81). Geological Society, Special Publications.
- Harris, N. B. W., Kelley, S., & Okay, A. I. (1994). Post-collision magmatism and tectonics in north-west Anatolia. *Contributions to Mineralogy and Petrology*, 117(4), 241-252.
- Harrison, T. M., & Watson, E. B. (1984). The behaviour of apatite during crustal anatexis: equilibrium and kinetic considerations. *Geochimica et Cosmochimica Acta*, 48(7), 1467-1477.
- Hattori, K., & Sato, H. (1996). Magma evolution recorded in plagioclase zoning in 1991 Pinatubo eruption products. *American Mineralogists*, 81(7-8) 982-994.
- Hawkesworth, C. J. (1982). Isotope characteristics of magmas erupted along destructive plate margins. In R. S. Thorpe (Ed.), *Orogenic Andesites and Related Rocks*. (pp.549-571). London: Wiley.
- Hawkesworth, C. J., Hergt, J. M., Ellam, R. M., & McDermott, F. (1991). Element fluxes associated with subduction-related magmatism. *Philosophical Transactions of the Royal Society, London A*, 335(1638), 393-405.
- Heflik, W., Parachoniak, W., Piekarski, K., Ratajczak, T., & Ryszka, J. (1975). Petrografia utworów staropaleozoicznych z okolic Myszkowa (Górny Śląsk). *Zeszyty Naukowe AHG 508, Geologia*, 1(4), 35-48 (in Polish).

- Heflik, W., Muszyński, M., & Parachoniak, W. (1977). Petrografia i warunki tworzenia się staropaleozoicznych skał podłoża Wyżyny Śląsko-Krakowskiej. *Geologia, Zeszyty Naukowe AHG Kwartalnik*, 3(4), 25-34 (in Polish).
- Heflik, W., Muszyński, M., & Pieczka, A. (1985). Lamprofiry z okolic Zawiercia. *Kwartalnik Geologiczny*, 29(3-4), 529-550 (in Polish).
- Heflik, W., Śliwiński, S., & Gładysz, J., (1989). Lamprofir z Piwoni koło Siewierza. *Rudy i Metale Nieżelazne*, 34(2) 36-40 (in Polish).
- Heflik, W., & Piekarski, K. (1992). Contact metamorphic rocks from the vicinity of Myszków (Upper Silesia). *Bulletin of the Polish Academy of Sciences, Earth Sciences*, 40(1), 31-42.
- Heflik, W., Moryc, W., & Muszyński M. (1992). Lamprophyres of the Silesia-Cracow Region. *Bulletin of the Polish Academy of Sciences, Earth Sciences*, 40(1), 23-29.
- Heflik, W., & Muszyński, M., (1993). A granitoid xenolith from rhyodacites of Zalas near Krzeszowice. *Bulletin of the Polish Academy of Sciences, Earth Sciences*, 41(4), 201-205.
- Herbich, E. (1981). Analiza tektoniczna sieci uskokuwej Górnośląskiego Zagłębia Węglowego. *Annales Societatis Geologorum Poloniae*, 51(3-4), 383-434 (in Polish).
- Hibbard, H. J. (1991). Textural anatomy of twelve magma-mixed granitoid systems. In J. Didier & B. Barbarin (Eds.), *Enclaves and Granite Petrology* (pp. 431-444). Amsterdam-Oxford-New York-Tokyo: Elsevier.
- Holtz, F., & Johannes, W. (1991). Genesis of peraluminous granites. I. Experimental investigation of melt composition at 3 and 5 kbar and various H₂O activities. *Journal of Petrology*, 32(5), 909-934.
- Hoshino, M., Kimata, M., Arakawa, Y., Shimizu, M., Nishida, N., & Nakai, S. (2007). Allanite-(Ce) as an indicator of the origin of granitic rocks in Japan: importance of Sr-Nd isotopic and chemical composition. *Canadian Mineralogist*, 45(6), 1329-1336.
- Hoskin, P. W. O., Kinny, P. D., Wyborn, D., & Chappell, B. W. (2000). Identifying accessory mineral saturation during differentiation in granitoid magmas: an integrated approach. *Journal of Petrology*, 41(9), 1365-1396.
- Huppert, H. E., & Sparks, R. S. J. (1988). The generation of granitic magmas by intrusion of basalt into continental crust. *Journal of Petrology*, 29(3), 599-624.
- İlbeyli, N., Pearce, J. A., Thirwall, M. F., & Mitchell, J. G., (2004). Petrogenesis of collision-related plutonics in Central Anatolia, Turkey. *Lithos*, 72(3-4), 163-182.
- Ishihara, S. (1977). The magnetite-series and ilmenite-series granitic rocks. *Mining Geology*, 27(5), 293-305.
- Ishihara, S., Kanaya, H., & Terashima, K. (1976). Genesis of the Neogene granitoids in the Fossa Magna region in Japan. *Marine Science Monthly*, 8, 523-528.
- Jachowicz, M. (2005). Ordowickie akritarchy bloku górnośląskiego. *Przegląd Geologiczny* 53(9), 756-762 (in Polish).
- Jachowicz-Zdanowska M. (2010). Palinologia kambru dolnego Bloku Górnośląskiego i prekambriu Bloku Małopolskiego w regionie krakowskim (Lower Cambrian palinology of the Upper Silesian Block and Precambrian palinology of the Małopolska Block in the Cracow region). In M. Jachowicz-Zdanowska & Z. Buła (Eds.), *Prekambr i Paleozoik Regionu Krakowskiego-model budowy geologicznej-jego aspekt użytkowy, Kraków 19 listopada 2010* (pp.67-92). Warszawa: Państwowy Instytut Geologiczny-Państwowy Instytut Badawczy (in Polish, English summary).
- James, D. E. (1982). A combined O, Sr, Nd and Pb isotopic and trace elements study of crustal contamination in central Andean lavas. 1- local geochemical variations. *Earth and Planetary Science Letters*, 57(1), 47-62.
- Janoušek, V., Braithwaite, C. J. R., Bowes, D. R., & Gerdes, A. (2004). Magma-mixing in the genesis of Hercynian calc-alkaline granitoids: an integrated petrographic and geochemical study of the Sazava intrusion, Central Bohemian Pluton, Czech Republic. *Lithos*, 78(1-2), 67-99.
- Jarmolowicz-Szulc, K. (1984). Datowania metodą K-Ar skał NE obrzeżenia GZW. *Kwartalnik Geologiczny*, 28(3-4), 749-750 (in Polish).
- Jarmolowicz-Szulc, K. (1985). Badania geochronologiczne K-Ar skał magmowych północno-wschodniego obrzeżenia Górnośląskiego Zagłębia Węglowego. *Kwartalnik Geologiczny*, 29(2), 343-354 (in Polish).
- Jayananda, M., Moyen, J-F., Martin, H., Peucat, J-J., Auvray, B., & Mahabaleswar, B. (2000). Late Archean (2550-2520 Ma) juvenile magmatism in the Eastern Dharwar craton, southern India: constraints from geochronology, Nd-Sr isotopes and whole rocks geochemistry. *Precambrian Research*, 99(3-4), 225-254.
- Jellinek, A. M., & DePaolo, D. J. (2003). A model for the origin of large silicic magma chambers. Precursors of caldera-forming eruptions. *Bulletin of Volcanology*, 65(5), 363-381.
- Jull, M., & Kelemen, P. B. (2001). On the conditions for lower crustal convective instability. *Journal of Geophysical Research*, 106(B4), 6423-6446.

- Jung, S., & Pfänder, J. A. (2007). Source composition and melting temperatures of orogenic granitoids: constraints from $\text{CaO}/\text{Na}_2\text{O}$, $\text{Al}_2\text{O}_3/\text{TiO}_2$ and accessory mineral saturation thermometry. *European Journal of Mineralogy*, 19(6), 859-870. DOI: 1127/0935-1221/2007/0019-1774
- Karwowski, Ł. (1988). Ewolucja fluidów mineralotwórczych waryscyjskiej formacji miedziowo-porfirowej Krakowidów na przykładzie rejonu Myszkowa-Mrzygłodu. *Prace Naukowe Uniwersytetu Śląskiego*, 929, 1-89 (in Polish).
- Kay, R. W., Mahlburg Kay, S., & Arculus, R. J. (1992). Magma genesis and crustal processing. In D. M. Fountain, R. Arculus & R. W. Kay (Eds.), *Continental Lower Crust* (pp. 423-445). Oxford: Elsevier.
- Koszowska, E., & Wolska, A. (1994a). Corundum from thermally-metamorphosed and hydrothermally altered Cambrian tuffaceous rocks, Będkowska Valley, S Poland. *Mineralogia Polonica*, 25(1), 29-42.
- Koszowska, E., & Wolska, A. (1994b). Cordierite from thermally metamorphosed Cambrian metasediments drilled in Będkowska Valley – preliminary report. *Mineralogia Polonica*, 25(2), 73-81.
- Koszowska, E., & Wolska, A. (2000a). Mineralogical and geochemical study of thermally altered country rock of granodiorite intrusion in the Będkowska Valley near Kraków (S Poland). *Annales Societatis Geologorum Poloniae*, 70(3-4), 261-281.
- Koszowska, E., & Wolska, A. (2000b). Contact metamorphism related to granodiorite intrusion from Będkowska Valley (South Poland). *Mineralogical Society of Poland Special Papers*, 17, 27-31.
- Kośnik, I., & Muszyński, M. (1990). Granitoidy z podłoża monokliny śląsko-krakowskiej – aktualny stan poznania. *Zeszyty Naukowe AGH, Geologia*, 16, 89-120 (in Polish).
- Kotas, A. (1982). Zarys budowy geologicznej GZW. In A. Rózkowski & J. Ślósarz (Eds.), *Przewodnik LIV Zjazdu Polskiego Towarzystwa Geologicznego, Sosnowiec 23-25 września 1982* (pp. 45-72). Warszawa: Wydawnictwa Geologiczne (in Polish).
- Kotas, A. (1985a). Uwagi o ewolucji strukturalnej Górnośląskiego Zagłębia Węglowego. In J. Trzpieczyński (Ed.), *Tektonika Górnośląskiego Zagłębia Węglowego. Materiały Konferencji Naukowej. Sosnowiec maj 31 - czerwiec 1* (pp. 17-46). Katowice: Wydawnictwo Uniwersytetu Śląskiego (in Polish).
- Kotas, A. (1985b). Structural evolution of the Upper Silesian Coal Basin (Poland). *10 International Congress of Carboniferous Stratigraphy and Geology, Madrid 12-17 september 1983* (pp.459-469). Preceedings Comptes Rendus, 3.
- Kozłowski, W., Domańska, J., Nawrocki, J., & Pecskey, Z. (2004). The provenance of the Upper Silurian greywackes from the Holy Cross Mountains (Central Poland). *Mineralogical Society of Poland Special Papers*, 24, 251-254.
- Kreutz, F. (1871). Skąły plutoniczne w okolicy Krzeszowic. *Rocznik c. k. Towarzystwa Naukowego Krakowskiego, Poczet trzeci, XIX*, 1-18 (in Polish).
- Królikowski, C., & Petecki, Z. (1995). *Gravimetric Atlas of Poland*. Warszawa: Państwowy Instytut Geologiczny.
- Kurbiel, H. (1978). Badania magnetyczne i grawimetryczne. *Prace Instytutu Geologicznego*, 83, 263-272 (in Polish).
- Leake, B. E., Wooley, A. R., Arps, C. E. S., Birch, W. D., Gilbert, M. C., Grice, J. D., Hawthorne, F. C., Kato, A., Kisch, H. J., Krivovichev, V. G., Linthout, K., Laird, J., Mandarino, J. A., Maresch, W. V., Nickel, E. H., Rock, N. M. S., Schumacher, J. C., Smith, D. C., Stephenson, N. C. N., Ungaretti, L., Whittaker, E. J. W., & Youzhi, G. (1997). Nomenclature of amphiboles: report of the Subcommittee on Amphiboles of the International Mineralogical Association, Commission on New Minerals and Mineral Names. *Canadian Mineralogist*, 35(1), 219-246.
- Le Maitre, R. W. (1989). *A Classification of Igneous Rocks and Glossary of Terms*. Oxford: Blackwell, 193 pp.
- Leshner, C. E. (1990). Decoupling of chemical and isotopic exchange during magma mixing. *Nature*, 344(6263), 235-237.
- Lewandowska, A., & Bochenek, K. (2001). New granitoid enclaves from Zalas rhyodacite Kraków area (S-Poland). *Mineralogical Society of Poland Special Papers*, 18, 106-108.
- Lewandowska, A., & Rospondek, M. (2003). Geochemistry of volcanic of the Zalas area near Kraków, South Poland. *Mineralogical Society of Poland Special Papers*, 23, 119-121.
- Lewandowska, A., Rospondek, M. J., & Nawrocki, J. (2010). Stephanian-Early Permian basaltic trachyandesites from the Sławków and Nieporaz-Brodła grabens near Kraków, Southern Poland. *Annales Societatis Geologorum Poloniae*, 80(3), 227-251.
- Lewandowski, M. (1994). Paleomagnetic constraints for Variscan mobilism of the Upper Silesian and Małopolska Massifs, southern Poland. *Geological Quarterly*, 38(2), 211-230.

- Liégeois, J.-P., & Black, R. (1987). Alkaline magmatism subsequent to collision in the Pan-African belt of the Adrar des Iforas. In J. G. Fitton & B. G. J. Upton (Eds.), *Alkaline Igneous Rocks* (pp. 381-401). The Geological Society, Blackwell Scientific Publications.
- Lustrino, M. (2005). How the delamination and detachment of the lower crust can influenced basaltic magmatism. *Earth-Science Review*, 72(1-2), 21-38.
- Łydka, K. (1973). Młodszy prekambry i sylur z rejonu Myszkowa. *Kwartalnik Geologiczny*, 17(4), 700-712 (in Polish).
- Mahan, K. H., Bartley, J. M., Coleman, D. S., Glazner, A. F., & Carl, B. S. (2003). Sheeted intrusion of the synkinematic McDoogle pluton, Sierra Nevada, California. *Geological Society of America Bulletin*, 115(12), 1570-1582.
- Malinowski, M., Żelaźniewicz, A., Grad, M., Guterch, A., & Janik, T. (2005). Seismic and geological structure of the crust in the transition from Baltica to Palaeozoic Europe in SE Poland – CELEBRATION 2000 experiment, profile CEL02. *Tectonophysics*, 401(1-2), 55-77.
- Maniar, P. D., & Piccoli, P. M. (1989). Tectonic discrimination of granitoids. *Geological Society of America Bulletin*, 101(5), 635-643.
- Markiewicz, J. (1984). Charakterystyka petrograficzna skał magmowych z rejonu Myszkowa-Mrzygodu. *Kwartalnik Geologiczny*, 28(3-4), 770-771 (in Polish).
- Markiewicz, J. (1994). Charakterystyka petrograficzna skał magmowych. In W. A. Rózkowski, J. Ślósarz & J. Żaba (Eds.), *Przewodnik 65. Zjazdu Polskiego Towarzystwa Geologicznego, Sosnowiec 22-24 września 1994* (pp. 191-195). Katowice: Wydawnictwa Uniwersytetu Śląskiego, Prace Naukowe Uniwersytetu Śląskiego w Katowicach, 1431 (in Polish).
- Markiewicz, J. (1998). Petrography of the apical zone of the Mrzygłód granitoids. *Biuletyn Instytutu Geologicznego*, 382, 5-34 (in Polish).
- Markiewicz, J. (2002). Przejawy kontaktowo-metasomatycznego oddziaływania granitoidowej intruzji mrzygłodzkiej. *Biuletyn Państwowego Instytutu Geologicznego*, 402, 101-132 (in Polish).
- Mason, R. (1990). *Petrology of Metamorphic Rocks*. London: Unwin Hyman Ltd. 230pp.
- Massonne, H. J. (2005). Involvement of crustal material in delamination of the lithosphere after continent-continent collision. *International Geology Review*, 47(8), 792-804.
- Matte, P. (1998). Continental subduction and exhumation of HP rocks in Palaeozoic orogenic belts: Uralides and Variscides. *Geologiska Föreningens i Stockholm Föreläsningar*, 120, 209-222.
- Matte, P. (2002). Variscides between the Appalachians and the Urals: similarities and differences between Paleozoic subduction and collision belts. *Special Papers – Geological Society of America*, 364, 239-251.
- Mazur, S., & Jarosiński, M. (2006). Budowa geologiczna głębokiego podłoża platformy paleozoicznej południowo-zachodniej Polski w świetle wyników eksperymentu sejsmicznego POLONAISE'97. *Prace Państwowego Instytutu Geologicznego*, 188, 203-222 (in Polish).
- McCulloch, M. T., & Perfit, M. R. (1981). $^{143}\text{Nd}/^{144}\text{Nd}$, $^{87}\text{Sr}/^{86}\text{Sr}$ and trace element constraints on the petrogenesis of Aleutian island arc magmas. *Earth and Planetary Science Letters*, 56(12), 167-179.
- Medaris, G., Jr., Wang, H., Jelinek, E., Mihaljević, M., & Jakeš, P. (2005). Characteristics and origins of diverse Variscan peridotites in the Gföhl Nappe, Bohemian Massif, Czech Republic. *Lithos*, 82(1-2), 1-23.
- Meyer, C., & Hemley, J. J. (1967). Wall rock alteration. In H. L. Barnes (Ed.), *Geochemistry of Hydrothermal Ore Deposits* (pp. 166-235). New York: Holt, Rinehart & Winston.
- Middlemost, E. A. K. (1994). Naming materials in their magma/igneous rocks systems. *Earth-Science Reviews*, 37(3-4), 215-224. DOI: 10.1016/0012-8252(94)90029-9.
- Mikrut, B. (1977). Wyniki badań petrograficznych skał magmowych z rejonu Myszkowa i Mrzygłodu. *Kwartalnik Geologiczny*, 21(4), 934-935 (in Polish).
- Moczyłowska, M. (1995). Neoproterozoic and Cambrian successions deposited on the East European Platform and Cadomian basement area in Poland. In D. G. Gee & M. Beckholmen (Eds.), *The Trans-European Suture Zone: EUROPROBE in Libice 1993* (pp. 276-285). Studia Geophysica Et Geodaetica, 39.
- Moyen, J.-F., Martin, H., & Jayananda, M. (2001). Multi-element geochemical modelling of crust-mantle interactions during late-Archean crustal growth: the Closepet granite (South India). *Precambrian Research*, 112(1-2), 87-105.
- Murphy, J. B., Pisarevsky, S. A., Nance, R. D., & Keppie, J. D. (2004). Neoproterozoic-Early Paleozoic evolution of peri-Gondwana terranes: implications for Laurentia-Gondwana connections. *International Journal of Earth Sciences*, 93(5), 659-682.
- Muszyński, M. (1995). Systematic position of igneous rocks from the northern margin of the Upper Silesian Coal Basin. *Mineralogia Polonica*, 26(1), 33-49.

- Muszyński, M., & Pieczka, A. (1994). Porphyry of the Dębnik laccolith. *Mineralogia Polonica*, 25(1), 15-28.
- Muszyński, M., & Pieczka, A. (1996). Potassium-bearing volcanic rocks from the northern margin of the Krzeszowice trough. *Mineralogia Polonica*, 27(1), 3-24.
- Muszyński, M., & Czerny, J. (1999). Granitoid autoliths from the porphyry of Zalas near Krzeszowice. *Mineralogia Polonica*, 30(2), 85-97.
- Naney, M. T., & Swanson, S. E. (1980). The effect of Fe and Mg on crystallization in granitic systems. *American Mineralogists*, 65(7-8), 639-653.
- Narkiewicz, M. (2005). Seria węglanowa dewonu i karbonu w południowej części bloku górnośląskiego. *Prace Państwowego Instytutu Geologicznego*, 182, 5-46 (in Polish).
- Narkiewicz, M. (2007). Development and inversion of Devonian and Carboniferous basins in the eastern part of the Variscan foreland (Poland). *Geological Quarterly*, 51(3), 231-256.
- Narkiewicz, K., & Nehring-Lefeld, M. (1993). Zastosowanie wskaźników CAI w analizie basenów sedimentacyjnych. *Przegląd Geologiczny*, 41(11), 757-763 (in Polish).
- Nawrocki, J., Żylińska, A., Buła, Z., Grabowski, J., Krzywiec, P., & Poprawa, J. (2004). Early Cambrian location and affinities of the Brunovistulian terrane (Central Europe) in the light of paleomagnetic data. *Journal of the Geological Society, London*, 161(3), 513-522.
- Nawrocki, J., & Poprawa, B. (2006). Development of Trans-European Suture Zone in Poland from Ediacaran lifting to Early Palaeozoic accretion. *Geological Quarterly*, 50(1), 59-76.
- Nawrocki, J., Lewandowska, A., & Fanning, M. (2007a). Isotope and paleomagnetic ages of the Zalas rhyodacites (S Poland). *Przegląd Geologiczny*, 55(6), 475-478.
- Nawrocki, J., Dunlop, J., Pecskey, Z., Krzemiński, L., Żylińska, A., Fanning, M., Kozowski, W., Salwa, S., Szczepanik, Z., & Trela, W. (2007b). Late Neoproterozoic to Early Palaeozoic palaeogeography of the Holy Cross Mountains (Central Europe): an integrated approach. *Journal of the Geological Society of London*, 164(2), 405-423.
- Nawrocki, J., Fanning, M., Lewandowska, A., Polechońska, O., & Werner, T. (2008). Palaeomagnetism and the age of the Cracow volcanic rocks (S Poland). *Geophysical Journal International*, 174(2), 475-488.
- Nawrocki, J., Krzemiński, L., & Pańczyk, M. (2010). ⁴⁰Ar-³⁹Ar ages of selected rocks and minerals from the Kraków-Lubliniec Fault Zone, and their relation to the Paleozoic structural evolution of the Małopolska and Brunovistulian terranes (S Poland). *Geological Quarterly*, 54(3), 289-300.
- Nelson, S. T., & Montana, A. (1992). Sieve-textured plagioclase in volcanic rocks produced by rapid decompression. *American Mineralogists*, 77(11-12), 1242-1249.
- Oberc, J. (1993). The role of longitudinal dislocation zones and strike-slip transversal deep fracture of Silesia-Lubusza (Hamburg-Kraków) in formation of main zone of meridional folds on Silesia and Moravia areas. *Kwartalnik Geologiczny*, 37(1), 1-18.
- Oberc, J. (1994). Uskoki (łuski, nasunięcia) podłużno-poprzeczne – specyfika strukturalno-ewolucyjna warwyscydów Śląska i Moraw. *Przegląd Geologiczny*, 42(2), 81-87 (in Polish).
- O'Connor, J. T. (1965). A classification for quartz-rich igneous rocks based on feldspar ratios. *United States Geological Survey Professional Paper*, 525B, 79-84.
- Orłowski, S. (1992). Cambrian stratigraphy and stage subdivision in the Holy Cross Mountains. *Geological Magazine*, 129(4), 471-474.
- Osborn, E. F. (1959). Role of oxygen pressure in the crystallization and differentiation of basaltic magma. *American Journal of Science*, 257(9), 609-647.
- Patiño Douce, A. E., & Beard, J. S. (1995). Dehydration-melting of Biotite Gneiss and Quartz Amphibolite from 3 to 15 kb. *Journal of Petrology*, 36(3), 707-738.
- Patiño Douce, A. E., & Harris, N. (1998). Experimental constraints on Himalayan anatexis. *Journal of Petrology*, 39(4), 689-710.
- Pearce, J. A. (1983). Role of sub-continental lithosphere in magma genesis at active continental margins. In C. J. Hawkesworth & M. J. Norry (Eds.), *Continental Basalts and Mantle Xenoliths* (pp. 230-249). Nantwich, U. K.: Shiva Press.
- Pearce, J. A. (1996). Sources and settings of granitic rocks. *Episodes*, 19(4), 120-125.
- Pearce, J. A., Harris, N. B., & Tindle, A. G. (1984). Trace element discrimination diagrams for the tectonic interpretation of granitic rocks. *Journal of Petrology*, 25(4), 956-983.
- Pearce, J. A., & Peate, D. W. (1995). Tectonic implications of the composition of volcanic arc magmas. *Annual Reviews of Earth and Planetary Sciences*, 23(1), 251-285.

- Peccerillo, R., & Taylor, S. R. (1976). Geochemistry of Eocene calc-alkaline volcanic rocks from the Kastamonu area, northern Turkey. *Contributions to Mineralogy and Petrology*, 58(1), 63-81.
- Phillips, G. N., Wall, V. J., & Clemens, J. D. (1981). Petrology of the Strathbogie batholiths: a cordierite-bearing granite. *Canadian Mineralogist*, 19(1), 47-63.
- Piekarski, K. (1982a). Aktualny stan badań okruszczowania paleozoiku północno-wschodniego obrzeżenia Górnośląskiego Zagłębia Węglowego. In A. Rózkowski & J. Ślósarz (Eds.), *Przewodnik LIV Zjazdu Polskiego Towarzystwa Geologicznego, Sosnowiec 23-25 września 1982* (pp. 26-38). Warszawa: Wydawnictwa Geologiczne (in Polish).
- Piekarski, K. (1982b). Litostratygrafia, tektonika, magmatyzm i okruszczowanie utworów staropaleozoicznych. In A. Rózkowski & J. Ślósarz (Eds.), *Przewodnik LIV Zjazdu Polskiego Towarzystwa Geologicznego, Sosnowiec 23-25 września 1982* (pp. 145-157). Warszawa: Wydawnictwa Geologiczne (in Polish).
- Piekarski, K. (1985). Analiza metalogeniczno-prognostyczna utworów paleozoicznych północno-wschodniego obrzeżenia Górnośląskiego Zagłębia Węglowego. *Annales Societatis Geologorum Poloniae*, 53(1-4), 207-234 (in Polish).
- Piekarski, K. (1994). Pozycja strukturalna i budowa złoża rud molibdenowo-wolframowo-miedziowych Myszków. In A. Rózkowski, J. Ślósarz & J. Żaba, (Eds.), *Paleozoik północno-wschodniego obrzeżenia Górnośląskiego Zagłębia Węglowego – Przewodnik LXV Zjazdu PTG, Sosnowiec, 22-24 września 1994* (pp. 58-68). Prace Naukowe Uniwersytetu Śląskiego 1431 (in Polish).
- Pietranik A., & Waight, T. E. (2008). Processes and sources during Late Variscan dioritic-tonalitic magmatism: insights from plagioclase chemistry (Gęsiniec intrusion, NE Bohemian Massif, Poland). *Lithos*, 86(3-4), 260-280.
- Pietranik A., & Koepke, J. (2009). Interactions between dioritic and granodioritic magmas in mingling zones: plagioclase record of mixing, mingling and subsolidus interactions in the Gęsiniec Intrusion, NE Bohemian Massif, SW Poland. *Contributions to Mineralogy and Petrology*, 158(1), 17-36.
- Pin, C., Binon, M., Belin, J. M., Barbarin, B., & Clemens, J. D. (1990). Origin of microgranular enclaves in granitoids: equivocal Sr-Nd evidence from Hercynian rocks in the Massif Central (France). *Journal Geophysical Research*, 95(B11), 17821-17828.
- Pin, C., & Santos Zalduegui, J. F. (1997). Sequential separation of light rare-elements, thorium and uranium, by miniaturized extraction chromatography: Application to isotopic analyses of silicate rocks. *Analytica Chimica Acta*, 339(1-2), 79-89.
- Pitcher, W. S. (1983). Granite: typology, geological environment and melting relationships. In M. P. Altherton & C. D. Gribble (Eds.), *Migmatites, Melting and Metamorphism* (pp. 277-287). Nantwich: Shiva Publications.
- Pitcher, W. S. (1993). *The Nature and Origin of Granite*. London: Blackie Academic and Professional Press. 321pp.
- Plonczyńska, I. (2000). Granitoids of the Silesian-Cracow monocline basement – mineralogical and geochemical characteristics and petrogenesis. *Mineralogical Society of Poland Special Papers*, 17, 63-71.
- Podemski, M., (Ed.), Buła, Z., Chaffee, M. A., Cieśla, E., Eppinger, R., Habryn, R., Karwowski, Ł., Lasoń, K., Markiewicz, J., Markowiak, M., Snee, L. W., Ślósarz, J., Truszel, M., Wybraniec, S., & Żaba, J. (2001). Palaeozoic Porphyry Molybdenum-Tungsten Deposit in the Myszków Area, Southern Poland. *Polish Geological Institute Special Papers*, 6, 87pp.
- Pożaryski, W., & Karnkowski, P. (1997). *Tectonic map of Poland during the Variscan time, 1:1 000 000*. Warszawa: Wydawnictwa Geologiczne.
- Pupier, E., Barbey, P., Toplis, M. J., & Bussy, F. (2008a). Igneous layering, fractional crystallization and growth of granitic plutons: the Dolbel Batholith in SW Niger. *Journal of Petrology*, 49(6), 1043-1068.
- Pupier, E., Duchene, S., & Toplis, M. J. (2008b). Experimental quantification of plagioclase crystal size distribution during cooling of basaltic liquid. *Contributions to Mineralogy and Petrology*, 155(5), 555-570.
- Ramsay, J. G. (1980). The crack-seal mechanism of rock deformations. *Nature*, 284(5752), 135-139.
- Rapp, R. P., & Watson, E. B. (1995). Dehydration melting of metabasalt at 8-32 kbar: implications for continental growth and crust-mantle recycling. *Journal of Petrology*, 36(4), 891-931.
- Rapp, R. P., Shimizu, N., & Norman, M. (2003). Growth of early continental crust by partial melting of eclogite. *Nature*, 425(6958), 605-609.
- Reid, J. B., Evans, O. C., & Fates, D. G. (1983). Magma mixing in granitic rocks of the central Sierra Nevada, California. *Earth Planetary Science Letters*, 66(1), 243-261.
- Rock, N. M. S. (1987). The nature and origin of lamprophyres, an overview. In J. G. Fitton & B. G. J. Upton (Eds.), *The Alkaline Rocks* (pp. 191-226). Special Publications Geological Society of London.

- Rollinson, H. R. (1993). *Using Geochemical Data: Evaluation, Presentation, Interpretation*. London: Longman Group UK Ltd. 352pp.
- Romer, R. L., Förster, H.-J., & Breitzkreuz, C. (2001). Intracontinental extensional magmatism with a subduction fingerprint: the late Carboniferous Halle Volcanic Complex (Germany). *Contribution to Mineralogy and Petrology*, 141(1), 201-221.
- Respondek, M., Lewandowska, A., Chocyk-Jamińska, M., & Finger, F. (2004). Residual glass of high-K basaltic andesites (shoshonites) from the Nieporaz-Brodla graben near Krzeszowice. *Mineralogical Society of Poland Special Papers*, 24, 337-440.
- Rozen, Z. (1909). Dawne lawy Wielkiego Księstwa Krakowskiego. *Rozprawy Wydziału Matematyczno-Przyrodniczego Akademii Umiejętności, Seria III*, 49 (pp. 293-368). Kraków (in Polish).
- Ryka, W. (1974). Asocjacja diabazowo-lamprofirowa północno-wschodniego obrzeżenia GZW. *Biuletyn Instytutu Geologicznego*, 278(12), 35-69 (in Polish).
- Sabatier, H. (1991). Vaugnerites: special lamprophyre-derived mafic enclaves in some Hercynian granites from Western and Central Europe. In J. Didier & B. Barbarin (Eds.), *Enclaves and Granite Petrology* (pp. 63-81). Amsterdam-N. York-Tokyo: Elsevier.
- Salisbury, M. J., Bohron, W. A., Clynne, M. A., Ramos, F. C., & Hoskin, P. (2008). Multiple plagioclase crystals populations identified by crystal size distribution and in situ chemical data: implications for timescales of magma chamber processes associated with the 1915 eruption of Lassen Peak, CA. *Journal of Petrology*, 49(10), 1755-1780.
- Sawka, W. N. (1988). REE and trace element variations in accessory minerals and hornblende from the strongly zoned McMurtry Meadows Pluton, California. *Transactions of the Royal Society of Edinburgh: Earth Sciences*, 79(2-3), 157-168. DOI: 10.1017/S0263593300014188.
- Schaltagger, U. (2000). U-Pb geochronology of the Southern Black Forest Batholith (Central Variscan Belt): timing of exhumation and granite emplacement. *International Journal of Earth Sciences*, 88(4), 814-828.
- Schmidt, M. W. (1992). Amphibole composition in tonalite as function of pressure: an experimental calibration of the Al in hornblende barometer. *Contributions to Mineralogy and Petrology*, 110(2), 304-310.
- Schott, B., & Schmeling, H. (1998). Delamination and detachment of a lithospheric root. *Tectonophysics*, 296(3-4), 225-247.
- Shand, S. J. (1943). *The Eruptive Rocks*. 2nd edn., N. York: John Wiley. 444pp.
- Shannon, W. M., Barnes, C. G., & Bickford, M. E. (1997). Grenville magmatism in West Texas: petrology and geochemistry of the Red Bluff Granitic Suite. *Journal of Petrology*, 38(10), 1279-1305.
- Shaw, D. M. (1968). A review of K-Rb fractionation trends by covariance analysis. *Geochimica et Cosmochimica Acta*, 32(6), 573-601.
- Shearer, C. K., Papike, J. J., & Laul, J. C. (1985). Chemistry of potassium feldspars from three zoned pegmatites, Black Hills, south Dakota: Implications concerning pegmatite evolution. *Geochimica et Cosmochimica Acta*, 49(3), 663-673.
- Shelly, D. (1993). *Igneous and Metamorphic Rocks Under Microscope*. London: Chapman and Hall. 445pp.
- Siedlecki, S., & Wieser, T. (1947). Porfir w dolinie Czernki. *Rocznik Polskiego Towarzystwa Geologicznego*, 17(1), 103-135 (in Polish).
- Siedlecki, S. (1954). Utwory paleozoiczne okolic Krakowa. *Biuletyn Instytutu Geologicznego*, 73, 1-415 (in Polish, English summary).
- Sisson T. W., Ratajeski, K., Hankins, W. B., & Glazner, A. F. (2005). Voluminous granitic magmas from common basaltic sources. *Contributions to Mineralogy and Petrology*, 148(5), 635-409. DOI: 10.1007/s004110-004-0632-9.
- Skorupa, J. (1953). Badania magnetyczne w obszarze na NE od Krzeszowic. *Biuletyn Instytutu Geologicznego*, 13(do użytku wewnętrznego), 1-23 (in Polish).
- Slaby, E. (1987). Adularization of plagioclases with accompanying processes in the rhyodacites from Zalas near Cracow. *Archiwum Mineralogiczne*, 42(2), 69-94.
- Slaby, E. (1990). Adularia from Miękinia. *Archiwum Mineralogiczne*, 46(1-2), 55-70.
- Slaby, E. (2000). Sodium and potassium feldspars; products of late-magmatic alteration, geology and petrology of the Upper Silesia and Małopolska terranes boundary zone. *Mineralogical Society of Poland Special Papers*, 17, 243-246.
- Slaby, E., & Götze, J. (2004). Feldspar crystallization under magma-mixing conditions shown by cathodoluminescence and geochemical modelling – a case study from the Karkonosze pluton (SW Poland). *Mineralogical Magazine*, 68(4), 541-557.

- Slaby, E., & Martin, H. (2008). Mafic and felsic magma interaction in granites: The Hercynian Karkonosze Pluton (Sudetes, Bohemian Massif). *Journal of Petrology*, 49(2), 353-391.
- Slaby, E., Götze, J., Wörner, G., Simon, K., Wrzalik, R., & Śmigielski, M. (2008). K-feldspar phenocrysts in microgranular magmatic enclaves: a cathodoluminescence and geochemical study of crystal growth as a marker of magma mingling dynamics. *Lithos*, 105(1-2), 85-97.
- Slaby, E., Żaba, J., Falenty, K., Falenty, A., Breitreuz, C., & Domańska-Siuda, J. (2009). The origin and the evolution of magmas of Permo-Carboniferous volcanism of the Kraków region. *Mineralogical Society of Poland Special Papers*, 34, 47-48.
- Slaby, E., Breitreuz, C., Żaba, J., Domańska-Siuda, J., Gadzik, K., Falenty, K., & Falenty, A. (2010). Magma generation in an alternating transtensional-transpressional regime, the Kraków-Lubliniec Fault Zone, Poland. *Lithos*, 119(3-4), 251-268.
- Solgadi, F., Vanderhaeghe, O., Moyen, J-F., Sawyer, E., & Reisberg, L. (2007). Generation of synorogenic Hercynian granites in the Livradois area, French Massif Central: the relative roles of crustal anatexis and mantle derived magmas. *Canadian Mineralogist*, 45(3), 581-606.
- Sparks, R. S. J., & Marshall, L. A. (1986). Thermal and mechanical constraints on mixing between mafic and silicic magmas. *Journal of Volcanology and Geothermal Research*, 29(1-4), 99-124.
- Stone, M. (1995). The main Dartmoor granites: petrogenesis and comparisons with the Carnmenellis and Isles of Scilly granites. *Proceedings of the Ussher Society*, 8, 379-384.
- Streckeisen, A., & Le Maitre, R. W. (1979). A chemical approximation to the modal QAPF classification of the igneous rocks. *Neues Jahrbuch für Mineralogie-Abhandlungen*, 136, 169-206.
- Sun, S. S., & McDonough, W. F. (1989). Chemical and isotopic systematic of oceanic basalts: implications for mantle composition and processes. In A. D. Saunders & M. J. Norry (Eds.), *Magmatism in the Ocean Basins* (pp.313-345). London: Geological Society of London, Special Publications, 42.
- Sun, C. H., & Stern, R. J. (2001). Genesis of Mariana shoshonites: contribution of the subduction component. *Journal of Geophysical Research*, 106(B1), 589-608.
- Sutowicz, E. (1982). Albitization of plagioclases in Permian volcanic rocks from Zalas. *Archiwum Mineralogiczne*, 38(1), 129-137.
- Ślósarz, J. (1982). Uwagi o warunkach geologicznych mineralizacji miedziowo-molibdenowej w paleozoiku okolic Myszkowa. *Przegląd Geologiczny*, 30(7), 329-335 (in Polish).
- Ślósarz, J. (1985). Stadia i strefowość mineralizacji kruszcowej w paleozoiku okolic Myszkowa. *Annales Societatis Geologorum Poloniae*, 53(1-4), 267-288 (in Polish).
- Ślósarz, J. (1994). Charakterystyka mineralogiczna okruszczowania miedziowo-molibdenowo-wolframowego. In A. Rózkowski, J. Ślósarz & J. Żaba (Eds.), *Przewodnik 65. Zjazdu Polskiego Towarzystwa Geologicznego, Sosnowiec 22-24 września 1994* (pp. 196-202). Katowice: Wydawnictwa Uniwersytetu Śląskiego, Prace Naukowe 1431 (in Polish).
- Tarney, J., & Saunders, A. D. (1979). Trace element constraints on the origin of cordilleran batholiths. In M. P. Atherton & J. Tarney (Eds.), *Origin of Granite Batholiths-Geochemical Evidence* (p. 90-105). Orpington, Kent: Shiva.
- Tatsumi, Y., & Hanyu, T. (2003). Geochemical modeling of dehydration and partial melting of subducting lithosphere: Toward a comprehensive understanding of high-Mg andesite formation in the Setouchi volcanic belt, SW Japan. *Geochemistry, Geophysics, Geosystems*, 4(9), 1525-2027. DOI: 10.1029/2003GC000530 issn1525-2027.
- Taylor, S. R., McLennan, S. M., Armstrong, R.L., & Tarney, J. (1981). The composition and evolution of the continental crust: rare earth element evidence from sedimentary rocks. *Philosophical Transactions of the Royal Society London A*, 301(1461), 381-399.
- Taylor, S. R., & McLennan, S. M. (1985). *The Continental Crust: its Composition and Evolution*. Blackwell, Oxford. 312 pp.
- Tepley, F. J., Davidson, J. P., Tilling, R. I., & Arth, J. G. (2000). Magma mixing, recharge and eruption histories recorded in plagioclase phenocrysts from El Chichon Volcano, Mexico. *Journal of Petrology*, 41(9), 1397-1411.
- Thiéblemont, D., & Cabanis, B. (1990). Utilisation d'un diagramme (Rb/100-Tb-Ta) pour la discrimination géochimique et l'étude pétrogénétique des roches magmatiques acides. *Bulletin de la Société Géologique de France*, 8(1), 23-35.
- Thorpe, R. S., Francis, P. W. O'Callaghan, L., Hutchison, R., & Turner, J. S. (1984). Relative roles of source composition, fractional crystallization and crustal contamination in the petrogenesis of Andean volcanic rocks. *Philosophical Transactions of the Royal Society London A*, 310(1514), 675-682.

- Tindle, A. G. (1991). Trace element behaviour in microgranular enclaves from granitic rocks. In J. Didier & B. Brabarin (Eds.), *Enclaves and Granite Petrology* (pp. 313-330), Amsterdam-Oxford- New York-Tokyo: Elsevier.
- Truszel, M. (1994). Charakterystyka petrograficzna skał metamorficznych starszego paleozoiku. In A. Rózkowski, J. Ślósarz & J. Żaba (Eds.), *Przewodnik 65. Zjazdu Polskiego Towarzystwa Geologicznego, Sosnowiec 22-24 września 1994* (pp. 187-191). Katowice: Wydawnictwa Uniwersytetu Śląskiego, Prace Naukowe Uniwersytetu Śląskiego 1431 (in Polish).
- Truszel, M., Karwowski, L., Lasoń, K., Markiewicz, J., & Żaba, J. (2006). Magmatism and metamorphism of the Kraków-Lubliniec tectonic zones as a clue to the occurrence of polymetallic deposits. *Biuletyn Instytutu Geologicznego*, 418, 55-103 (in Polish).
- Unrug, R., Harańczyk, Cz., & Chocyk-Jaminski, M. (1999). Easternmost Avalonian and Armorican-Cadomian terranes of Central Europe and Caledonian-Variscan evolution of the polydeformed Kraków mobile belt: geological constraints. *Tectonophysics*, 302(1-2), 133-157.
- Vance, D., & Thirwall, M. (2002). An assessment of mass discrimination in MC-ICPMS using Nd isotopes. *Chemical Geology*, 185(3-4), 227-240.
- Vernon, R. H. (1983). Restite, xenoliths and microgranitoid enclaves in granites. *The Journal and Preceeding of the Royal Society of New South Wales*, 116(3-4), 77-103.
- Vernon, R. H. (1984). Microgranitoid enclaves in granites: globules of hybrid magma quenched in a plutonic environment. *Nature*, 309(5967), 438-439.
- Vernon, R. H. (1990). Crystallization and hybridism in microgranitoid enclave magmas: microstructural evidence. *Journal of Geophysical Research*, 95(B11), 17849-17859.
- Vernon, R. H. (1991). Interpretation of microstructures of microgranitoid enclaves. In J. Didier & B. Brabarin (Eds.), *Enclaves and Granite Petrology* (pp.277-290), Amsterdam-Oxford-New York-Tokyo: Elsevier.
- Vernon, R. H., & Paterson, S. R. (2008). How late are K-feldspar megacrysts in granites ? *Lithos*, 104(1-4), 327-336.
- Vogel, T. A., & Wilband, J. T. (1978). Coexisting acidic and basic melts: geochemistry of composite dike. *The Journal of Geology*, 86(3), 353-371.
- Voshage, H., Hofmann, A. W., Mazzucchelli, M., Rivalenti, S., Sionigoi, S., & Demarchi, G. (1990). Isotopic evidence from Ivrea zone for a hybrid lower crust formed by magmatic underplating. *Nature*, 347(6295), 731-736.
- Waight, T. E., Weaver, S. D., Muir, R. J., Maas, R., & Eby, N. (1998). The mid-Cretaceous Hohonu Batholith of North Westland New Zealand: granitoid compositions controlled by source H₂O contents and generated during tectonic transition. *Contributions to Mineralogy and Petrology*, 130(3), 225-239.
- Waight, T. E., Maas, R., & Nicholls, I. A. (2000). Fingerprinting feldspar phenocrysts using crystal isotopic composition stratigraphy: implications for crystal transfer and magma mingling in S-type granites. *Contributions to Mineralogy and Petrology*, 139(2), 227-239.
- Wang, H. F., Bonner, B. P., Carlson, S. R., Kowallis, B. J., & Heard, H. C. (1989). Thermal stress cracking in granite. *Journal of Geophysical Research*, 94(B2), 1745-1758. DOI: 10.1029/JB094iB02p01727.
- Warner, S., Martin, R. F., Abdel-Rahman, A-F. M., & Doig, R. (1998). Apatite as a monitor of fractionation, degassing, and metamorphism in the Sudbury Igneous Complex, Ontario. *Canadian Mineralogist*, 36(4), 981-999.
- Weaver, B. L., & Tarney, J. (1984). Empirical approach to estimating the composition of the continental crust. *Nature*, 310(5978), 575-577.
- White, A. J. R., & Chappel, B. W. (1977). Ultrametamorphism and granitoid genesis. *Tectonophysics*, 43(1-2), 7-22.
- White, A. J. R., & Chappel, B. W. (1983). Granitoid types and their distribution in the Lachlan Fold Belt, southeastern Australia. In J. A. Roddick (Ed.), *Circum-Pacific Plutonic Terranes* (pp. 21-34). Geological Society of America, Memoir 159.
- White, W. M., & Patchett, J. (1984). Hf-Nd-Sr isotopes and incompatible element abundances in island arcs: implications for magma origins and crust-mantle evolution. *Earth and Planetary Science Letters*, 67(2), 167-185.
- White, W. M., & Duprè, B. (1986). Sediment subduction and magma genesis in the lesser Antilles: isotopic and trace element constraints. *Journal of Geophysical Research*, 91(B6), 5927-5941. DOI: 10.1029/JB091iB06p05943.

- White, A. J. R., Chappel, B. W., & Wyborn, D. (1999). Application of the restite model to the Deddick granodiorite and its enclaves – a reinterpretation of the observations and data of Maas et al. *Journal of Petrology*, 40(3), 413-421.
- Wiebe, R. A. (1968). Plagioclase stratigraphy: a record of magmatic conditions and events in a granite stock. *American Journal of Science*, 266(8), 690-703.
- Wiebe, R. A., Manon, M.R., Hawkins, D. P., & McDonough, W. F. (2004). Late-stage mafic injection and thermal rejuvenation of the Vinalhaven granite, coastal Maine. *Journal of Petrology*, 45(11), 2133-2153.
- Wilson, J. T. (1966). Did the Atlantic close and re-open ? *Nature*, 211(5050), 676-681.
- Wilson, M. (1989). *Igneous Petrogenesis A Global Tectonic Approach*. Springer. 466 pp.
- Winchester, J. A., & Team, T. P. T. N. (2002). Palaeozoic amalgamation of Central Europe: new results from recent geological and geophysical investigations. In H. Thybo, T. Pharach & A. Guterch (Eds.), *Geophysical Investigations of the Trans-Europe Suture Zone II, Nice, France 25-29 April 2000* (pp.5-21). Tectonophysics, 360 (1-4).
- Winkler, H. G. F. (1974). *Petrogenesis of metamorphic rocks*. (3rd edition). New York: Springer. 320 pp.
- Winkler, H. G. S. (1986). *Petrogenesis of metamorphic rocks*. Berlin: Springer. 348 pp.
- Wolska, A., (1984). Skład petrograficzny i chemiczny diabazu z Niedźwiedziej Góry. *Przegląd Geologiczny*, 32(7), 391-396 (in Polish).
- Wolska, A. (2000). Hydrothermal alterations of granodiorite from Będkowska Valley (southern Poland). *Mineralogical Society of Poland Special Papers*, 17, 75-77.
- Wolska, A. (2001). Alteration of the porphyry copper deposits type in the granodiorite from Pilica area (southern Poland). *Mineralogical Society of Poland Special Papers*, 19, 184-186.
- Wolska, A. (2004). High-temperature restite enclaves as an evidence of deep-seated parent magma melting of the Będkowska Valley granodiorite (Silesian-Cracow area, South Poland) – preliminary petrographic and mineralogical study. *Annales Societatis Geologorum Poloniae*, 74(1), 21-33.
- Wolska, A. (2009). Enclaves in granodiorite intrusion from the Paleozoic basement of Silesian-Kraków area, Southern Poland. *Mineralogia Special Papers*, 34, 32-33.
- Wyllie, P. J., Cox, K. G., & Biggar, G. M. (1962). The habit of apatite in synthetic systems and igneous rocks. *Journal of Petrology*, 3(2), 238-243.
- Zaręczny, S., (1894). *Atlas geologiczny Galicji. Tekst do zeszytu III. 4 arkusze mapy geologicznej 1:75 000*. Komisja Fizjograficzna Akademii Umiejętności, Kraków (in Polish).
- Zen, E-A. (1986). Alumina enrichment in silicate melts by fractional crystallization, some mineralogic and petrographic constraints. *Journal of Petrology*, 27(5), 1095-1118.
- Zen, E-A. (1988). Phase relations of peraluminous granitic rocks and their petrogenetic implications. *Annual Review of Earth and Planetary Sciences*, 16(1), 21-52.
- Zorpi, M. J., Coulon, C., Orsini, J. B., & Cocirca, C. (1989). Magma mingling, zoning and emplacement in calc-alkaline granitoid plutons. *Tectonophysics*, 157(4), 315-329.
- Zuber, R. (1886). Skąły wybuchowe z okolicy Krzeszowic. *Rozprawy Wydziału Matematyczno-Przyrodniczego Akademii Umiejętności*. Kraków (in Polish).
- Zulauf, G. (1997). Von der Anchizone bis zur Eklogitfazies: Angekippte Krustenprofile als Folge der cadomischen und variscischen Orogenese im Teplá-Barrandium (Böhmische Masse). *Geotektonische Forschungen*, 89, 1-302.
- Żaba, J. (1994). Ewolucja strukturalna paleozoicznych skał krystalicznych w rejonie Myszkowa i Mrzygłodu na przykładzie otworu Pz-10. In A. Rózkowski, J. Ślósarz & J. Żaba (Eds.), *Przewodnik 65 Zjazdu Polskiego Towarzystwa Geologicznego, 22-24 września 1994, Sosnowiec* (pp.141-154). Wydawnictwo Uniwersytetu Śląskiego, Prace Naukowe Uniwersytetu Śląskiego 1431 (in Polish).
- Żaba, J. (1995). Uskoki przesuwcze strefy krawędziowej bloków Górnośląskiego i Małopolskiego. *Przegląd Geologiczny*, 43(10), 838-842 (in Polish).
- Żaba, J. (1996). Późnokarbońska aktywność przesuwcza strefy granicznej bloków Górnośląskiego i Małopolskiego. *Przegląd Geologiczny*, 44(2), 173-180 (in Polish).
- Żaba, J. (1999). Structural evolution of Lower Palaeozoic succession in the Upper Silesia block and Małopolska block zone. *Prace Państwowego Instytutu Geologicznego*, 166, 5-162.
- Żaba, J. (2000). Tectono-magmatic activity of the Upper Silesia terrane and Małopolska terrane edge (Southern Poland). *Mineralogical Society of Poland Special Papers*, 17, 81-83.
- Żelaźniewicz, A., Buła, Z., Jachowicz, M., & Żaba, J. (1997). The crystalline basement SW of the Trans-European Suture Zone in Poland: Neoproterozoic (Cadomian?) orogen. *Terra Nostra*, 11, 167-171.

- Żelaźniewicz, A. (1998). Rodinian-Baltican link of the Neoproterozoic orogen in southern Poland. *Acta Universitatis Carolinae Geologica*, 42(3-4), 509-515.
- Żelaźniewicz, A., Buła, Z., & Jachowicz, M. (2002). Neoproterozoic granites in the Upper Silesia Massif of Bruno-Vistulicum, S Poland: U-Pb SHRIMP evidence. *Schriftenreihe der Deutschen Geologische Gesellschaft*, 21, 361-362.
- Żelaźniewicz, A., Pańczyk, M., Nawrocki, J., & Fanning, M. (2008). A Carboniferous/Permian, calc-alkaline, I-type granodiorite from the Małopolska Block, Southern Poland: implications from geochemical and U-Pb zircon age data. *Geological Quarterly*, 52(4), 301-308.
- Żelaźniewicz, A., Buła, Z., Fanning, M., Seghedi, A., & Żaba, J. (2009). More evidence on Neoproterozoic terranes in Southern Poland and southeastern Romania. *Geological Quarterly*, 53(1), 93-124.
- Żylińska, A. (2002). Stratigraphic and biogeographic significance of Late Cambrian trilobites from Łysogóry (Holy Cross Mountains, central Poland). *Acta Geologica Polonica*, 52(1-2), 217-238.